Thèse de doctorat

pour l'obtention du titre de

Docteur en Sciences Mathematiques

de Cergy Paris Université

Presentée par

Anna MELNYKOVA

Statistical and numerical analysis
of jump and diffusion models in biology

Thèse dirigée par

Eva LÖCHERBACH et Adeline SAMSON

Soutenué le 8 decembre 2020 devant le jury composé de

Mme Evelyn BUCKWAR	*Examinatrice*	Professeure
Mme Magalie FROMONT RENOIR	*Examinatrice*	Professeure
M Arnaud GLOTER	*Rapporteur*	Professeur
M Antoine LEJAY	*Rapporteur*	DR Inria
Mme Eva LÖCHERBACH	*Directrice de thèse*	Professeure
Mme Adeline SAMSON	*Directrice de thèse*	Professeure

Richtiges Auffassen einer Sache

und Mißverstehn der gleichen Sache

schließen einander nicht vollständig aus.

FRANZ KAFKA

ACKNOWLEDGEMENTS

will, lightfast brain and well-documented code. Susanne Ditlevsen for my time in Copenhagen and her incomparable scientific energy.

I thank PhDs of LJK (past or present) for making the world a bit a better place, and also the administration in Grenoble and Cergy, especially Laurence Wazné, Linda Isone, Juana Dos Santos and Frederick Audra. And... okay, okay, here we go, I thank Mitya for sharing the office with me for these 3 years (even if we didn't talk for some periods and argued for 90% percent of the remaining time). Let's put it like this: you have trained me to stay focused and work no matter what. Also, we had quite a lot of productive swimming and pull-up sessions, so in retrospective it was even not so bad, you're a funny guy.

On a less professional level, I send a lot of warm thanks for my cat-obsessed crew in Grenoble, Nastya and Vlad, for all the fun we had on hikes, on that boat concert in Sweden, Rocky Horror Picture Show, for the dinners, good Spotify playlists, Korean movies, lockdown jogging sessions and all those things. Also, I thank all the (former) Inria crew, Federico, Daan, Konstantin, and all the others with whom we've shared hikes, or parties, or climbing sessions, without you Grenoble wouldn't be Grenoble anymore. Thanks to my former mathematical crew in Ulm, of which I keep only the warmest memories all the past years (5 years!), especially Anya and Nikita, for keeping contact, for sharing, for discussing, for just being somewhere there, you are cool guys.

If someone is still reading this quite long and pathetic acknowledgment, here is another short story to entertain you: in 1965, an 18-years old girl Nina Tschaïka was preparing to apply for a mathematical faculty of Odessa university, but was convinced against it by her environment, since "it is very difficult for a girl". So, finally she has became a midwife. In 1987, a 17-years old girl Valya Bondar, wanted to apply to a Physical-Mathematical faculty in University of Kiev... but was talked against it, because "it is very difficult for a girl", so she has became a sociologist. In 2010, at the age of 16, I have applied for a Physical-Mathematical faculty in Kiev Polytechnic Institute, enjoying a full support from my family, most notably from Valya Bondar (who has ended up being my mom), and Nina Tschaïka (my grandma). And — guess what, in 2020 I have ended up with a PhD diploma in Mathematics! So, let me assure you, with a little bit of supporting environment, it is not that difficult at all ("even for a girl"!).

Talking about the supporting environment, I finally thank Pierre, and the cat, for all our travels and the lockdowns spent together, your exceptionally wide taste in music, literature and movies, lust for life, and also a remarkable appreciation of satirically-depressive slavic sense of humor. Just imagine all those nice restaurants we will surely try once the Covid pandemics is over, the journey has just began!

A B S T R A C T

There exist a lot of biological phenomena which are difficult to observe and explain. For example, the generation and processing of the information in our brains, the immune response of our bodies to different diseases, the reaction of living cells to different stimuli and so on. Thanks to the recent advances in biology, medicine and computer science those processes can be observed and recorded (at least partly) with a high level of precision. Consequently, there is an increasing demand in translating the data, gathered by biologists and neuroscientists, into interpretable mathematical models. The aim of this thesis is to contribute to the study of stochastic mathematical models of real-world phenomena, and analyze these models both numerically and theoretically.

In the first part of this thesis we are studying the link between individual-based stochastic models (birth-and-death processes, Hawkes processes) and their respective continuous approximations (stochastic diffusions, partial differential equations), obtained at a larger scale. In particular, we are tackling the question of the numerical simulation of stochastic and deterministic processes with the help of splitting and implicit numerical schemes, which preserve the asymptotic behavior of the process. On the applied level, we consider mathematical models of interacting networks of biological neurons, as well as bacteria populations.

In the second part of the manuscript we are dealing with statistics for stochastic differential equations, such as parametric inference for diffusions with degenerate noise, and hypothesis testing for the covariance matrix rank from discrete observations. For the parametric estimation we use quasi-maximum likelihood estimators (also known as contrast estimators), where the contrast is built on the density approximated with the local linearization scheme. For the second problem, we study a non-asymptotic regime (i.e., the case when the observations are available with a fixed time step). We consider the case when the distribution of the test statistics can be written explicitly (for example, when the drift is known and the dimension is 1 or 2). Then, we use concentration inequalities to derive the tail properties and use them to obtain a non-asymptotic control of the Type I and Type II errors.

Keywords. *Statistics:* parametric inference, maximum likelihood estimators, concentration inequalities, statistical tests. *Probability:* stochastic diffusions, hypoellipticity, Hawkes processes, birth-and-death processes. *Numerics:* splitting schemes, high-order approximation schemes, asymptotic-preserving schemes for PDEs, thinning algorithms.

R É S U M É

Beaucoup de phénomènes biologiques sont difficiles à observer et à expliquer. Par exemple, la génération et le traitement des informations dans notre cerveau, la réponse immunitaire de notre corps à différentes maladies, la réaction des cellules vivantes à différents stimuli, etc. Grâce aux progrès récents de la biologie, de la médecine et de l'informatique, ces processus peuvent être observés et enregistrés (au moins en partie) avec un haut niveau de précision. Par conséquent, il existe une demande croissante pour traduire les données recueillies par les biologistes et les neuroscientifiques en modèles mathématiques interprétables. Le but de cette thèse est de contribuer à l'étude des modèles mathématiques stochastiques des phénomènes du monde réel, et d'analyser ces modèles à la fois numériquement et théoriquement.

Dans la première partie de cette thèse, nous étudions le lien entre les modèles stochastiques indivu-centrés (processus de naissance et de mort, processus de Hawkes) et leurs approximations continues respectives (diffusions stochastiques, l'équations aux dérivées partielles), obtenues à plus grande échelle. En particulier, nous abordons la question de la simulation numérique des processus stochastiques et déterministes à l'aide de schémas par fractionnement (splitting) et numériques implicites, qui préservent le comportement asymptotique du processus. Au niveau appliqué, nous considérons des modèles mathématiques d'interaction de réseaux de neurones biologiques, ainsi que des populations de bactéries.

Dans la deuxième partie du manuscrit, nous traitons de statistique pour les équations différentielles stochastiques, telles que l'inférence paramétrique pour les diffusions avec bruit dégénéré, et le test d'hypothèses pour le rang de la matrice de covariance à partir d'observations discrètes. Pour l'estimation paramétrique, nous utilisons des estimateurs de quasi-maximum de vraisemblance (également appelés estimateurs de contraste), où le contraste est construit sur la densité approchée avec le schéma de linéarisation locale. Pour le deuxième problème, nous étudions un régime non asymptotique (c'est-à-dire le cas où les observations sont disponibles avec un pas de temps fixe). On considère le cas où la distribution des statistiques de test peut être écrite explicitement (par exemple, lorsque la dérive est connue et que la dimension est 1 ou 2). Ensuite, nous utilisons des inégalités de concentration pour évaluer les erreurs du 1ère et 2ème espèces du test.

Mots clés. *Statistiques:* inférence paramétrique, estimateurs du maximum de vraisemblance, inegalités de concentration, tests statistiques. *Probabilité:* diffusions stochastiques, hypoellipticité, processus de Hawkes, processus de naissance et mort. *Numérique:* schémas de division, schémas d'approximation d'ordre élevé, schémas consistentes pour l'EDP, algorithmes de thinning.

S U M M A R Y

This PhD thesis is devoted to stochastic models in biology, with a primal focus being neuronal models. First, we treat some questions related to the simulation of stochastic processes which describe the biological phenomena (neuronal activity, bacterial populations and so on). Second, we contribute to some statistical problems (parametric inference, hypothesis testing) which are often faced by statisticians and biologists who work with neuronal data.

The manuscript consists of 8 chapters, which are divided in 4 parts. **Part i** is an Introduction, which is devoted to the biological motivation behind the problems, treated in the other parts, the state of the art and the overview of the thesis's contributions. It contains 3 Chapters: *Existing models and probabilistic preliminaries*, *Objectives, methods and related works* and the *Outline of the contributions*. In this part a short summary of the results presented in Parts ii-iii is made, and their relevance to the recent advances in adjacent fields, as well as possible extensions are discussed.

Chapter 1 (*Existing models and probabilistic preliminaries*) is organized as follows: first, we give a very brief introduction to the biological problems which have (partly) motivated this thesis. Then, we present necessary mathematical tools which are used to model the described phenomena. We group the models by three categories: deterministic, stochastic diffusions and point processes. This division should be considered as a mere convenience for the author and the reader. It will be shown in the next chapters that those three families of models can be used interchangeably depending on the exact problem and the level of abstraction one is working on.

Chapter 2 (*Objectives, methods and related works*) aims to give an overview of the recent advances in numerical analysis and statistics for the deterministic and stochastic models described in the previous chapter. Of course, it is not possible to give an exhaustive picture within the page limits of PhD Thesis' Introduction, thus some important statistical issues are deliberately omitted. Our primary goal is not to cover all important subjects, but rather to place our contributions in a suitable context and explain how they are related to other published works. It is what **Chapter 3** (*Outline of the contributions*) is devoted to. In this chapter we give a short overview of models we were working on, the ultimate goal of the work and the results we have achieved.

Part ii (*Numerical analysis*) and **Part iii** (*Statistics*) contain two chapters each. They present the author's own contribution to the field and are primarily based on published or submitted articles, except for Chapter 7 which presents work in progress. Thematically, **Part ii** investigates the links between counting processes and processes with a smooth dynamics (like partial differential equations and stochastic differential equations), while **Part iii** is focused on stochastic diffusions.

More precisely, **Chapter 4** is devoted to the numerical and theoretical study of Hawkes processes with Erlang memory kernel and their diffusion aproximation. These processes are used to describe an activity of a system of interacting neurons, structured by several populations according to their

functionality. It is shown in Ditlevsen and Löcherbach (2017) that in a mean-field limit the piece-wise deterministic Markov process (PDMP), associated with the Hawkes process, is approximated by a hypoelliptic diffusion. In this Chapter we prove a strong error bound between the PDMP and the diffusion, develop a numerical splitting scheme for the diffusion and prove that it preserves its properties (ergodicity and moment bounds), and propose an efficient algorithm for simulating the PDMPs, based on the thinning procedure.

Chapter 5 studies mathematical models which describe the Horizontal Gene Transfer in bacteria population on different scales. We start with the macroscopic scale, where the dynamics of the population is described by a classical death-and-birth process. We simulate this process and study its behaviour in a cyclic regime, which is ensured by the evolutionary rescue phenomena. This phenomena means that under certain conditions, the vast majority of the population is driven by extinction, but in the absence of the competition between the individuals, the few remaining organisms manage to repopulate the environment. On the next step, we consider the case when the size of the population increases, and it becomes too difficult (and computationally costly) to consider the individual-based model. We thus pass to a density-based model based on partial differential equations (PDE), first considered in Billiard et al. (2015, 2016a). In order to go even further, to an evolutionary time scale, one needs to consider a special, Hamilton-Jacobi type PDE. This model is more convenient to analyze with mathematical tools, but is more difficult to simulate. We thus propose an asymptotic-preserving simulation scheme which allows to empirically investigate the difference of the observed dynamics on a different level of abstraction.

Chapter 6 is devoted to the parameter estimation for hypoelliptic diffusions with full observations. We consider a two-dimensional diffusion, where one coordinate is driven by the Brownian motion, and the other one is not. The diffusion coefficient is thus degenerate, and it makes the application of standard statistical procedures more complicated. We show under which conditions this diffusion is hypoelliptic, which ensures the existence of smooth transition density. For the parameter estimation we adopt a classical approach, based on the pseudo-maximum likelihood. As a first step, we develop an approximation scheme, based on the Local Linearization method (Ozaki, 1989, Biscay et al., 1996, Jimenez and Carbonell, 2015), and write its discrete transition density. On the second step, we propose a maximum likelihood estimator based on the obtained expression and propose a single criteria for estimating the parameters of the drift and the variance coefficient. We prove that this estimator is consistent and asymptotically normal. Finally, we illustrate our results on the hypoelliptic neuronal FitzHugh-Nagumo model.

Chapter 7 treats the estimation of the covariance matrix rank in diffusion models from discretely observed data. Estimating the rank of the matrix helps to differentiate between elliptic and hypoelliptic models. On an applied level, this information sheds some light upon the nature of the noise in neuronal models. We work in a non-asymptotic setting, meaning that the observations of the processes are only available at fixed time steps. The main difficulty imposed in this case consists in choosing a meaningful hypothesis: indeed, when the observation time step is fixed, we cannot really infer the information about strictly degenerate (i.e., identically equal to zero) diffusion coefficients. Instead, we

are focusing on estimating if a given diffusion coefficient is smaller than a given threshold or not, thus complementing the results of Jacod et al. (2008). We start with simple examples of systems where the distribution of the test statistics can be found explicitly. In more general cases, when the probabilistic law cannot be written explicitly, we use concentration inequalities to evaluate the distribution of the test statistics.

The manuscript is concluded with **Part iv** which is an Afterword. It contains the only Chapter 8, where we discuss possible expansions of the results obtained in previous two Parts.

CONTENTS

LIST OF FIGURES

$\mathbb{E}$ Expectation

$\mathbb{P}$ Probability

Ω Probability space

$\mathbb{N}$ Space of natural numbers

$\mathbb{R}$ Space of real numbers

$\mathcal{A}$ Infinitesimal generator

$\mathcal{N}$ Normal distribution

$\mathcal{U}$ Uniform distribution

$\mathcal{E}$ Exponential distribution

$Pois$ Poisson distribution

$\sim$ follows the probability law

$\equiv$ equivalence

$\approx$ approximately equal

$\triangleq$ defined as

$\xrightarrow{\mathcal{D}}$ convergence in distribution

$\xrightarrow{\mathbb{P}}$ convergence in probability

Part I

INTRODUCTION

EXISTING MODELS AND PROBABILISTIC PRELIMINARIES

Ce qui est simple est toujours faux. Ce qui ne l'est pas est inutilisable.

Paul Valéry

Mathematics is used for modeling a vast amount of real-world phenomena. The main objective of this thesis is to tackle some of the existing mathematical challenges, related to biology. Biological phenomena are described by different classes of models: deterministic (given by differential equations) and stochastic (stochastic differential equations and piece-wise deterministic Markov processes). Despite the fact that this manuscript is mostly focused on processes described by stochastic differential equations (more precisely, stochastic diffusions), it is sometimes indispensable to work with other classes.

Why different types of models are needed? Consider a dozen of hares feeding on a vast field of grass next to a small village. If we decide to predict the dynamics of population of this (or equivalent) dozen of hares living next to this (or equivalent) small village, the most natural approach to adopt would be to consider a birth-and-death process. The data gathered by generations of villagers would permit to estimate the birth and the death rates from natural causes, hungry wolves (or villagers) or global warming. In turn, it would allow to give a fairly accurate estimate of the hare population in the coming years. If we decide to consider the same task, but for the hare population in whole Europe, the birth-and-death approach would touch its limits. On this scale, the density-based models (given as a differential or partial differential equation) could be more suitable and easy to treat.

Thus, the primary goal of the first chapter of this introduction is to give an overview of biological phenomena which give rise to yet unsolved mathematical problems. Our aim is to give examples of biological systems and provide a necessary statistical and probabilistic background without limiting to a specific class of mathematical models. Questions we are going to consider include, but are not limited to, an activity of the human brain, antibiotic resistance in bacteria, cancer tumor growth etc. Later, in Chapter 2 we will rely on the presented notions to introduce a set of numerical and statistical tools, on which the contributions of the thesis are primarily based.

We start with **deterministic models** (Section 1.1), as the most classical and well-studied framework. Within this manuscript we focus on ordinary and partial differential equations (ODEs and PDEs). The advantage of the deterministic models is that they are versatile, relatively easy to analyze and fast to simulate. However, the use of purely deterministic models is often limited to studying the

"average" behavior, or to the settings where the stochasticity plays little to no role (for example, in a large population limit in certain biological networks), since they cannot take into account the random nature of inputs which often shape the biological processes. In the setting when the influence of random force is not negligible, it is more common to work with the stochastic models.

Most of the stochastic biological models can be divided in two large classes: **diffusion processes** and **point processes**. By diffusion processes we mean the solutions of stochastic differential equations (SDEs). They are a natural extension of deterministic models (usually presented by ordinary- or partial differential equations). We devote Section 1.2 of this chapter to the diffusion processes. We present some concepts from probability theory which will be used throughout this thesis. Among other things, we give a formal definition of a hypoelliptic class of diffusions. They are in the focus of Chapters 4 and 6 of this thesis. We also show how the hypoellipticity can be verified on concrete examples, and briefly discuss the influence of noise in stochastic systems. Finally, we complete the picture by talking about the point processes belonging to a family of piecewise deterministic Markov processes (PDMP). They are defined by a sequence of jumps, occurring with a certain intensity, and the deterministic flow, given by a solution of an ordinary differential equation. Section 1.3 briefly present simple birth-and death processes, Poisson processes and Hawkes processes.

Let us now give a brief description of the real-world motivation behind the numerical and statistical problems we consider. An important field, which has gained a lot of attention in recent years is **neuroscience**. Cheap and almost unlimited computational power, which is shaping the science of the XXI century, has allowed to record, process and analyze the brain activity with high precision. More precisely, it is possible to record the spikes emitted by a neuronal cell or a group of cells (*extracellular recording*), or to place an electrode into a cell body (see the right panel of Figure 1.1) and record the changes of the membrane potential (*intracellular recording*). The latter process (see plot on the left panel of Figure 1.1) allows to observe how the neuron reacts to the change of the external stimuli (for example, the electric current run through the cell).

We start the brief excursion into the mathematical neuroscience with the building block of our neural circuits: neurons. Neurons are excitable cells which are the main information transmitters in the brain. The body of a neuron consists of a cell body (soma), an axon and an axon terminal (illustrated on the left panel of Figure 1.1). The cell body receives the stimuli from the environment via dendrites. Then, under the influence of the stimuli, the concentration of sodium and potassium inside the cell changes and under certain circumstances the neuron emits a spike (also called an *action potential*), which then travels through the axon body to the axon terminal, emitting a signal to the other neurons in a network through synapses.

Similarly to the example with hares in the beginning of this section, there exist different approaches to describe a neuronal activity. If we are interested primarily in the firing pattern of an individual neuron, or a small group of neurons, the most natural approach would be to use the framework of point processes (Poisson, Hawkes, etc.). If we decide to focus on how the firing activity of a neuron depends on the biochemical processes inside the body of neuron, it is more accurate to use models, described by differential or stochastic differential equations (see Examples 1.1, 1.2 and 1.8).
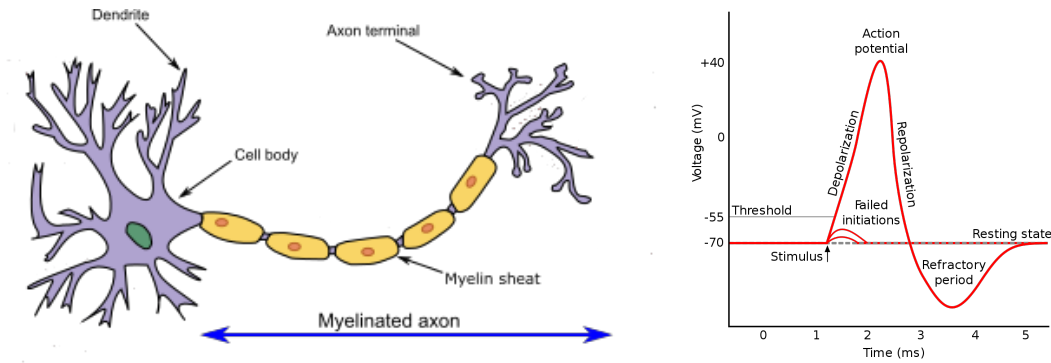
Figure 1.1: The structure of a biological neuron and the action potential. Source: https://en.wikipedia.org/wiki/Neuron, https://en.wikipedia.org/wiki/Action_potential

Often, the choice of the suitable model is dictated by a practical convenience rather than strict mathematical arguments. For example, it is rather bold to assume that the action potential corresponds to a completely deterministic process. But how strong is the influence of the stochasticity? Is it even important to take it into account, or a deterministic model is precise enough? The answer to these questions lies in treating the neuronal data. For that, a solid statistical tool set at hand is indispensable. Contributing to such a tool set is one of the goals of this thesis.

Another important field where the mathematical expertise is required is **evolutionary biology**. This field covers a lot of important medical applications: for example, the problem of development of antibiotic resistance in bacteria, evolutionary and spatial dynamics of cancer cell populations and their resistance to treatment, and many others. The following problems are often faced by biologists: how to find the ideal trade-off between the toxicity and the efficiency of a certain drug treatment? What would be the optimal dose of antibiotics which would kill the malicious bacteria with a minimal impact on a natural flora of human guts? Is it possible to predict the growth rate of a cancerous tumor in different environments? Those and other questions can be answered, at least partly, with the help of numerical analysis of mathematical models, which is is another motivation of this thesis.

The aim of this chapter is to give a short overview of the existing models, addressing of the issues described above. Section 1.1 is devoted to the deterministic models, described by Ordinary or Partial Differential Equations (ODE and PDE respectively), as the most common and well-studied class. On the next step, we consider a family of diffusions, described by Stochastic Differential Equations (SDEs), which is the subject of Section 1.2. Finally, we briefly discuss the class of counting processes (or point processes) in Section 1.3.

1.1   DETERMINISTIC MODELS

We start the excursion into the existing models from the simplest deterministic case, an ordinary differential equation (ODE), written as

$$dX_t = b(t, X_t)dt, \quad X_0 = x_0, \tag{1.1}$$

where $b \in \mathbb{R}^{d+1} \to \mathbb{R}^d$. We refer the reader to textbooks like Chicone (2006), Evans (2010) for the conditions of existence of solutions of ODEs and PDEs, presented further in this section. ODEs (1.1) are widely used in neuronal modeling. There exist several models which aim to describe the process of firing in neurons with a different level of abstraction. One of the most famous examples is the Hodgkin-Huxley synaptic-based model (see Example 1.1). It was awarded a Nobel prize in 1968 and since then has served as a starting point for developing more sophisticated (or, on the contrary, simplified) models.

Example 1.1 (Hodgkin-Huxley neuronal model (Hodgkin and Huxley, 1952)). *The dynamics of the membrane potential and the synapses is described by the following system:*

$$\begin{cases} I = C_m \frac{dV_m}{dt} + \bar{g}_K n^4 (V_m - V_K) + \bar{g}_{Na} m^3 h (V_m - V_{Na}) + \bar{g}_l (V_m - V_l), \\ \frac{dn}{dt} = \alpha_n(V_m)(1 - n) - \beta_n(V_m)n, \\ \frac{dm}{dt} = \alpha_m(V_m)(1 - m) - \beta_m(V_m)m, \\ \frac{dh}{dt} = \alpha_h(V_m)(1 - h) - \beta_h(V_m)h, \end{cases}$$

where I is the input current (stimulation of the other neurons or the current controlled by the experimenter), V_m is the voltage of the membrane, and α_i and β_i are rate constants for the i-th ion channel, which depend on voltage but not time. $\bar{g}_n$ is the maximal value of the conductance. n, m, and h are dimensionless quantities between 0 and 1 that are associated with potassium channel activation, sodium channel activation, and sodium channel inactivation, respectively. For $p = (n, m, h)$, α_p and β_p take the form

$$\alpha_p(V_m) = p_\infty(V_m)/\tau_p$$
$$\beta_p(V_m) = (1 - p_\infty(V_m))/\tau_p.$$

p_∞ and $(1 - p_\infty)$ are the steady state values for activation and inactivation, respectively, and are usually represented by Boltzmann equations as functions of V_m.

The Hodgkin-Huxley equations model with a very high precision the potassium channel activation and sodium channel activation and deactivation. Once the voltage (or the action potential), given by the variable V_m, exceeds a certain threshold, the Hodgkin-Huxley model undergoes a bifurcation. It results in a sudden jump in an action potential, which is interpreted as a "firing" of a neuron (see the right panel of Figure 1.1). After the firing, the neuron goes into a refractory period, during which another spike is not possible.

The price to pay for the biological precision is that the Hodgkin-Huxley model is very difficult to study from a mathematical point of view. The first reason is that it is highly non-linear and its solution cannot be written explicitly. The second reason is that it is high-dimensional. For modeling purposes it is often more convenient to work with other self-exciting models which mimic the neuronal activity in a simplified way.

Indeed, there exist numerous models based on the Hodgkin-Huxley. The aim of some of them is to achieve a higher precision (adding more information to the system), while others try to simplify the model, making it easier to analyze from a mathematical point of view. The most common simplification is to replace the three last equations in Hodgkin-Huxley equation by an abstract variable, summarizing dynamics of all ion channels. The closest to the original model is the Morris-Lecar system (Morris and Lecar, 1981), where the dynamics of the recovery variable is approximated by a first-order linear differential equation for the probability of channel opening:

Example 1.2 (Morris-Lecar neuronal model (Morris and Lecar, 1981))**.** *The oscillatory activity of a neuron is described by the following 2-dimensional ODE:*

$$\begin{cases} C\frac{dV}{dt} = I - g_{\mathrm{L}}(V - V_{\mathrm{L}}) - g_{\mathrm{Ca}}M_{\mathrm{ss}}(V - V_{\mathrm{Ca}}) - g_{\mathrm{K}}N(V - V_{\mathrm{K}}), \\ \frac{dN}{dt} = \frac{N_{\mathrm{ss}} - N}{\tau_N}, \end{cases}$$

where V is the membrane potential, N is the recovery variable, which can be regarded as the probability that the $K+$ channel is conducting, and

$$M_{\mathrm{ss}} = \frac{1}{2} \cdot \left(1 + \tanh\left[\frac{V - V_1}{V_2}\right]\right),$$

$$N_{\mathrm{ss}} = \frac{1}{2} \cdot \left(1 + \tanh\left[\frac{V - V_3}{V_4}\right]\right),$$

$$\tau_N = 1 / \left(\varphi \cosh\left[\frac{V - V_3}{2V_4}\right]\right).$$

Even further, the model can be simplified by replacing the hyperbolic functions by polynomials. It gives one of the most widely used simple self-exciting models, namely a 2-dimensional FitzHugh-Nagumo model (Fitzhugh, 1961, Nagumo et al., 1962):

Example 1.3 (Deterministic FitzHugh-Nagumo model (Fitzhugh, 1961, Nagumo et al., 1962))**.** *The spiking activity of a neuron is described by the following equation:*

$$\begin{cases} dV_t = \frac{1}{\varepsilon}\left(V_t - V_t^3 - U_t - s\right)dt \\ dU_t = \left(\gamma V_t - U_t + \beta\right)dt, \end{cases}$$

where V_t is the membrane potential, and U_t summarizes the input of ion channels. The parameters of the systems do not have the same explicit biological meaning as in the Hodgkin-Huxley model (see Example 1.1). In particular, ε is a scaling parameter, which regulates the time difference between the membrane voltage V_t, which changes at a faster scale than the recovery variable U_t, s describes the stimuli current, γ and β are abstract variables determining the spiking or oscillatory behaviour of a neuron.
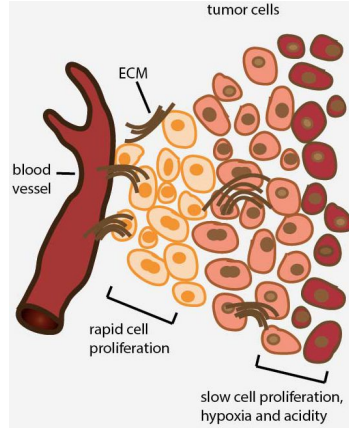
Figure 1.2: Cancer cell growth in oxygenated and hypoxic environment. Source: Zhang et al. (2015).

The same model will be presented in the next Section in its stochastic version (see Example 1.8). Since the examples presented in this manuscript are by no mean exhaustive, we refer to the books Gerstner and Kistler (2002), Tuckwell (2005), Izhikevich (2007) for a more complete overview of the existing neuronal models.

Another important class of deterministic models are PDE models. They are heavily used in the evolutionary biology and cancer research for studying the drug resistance in bacteria, viruses, tumors, as well as natural selection, mutation and other phenomena. PDE-based model are usually focused on the dynamics of a population of biological cells or individuals, structured by phenotypic traits, in time and/or space. Most of them can be viewed as an "averaged" version of a birth-and-death process for large populations (see Example 1.9 in Section 1.3). While in a classical birth-and-death process the number of individuals in a population is countable and finite, the PDE approach assumes an infinite number of cells. These models study the evolution of the density of a certain type of cells rather than the dynamics of separate individuals. There exist numerous works which prove the link between the stochastic individual based models and density-based PDE models, applied to bacteria or cancer cell evolution, see, in particular, Billiard et al. (2016a, 2015), Champagnat et al. (2008).

The following example provides a density-based model of the evolution of the cancer cells in hypoxic and oxygenated environment (see Figure 1.2 for an illustration). It is used for studying the influence of certain types of treatment on the proliferation rate of the cancer cells:

Example 1.4 (Cancer cell dynamics (Lorz et al., 2015, Lorenzi et al., 2018))**.** *Denote a state space* $\Omega \in \mathbb{R}^3$*, where* Ω *represents a solid tumor, and by* $x \in \Omega$ *— a position in this tumor. Further,* $y \in [0,1]$ *denotes a hypoxia responsive gene and* $s(t,x)$ *the concentration of oxygen at time* t*. We denote the population density at time* t *and position* x *by* $n(t,x,y)$*. Then, the dynamic of the system is described by the following PDE:*

$$\begin{cases} \frac{\partial n(t,x,y)}{\partial t} = \left(f(y) + r(y,s(t,x)) - d\rho(t,x,y) \right) n(t,x,y) \\ \rho(t,x,y) = \int_0^1 n(t,x,u)du. \end{cases}$$

Here $f(y)$ *and* $r(y,s(t,x))$ *are deterministic functions which represent the proliferation rate (i.e. the speed of reproduction) in hypoxic and oxygenated environments respectively,* y *encodes the genetic*

information, which controls cell proliferation and drug resistance, and d is a death rate from the competition between individuals. The mean phenotype at position x can be computed as follows:

$$\mu(t, x) = \frac{1}{\rho(t, x)} \int_0^1 y\, n(t, x, y) dy.$$

Deterministic models are not in the main focus of the thesis, but they often serve as a basis for more sophisticated models. For example, if our goal is to see how the dynamics of a particular system can be influenced by some unknown (considered random) inputs of the outer world, we are naturally lead to stochastic models of diffusion type, presented in the following section.

1.2   STOCHASTIC DIFFERENTIAL EQUATIONS

Not all real-world forces are of deterministic nature or, to be more precise, it is not always convenient to encipher all possible influences in a form of deterministic parameters. For example, consider a single neuronal cell, whose activity is described with the Hodgkin-Huxley model (see Example 1.1). This model (despite being very precise!) does not take into account, for example, the signals coming from the other cells, the temperature of the environment etc., which can slightly modify the voltage dynamics. If we are interested in studying the influence of these unknown phenomena, we can upgrade the ODE by adding a random process with a volatility (or diffusion) parameter, which would mimic the influence of the other, "less important", forces.

The most widely used approach is to add a Wiener Process (also called a Brownian motion), thus transforming a system of ODEs (or PDEs) into a Stochastic Differential Equation (SDEs) (or SPDEs, respectively). Consider a probability space $(\Omega, \mathcal{F}, \mathbb{P})$. By stochastic diffusion we mean a solution of the autonomous d-dimensional stochastic differential equation (SDE) in Itô sense, written as follows:

$$dX_t = b(X_t)dt + \sigma(X_t)dW_t, \quad X_0 = x_0, \tag{1.2}$$

where $b \in \mathbb{R}^d \to \mathbb{R}^d$ is a drift term, $\sigma \in \mathbb{R}^d \to \mathbb{R}^d \times \mathbb{R}^q$, $W_t \in \mathbb{R}^q$ is a standard Brownian motion, x_0 is a random variable such that $\mathbb{E}[x_0^2] < \infty$. By "autonomous" we mean that the drift and the variance coefficients do not depend on time. We refer to classical textbooks like Karatzas and Shreve (1987), Oksendal (2003) for conditions of existence of solutions and other properties of (1.2).

To give an example of a SDE having an explicit solution, let us consider a linear homogeneous system of equations. The solution of this equation is called an Ornstein-Uhlenbeck process, which is studied by numerous authors (Gikhman and Skhorokhod (1968) being one of the most classical references).

Example 1.5 (Linear Homogeneous system). *Consider the following d-dimensional SDE:*

$$dX_t = (AX_t + a)dt + \sigma dW_t, \quad X_0 = x_0 \equiv const$$

where A is a square $d \times d$ constant matrix of full rank, $a \in \mathbb{R}^d$ is a constant vector, σ is a constant $d \times q$ matrix with at least one non-zero entry, $W_t \in \mathbb{R}^q$ is a standard Brownian motion. This system can be solved explicitly and its solution at time $t > 0$ is given by

$$X_t = e^{At} \left(x_0 + \int_0^t e^{-As} a\, ds + \int_0^t e^{-As} \sigma\, dW_s \right).$$

The process $(X_t)_{t \geq 0}$ is Gaussian and has the following expectation and variance:

$$\mathbb{E}\left[X_t\right] = e^{At} \left(x_0 + \int_0^t e^{-As} a\, ds \right),$$

$$Var\left[X_t\right] = \mathbb{E}\left[\left(\int_0^t e^{A(t-s)} \sigma\, dW_s \right) \left(\int_0^t e^{A(t-s)} \sigma\, dW_s \right)^T \right].$$

Example 1.5 is interesting, because the process described by the solution of a linear homogeneous SDE has a smooth Gaussian transition density even when $\sigma \sigma^T$ is not of full rank. In general, the case when $rank(\sigma \sigma^T) < d$ is much more difficult to study, since the solution of (1.2) cannot be analyzed by standard tools, requiring a non-degenerate covariance matrix. Depending on the rank of the matrix $\sigma \sigma^T$, this process has different properties, because it belongs to different classes of processes: elliptic and hypoelliptic. More precisely,

- when $rank(\sigma \sigma^T) = d$, the system is said to be *elliptic*;

- when $rank(\sigma \sigma^T) < d$, the elliptic assumption does not hold. However, under special conditions, the usual properties of the system (such as existence of transition density), can be proven under milder conditions, known as *hypoellipticity*.

The main focus of this thesis is made on the diffusions satisfying the *hypoelliptic assumption*. However, in order to keep a consistent narrative, we will first shortly discuss the "classical" diffusions, satisfying the elliptic condition.

Most of the first stochastic models applied in neuroscience belong to the class of **elliptic diffusions**. We refer, for example, to Gerstein and Mandelbrot (1964) for a firing model based on Wiener process, or Stevens and Zador (1998) for a simple model of a firing neuron, given by a particular case of the linear homogeneous equation (see Example 1.5), to the elliptic Morris-Lecar model (as in Example 1.2) studied by Ditlevsen and Samson (2012), Ditlevsen and Greenwood (2013) and many others.

Example 1.6 (Stochastic Leaky Integrate-and-fire model (Stevens and Zador, 1998))**.** *In this model the membrane potential is associated with a continuous stochastic process, where spikes occur when the membrane potential crosses a certain (deterministic threshold). The dynamics of the membrane potential under the threshold is described by Ornstein-Uhlenbeck process:*

$$dV_t = \left(-\frac{V_t - V_0}{\tau} + I \right) dt + \sigma\, dW_t, \quad V_0 = v_0.$$

In this example the neuron fires at time $s = \min_s \{V_s > v\}$, and then the membrane takes its initial value v.

Before focusing on **hypoelliptic diffusions**, let us formally define what hypoellipticity refers to. In the sense of stochastic calculus of variations (Malliavin and Thalmaier, 2006, Nualart, 2006) the definition is the following:

Definition 1.1 (Hypoellipticity). *The Lie bracket $[A_1, A_2]$ of the two vectors $A_m = \sum_{i=1}^{d} A_m^i e^i$, $m = 1, 2$, is given by*

$$[A_1, A_2] := J_{A_2} A_1 - J_{A_1} A_2 = \sum_{i=1}^{d} \left(\sum_{j=1}^{d} (A_1^j \partial_j A_2^i - A_2^j \partial_j A_1^i) \right) e^i,$$

*where J_{A_m} denotes the Jacobian of matrix A_m. The **Lie algebra** $\mathbf{A}$ generated by the d vector fields $A_1, \ldots, A_d$ is defined as the vector space of all fields obtained as linear combinations with constant coefficients of the*

$$A_k, \ [A_k, A_l], \ [[A_k, A_l], A_s], \quad etc.$$

*Given $r \in \mathbb{R}^d$, let $\mathbf{A}(r) \triangleq \{\zeta \in \mathbb{R}^d | \zeta = Z(r) \text{ for some } Z \in \mathbf{A}\}$. We say that vector fields $A_1, \ldots, A_d$ satisfy the **Hörmander criterion for hypoellipticity** if $A_1, \ldots, A_d$ are infinitely often differentiable and if*

$$\mathbf{A}(r) = \mathbb{R}^d \quad \forall r \in \mathbb{R}^d.$$

Let us explain how Definition 1.1 can be verified in practice and give an intuition of it. First, the coefficients of (1.2) must be written the Stratonovich form, which is the following:

$$dX_t = \left(b(X_t) - \frac{1}{2} \partial_x \sigma(X_t) \sigma(X_t) \right) dt + \sigma(X_t) \circ dW_t, \tag{1.3}$$

where the notation $\sigma(X_t) \circ dW_t$ is commonly used to distinguish the stochastic integrals defined in Stratonovich sense from the analogous Itô form (typically denoted as $\sigma(X_t) dW_t$). Both equations (1.3) and (1.2) refer to the same process, but the rules of integration slightly differ.

The goal is to compute the Lie bracket of the following two vectors:

$$A_1 = b(X_t) - \frac{1}{2} \partial_x \sigma(X_t) \sigma(X_t), \quad A_2 = \sigma(X_t).$$

The hypoellipticity is implied by the fact that A_2 and $[A_1, A_2]$ span the space $\mathbb{R}^d$.

Informally speaking, hypoellipticity holds when some of the coordinates in system (1.2) are not perturbed by noise directly (they are often called "smooth"), but they depend at least on one of the "rough" variables. In two-dimensional systems it implies that the derivative of the drift coefficient of the smooth variable with respect to the rough one should be non-zero. Then, as illustrated in Examples 1.7-1.8, the respective Lie brackets of the process span the whole state space and the Hörmander condition holds.

Hypoellipticity also implies that all the coordinates are perturbed by a Brownian motion, but at different rate. This means, in particular, that the degenerate diffusion coefficient may be "complemented" by higher-order terms, obtained as an integrated Brownian motion from noisy coordinates. A formal derivation of an "extended" diffusion term for a multidimensional hypoelliptic diffusion is presented in a recent preprint Pigato (2020).

Now let us give some examples of 2-dimensional hypoelliptic systems and illustrate how the definition 1.1 can be verified in practice. We start with the following important class of stochastic diffusions:
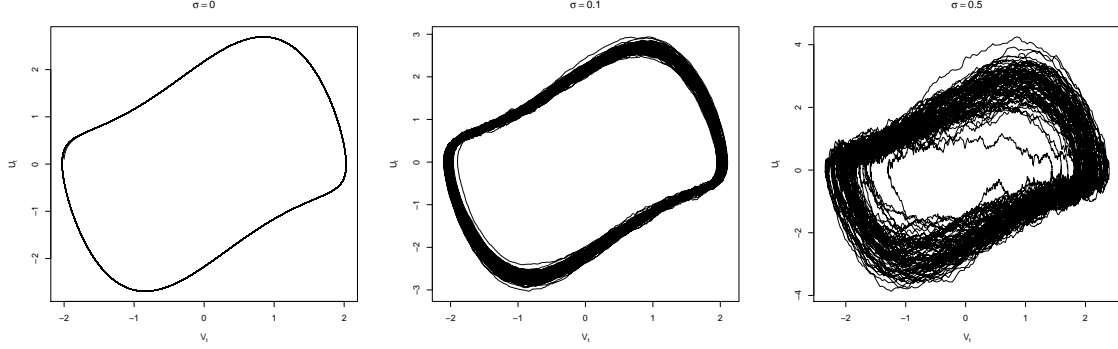
Figure 1.3: Phase portrait of a Van Der Pol oscillator (Example 2.1) under different random perturbation forces.

Example 1.7 (Stochastic Damping Hamiltonian system)**.** *Consider the process $X = (V, U)$, given as a solution of the following SDE:*

$$\begin{cases} dV_t = U_t dt \\ dU_t = \left(C(V_t, U_t)U_t + G'(V_t) \right) dt + \sigma(V_t, U_t) dW_t, \end{cases} \tag{1.4}$$

where $(V_0, U_0) \in \mathbb{R}^2$, the potential $G(V_t)$ is lower bounded and continuously differentiable over $\mathbb{R}$, the damping coefficient $C(V_t, U_t) \in \mathbb{R}^2 \to \mathbb{R}$ is continuous, the diffusion coefficient $\sigma \in \mathbb{R}^2 \to \mathbb{R}$ is positive and infinitely differentiable. System (1.4) is defined by the following vectors, which correspond to its drift and diffusion coefficients written in form (1.3):

$$A_1(V_t, U_t) = \begin{pmatrix} U_t \\ C(V_t, U_t)U_t + G'(V_t) - \frac{1}{2}\partial_u \sigma(V_t, U_t)\sigma(V_t, U_t) \end{pmatrix}, \quad A_2(V_t, U_t) = \begin{pmatrix} 0 \\ \sigma(V_t, U_t) \end{pmatrix}.$$

Their respective Lie bracket is computed as follows:

$$[A_1, A_2] = \begin{pmatrix} A_1^1 \partial_v A_2^1 - A_2^1 \partial_v A_1^1 + A_1^2 \partial_u A_2^1 - A_2^2 \partial_u A_1^1 \\ A_1^1 \partial_v A_2^2 - A_2^1 \partial_v A_1^2 + A_1^2 \partial_u A_2^2 - A_2^2 \partial_u A_1^2 \end{pmatrix} = \begin{pmatrix} -\sigma(V_t, U_t) \\ g(V_t, U_t) \end{pmatrix},$$

where $g(V_t, U_t) = U_t \partial_v \sigma + \left(CU_t + G' - \frac{1}{2}\partial_u \sigma \sigma \right) \partial_u \sigma - \sigma \partial_u \left(CU_t + G' - \frac{1}{2}\partial_u \sigma \sigma \right)$. Note that the vector fields A_2 and $[A_1, A_2]$ generate $\mathbb{R}^2$ when $\sigma \neq 0$. Thus, the system is hypoelliptic if $\sigma(v, u) \neq 0 \, \forall v, u \in \mathbb{R}^2$. In this case the covariance matrix of the process may be then written as follows:

$$\Sigma(V_t, U_t) = \sigma^2(V_t, U_t) \begin{pmatrix} \frac{t^3}{3} & \frac{t^2}{2} \\ \frac{t^2}{2} & t \end{pmatrix}.$$

The class of Stochastic Damping Hamiltonian systems includes, in particular, a stochastic version of the Van der Pol oscillator (Van der Pol, 1920) (with $C(V_t, U_t) = V_t^2 - 1$ and $G(V_t) = \frac{1}{2}V_t^2$), or Duffing oscillator (with $C(V_t, U_t) \equiv C > 0$ and $G(V_t)$ being a lower bounded polynomial). On Figure 1.3 we plot a phase portrait of the Van de Pol oscillator in order to illustrate the influence of the noise. As we can see, even though only one coordinate is perturbed by the Brownian motion, it propagates in both directions. Some important properties of Stochastic Damping Hamiltonian diffusions, such as existence of the invariant measure, Feller property and ergodicity are proven in Wu (2001).
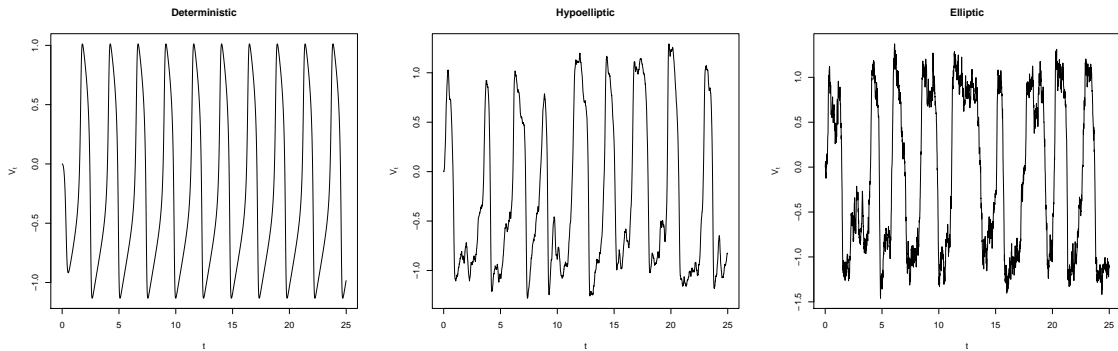
Figure 1.4: Membrane potential V_t of a neuron in a FitzHugh-Nagumo neuronal model in the deterministic, hypoelliptic and elliptic cases.

To give an example of a neuronal model, we consider a hypoelliptic FitzHugh-Nagumo model (a deterministic version of it is presented in Example 1.3 from the previous Section). It can be viewed as a simplification of a neuronal Hodgkin-Huxley model (see Example 1.1), which is widely used in neuronal modeling. Due to the fact that FitzHugh-Nagumo model is 2-dimensional and has a polynomial drift, it is much easier to analyze from a mathematical point of view.

Example 1.8 (Hypoelliptic FitzHugh-Nagumo model (Fitzhugh, 1961, Nagumo et al., 1962))**.** *The spiking activity of a neuron is described by the following equation:*

$$\begin{cases} dV_t = \frac{1}{\varepsilon}\left(V_t - V_t^3 - U_t - s\right)dt \\ dU_t = \left(\gamma V_t - U_t + \beta\right)dt + \sigma dW_t, \end{cases}$$

where V_t is the membrane potential, and U_t summarizes the input of ion channels. Note that this system does not satisfy Lipschitz assumptions. The solution, however, exists, has an invariant measure and is ergodic. These and other properties are proven in works Leon and Samson (2018), Uda (2019). An interesting observation is that the FitzHugh-Nagumo can be regarded as a particular case of a Stochastic Damping Hamiltonian System (see Leon and Samson (2018)).

The hypoellipticity of FitzHugh-Nagumo model can be proven by definition (1.1), as in the previous example. Note that the Itô (1.2) and Stratonovich (1.3) forms of SDE coincide, since the diffusion coefficient σ is constant. The system is hypoelliptic if the following vector fields generate $\mathbb{R}^2$:

$$A_2 = \begin{pmatrix} 0 \\ \sigma \end{pmatrix} \qquad [A_1, A_2] = \begin{pmatrix} -\frac{\sigma}{\varepsilon} \\ -\sigma \end{pmatrix}$$

As we see, this condition holds everywhere if $\sigma \neq 0$, thus the Hörmander criterion for the hypoellipticity holds. The covariance matrix of X can be written as follows (see Ditlevsen and Samson (2017), Melnykova (2020)):

$$\Sigma(V_t, U_t) = \sigma^2 \begin{pmatrix} \frac{1}{\varepsilon^2}\frac{t^3}{3} & \frac{1}{\varepsilon}\frac{t^2}{2} \\ \frac{1}{\varepsilon}\frac{t^2}{2} & t \end{pmatrix}.$$

Figure 1.4 illustrates the difference between the elliptic, hypoelliptic and deterministic approaches on example of FitzHugh-Nagumo model. The left panel depicts the oscillatory dynamics of a membrane

potential in a deterministic case, when its diffusion coefficient is equal to 0. The middle panel is a hypoelliptic case (as in Example 1.8), with $\sigma = 0.6$. We see that even though the variable V_t is not influenced by the Brownian motion directly, its trajectory is more chaotic than the one on the left. Finally, in the elliptic case (right panel), we add another source of independent Brownian motion with both diffusion coefficients being equal to 0.6. An interesting observation is that it is rather difficult to distinguish between the two last types of models by examining the trajectories. A more detailed study on the effects of noise in FitzHugh-Nagumo models is done in Lindner and Schimansky-Geier (1999), Lindner et al. (2004). In Chapter 6 of this thesis we study the parameter estimation in the hypoelliptic FitzHugh-Nagumo model.

Other examples of hypoelliptic models used in neuroscience would be the hypoelliptic Hodgkin-Huxley model (as studied in Höpfner et al. (2016b,a, 2017)), the Jensen-Rit neuronal mass model (Ableidinger et al., 2017), the cascade diffusion which approximates the integrated intensity of the interacting network of neurons (Ditlevsen and Löcherbach, 2017, Löcherbach, 2019, Duarte et al., 2019, Chevallier et al., 2020) and many others.

1.3   POINT PROCESSES

In this section we give a very brief overview of point processes or, more precisely, *Piece-Wise Deterministic Markov Process* (PDMP). Very roughly speaking, this family of processes is characterized by a sequence of jumps (or rather jump times), which happen with a certain intensity. The dynamics of the process between jumps is determined by a deterministic process, often ODE.

We start this introduction with the class of **Poisson processes**. They are widely used in mathematical modeling for biology, in particular in genetics, oncology and neuroscience (see Moran (1958), Rudnicki and Tyran-Kamińska (2017) and many others). A homogeneous Poisson point process can be viewed as a counting process $(N_t)_{t \geq 0}$, which counts the number of events, happened before time t. The Poisson process is a process possessing no memory. It means that a future event will happen with the same probability disregarding of how many events have already happened before. The increments of a Poisson process follow the Poisson distribution. This means, in particular, that the waiting times between the successive events are exponentially distributed and that the expected number of events on each fixed time interval of size t is equal to λt. The probability of having a given number of events up to time t is computed as follows:

$$\mathbb{P}\left(N_t = n\right) = \frac{(\lambda t)^n}{n!} e^{-\lambda t}.$$

An important class of Poisson processes is a **birth-and-death process** (see Feller (1939), Kendall et al. (1948)). In its simplest form it can be defined like follows:

Example 1.9. *Consider a population of biological cells (for example: cancerous cells, bacterial cells etc.). Denote by ν_t a point measure, which counts the number of cells in the environment at time t.*
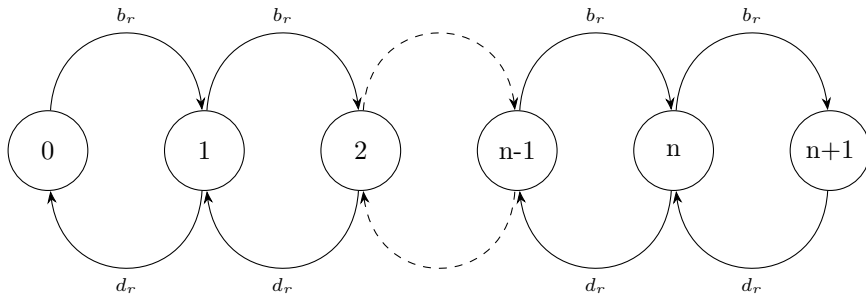
Figure 1.5: Transition between the states in birth and death process

During time interval Δ, each cell can either give birth to another cell with probability $b_r\Delta$, either die with probability $d_r\Delta$. Then, for Δ sufficiently small, the following holds:

$$\mathbb{P}\left(\nu_{t+\Delta} = j | \nu_t = i\right) = \begin{cases} ib_r\Delta, & \text{if } j = i+1, \\ id_r\Delta, & \text{if } j = i-1, \\ 1-(b_r+d_r)i\Delta & \text{if } j = i, \\ 0 & \text{otherwise.} \end{cases}$$

The transition between the states is summarized on Figure 1.5.

As its name presumes, birth-and-death processes are often used to model dynamics of biological systems: bacterias, cancer cells, but also larger organisms (animals, humans etc.). Of course, the model presented in Example 1.9 is too simple to be applied directly to any real-life phenomenon. Often, birth-and-death processes include other types of transition between the states: for example, the individuals can mutate, compete with the others for the resources (the amount of which is often limited), and the birth/death rate usually depends on the fitness of the individual and/or the current state of the system. We refer the reader to Baar et al. (2016), Costa et al. (2016), West et al. (2016) as examples. A birth-and-death process which models the evolution of a bacterial population is the subject of Chapter 5 of this thesis (see also the related paper Calvez, Vincent et al. (2020)).

Note that because of their memory-less nature, the Poisson processes are not capable of reflecting the dependency between the current state of the real-world process and its previous states. The need of introducing a "memory" has spawned another family of point processes: **Hawkes processes** (Hawkes, 1971, Hawkes and Oakes, 1974). They are called self-exciting, because the occurrence of one event triggers the occurrence of even more future events. In other words, while the "jumps" in a Poisson process appear with some deterministic rate (intensity), which does not depend on the state of the process, in a Hawkes process the intensity is determined by the previous states of the process. The intensity of the Hawkes process $(N_t)_{t \geq 0}$ is usually defined as follows:

$$\lambda_t = \mu_t + \int_0^t h(t-s)dN_s,$$

where μ_t is a deterministic function, which expresses the autonomous part of the intensity, and $h : \mathbb{R}^+ \to \mathbb{R}^+$ is a memory kernel, which encodes the influence of all the past events on the current state.

Being endowed with memory, Hawkes processes allow to model phenomena where one event can cause the occurrence of other stereotypical events. This approach was initially applied to the study of earthquakes (Ogata, 1988), but has found applications in various other fields. For example, it was observed that a confrontation between criminal gangs which happened at some point of time can cause a significant increase in criminal fights shortly afterwards (Mohler et al., 2011). Also the spread of a new coronavirus, paralyzing the world at the time of writing this manuscript, can be described as a self-exciting process (Juditsky et al., 2020).

The motivation for studying Hawkes processes in this manuscript mainly comes from neuroscience. Hawkes processes permit to model with a very high precision the dynamics of an interacting network of neurons. By "interacting" we mean that the occurrence of spikes in one part of the system can trigger the neurons in the "connected" part to spike as well. A particular case of Hawkes processes is studied in Chapter 4 of this thesis.

<div style="text-align: right">

2

</div>

OBJECTIVES, METHODS AND RELATED WORKS

The models described in Chapter 1 provide a set of tools which allow to analyze the intrinsic biological problems from a purely mathematical point of view. However, in order to use the full force of the models presented in the previous chapter and draw meaningful conclusions from the data gathered by scientists from the other fields, numerical and statistical expertise is required. Otherwise, how can we be sure that the mathematical abstractions are able to capture and describe the properties of the phenomena of interest?

In this Chapter we present the main challenges associated with mathematical models in biology and provide a brief overview of the existing literature. Section 2.1 is devoted to the **simulation methods**, which can be considered as a prerequisite to the Part ii of this thesis. There are two main reasons why the numerical simulation is important. First of all, the inference from the real-world biological data often means that the observations are not complete or not precise enough: that is, some of the variables are physically inobservable (ion concentration in neurons), or only one small part of the biological system is recorded (few hundred bacterias from a population of few millions). As a consequence, the application of any statistical method may require the simulation of the missing parts, or the data augmentation. Moreover, some inference procedures heavily rely on a simulated data (for instance, Bayesian simulation-based statistics).

Second, the efficiency of any statistical procedure must be measured first on a "good" data set, where the ground truth is available. This means, for example, that in order to estimate the firing rate of biological neurons, we must be able to estimate it from artificial spikes, simulated with a known intensity. Finally, the numerical analysis can be used as an empirical evidence in favor of one or another mathematical model. For example, in Chapter 4 we use the simulation methods in order to illustrate that the SDE-based model of the interacting populations of neurons shares the properties of the point process, describing the same phenomena. Furthermore, in Chapter 5 we use the numerical simulation in order to highlight the differences and similarities between individual-based and density-based approach when studying the bacteria population.

Section 2.2 is focused on **statistical inference**, i.e. estimation of the parameters of the system from discretely or continuously observed data. The focus is made on diffusion-type models. More precisely, in Chapter 6 of this thesis we treat the parameter estimation in diffusions of the hypoelliptic type (as Example 1.8). The real-world application of the parametric inference is, for example, the estimation of the concentration of potassium and sodium inside a cell during the firing activity of a

neuron, or its firing rate. In this thesis we work primarily with simplified models, whose parameters do not necessarily have an explicit biological meaning (see, for instance, FitzHugh-Nagumo model in Example 1.8). The reason is that complex models (as Hodgkin-Huxley in Example 1.1) are much more difficult to treat, especially in hypoelliptic case.

Further, in Section 2.2.2 we discuss some questions related to the **hypothesis testing** in stochastic diffusions. We are interested in the following question: how strong is the influence of the Brownian motion in the stochastic processes? In neuronal models of Hodgkin-Huxley type (Example 1.1), for example, this hypothesis corresponds to determining the number of stochastic imputs, which can come either from inside the cell, or from the environment. This question is often discussed in literature (see Goldwyn and Shea-Brown (2011) for details). The mathematical formulation of the problem is tightly related to the question of the random matrix rank estimation, with the principal object of study being the covariance matrix of the process. The principal statistical tool consists in testing a null hypothesis (covariance matrix of noise being of a certain rank) against the alternative (rank being smaller or bigger than the reference value). We present the main statistics of test, used by Jacod et al. (2008), Jacod and Podolskij (2013), explain the idea of the testing procedure and the limitations which are imposed by different settings.

Before we proceed, let us fix the following notations, which will be used throughout this Chapter:

- $(X_t)_{t \geq 0}$ denotes the continuous process, usually the solution of (1.2) (unless otherwise stated)

- $(X_{t_i})_{i \in \mathbb{N}_+}$ denotes the discrete sampling of the process defined above. Unless otherwise stated, the sampling is assumed to be equidistant, that is, $\forall i \in \mathbb{N}_+ : \quad t_{i+1} - t_i = \Delta$, where Δ is a strictly positive fixed time step.

- $(\tilde{X}_{t_i})_{i \in \mathbb{N}_+}$ denotes the numerical approximation of the process $(X_t)_{t \geq 0}$. Unless otherwise stated, the process is simulated on the equidistantly partitioned fixed time interval $[0 = t_0, \ldots, t_i, \ldots, t_n = T], T \geq 0$, that is, $\forall i \in \mathbb{N}_+ : \quad t_{i+1} - t_i = \Delta$, where Δ is a strictly positive fixed time step.

2.1   SIMULATION METHODS

The first question related to the study of dynamical systems (either of deterministic or stochastic type) is how to reproduce it numerically? Unfortunately, in a vast majority of cases the systems of equations described in the previous chapter, cannot be solved explicitly. In the case of point processes with a random intensity, the problem of numerical simulations is linked to the problem of evaluating this intensity. In this section we aim to provide an overview (by no means exhaustive) of the typical strategies used for the simulation of deterministic or stochastic processes. Note also that the content of this section is limited to a very few examples and methods which are used later in Chapters 4, 5 and 6 of this manuscript. For a more complete picture the readers are referred to the following classical books on simulation methods: Smith et al. (1985), Lapidus and Pinder (2011) for deterministic models, Kloeden et al. (2003) for stochastic differential equations and Moller and Waagepetersen (2003) for

point processes. This section presents the most common simulation techniques for the processes described in Chapter 1: deterministic processes, stochastic diffusions and, finally, point processes.

2.1.1 *Simulation of ODEs*

Consider an equidistant partition $[0 = t_0, \ldots, t_i, \ldots, t_n = T], T \geq 0$ with a time step Δ. The most classical first-order methods to approximate the solution of (1.2) are based on the following approximations, when Δ is small:

$$dX_{t_{i+1}} \approx \frac{X_{t_{i+1}} - X_{t_i}}{\Delta}, \tag{2.1}$$

$$\int_{t_i}^{t_{i+1}} b(s, X_s)ds \approx \Delta b(t_i, X_{t_i}). \tag{2.2}$$

By this rule the solution of (1.1) can be recursively approximated by a process $\tilde{X}$ as follows:

$$\tilde{X}_{t_{i+1}} = \tilde{X}_{t_i} + \Delta(t_i, \tilde{X}_{t_i}).$$

This method is called a first-order Euler scheme. There exist other schemes, which improve approximations (2.1)-(2.2), using the finite element and finite difference methods (Smith et al., 1985, Lapidus and Pinder, 2011). In Chapter 5 of this manuscript we show the limitations of the explicit Euler scheme when applied to a PDE of Hamilton-Jacobi type and propose an asymptotic-preserving simulation scheme in the spirit of Klar (1998, 1999).

Another popular approach consists in simulating an ODE as a convolution of its subparts which can be explicitly solved (Strang, 1968, Mclachlan and Quispel, 2002). This method is proven to be especially advantageous when applied to models with an oscillatory dynamics, such as Hodgkin-Huxley as in Example 1.1 (see Chen et al. (2020)). The idea of the splitting can be summarized as follows. Consider ODE (1.1). Let the function b do not depend on time t and assume that it can be written as follows:

$$b(x) = \sum_{j=1}^{m} b^{[j]}(x).$$

The goal is to find a combination of functions $b^{[j]}$, such that the resulting sub-equations

$$dx^{[j]} = b^{[j]}(x^{[j]}), \quad j \in \{1, ..., m\} \tag{2.3}$$

are explicitly solvable. The next step is to find a proper composition of the resulting solutions. Two standard procedures are the so-called Lie-Trotter splitting and the Strang splitting. Let $\varphi_t^{[j]}(x)$ denote the exact flows of the sub-equations in (2.3) at time t and starting from x. Then, the Lie-Trotter composition is given by

$$\left(\varphi_\Delta^{[1]} \circ ... \circ \varphi_\Delta^{[m]} \right)(x), \tag{2.4}$$

and the Strang composition is given by

$$\left(\varphi_{\Delta/2}^{[1]} \circ ... \circ \varphi_{\Delta/2}^{[d-1]} \circ \varphi_\Delta^{[m]} \circ \varphi_{\Delta/2}^{[m-1]} \circ ... \circ \varphi_{\Delta/2}^{[1]} \right)(x). \tag{2.5}$$

The discrete process obtained recursively by compositions (2.4)-(2.5) is proven to approximate the solution of ODE (1.1) (Mclachlan and Quispel, 2002, Blanes et al., 2009). Such splitting methods can be also extended to stochastic equations (Petersen, 1998, Shardlow, 2003). Differently from commonly used schemes, they allow to prove the preservation of the underlying model properties even when the time step is relatively big. We note that usually the splitting schemes perform better than the analogous approximations, since they usually exploit a structure of the system instead of breaking it down into piece-wise constant equations (like in the case of Euler scheme). The price to pay is that the splitting schemes are usually more difficult to develop. The first reason is that finding a good scheme requires some insight about the theoretical properties of the considered system, while the application of schemes of Euler type is straightforward for any system. Second, the choice of the subsystems is usually not unique and choosing the best splitting is not a trivial question. That is why this choice is often backed up solely by empirical evidence of the performance of the scheme, since the theoretical justifications are not always possible to obtain.

2.1.2 *Simulation of SDEs*

The simulation of SDEs does not significantly differ from that of ODEs. The only new step is the simulation of a stochastic integral, which is easily done by following the definition of an Itô integral and choosing some equidistant partition of the time interval $[0, T]$:

$$\int_0^T Y_t dW_t = \lim_{n \to \infty} \sum_{i=0}^n Y_{t_{i-1}}(W_{t_i} - W_{t_{i-1}}) \approx \sqrt{\Delta} \sum_{i=0}^n Y_{t_{i-1}} \xi_i,$$

where $\xi_i \sim \mathcal{N}(0, 1)$, i.i.d. To illustrate how it is used in practice, we provide the most classical simulation scheme, based on a modified Euler method for simulating ODEs (see the previous subsection). This scheme often serves as a benchmark for the new methods. Consider an equidistant partition $[0, t_1, \ldots, t_i, \ldots, T]$, where $T = i_{\max}\Delta$. The numerical solution of (1.2) is then given recursively by

$$\tilde{X}_{t_{i+1}} = \tilde{X}_{t_i} + \Delta b(\tilde{X}_{t_i}) + \sqrt{\Delta}\sigma(\tilde{X}_{t_i})\xi_{i+1},$$

where ξ_i, $i = 1, \ldots, n$ are i.i.d. standard normal d-dimensional vectors. Note that

$$\tilde{X}_{t_{i+1}}|\tilde{X}_{t_i} \sim \mathcal{N}\left(\Delta b(\tilde{X}_{t_i}), \Delta\Sigma(\tilde{X}_{t_i})\right),$$

where $\Sigma(\tilde{X}_{t_i}) = \sigma(\tilde{X}_{t_i})\sigma^T(\tilde{X}_{t_i})$. Even if the Euler-Maruyama scheme is popular and widely used due to its simplicity, it has a number of limitations when applied to certain models. To begin with, the fixed-step Euler-Maruyama method may fail to converge to the true solution when (1.2) does not satisfy Lipschitz conditions (see Hutzenthaler and Jentzen (2015), Beyn et al. (2016)). A non-Lipschitz drift is often encountered among the systems describing oscillatory dynamics (recall, for example, the FitzHugh-Nagumo model from Example 1.8).

The second problem is that even in the case when the underlying diffusion process X, defined as a solution of (1.2), is ergodic, its discrete approximation $\tilde{X}$, obtained with the Euler-Maruyama schemes, does not necessarily preserve this property (see Mattingly et al. (2002)). It means that even if the

scheme converges asymptotically, i.e. when $\Delta \to 0$, in practice the dynamics of the approximated process does not necessarily correspond to that of the true process when $\Delta \equiv const > 0$. Finally, in the hypoelliptic case the application of the Euler-Maruyama method leads to a (piece-wise) degenerate density of the approximated process. It does not always cause the convergence issues, but poses a problem if the approximation is coupled with a method of statistical inference. It is crucial, for example, if the classical maximum likelihood or Bayesian methods are applied, where an explicit expression for an (approximate) non-degenerate density is required.

Sometimes these issues can be overcome by using the approximations based on the Euler-Maruyama scheme with a varying time step (see, for example Lamba et al. (2007)), or an Itô-Taylor expansion of the generator of the solution of (1.2). An exhaustive reference for the schemes based on the Itô-Taylor expansion are the books Milstein (1994), Kloeden et al. (2003).

Another idea, which gained attention in recent years in application to neuronal models, is to use a splitting approach. Splitting methods for SDEs follow the same principle as a splitting for ODEs (see Section 2.1.1) and become popular in recent years, especially when applied to neuronal models (see Mattingly et al. (2002), Ableidinger et al. (2017), Tubikanec et al. (2020)). The limitations of the Euler-Maruyama scheme for non-linear models can be illustrated on the Van der Pol oscillator. It is a particular case of a Stochastic Damping Hamiltonian System (see Example 1.7). In the following example we propose a splitting scheme and compare its performance to the classical Euler-Maruyama method:

Example 2.1 (Stochastic Van der Pol oscillator)**.** *Consider the following two-dimensional equation:*

$$\begin{cases} dV_t = U_t dt \\ dU_t = (\mu(1 - V_t^2)U_t - V_t)dt + \sigma dW_t \end{cases} \tag{2.6}$$

with $V_0 = v_0, U_0 = u_0$. We can rewrite (2.6) as follows:

$$dX_t = b(X_t)dt + \sigma^* dW_t,$$

where $\sigma^* = (0, \sigma)^T$ and

$$b(X_t) = \begin{pmatrix} U_t \\ (\mu(1 - V_t^2)U_t - V_t) \end{pmatrix} = \begin{pmatrix} U_t \\ -V_t \end{pmatrix} + \begin{pmatrix} 0 \\ (\mu(1 - V_t^2)U_t) \end{pmatrix} =: b^{[1]}(X_t) + b^{[2]}(X_t).$$

Thus, system (2.6) can be splitted into two subsystems:

$$dX_t^{[1]} = b^{[1]}(X_t^{[1]}) + \sigma^* dW_t$$
$$dX_t^{[2]} = b^{[2]}(X_t^{[2]}).$$

Note that both equations can be solved explicitly. The first one is a linear homogeneous equation (see Example (1.5)), and one of the coordinates in the second equation is constant. The respective solutions at time t are thus given as follows:

$$\varphi_t^{[1]}(x_0) = e^{A^{[1]}t}x_0$$
$$\varphi_t^{[2]}(x_0) = A^{[2]}x_0 + \sigma^* \int_0^t dW_s,$$
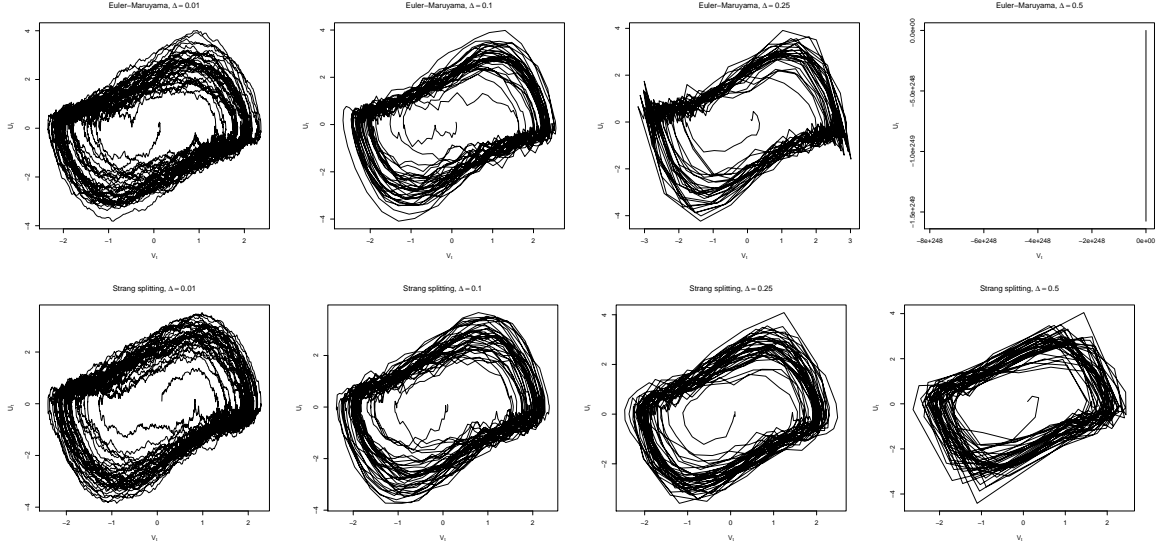
Figure 2.1: Comparison of the performance of the Euler-Maruyama and Strang splitting schemes, applied to the stochastic Van der Pol oscillator (Example 2.1). Parameters used for simulation: $\mu = 1, \sigma = 0.5$. Top row: phase portrait of the process, simulated with the Euler-Maruyama approximation, bottom row: phase portrait of the process, simulated with the Strang splitting. Step size $\Delta = 0.01, 0.1, 0.25, 0.5$ respectively, time interval is $[0, 250]$, initial values $(0.1, 0.1)$.

where $A^{[1]} = \begin{pmatrix} 0 & 1 \\ -1 & 0 \end{pmatrix}$ *and* $A^{[2]} = \begin{pmatrix} 1 & 0 \\ 0 & e^{\mu t(1-v_0^2)}s \end{pmatrix}$. *The solution of* (2.6) *can be obtained recursively using Lie-Trotter or Strang composition, that is:*

$$X_{t_{i+1}}^{LT} = (\varphi_\Delta^{[1]} \circ \varphi_\Delta^{[2]})\left(X_{t_i}^{LT}\right) = e^{A^{[1]}\Delta}\left(A^{[2]}X_{t_i}^{LT} + \sqrt{\Delta}\sigma^*\xi_{i+1}\right)$$

$$X_{t_{i+1}}^{S} = (\varphi_{\frac{\Delta}{2}}^{[1]} \circ \varphi_\Delta^{[2]} \circ \varphi_{\frac{\Delta}{2}}^{[1]})\left(X_{t_i}^{S}\right) = e^{A^{[1]}\frac{\Delta}{2}}\left(A^{[2]}e^{A^{[1]}\frac{\Delta}{2}}X_{t_i}^{S} + \sqrt{\Delta}\sigma^*\xi_{i+1}\right),$$

where $\xi_i \sim \mathcal{N}(0,1)$, *independently in* i.

Sample trajectories of the stochastic Van der Pol oscillator, simulated with the Strang splitting and Euler-Maruyama scheme, are given on Figure 2.1. We see that the phase portrait starts to look distorted for $\Delta = 0.25$, if the Euler-Maruyama scheme is used. For $\Delta = 0.5$ the simulated process blows up. It is not the case with the Strang splitting: even if the shape of the attractor is slightly distorted, the trajectory stays within its usual limits. Further practical and theoretical advantages of using splitting schemes over the standard simulation methods are discussed in Chapter 4 of this thesis, where we apply splitting to a high-dimensional hypoelliptic diffusion, describing the dynamics of interacting populations of neurons (see Ditlevsen and Löcherbach (2017)).

2.1.3   *Simulation of point processes*

A simulation of any point process boils down to computing the arrival times of events of interest. In the case of homogeneous Poisson process with a constant rate λ, the arrival times can be simulated straightforwardly, since they follow the exponential distribution. As an example, let us consider a

simple birth-and-death process (see Example 1.9), where each individual in a community can either proliferate or die with a rate b_r and d_r respectively. A waiting time till the next event is an exponential random variable with the rate $b_r N_t$ and $d_r N_t$ for birth and death respectively, where N_t is the number of individuals in a population at time t. Then, the dynamics of the population of cells on an interval $[0, T]$ is described by the Markov jump process $(N_t)_{t \in [0,T]}$, and it can be numerically simulated as summarized in Algorithm 1.

A simulation of more complicated birth-and-death processes follows essentially the same principle. The difference lays usually in additional dependencies: for example, competition terms, dependency on the state of the environment etc. In Chapter 5 we use a similar algorithm for a simulation of a bacterial population, structured by phenotypic traits.

Algorithm 1: Simulation of a birth-and-death process

Input: Birth and death rate b_r and d_r

Output: Point process $(N_{t_i})_{t_i \in [0,T]}$

Initialization: $t_0 = 0, N_0 = n_0$;

while $t_i \leq T$ **do**

    $\Delta_b \sim \mathcal{E}(b_r N_{t_i}); \Delta_d \sim \mathcal{E}(d_r N_{t_i})$;

    if $\Delta_b < \Delta_d$ **then**

        $t_{i+1} = t_i + \Delta_b$;

        $N_{t_{i+1}} = N_{t_i} + 1$;

    else

        $t_{i+1} = t_i + \Delta_d$;

        $N_{t_{i+1}} = N_{t_i} - 1$;

    $i = i + 1$

For the inhomogeneous Poisson process, the standard (but not unique) procedure is thinning. It is a sampling-rejection method. The main idea of the thinning is the following. The counting process $(N_t)_{t \geq 0}$ with a time-dependent rate λ_t cannot be simulated directly, since the rate depends on yet unknown moment of the future. However, it is usually possible to simulate a *dominating* process $(\tilde{N}_t)_{t \geq 0}$ with a dominating (constant) rate $\tilde{\lambda} \geq \lambda_t \quad \forall t$, and then determine the points which belong to $(\tilde{N}_t)_{t \geq 0}$, but not to $(N_t)_{t \geq 0}$. The procedure is schematically described in Algorithm 2. Given a "possible" inter-arrival time t^*, which follows law $\mathcal{E}(\tilde{\lambda})$, we check if this is also an arrival time of the process $(\tilde{N}_t)_{t \geq 0}$. For that, we draw a uniform random variable $U \sim \mathcal{U}([0, 1])$ and see if the condition $\frac{\lambda_{t^*}}{\tilde{\lambda}} < U$ holds. Points of time where this condition is satisfied are accepted. Graphically, the acceptance-rejection procedure is illustrated on Figure 2.2. From this plot one can deduce that the efficiency of the procedure would depend on the sharpness of the computed domination bound: the less points are rejected, the faster is the simulation.

Simulation of Hawkes processes via thinning shares the same principle, with the difference that the dominating intensity $\tilde{\lambda}$ is (in general) more difficult to compute. Note that on the contrary to the simulation of the diffusion or deterministic processes, the generation of the point processes is "perfect".
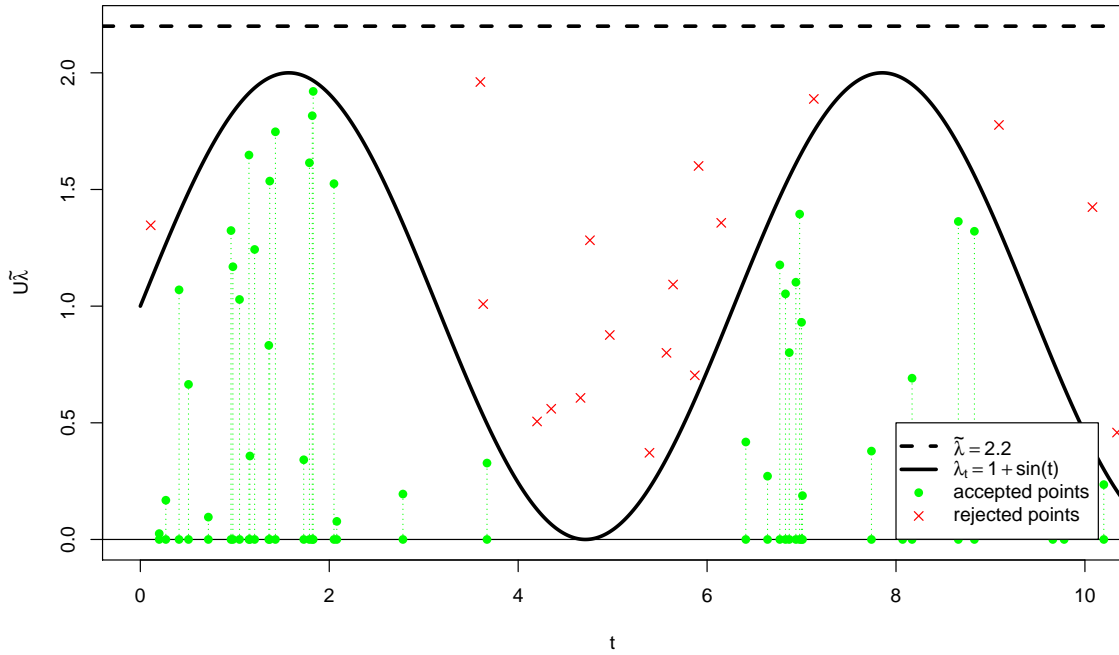
Figure 2.2: Illustration of the acceptance-rejection method: spiking times t_i are generated by law $\mathcal{E}(\tilde{\lambda})$ and accepted, if $U\tilde{\lambda} < \lambda_{t_i}$, where $U \sim \mathcal{U}([0,1])$. Plotted points are values of $U\tilde{\lambda}$ at times t_i.

By that we mean that there is no discretization error present, and the number of simulated events correspond, in average, to the expected number of events on a given interval. It also implies that it takes a longer time to simulate the high-intensity process than the process with a lower intensity on the same time interval. Note that in addition to the "true" intensity λ, the efficiency of simulation algorithm heavily depends on the sharpness of the "dominating" intensity $\tilde{\lambda}$. Thus, the most delicate part of developing a simulation algorithm for inhomogeneous Poisson or Hawkess process consists in proposing a sharp domination bound.

For example, it is common to compute the dominating intensity not on the whole time interval $[0, T]$, but on some limited time interval of a fixed time step. The interest of this approach can be intuitively explained with the help of Figure 2.2. Note that the proposed constant bound $\tilde{\lambda}$ is rather sharp when λ_t is close to its maximal value. But when λ_t approaches its minimum, the bound is not sharp at all and a lot of simulated points are rejected (as on time interval $[4, 6]$ on the plot). Choosing a piece-wise constant dominating intensity $\tilde{\lambda}$ computed on a partitioned time horizon, can give sharper bounds and thus increase the efficiency of the simulation procedure, especially when the intensity is given by a highly non-linear function.

For a further discussion of the utility of the local bounds the reader is referred to Chapter 4 of this manuscript, where an adapted thinning algorithm for the Hawkes processes with Erlang memory kernels is proposed.

Algorithm 2: Simulation of a inhomogeneous Poisson process

    Input: Time-changing rate λ_t, dominating intensity $\tilde{\lambda} \geq \lambda_t \quad \forall t \in [0, T]$

    Output: Spiking times $(t_i)_{i \in \mathbb{N}}$

    Initialization: $t_0 = 0$;

    while $t \leq T$ **do**

        $t^* \sim \mathcal{E}(\tilde{\lambda})$;

        $t = t + t^*$;

        $U \sim \mathcal{U}([0, 1])$;

        if $\frac{\lambda_t}{\tilde{\lambda}} < U$ *and* $t < T$ **then**

            $t_i = t$;

            $i = i + 1$;

2.2 STATISTICAL INFERENCE

In this Section we address a number of statistical challenges associated with biological data, focusing on a parametric inference and statistical tests for SDEs. To assess a more complete picture of existing problems and methods the interested reader is referred to some classical textbooks, like Rao (1973) for a basic overview of statistics for stochastic processes, Jacod and Protter (2011) for the discretization of processes, Rao (1999) for the inference of diffusion-type processes, Ibragimov and Khasminskii (2013), Kutoyants (2013) for statistical inference in ergodic diffusions, Rao (2014) for non-parametric inference, Ozaki (2012) for some discretization, inference and filtering problems for neuroscience models.

This Section is organized as follows: in Subsection 2.2.1, we present the state-of-the-art of the parametric inference for diffusion-type models, first elliptic and then hypoelliptic. We explain the challenges, associated with the parameter estimation for hypoelliptic models, which are addressed in Chapter 6. Then, in Subsection 2.2.2 we discuss the problem of determining the class of diffusions (elliptic or hypoelliptic) the discretely observed process belongs to. As we have previously mentioned in Section 1.2, the principal difference between two classes of models lies in the rank of the diffusion matrix. We first present the available methods of estimating the rank of the covariance matrix of the process, and then discuss the limitations, which motivate Chapter 7 of this thesis.

2.2.1 *Parametric inference in diffusion-type models*

There are several methods of parameter estimation. Chapter 6 of this manuscript is devoted to the estimation by means of a so-called contrast function, which is widely used in a frequentist approach. In this subsection we recall the most influential works devoted to the parametric estimation by the means of the contrast functions and explain the motivation behind the contribution of this thesis. We start with a simple illustration of a drift and diffusion term estimator in the case of an explicitly solvable system.

Example 2.2 (Parameter estimation for the linear SDE (Le-Breton and Musiela, 1985))**.** *Consider a particular case of a linear system as in Example 1.5:*

$$dX_t = A_t X_t dt + \sigma dW_t,$$

where A is a $d \times d$ stable constant matrix, and $\sigma \in \mathbb{R}^{d \times q}$ a constant matrix, and $W_t \in \mathbb{R}^q$ is a q-dimensional Brownian motion. Under these conditions (we refer to Le-Breton and Musiela (1985) for details), the process $(X_t)_{t \geq 0}$ satisfies (at least) the Hörmander condition and is thus hypoelliptic. In particular, it means that its covariance matrix is non-singular and is given by

$$\Sigma_t = \int_0^t e^{As} \sigma \sigma^T \left(e^{As} \right)^T ds.$$

Σ_t can be estimated as follows:

$$\widehat{\Sigma}_t = \frac{1}{t} \int_0^t X_s X_s^T ds.$$

Asymptotically, $\lim_{t \to \infty} \widehat{\Sigma}_t = \Sigma_\infty$ almost surely. The drift matrix A can be, in turn, estimated by the maximum likelihood estimator, defined as follows:

$$\widehat{A}_t = \left[\frac{1}{t} \int_0^t dX_s X_s^T \right] \left[\frac{1}{t} \int_0^t X_s X_s^T ds \right]^T.$$

This estimator is also strongly consistent in asymptotic sense, $\lim_{t \to \infty} \widehat{A}_t = A$ almost surely.

The above approach is not easy to apply to a general class of models. First, it assumes that the continuous data are available, which is not realistic in practice. Second, the consistent estimators presented in Example 2.2 are based on the fact that the transition density is explicitly known. Of course, it is not the case in the majority of settings.

In the case when the density of the process $(X_t)_{t \geq 0}$ is not known explicitly, pseudo-likelihood (also known as contrast estimators) comes to the rescue. The idea of **quasi-maximum likelihood based methods** is the following: first, the density of the process $(X_t)_{t \geq 0}$ is replaced by its discrete approximation with the help of an appropriate approximation scheme. Denote the transition density of X by $p(X_t; \theta)$, where θ is an unknown vector of parameters. Recall that the likelihood (or "pseudo-likelihood" if the approximated density is used) is written as:

$$L_n(\theta) = \prod_{i=1}^n p(X_{t_i}; \theta | X_{t_{i-1}}) p_\theta(X_0).$$

The parameters are typically estimated by minimizing a so-called "contrast function", which is defined as $\mathcal{L}((\theta; (X_{t_i})_{i \in 1,n})) := -\sum_{i=1}^n \log L_n(\theta)$. We show how the contrast function can be written when the density is approximated by the Euler-Maruyama scheme (see Section 2.1.2):

Example 2.3 (Contrast estimator based on the Euler-Maruyama scheme (Kessler, 1997))**.** *Consider a discrete approximation of the solution of (1.2), obtained with the Euler-Maruyama scheme. Assume that SDE (1.2) is elliptic. The pseudo log-likelihood of the discrete process $(X_{t_i})_{i \in 1,n}$ can be written*

as follows, where we stress the dependency of the drift and the variance coefficients on some vector of parameters θ:

$$\mathcal{L}\left(\theta;(X_{t_i})_{i\in 1,n}\right) = \sum_{i=1}^{n}\left(X_{t_{i+1}} - X_{t_i} - \Delta b(X_{t_i};\theta)\right)\Sigma^{-1}(X_{t_i};\theta)\left(X_{t_{i+1}} - X_{t_i} - \Delta b(\tilde{X}_{t_i};\theta)\right)^T +$$

$$\frac{1}{2}\sum_{i=1}^{n}\log\det\Sigma(X_{t_i};\theta)$$

where $\Sigma(X_{t_i};\theta) = \sigma(X_{t_i};\theta)\sigma^T(X_{t_i};\theta)$. The parameters of the equation (1.2) *can be then estimated as follows:*

$$\widehat{\theta} = \arg\min_{\theta}\mathcal{L}\left(\theta;(X_{t_i})_{i\in 1,n}\right)$$

Contrast-type estimators are very well studied and have been applied to a wide range of elliptic models. To name few, let us mention Genon-Catalot and Jacod (1993), Kessler (1997), Genon-Catalot et al. (1999), Gloter (2001), Aït-Sahalia (2002), Gloter (2006), Gloter and Sørensen (2009). The advantage of these methods is that they usually possess good theoretical properties, and are not costly to apply from a computational point of view.

Note however that when $rank(\Sigma) < d$, then the estimator from Example 2.3 is not applicable, since Σ is not invertible. Thus, the Euler-Maruyama approximation cannot be used for statistical inference based on the discretized maximum likelihood when the system (1.2) is hypoelliptic. Thus, the usual approach is to use higher-order schemes. They give a tractable discrete density, but are, in general, more difficult to analyze from a theoretical point of view.

In the hypoelliptic setting, there are numerous works devoted to the parametric inference based on the maximum likelihood-based methods for Stochastic Damping Hamiltonian Systems (Gloter, 2000, Pokern et al., 2007, Samson and Thieullen, 2012), and also to linear homogeneous SDEs (Le-Breton and Musiela, 1985, Ozaki, 1989, León et al., 2018). However, not all of the methods adapted for Hamiltonian or linear systems can be adapted for a wider class. For general systems the first reference to give is Ditlevsen and Samson (2017), where the maximum likelihood estimators are constructed on marginal densities of "rough" and "smooth" variables of the SDE (1.2). This method performs good in practice, but the work does not explore the properties of the estimator when the minimization is performed with respect to the parameters of all the variables with different variances at the same time, without fixing the parameters partially to their true value. Recently, Gloter and Yoshida (2020) proposed an adaptive estimator for hypoelliptic diffusions in higher dimension.

Chapter 6 of this manuscript contributes to the study of contrast estimators for the hypoelliptic systems, where we propose a single estimation criterion for a two-dimensional hypoelliptic SDE. The estimator based on this criteria is shown to be consistent and asymptotically normal. In practice this estimator performs similarly to Ditlevsen and Samson (2017), with the difference that the minimization is performed on a single estimation criteria, without using the marginal densities.

2.2.2 *Hypothesis testing in stochastic diffusions*

The inference methods described above are taking for granted that the type of the system (elliptic or hypoelliptic) is known. In most of the cases, however, there is no reason to assume that this information is available in advance. Thus, it is of utmost interest to derive the information about the dimensionality of noise in a given process, from its discrete observations. Ideally, one needs a statistical test which could assign a certain level of confidence to the claim that the given system is elliptic or hypoelliptic. There are very few works which are devoted to the covariance matrix rank estimators and matrix rank tests for the diffusions.

Given discrete observations of a d-dimensional process $(X_t)_{t\geq 0}$, defined as a solution of a d-dimensional SDE (1.2), the following matrices of increments are considered:

$$\Phi_i := \begin{pmatrix} \frac{X^{(1)}_{t_{id+1}}-X^{(1)}_{t_{id}}}{\sqrt{\Delta}} & \frac{X^{(1)}_{t_{id+2}}-X^{(1)}_{t_{id+1}}}{\sqrt{\Delta}} & \cdots & \frac{X^{(1)}_{t_{id+d}}-X^{(1)}_{t_{id+d-1}}}{\sqrt{\Delta}} \\ \frac{X^{(2)}_{t_{id+1}}-X^{(2)}_{t_{id}}}{\sqrt{\Delta}} & \frac{X^{(2)}_{t_{id+2}}-X^{(2)}_{t_{id+1}}}{\sqrt{\Delta}} & \cdots & \frac{X^{(2)}_{t_{id+d}}-X^{(2)}_{t_{id+d-1}}}{\sqrt{\Delta}} \\ \cdots & \cdots & \cdots & \cdots \\ \frac{X^{(d)}_{t_{id+1}}-X^{(d)}_{t_{id}}}{\sqrt{\Delta}} & \frac{X^{(d)}_{t_{id+2}}-X^{(d)}_{t_{id+1}}}{\sqrt{\Delta}} & \cdots & \frac{X^{(d)}_{t_{id+d}}-X^{(d)}_{t_{id+d-1}}}{\sqrt{\Delta}} \end{pmatrix}, \tag{2.7}$$

where $X^{(i)}$ denotes $i-$th variable of the process X. It may be not clear from the first glance why this representation (and not the empirical covariance matrix) is chosen for study. But in fact studying the matrix (2.7) has several statistical advantages. First, its entries are normally distributed and, under certain conditions on the process $(X_t)_{t\geq 0}$, are independent. Second, the order of the discriminant and the minors of matrix (2.7) corresponds to that of the sample covariance matrix. In particular, if the sample covariance matrix is not of full rank, then Φ_i^2 is also not of full rank. Finally, the law of matrices (2.7), as well as the law of their determinant, is relatively well studied (Girko, 1990, Nguyen and Vu, 2014).

Let us denote by r_0 the **Brownian dimension** of the process $(X_t)_{t\geq 0}$, which is a number of independent sources of a Brownian motion, influencing the process. r_0 also equals to the rank of the covariance matrix of this process. The ultimate objective is to propose the following statistical test:

$$\begin{aligned} H_0 &: r_0 = r \\ H_1 &: r_0 \neq r. \end{aligned} \tag{2.8}$$

The very first method of determining the rank of Φ_i^2 is proposed by Jacod et al. (2008). It can be roughly described as follows: it is known that if the matrix Φ_i defined in (2.7) is of rank $r_0 < d$, then all the minors (submatrices) of Φ_i^2 of dimension $d \times d, d-1 \times d-1, \ldots, r_0+1 \times r_0+1$ are zero. A natural idea is to check if the minors of a certain dimension r are smaller than a some given threshold δ (or a sequence of thresholds $\{\delta_i\}_{i\geq 0}$). If the minors are "too small", then the true dimension r_0 is smaller than r. Ultimately, r_0 is estimated as a first dimension trespassing a threshold.

Let us explain where this idea comes from. Note that the approximation of a solution of SDE (1.2) can be written, for example, with the Euler-Maruyama scheme (see Section 2.1.2). With the

approximated process it is easy to see that the diffusion part of the process is of order $\sqrt{\Delta}$, and the drift part is of order Δ. As a consequence, the matrix Φ_i can be expressed as a sum of its diffusion part $\sigma(\Phi_i) \in \mathbb{R}^{d \times d}$ (which is a random matrix with the Gaussian entries) and a non-random drift part $\sqrt{\Delta} b(\Phi_i) \in \mathbb{R}^{d \times d}$. Then, one can use the fact (see Jacod and Podolskij (2013)) that the determinant of Φ_i can be expressed as follows:

$$\det \Phi_i = \det \left(\sigma(\Phi_i) + \sqrt{\Delta} b(\Phi_i) \right) =$$

$$\det \sigma(\Phi_i) + \sqrt{\Delta} \gamma_{d-1}(\sigma(\Phi_i), b(\Phi_i)) + \cdots + \Delta^{(d-r)/2} \gamma_r(\sigma(\Phi_i), b(\Phi_i)) + \cdots + \Delta^{d/2} \det b(\Phi_i), \quad (2.9)$$

where

$$\gamma_r(\sigma(\Phi_i), b(\Phi_i)) = \sum_{G \in \mathcal{M}^r_{\sigma(\Phi_i), b(\Phi_i)}} \det(G).$$

Here $\mathcal{M}^r_{A,B}$ denotes the class of $d \times d$ matrices, created as a combination of r columns from A and $d - r$ columns of B (without shifts). Its formal definition reads as follows:

$$\mathcal{M}^r_{A,B} = \{G \in \mathcal{M} : G_i = A_i \text{ or } G_i = B_i, \#\{i : G_i = A_i\} = r\},$$

where A_i denotes the i-th columns of matrix A. In other words, the function $\gamma_r(A, B)$ is a sum of determinants of all possible combinations of matrices containing r columns from matrix A and $d - r$ of matrix B. An important message to take from this decomposition is that the order of $\det \Phi_i^2$ directly depends on the rank of $\sigma(\Phi_i)$: if the Brownian dimension of the process X is equal to r_0, then $\det \Phi_i^2 = O(\Delta^{d-r_0})$. Then, the testing procedure is based on "extracting" the value of r_0 from the test statistics, which is defined in Jacod et al. (2008) as

$$S = \frac{1}{n} \sum_{i=1}^{n} \det \Phi_i. \quad (2.10)$$

This statistics has the same order of magnitude with respect to Δ as the covariance matrix of the process X, thanks to the property of the determinant expansion (2.9). The main drawback of the method is that the sequence of thresholds must be chosen very carefully: the accuracy of the estimation depends on the chosen values.

A bit different approach, employing no thresholds, is proposed in Jacod and Podolskij (2013). They propose to estimate r_0 by constructing the statistics (2.10) with a different discretization step (for example, Δ and 2Δ) and taking the log-ratio of the obtained determinants. The log-ratio of statistics sampled with a different time step provides, at least asymptotically, the value of r_0. A central limit theorem proved in Jacod and Podolskij (2013) allows then to construct an asymptotic test (2.8).

Both methods (threshold-based and ratio-based) provide a good estimate of the matrix rank in an asymptotic regime (when the discretization step $\Delta \to 0$), i.e. when the observations are available in a continuous time. However, they are not very well adapted to the case when the observations are available at discrete times with a fixed time step Δ. Indeed, when the time step is fixed, the higher-order term in (2.9) does not necessarily correspond to the one giving the "true" value of the matrix rank. Thus, in the non-asymptotic setting, it is more correct to consider the hypothesis that certain diffusion coefficients are negligible at a given step size.

In Chapter 7 of this manuscript we explore the probabilistic properties of statistics (2.10) in non-asymptotic setting, assuming Δ fixed. In particular, we propose a test based on the exact distribution in the one- and two-dimensional cases with constant drift and diffusion, assuming the drift is known. We demonstrate under which conditions the Type I and Type II error can be controlled. Then, we consider a general case and study the distribution of statistics (2.10). In particular, we study the tail distribution of S with the help of concentration inequalities. We conclude with a discussion and open questions.

3

OUTLINE OF THE CONTRIBUTIONS

The contributions of this thesis are essentially divided in two parts. Part ii is devoted to the Numerical Analysis and contains Chapters 4 (Numerical analysis of the PDMP and their diffusion approximation) and 5 (Numerical analysis of the birth-and-death process and their PDE approximation). Both chapters presented in Part ii are thought to complement the results discussed in Section 2.1 and, on a more general level, to investigate the link between the jump processes and the diffusion-type models with the help of numerical experiments.

Part iii (Statistics) is devoted to some statistical problems, discussed in Section 2.2 of the previous chapter. It is focused exclusively on stochastic diffusions. More precisely, in Chapter 6 we treat the parameter estimation problem for SDEs (1.2) of hypoelliptic type, using a contrast function (see Section 2.2.1 for reference). In Chapter 7 we propose a statistical test which helps to determine if the observations of a multidimensional diffusion process come from an elliptic or hypoelliptic model. The key object of our study is the rank of the covariance matrice of the stochastic process (also called a Brownian dimension by some authors).

Note that this Chapter can be in parts redundant with the introduction of the respective chapters. Also note that the meaning of some numerical parameters designated by the same letter in different chapters may not coincide.

3.1 PART II: NUMERICAL ANALYSIS

3.1.1 *Numerical analysis of the PDMPs and their diffusion approximation*

This chapter is based on the article Chevallier et al. (2020), written in collaboration with Julien Chevallier (Université Grenoble Alpes, France) and Irene Tubikanec (JKU Linz, Austria). It is currently under review in "Journal of Applied Probability". Me and Irene Tubikanec have enjoyed the support of Mathematisches Forschungsinstitut Oberwolfach, where we have stayed in January 2020 within the scope of Research in Pairs program.

Chapter 4 is treating a specific type of hypoelliptic diffusions arising as an approximation of multivariate Hawkes processes with Erlang memory kernels. These processes model the interaction between several neuronal populations. The spiking activity of each population is described by the intensity functions and the associated Piece-wise Deterministic Markov Process (PDMP). More

precisely, we consider a network of K large populations of neurons, where the number of neurons in the k-th population is denoted by N_k and the total number of neurons in the network is $N = N_1 + \cdots + N_K$. Let $Z_t^{k,n}$ represent the number of spikes of the n-th neuron belonging to the k-th population during the time interval $[0, t]$. The sequence of counting processes $\{(Z_t^{k,n})_{t \geq 0}, 1 \leq k \leq K, 1 \leq n \leq N_k\}$ is characterized by the intensity processes $(\lambda^{k,n}(t))_{t \geq 0}$, which are formally defined through the relation

$$\mathbb{P}(Z_t^{k,n} \text{ has a jump in } (t, t+dt]|\mathcal{F}_t) = \lambda^{k,n}(t)dt,$$

where $\mathcal{F}_t$ contains the information about the processes $(Z_t^{k,n})_{t \geq 0}$ up to time t. The mean-field framework considered here corresponds to intensities $\lambda^{k,n}(t)$ given by

$$\lambda^{k,n}(t) = f_k\left(\sum_{l=1}^{K} \frac{1}{N_l} \sum_{1 \leq m \leq N_l} \int_0^t h_{kl}(t-s)dZ_s^{l,m}\right), \tag{3.1}$$

where $\{h_{kl} : \mathbb{R}_+ \to \mathbb{R}\}$ is a family of *synaptic weight functions* (also called memory kernels), which model the influence of population l on population k. The function $f_k : \mathbb{R} \to \mathbb{R}_+$ is the *spiking rate function* of population k. The expression "mean-field framework" refers to the fact that the intensity $\lambda^{k,n}(t)$ depends on the whole system only through the "mean-field" behaviour of each population, namely $\frac{1}{N_l} \sum_{1 \leq m \leq N_l} dZ_s^{l,m}$. Also, it implies that the proportion of neurons of different types is constant, so that $\frac{N_k}{N} =: p_k$. Here, we consider Erlang-type memory kernels and a cyclic feedback system of interactions, which was first considered in Ditlevsen and Löcherbach (2017). This means that for each k, population k is only influenced by population $k+1$, where we identify $K+1$ with 1. In this case, all the memory kernels are null except the ones given by

$$h_{kk+1}(t) = c_k e^{-\nu_k t} \frac{t^{\eta_k}}{\eta_k!}, \tag{3.2}$$

where $c_k = \pm 1$. This constant determines whether the population has an *inhibitory* ($c_k = -1$) or *excitatory* ($c_k = +1$) effect. The parameter $\eta_k \geq 1$ is an integer number, determining the memory order for the interaction function from population $k+1$ to population k.

We are interested in the processes $\{(\bar{X}_t^{k,1})_{t \geq 0}, 1 \leq k \leq K\}$, which are the arguments of the function f_k in Equation (3.1) and are defined by

$$\bar{X}_t^{k,1} = \frac{1}{N_{k+1}} \sum_{1 \leq m \leq N_{k+1}} \int_0^t h_{kk+1}(t-s)dZ_s^{k+1,m}. \tag{3.3}$$

When the memory kernels are given in form (3.2), the processes defined in (3.3) can be obtained as marginals of the process $(\bar{X}_t)_{t \geq 0} = \{(\bar{X}_t^{k,j})_{t \geq 0}, 1 \leq k \leq K, 1 \leq j \leq \eta_k + 1\}$ which solves the following system of dimension $\kappa = \sum_{k=1}^{K}(\eta_k + 1)$:

$$\begin{cases} d\bar{X}_t^{k,j} = \left[-\nu_k \bar{X}_t^{k,j} + \bar{X}_t^{k,j+1}\right] dt, \text{ for } j = 1, \ldots, \eta_k, \\ d\bar{X}_t^{k,\eta_k+1} = -\nu_k \bar{X}_t^{k,\eta_k+1} dt + c_k d\bar{Z}_t^{k+1}, \\ \bar{X}_0 = x_0 \in \mathbb{R}^\kappa, \end{cases} \tag{3.4}$$

where $\bar{Z}_t^{k+1} = \frac{1}{N_{k+1}} \sum_{n=1}^{N_{k+1}} Z_t^{k+1,n}$, each $Z_t^{k+1,n}$ jumping at rate $f(\bar{X}_{t-}^{k+1,1})$. This type of equation is called a Markovian cascade in the literature. The process $(\bar{X}_t)_{t \geq 0}$ summarizes and averages the

influence of the past events. This process, along with the firing rate functions f_k, determines the dynamics of $(Z_t^{k,n})_{t\geq 0}$, described by its intensity (3.1). In Ditlevsen and Löcherbach (2017) it is proven that (3.4) converges weakly to a stochastic diffusion of the following form:

$$\begin{cases} dX_t^{k,j} = \left(-\nu_k X_t^{k,j} + X_t^{k,j+1}\right) dt, \text{ for } j = 1, \dots, \eta_k, \\ dX_t^{k,\eta_k+1} = \left(-\nu_k \bar{X}_t^{k,\eta_k+1} + c_k f_{k+1}(X^{k+1,1})\right) dt + \frac{c_k}{\sqrt{p_{k+1}}} \sqrt{f_{k+1}(X^{k+1,1})} dW_t^{k+1}, \\ X_0 = x_0 \in \mathbb{R}^\kappa. \end{cases} \quad (3.5)$$

More precisely, the following bound holds:

Theorem 3.1 (Ditlevsen and Löcherbach (2017)). *Suppose that all spiking rate functions f_k belong to the space C_b^5 of bounded functions having bounded derivatives up to order 5. Then there exists a constant C depending only on $f_1, \dots, f_n$ and the bounds on its derivatives such that $\forall \varphi \in C_b^4(\mathbb{R}^\kappa; \mathbb{R})$,*

$$\left\| P_t^{\bar{X}} \varphi - P_t^X \varphi \right\|_\infty \leq Ct \frac{\|\varphi\|_{4,\infty}}{N^2},$$

where $P_t^{\bar{X}}$ and P_t^X are the Markovian semigroups, associated with the respective processes.

This result states that the diffusion (3.5) approximates the PDMP process (3.4) with a high precision when the number of neurons N is large, but this approximation becomes worse as time t increases. This means that it must be possible to rely on the numerical simulation of (3.5) (which is, in general, less costly to compute) to study the behaviour of (3.4). In order to do that, it is important to find a "good" simulation scheme, which would replicate the highly non-linear dynamics.

Chapter 4 aims to answer those questions. To answer the first one, we prove a strong error bound between the PDMP and the stochastic diffusion process. It complements the result of a weak error bound, obtained in Theorem 3.1. In particular, we show that in comparison to Theorem 3.1 PDMP (3.4) converges strongly to (3.5) at a slower rate with respect to N, and diverges faster with respect to t. Then, we prove that the diffusion (3.5) is ergodic and find its moment bounds. These results complement the ones presented in Ditlevsen and Löcherbach (2017), Löcherbach (2019). The ergodicity and the moment bounds are needed to verify the properties of the future approximation scheme.

On the next step, our interest is to illustrate the obtained theoretical properties with a numerical study. For this purpose, we need to simulate both the PDMP (3.4) and the stochastic diffusion (3.5). For the diffusion, we propose an approximation scheme, based on the numerical splitting. We show that our scheme outperforms the classical Euler-Maruyama scheme (see Section 2.1.1 for reference), even though they are proven to converge with the same mean square rate 1. More precisely, we demonstrate that the splitting scheme is more stable when the discretization time step Δ is large. It is due to the fact that the splitting preserves the most important properties of the diffusion: in particular, the first and the second moment bounds, as well as the ergodicity, obtained on the previous step.

Another interesting part of developing a splitting scheme for this cascade diffusion is that the dimension of the system depends on the parameters η_k. The numerical splitting scheme allows to simulate the process in any dimension. It is a prominent advantage over schemes based on high-order

Itô-Taylor expansion since in the latter case one would be forced to increase the order of the scheme when the dimension grows, otherwise the vital properties (as, for example, hypoellipticity), would not be preserved.

For the PDMP, we adapt a classical thinning algorithm (as in Algorithm 2) to the case of multiple neuronal populations. At the moment of writing this manuscript, there is no available analogous simulation technique for Hawkes processes with Erlang kernel and arbitrary intensity function. The only reference, which treats a particular case of linear intensity, is Duarte et al. (2019). The performance of our algorithm (which we measure by a computational speed) only slightly outperforms their method in the case of linear kernel. It is due to the fact that in the case of a linear kernel, the absolute dominating bound, as used in Duarte et al. (2019), is sharp. However, when tested on the exponential intensity function, we observe a 2 times decreased computational time in comparison to their method. It demonstrates the advantage of using a localized upper bound on the intensity function over the often used "naïve" uniform upper bound. Note, however, that due to the acceptance-rejection procedure, the simulation of the PDMP usually takes a much longer time than the simulation of the diffusion process even when a sharp bound is used.

The general aim of this work was to show that the stochastic diffusions can be used for studying the properties of the PDMP at a negligible computational cost. In particular, our numerical experiments show that the empirical densities of both processes coincide.

3.1.2 *Numerical analysis of the birth-and-death processes and their PDE approximation*

The works presented in Chapter 5 are based on the article Calvez, Vincent et al. (2020), written in a collaboration with Vincent Calvez, Susely Figueroa Iglesias, Hélène Hivert, Sylvie Méléard and Samuel Nordmann during the CEMRACS research session in July-August 2018, and published in SIAM: Proceedings and Surveys.

We start with considering a birth-and-death process (see Example 1.9), which models the bacteria population. This population is structured by so-called traits, which are in fact some numerical parameters encoding the genetic information. On the contrary to the classical birth-and-death model (as in Example 1.9), each cell can not only reproduce and die, but also transmit its genetic information to other individuals. This phenomenon is called horizontal gene transfer (HT) in literature. In this work we consider unilateral gene transfer, which means that after the exchange of genetic information the "recipient" cell becomes genetically identical to the "donor" (see Figure 3.1 for an illustration). Horizontal transfer of genes is believed to be the principal mechanism of developing the antibiotic resistance in bacteria. Further, each time the cell gives birth to another, there is a certain probability that the new cell will not inherit the trait of its "parent", but will develop a mutation. If it is the case, the new trait is picked up from a normal distribution, centered around the "old" trait. Finally, we assume the birth and death rate are depending on the trait of the individual. That means that certain groups are more "fit" than the others and thus have more chances to survive on a long time scale.
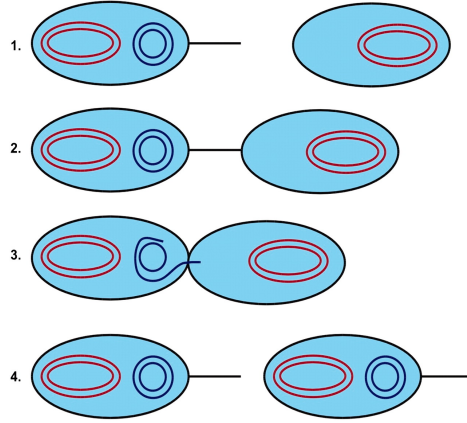
Figure 3.1: Unilateral horizontal gene transfer. Picture from Raz and Tannenbaum (2010).

Formally, we consider a stochastic model describing the evolution of a population structured by phenotype. In the general case it is described at each time t by the point measure

$$\nu_t^K(dx) = \frac{1}{K} \sum_{i=1}^{N_t^K} \delta_{X_i(t)}(dx),$$

where the parameter K is a scaling parameter, referred to as the *carrying capacity*. It stands for the maximal number of individuals that the underlying environment is able to host (K can represent, for example, the amount of available resources). $N_t^K = K \int \nu_t^K(dx)$ is the size of the population at time t, and $X_i(t) \in \mathbb{R}^n$ is the trait of the i-th individual living at t, which summarizes the phenotype information. In this work we assume $n = 1$, that is, the trait is given by a point on a real line.

The demography of the population is regulated, first of all, by its birth and death rates. An individual with a trait x gives birth to a new individual with rate $b(x)$. The trait y of the offspring is chosen from a probability distribution $m(x - y)dy$ (by that we mean that $\int_{\mathbb{R}} m(x - y)dy = 1$). We will refer to it as the *mutation kernel*. An individual with a trait x dies according to an intrinsic death rate $d(x)$ plus an additional death rate $C\frac{N_t^K}{K}$ (independent of x) which stands for the competition between individuals.

Finally, an individual with a trait x can induce a *unilateral* HT to an individual with trait y at rate $h_K(x, y, \nu)$, such that the pair (x, y) becomes (x, x). In the literature this kind of transfer is sometimes referred to as a *conjugation*. For simplicity, we assume $h_K(x, y, \nu)$ to be in the particular form

$$h_K(x, y, \nu) = h_K(x - y, N) = \tau_0 \frac{\alpha(x - y)}{N/K},$$

where $N = K \int_{\mathbb{R}} \nu(dx)$ is the number of individuals, $\tau_0 > 0$ is a constant and α is the Heaviside function.

For a population $\nu = \frac{1}{K}\sum_{i=1}^{N}\delta_{x_i}$ and a generic measurable bounded function F, the generator of the process is then given by:

$$L^K F(\nu) = \sum_{i=1}^{N} b(x_i)\int_{\mathbb{R}}\left(F\left(\nu + \frac{1}{K}\delta_y\right) - F(\nu)\right)m(x_i, dy)$$

$$+ \sum_{i=1}^{N}\left(d(x_i) + C\frac{N}{K}\right)\left(F\left(\nu - \frac{1}{K}\delta_{x_i}\right) - F(\nu)\right)$$

$$+ \sum_{i,j=1}^{N} h_K(x_i, x_j, \nu)\left(F\left(\nu + \frac{1}{K}\delta_{x_i} - \frac{1}{K}\delta_{x_j}\right) - F(\nu)\right).$$

It is standard to construct the measure-valued process ν^K as the solution of a stochastic differential equation driven by Poisson point measures and to derive moment and martingale properties (see for instance Fournier and Méléard (2004)).

In this work we are interested to see what happens in a large time scale, when the size of the population grows and the occurring mutations are *almost* negligible (but are instead observed on a very long period of time). We conduct a numerical study of the behaviour of the birth-and-death process which undergoes two limiting procedures: first, the individual-based jump process is replaced by a PDE (or, more precisely, by an integro-differential equation in partial derivatives), which models the density of the population, structured by traits. This PDE has first been considered in Billiard et al. (2016a, 2015). Second, we rescale the mutation kernel: if before the mutation of each new individual in the population was obeying a normal law, in the evolutionary time scale (i.e., when the mutations are infinitely small, but happen infinitely often) its density kernel transforms into a Dirac mass. The PDE then transforms (by applying a Hopf-Cole transformation) into a Hamilton-Jacobi PDE, which provides a convenient framework for studying the dynamics of the system.

To be more precise, it is proven (Billiard et al., 2016b) that for $K \to +\infty$ the stochastic process defined by the sequence of point measures given by (5.1) converges in probability to the unique solution of a non-linear integro-differential equation. This equation is given by:

$$\partial_t f(t, x) = -(d(x) + C\rho_1(t))f(t, x) + \int_{\mathbb{R}^n} m(x - y)b(y)f(t, y)dy +$$

$$f(t, x)\int_{\mathbb{R}^n}\tau(x - y)\frac{f(t, y)}{\rho_1(t)}dy, \text{ in } \mathbb{R}_+ \times \mathbb{R}^n, \quad (3.6)$$

where $\rho_1(t) = \int_{\mathbb{R}} f(t, x)dx$, $f(0, x) = f^0(x) > 0$ and $f(t, x)$ is the macroscopic density of the population with trait x at time t, $b(x)$, $d(x)$ and C are the birth, death and competition rate respectively, m is the mutation kernel, and

$$\tau(y - x) := \tau_0\left[\alpha(x - y) - \alpha(y - x)\right]$$

is the horizontal transfer flux. This result describes the dynamics of the system in the case of an infinite population. In our work we are interested in what happens in infinite time. In order to expand the horizon of events, we rescale the mutation kernel by introducing a scaling parameter ε. This rescaling is introduced as follows: $m(y - y') \longleftrightarrow \frac{1}{\varepsilon}m\left(\frac{y - y'}{\varepsilon}\right)$. Note that the parameter ε entering in the mutation kernel is responsible for reducing the variance of the mutation, and $\frac{1}{\varepsilon}$ used
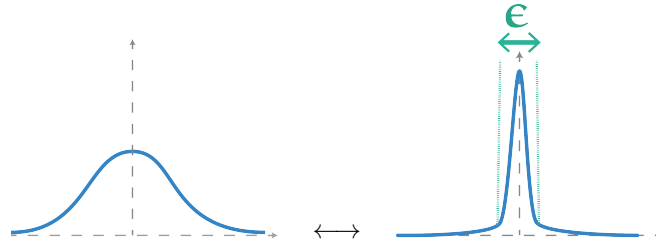
Figure 3.2: Shape of $\frac{f_e}{\rho_e}$ under the time rescaling

as a multiplicative factor which increases the time horizon. Informally speaking, we assume that on each infinitely small interval of time an infinitely small mutation is happening. The rescaled version of (3.6) is written as follows:

$$\partial_t u_\varepsilon = -(d(x) + C\rho_\varepsilon(t)) + \int_{\mathbb{R}^n} m(z)b(x + \varepsilon z) \exp\left\{\frac{u_\varepsilon(t, x + \varepsilon z) - u_\varepsilon(t, x)}{\varepsilon}\right\} dz +$$
$$\int_{\mathbb{R}^n} \tau(x - y)\frac{f(t, y)}{\rho_\varepsilon(t)} dy, \quad (3.7)$$

where $u_\varepsilon(t, x) := \varepsilon \ln(f(t, x)), \rho_\varepsilon = \int_{\mathbb{R}} f(t, x)dx$. When ε converges to 0, the density of a population ρ_1 in (3.6) coverges to a Dirac mass centered around a dominating trait, as graphically shown on Figure 3.2. The equation (3.6) itself converges in asymptotics to a Hamilton-Jacobi equation, given by

$$\partial_t u_\varepsilon = -(d(x) + C\rho_\varepsilon(t)) + b(x)\int_{\mathbb{R}^n} m(z)\exp^{z \cdot \nabla_x u} dz + \tau(x - \bar{x}(t)), \quad (3.8)$$

where $\rho(t) \geq 0$ is the weak limit of $\rho_\varepsilon(t)$ and $\bar{x}(t) = \arg\max u(t, \cdot)$. The resulting limit equation is new in the literature, and constitutes the first important contribution of the chapter. We note however that a description of a concentration phenomenon by the means of Hamilton-Jacobi PDE is often applied to other biological models which describe the evolution of a population. The reader is referred to the recent thesis Figueroa Iglesias (2019) for applied examples and a bibliographic overview.

What are we especially interested in is the phenomenon of the "evolutionary rescue", which appears when the majority of the population is killed because of unfavourable mutations and/or limited amount of resources in the hosting system, but the remaining few individuals manage to repopulate the environment. The question we were trying to answer is the following: will this phenomena be still observable after the two limiting procedures?

To answer this question, we conduct a numerical analysis. First, we simulate the birth-and-death process and try to determine (numerically) the parameters under which the extinction and the evolutionary rescue phenomena occur. Note that finding those parameters theoretically is a highly complicated subject in a stochastic setting. However, once we have passed to a Hamilton-Jacobi type equation (3.8), we can give an estimate of thresholds for the occurrence of extinction, or cycles of evolutionary rescue and extinction, or the convergence to a stable state around an optimal phenotypic trait. Such thresholds and their comparison to the behaviour of the individual-based system are the first result of this chapter. Thus, we are interested to see if the simulation of a stochastic individual-based system corresponds to the thresholds computed with the Hamilton-Jacobi approach.

Second, we are interested to see how the system behaves in a small mutation limit, that is, what happens when the equation (3.6) transforms into (3.8) as $\varepsilon \to 0$. To be able to track this transformation

numerically, the use of an asymptotic-preserving scheme is required. By an "asymptotic-preserving" we mean a scheme which does not blow up when $\varepsilon \to 0$ in (3.7). Also, it is important to preserve the accuracy when $\rho_\varepsilon \to 0$, that is, when the population is driven to the extinction. The development of this scheme is another important result of this chapter.

In the concluding part of the chapter, devoted to the numerical experiments, we illustrate that the threshold values for the death, birth and HT rate, computed from the Hamilton-Jacobi equation (3.8), coincide with the threshold values observed empirically for the individual-based system.

3.2 PART III: STATISTICAL INFERENCE

In this part we focus on the statistical inference for stochastic diffusions. In Chapter 6 we construct a contrast estimator for a 2-dimensional hypoelliptic ergodic diffusion and prove its asymptotic properties. Chapter 7 is devoted to the estimation of the covariance matrix rank in non-asymptotic setting.

3.2.1 *Parametric inference for hypoelliptic ergodic diffusions*

Chapter 6 is addressing problems of parametric inference in SDEs (1.2) of hypoelliptic type (see Definition 1.1). It is based on the article Melnykova (2020), which is published in *Statistical Inference for Stochastic Processes*.

We consider a two-dimensional SDE, where only one variable is driven by a Brownian motion, namely:

$$\begin{cases} dV_t = b_1(V_t, U_t; \theta_1)dt \\ dU_t = b_2(V_t, U_t; \theta_2)dt + \sigma(V_t, U_t; \sigma_0)dW_t, \end{cases} \tag{3.9}$$

where $\theta = (\theta_1, \theta_2, \sigma_0)$ is the vector of unknown parameters, W is a Brownian motion. This diffusion is hypoelliptic when $\partial_u b_1 \neq 0 \quad \forall v, u \in \mathbb{R}^2$. The interest of these diffusions is that they are often used for modeling neuronal activity (see, in particular, Section 1.2 of this thesis). Our aim is to provide a tool which allows to estimate the parameters of the model from discrete observation of the process. The difficulty of the hypoelliptic setting is that, first of all, standard approximation methods (like the Euler-Maruyama scheme, see Section 2.1.2 for reference) lead to a degenerate transition density, which does not permit to use classical maximum likelihood methods. Second, each variable has a variance of different order, which needs to be taken into account when constructing an estimation criteria.

The first problem is usually solved by using a method of density approximation which gives a non-degenerate diffusion matrix. It is always possible when the diffusion is hypoelliptic (see Section 1.2). There are numerous works which treat the parameter estimation problem in the case $b_1(V_t, U_t; \theta_1) \equiv U_t$, for example the contrast estimation of the diffusion coefficient in Gloter (2000), Pokern et al. (2007), where a Bayesian approach is applied for estimating both drift and diffusion parameters. However, the results in Pokern et al. (2007) are not very encouraging for the drift parameters. The papers Ozaki

(1989), León et al. (2018) use the idea of constructing a 2-dimensional contrast estimator with the help of a discretization scheme. The scheme is based on Local Linearization, meaning that the solution of (3.9) on small Δ-intervals is approximated recursively by a solution of a Linear Homogeneous equation (see Example (1.5)).

Another idea was proposed by Samson and Thieullen (2012), where a one-dimensional estimator is constructed based on a marginal density of the second variable, approximated with the Euler-Maruyama scheme. Finally, in Ditlevsen and Samson (2017) the general case (3.9) is treated, where they propose two separate estimators for the rough and the smooth variables.

Our aim is to adapt the idea of using the linearization scheme to the general SDE case and propose a two-dimensional criteria for the parameter estimation. Thus, the contribution of Chapter 6 can be logically splitted in two steps. First, we provide an approximation scheme in order to get a tractable discrete density, using an adapted version of a Local Linearization scheme (see in particular Ozaki (1989), Biscay et al. (1996), Jimenez and Carbonell (2015)). In other words, we assume the solution of (1.2) to be piece-wise linear.

Thanks to this approach we can obtain an invertible covariance matrix, given as follows:

$$\Sigma_\Delta(\tilde{V}_{t_{i+1}}, \tilde{U}_{t_{i+1}}; \theta) := \sigma^2(\tilde{V}_{t_i}, \tilde{U}_{t_i}) \begin{pmatrix} (\partial_y a_1)^2 \frac{\Delta^3}{3} & \partial_y a_1 \frac{\Delta^2}{2} \\ \partial_y a_1 \frac{\Delta^2}{2} & \Delta \end{pmatrix}, \tag{3.10}$$

where all derivatives are computed at time $i\Delta$. Note that here and in the following we drop the dependency on the parameters for readability. The component-wise approximation for (3.9) is given recursively by the following formulas:

$$\tilde{V}_{t_{i+1}} = \tilde{V}_{t_i} + \bar{B}_1(\tilde{V}_{t_i}, \tilde{U}_{t_i}; \theta) + \xi_{1,i+1}$$
$$\tilde{U}_{t_{i+1}} = \tilde{U}_{t_i} + \bar{B}_2(\tilde{V}_{t_i}, \tilde{U}_{t_i}; \theta) + \xi_{2,i+1}$$

where $(\xi_{1,i})$ and $(\xi_{2,i})$ are normal random sequences with zero means, independent in i, such that the covariance matrix of vector $(\xi_{1,i}, \xi_{2,i})$ is given by (3.10), and $\bar{B}_1, \bar{B}_2$ are given as follows:

$$\bar{B}_1(\tilde{V}_{t_i}, \tilde{U}_{t_i}; \theta) := \tilde{V}_{t_i} + \Delta b_1(\tilde{V}_{t_i}, \tilde{U}_{t_i}) +$$
$$\frac{\Delta^2}{2} \left(\frac{\partial b_1(\tilde{V}_{t_i}, \tilde{U}_{t_i})}{\partial v} b_1(\tilde{V}_{t_i}, \tilde{U}_{t_i}) + \frac{\partial b_1(\tilde{V}_{t_i}, \tilde{U}_{t_i})}{\partial u} b_2(\tilde{V}_{t_i}, \tilde{U}_{t_i}) \right) +$$
$$\frac{\Delta^2}{4} \sigma^2(\tilde{V}_{t_i}, \tilde{U}_{t_i}) \partial^2_{uu} b_1(\tilde{V}_{t_i}, \tilde{U}_{t_i})$$
$$\bar{B}_2(\tilde{V}_{t_i}, \tilde{U}_{t_i}; \theta) := \tilde{U}_{t_i} + \Delta b_2(\tilde{V}_{t_i}, \tilde{U}_{t_i}) +$$
$$\frac{\Delta^2}{2} \left(\frac{\partial b_2(\tilde{V}_{t_i}, \tilde{U}_{t_i})}{\partial v} b_1(\tilde{V}_{t_i}, \tilde{U}_{t_i}) + \frac{\partial b_2(\tilde{V}_{t_i}, \tilde{U}_{t_i})}{\partial u} b_2(\tilde{V}_{t_i}, \tilde{U}_{t_i}) \right) +$$
$$\frac{\Delta^2}{4} \sigma^2(\tilde{V}_{t_i}, \tilde{U}_{t_i}) \partial^2_{uu} b_2(\tilde{V}_{t_i}, \tilde{U}_{t_i}).$$

As a result, on small intervals of time the transition density of the original process can be replaced by the transition density of a solution of a linear SDE which is non-degenerate Gaussian.

On the second step, we closely follow the classical maximum-likelihood based approach, constructing a contrast estimator for estimating the parameters of the drift and diffusion coefficients. First, we write the pseudo-likelihood of the 2-dimensional process $X = (V, U)$:

$$\mathcal{L}_{n,\Delta_n}(\theta; X_{t_{0:n}}) = \frac{1}{2} \sum_{i=0}^{n-1} (X_{t_{i+1}} - \bar{B}(X_{t_i}; \theta))^T \Sigma_\Delta^{-1}(X_{t_i}; \theta)(X_{t_{i+1}} - \bar{B}(X_{t_i}; \theta))$$

$$+ \sum_{i=0}^{n-1} \log \det(\Sigma_\Delta(X_{t_i}; \theta)),$$

where $\bar{B} = (\bar{B}_1, \bar{B}_2)$, the inverse matrix Σ_Δ^{-1} is computed as the inverse of (3.10). Then the Local Linearization (LL) estimator is defined as:

$$(\hat{\theta}_{n,\Delta}, \hat{\sigma}_{n,\Delta}^2) = \underset{\theta,\sigma^2}{\arg\min} \, \mathcal{L}_{n,\Delta}(\theta, \sigma^2; Z_{0:n}), \tag{3.11}$$

where $\hat{\theta}_{n,\Delta} = (\hat{\theta}_1)_{n,\Delta}, (\hat{\theta}_2)_{n,\Delta}$. We prove that the proposed estimator is consistent and asymptotically normal as $T\Delta \to \infty, T\Delta^2 \to 0$ while $\Delta \to 0$. More precisely, $(\hat{\theta}_1)_{n,\Delta}$ converges to θ_1^0 with the speed $\sqrt{\frac{\Delta}{n}}$, $(\hat{\theta}_2)_{n,\Delta}$ converges to θ_2^0 at rate $\sqrt{\frac{1}{n\Delta}}$, and the diffusion coefficient $\hat{\sigma}^2 \to (\sigma^0)^2$ at rate $\sqrt{\frac{1}{n}}$. In addition to the contrast esimator, defined by (3.11), we consider also the Conditional Least Squares Estimator (CLSE) for estimating the parameters of the drift as follows:

$$(\widehat{\theta_1})_{n,\Delta}^{LSE} = \underset{\theta_1}{\arg\min} \sum_{i=0}^{n-1} \frac{(V_{t_{i+1}} - \bar{B}_1(X_{t_i}; \theta))}{\Delta^3}$$

$$(\widehat{\theta_2})_{n,\Delta}^{LSE} = \underset{\theta_2}{\arg\min} \sum_{i=0}^{n-1} \frac{(U_{t_{i+1}} - \bar{B}_2(X_{t_i}; \theta))}{\Delta}$$

In the numerical study, we test all the estimators on the hypoelliptic FitzHugh-Nagumo model (see Example 1.8).

3.2.2 *Non-asymptotic test and concentration inequalities for the covariance matrix rank estimator*

In Chapter 7 we explore non-asymptotic statistical properties of the discriminant of a random matrix. Our aim is to construct a non-asymptotic statistical test of a matrix rank from discrete observations of a d-dimensional stochastic diffusion, following Jacod et al. (2008), Jacod and Podolskij (2013) (see Section 2.2.2 of the previous Chapter). The content of this chapter is based on the ongoing work in collaboration with Adeline Samson and Patricia Reynaud-Bouret.

Here by a "non-asymptotic" setting we mean two features. First, we assume that the discrete observations of the process are available with a fixed time step Δ. Our aim is to propose a meaningful test procedure when Δ does not tend to 0. The second point, we assume the process — and, respectively, its covariance matrix — being of a fixed dimension d. The main setback is that non-asymptotic results in a random matrix theory are surprisingly scarce. The law of the determinant of a random matrix and its logarithm are well studied when the dimension of the matrix is relatively large (see, for example, Nguyen and Vu (2014)), or when the entries of the matrix follow some specific law or a centered around zero (see Nyquist et al. (1954), Girko (1990)). However, it is not the case in our

setting: typically, the dimension of a neuronal model is between 2 and 6 variables, so the asymptotic theory cannot be applied, and the entries of the matrix in consideration are not necessarily centered and not necessarily identically distributed.

Even to state a test hypothesis is a more challenging task: as discussed in Section 2.2.2, the order of magnitude of the test statistics in non-asymptotic case does not necessarily give the information about the covariance matrix rank. But in order to be able to construct the test, we need to study the behaviour of the test statistics in a non-asymptotic setting. We do it in several steps: first, we reduce the problem to the evaluation of the norms of the corresponding vector-columns. It allows us to use a powerful theory of quadratic forms of random variables (see a book Mathai and Provost (1992)). Using this trick, we obtain upper and lower concentration bounds on the test statistics. This approach gives the concentration bounds, which can be used for constructing a test.

To be more precise, the random matrices of interest are constructed as follows. We denote by $mat(a^1, a^2, \ldots, a^d)$ a matrix which is defined by its vector-columns $a^1, a^2, \ldots, a^d$. The, we consider a sequence of $d \times d$-dimensional matrices $(\Xi_i)_{i \geq 1}$, where each entry is given by

$$\Xi_i = mat(\xi_i^1, \xi_i^2, \ldots, \xi_i^d), \tag{3.12}$$

and ξ_i^j are given by the increments of the process X, defined in (7.1) as follows:

$$\xi_i^j := \frac{X_{(di+j)\Delta} - X_{(di+j-1)\Delta}}{\sqrt{\Delta}} \quad \forall j, i.$$

In other words, to construct the first matrix Ξ_1 we take first d increments of the process and write them column-wise (thus, obtaining a aquare $d \times d$ matrix), for the next matrix we start with the $d + 1$-th increment and so on. Note that matrix (3.12) is analogous to a random matrix defined in (2.7). Then, the principal statistics (first introduced in Jacod et al. (2008), Jacod and Podolskij (2013)) is written as follows:

$$S = \frac{1}{n} \sum_{i=1}^n \det\left(\Xi_i^2\right). \tag{3.13}$$

The statistical properties of (3.13) are linked to the properties of the determinants of matrices (3.12). A lot of results about the distribution and statistical properties of the random matrix determinants exists when the entries follow some specific probabilistic law. For example, they are Rademacher or standard normal variables . In particular, it is known that when the entries of the matrix are standard normal and independently distributed, then the determinant can be seen as a product of independent chi-squared variables. But any relaxation of those assumptions (non-unit variance, dependency between the variables or the non-zero expectation) is much harder to analyze.

In Chapter 7 the tail distribution of S is evaluated with the help of concentration inequalities, for the case when the entries of Ξ_i are independent in j. More precisely, we obtain the following upper and lower bound. In particular, the following inequality holds:

$$\mathbb{P}\left(S - \mathbb{E}[S] \leq -\varepsilon\right) \leq \exp\left(\frac{-\varepsilon^2 n^2}{4 \sum_{i=1}^n \mathbb{E}[\det \Xi_i^4]}\right).$$

In other words, the lower tail of S is sub-Gaussian. For the upper tail, the expression is more complicated, since the statistics are not bounded from above. The following bound holds:

$$\mathbb{P}\left(S - \mathbb{E}[S] \geq \varepsilon\right) \leq \exp\left(-\frac{2\varepsilon^2 n^2}{\sum_{i=1}^{n}\prod_{j=1}^{d}\left(\mathbf{tr}\left(\Sigma_i^j\right) + \|\mu_i^j\|^2 + c_i^j\right)}\right) + dne^{-c}, \qquad (3.14)$$

where c_i^j and c are constants, which will be further specified in Chapter 7, μ_i^j and Σ_i^j being the expectation and the covariance matrix of vector column ξ_i^j respectively. These bounds is a preliminary step toward constructing a non-asymptotic test. Before doing so, we need an accurate estimate or an explicit expression for the first and the second moments of S. They are difficult to obtain in the case of non-centered entries. Also, Hadamard inequality which is used to obtain (3.14), is not sharp in general and a lot of information about the distribution of S is lost. Thus, in order to build an accurate test, the bound (3.14) needs to be improved.

In order to better understand the behaviour of the statistics, in Chapter 7 we also consider two special cases, when the law of S can be written explicitly. More precisely, we study the case of one- and two-dimensional systems with constant drift and diffusion coefficients. It allows us to write the explicit probabilistic law of the test statistics (2.10) (first introduced in Jacod et al. (2008), Jacod and Podolskij (2013)), and write the test based on the explicitly known distribution. We give the conditions when the Type I and Type II error can be controlled.

For a 2-dimensional system we consider the following toy model. It is a two-dimensional process defined by the solution of:

$$dX_t = bdt + \sigma dW_t,$$

where $b = (b_1, b_2)^T$ is a drift vector and σ is a diagonal diffusion matrix with constant coefficients σ_1 and σ_2 on the main diagonal, W is a 2-dimensional Brownian motion. The goal is to construct the test of the following hypothesis:

$$H_0 : \sigma_1^2\sigma_2^2 = \delta$$
$$H_1 : \sigma_1^2\sigma_2^2 \geq \delta,$$

where δ is some chosen "sensitivity" threshold. H_0 and H_1 correspond roughly to the case of the covariance matrix being of a full rank or not, as δ can be arbitrarily close to 0. Then, if we modify the statistics defined in (3.13) by centering each column around its expectation $\sqrt{\Delta}b$, the following bound holds under H_0:

$$\mathbb{P}_0\left(\dot{S} \geq q_\alpha\right) \leq \alpha,$$

where q_α is a quantile defined as follows:

$$q_\alpha = \delta\left(1 + W\left(-\frac{\alpha^{1/n}}{e}\right)\right)^2,$$

and W is the Lambert W-function (see Appendix of Chapter 7 for its definition and basic properties). It gives a control over the Type I error of the test (fixed to α). The Type II error is bounded by β under the following conditions:

$$\sigma_1^2 \sigma_2^2 \geq \delta \left(\frac{1 + W\left(-\frac{\alpha^{1/n}}{e}\right)}{1 + W\left(-\frac{(1-\beta)^{1/n}}{e}\right)} \right)^2.$$

Part II

NUMERICAL ANALYSIS

THEORETICAL ANALYSIS AND SIMULATION METHODS FOR HAWKES PROCESSES AND THEIR DIFFUSION APPROXIMATION

This chapter is based on the article Chevallier et al. (2020), which is written in collaboration with Julien Chevallier (Université Grenoble Alpes) and Irene Tubikanec (JKU Linz, Austria).

Abstract. Oscillatory systems of interacting Hawkes processes with Erlang memory kernels were introduced in Ditlevsen and Löcherbach (2017). They are piecewise deterministic Markov processes (PDMP) and can be approximated by a stochastic diffusion in the large population limit. First, a strong error bound between the PDMP and the diffusion is proved. Second, moment bounds for the resulting diffusion are derived. Third, approximation schemes for the diffusion, based on the numerical splitting approach, are proposed. These schemes are proved to converge with mean-square order 1 and to preserve the properties of the diffusion, in particular the hypoellipticity, the ergodicity and the moment bounds. Finally, the PDMP and the diffusion are compared through numerical experiments, where the PDMP is simulated with an adapted thinning procedure.

Résumé: Les systèmes oscillatoires des processus Hawkes en interaction avec les noyaux de mémoire Erlang ont été introduits dans Ditlevsen and Löcherbach (2017). Ce sont des processus de Markov déterministes par morceaux (PMDM) qui peuvent être approximés par une diffusion stochastique dans une limite de grande population. Tout d'abord, un contrôle de l'erreur forte liée entre le PMDM et la diffusion est prouvée. Deuxièmement, des bornes de moment pour la diffusion résultante sont dérivées. Troisièmement, des schémas d'approximation pour la diffusion, basés sur l'approche de splitting numérique, sont proposés. Il est prouvé que ces schémas convergent avec un de moyenne quadratique 1 et préservent les propriétés de la diffusion, en particulier l'hypoellipticité, l'ergodicité et les bornes de moment. Enfin, le PMDM et la diffusion sont comparés à travers d'expériences numériques, où le PMDM est simulé avec une procédure d'amincissement adaptée.

Keywords: Piecewise deterministic Markov processes, Hawkes processes, stochastic differential equations, diffusion processes, neuronal models, numerical splitting schemes

4.1 INTRODUCTION

Fast and accurate simulation of a biological neuronal network is one of the most extensively studied problems in computational neuroscience. The general goal is to understand how information is processed and transmitted in the brain. One of the widely used approaches is to assume that the

spike occurrences in a network are described by a point process. Poisson processes, as "memory less" Markovian processes, can neither take into account a refractory period between two consecutive spikes nor the interaction between neurons, and are thus no proper candidates. Therefore, it is common to model the neuronal activity with Hawkes processes, which are self-exciting point processes with a memory (Chevallier et al., 2015, Chornoboy et al., 1988, Johnson, 1996, Pernice et al., 2011, Reynaud-Bouret et al., 2014). The price to pay for using Hawkes processes to model spiking activity is that their investigation is more difficult, since the Markovian theory cannot be directly applied.

However, for a certain type of memory kernels, so-called Erlang kernels, the dynamics of the point process can be described by a piece-wise deterministic Markov process (PDMP), whose dimension is determined by the "memory length" of the underlying Hawkes process (Ditlevsen and Löcherbach, 2017). This PDMP, also called "Markovian cascade of successive memory terms" in the literature, is a convenient framework to study the long-time behaviour of the particle system. In particular, it is proved that it is positive Harris recurrent and converges to its unique invariant measure exponentially fast in Wasserstein distance (Duarte et al., 2019, Theorems 1 and 2).

This Markovian cascade and its associated point process can be simulated thanks to the thinning procedure (Ogata, 1981), which is a common way to simulate general point processes even without any Markovian assumption. The only requirement in order to apply this method is to provide an upper-bound for the spiking rate of the neurons, which is highly related to the model under consideration (Dassios et al., 2013, Duarte et al., 2019). This procedure yields an exact simulation algorithm but is costly to compute, especially when the number of neurons is large. This results from the fact that the computation time scales linearly with the number of neurons.

In the brain, neurons are clustered in populations with similar behaviours (excitatory, inhibitory, etc). When the network size grows, but the proportion of neurons in each population remains constant, the Markovian cascade can be approximated by a stochastic differential equation (SDE) of the same dimension. In other words, the diffusion approximation theory allows to replace the stochastic term, described by jumps in the PDMP, by a multi-dimensional Brownian motion. Passing from a Hawkes process to a diffusion process substantially simplifies the analysis of the system behaviour. In particular, the simulation of the diffusion process is much less computationally expensive than that of the Markovian cascade, especially when the number of neurons is large. This results from the fact that the computational time for the SDE does not depend on the number of neurons. However, the SDE cannot be solved explicitly, and thus the construction of a reliable approximation scheme is required.

Note that the main difficulty does not lie in the construction of convergent numerical schemes. For example, standard methods such as the Euler-Maruyama or Milstein schemes converge in the mean-square sense when the time discretization step tends to zero. In practice, however, the solution is approximated with a strictly positive time step. As a consequence, even if the discrete solution is known to converge to the continuous process as the time step tends to zero, it does not imply that both processes share the same properties for a fixed discretization step. Thus, the approximation scheme should not be used to study the behaviour of the original model without further analysis of its

qualitative properties. Constructing approximation schemes, which are not only convergent, but also preserve the properties of the model, constitutes the main difficulty.

In our case, the first challenge is that the diffusion term of the SDE is highly degenerate and that frequently applied numerical schemes, such as the Euler-Maruyama method, do not preserve the "propagation of noise property" (formally known as *hypoellipticity*). Second, standard integrators may also fail in preserving second moment properties (see Mattingly et al. (2002)), especially when the equation describes oscillatory dynamics, which is the case here. For example, Higham and Strømenn Melbø (2004) prove that the Euler-Maruyama method does not preserve the second moment of linear stochastic oscillators. It is expected that this and similar negative results also extend to higher-dimensional and non-linear stochastic oscillators, see, e.g., Ableidinger et al. (2017). Even if higher-order Taylor approximation schemes may solve the problem of degenerate noise structure, they got two major drawbacks. They highly depend on the dimension of the system (which is determined by a parameter in our model) and they commonly fail in preserving ergodic properties.

To overcome these problems, we construct numerical schemes based on the so-called splitting approach. This approach was first developed for ordinary differential equations (ODEs). We refer to Blanes et al. (2009) and Mclachlan and Quispel (2002) for an exhaustive discussion. For an extension to SDEs, see, e.g., Ableidinger and Buckwar (2016), Ableidinger et al. (2017), Bréhier and Goudenège (2019), Leimkuhler and Matthews (2015), Leimkuhler et al. (2016), Milstein and Tretyakov (2004), Misawa (2001), Petersen (1998), Shardlow (2003). The main idea of the numerical splitting approach is to decompose the system into explicitly solvable subequations and to find a proper composition of the derived explicit solutions. Such methods usually preserve the properties of the underlying model through the explicitly solved subparts.

The main contributions of this work can be divided into three steps. First, a strong error bound between the Markovian cascade and the stochastic diffusion is proved. This complements the results presented in Ditlevsen and Löcherbach (2017), Löcherbach (2019). Second, moment bounds of order one and two for the stochastic diffusion are derived. Third, simulation algorithms for the diffusion and the PDMP are provided. For the diffusion, two splitting schemes, based on the Lie-Trotter and the Strang approach (Mclachlan and Quispel (2002), Strang (1968)), are proposed. They are proved to converge with order one in the mean-square sense. Moreover, they are proved to preserve the ergodic property of the continuous process and to accurately reconstruct the moment bounds obtained in the second step. The simulation method for the PDMP is exact and based on the thinning procedure. In order to apply this method, an explicit upper-bound and a sharper one, involving the numerical computation of polynomial roots, are obtained. Their performances, with respect to the parameters of the model, are discussed.

This Chapter is organized as follows. In Section 4.2, the finite particle system, the corresponding piece-wise deterministic Markov process and the main notations are introduced. Section 4.3 is devoted to the stochastic diffusion and to its properties. Section 4.4 presents the approximation schemes for the stochastic diffusion. Section 4.5 describes the simulation algorithm for the PDMP. Finally, Section 4.6 provides a numerical study, illustrating the theoretical results.

4.2   MODEL AND NOTATIONS

The system considered in this chapter consists of several populations of neurons, each of them representing a different functional group of neurons (layers in the visual cortex, pools of excitatory and inhibitory neurons in a network, etc.). This system is described by a multivariate counting process, which counts the spike occurrences. In a certain setting, it can be approximated by a stochastic diffusion in the large population limit (Ditlevsen and Löcherbach, 2017). The resulting diffusion is the subject of study in Section 4.3.

4.2.1   *Finite particle system*

Let us consider a network, consisting of K large populations of neurons, where the number of neurons in the k-th population is denoted by N_k and the total number of neurons in the network is $N = N_1 + \cdots + N_K$. Let $Z_t^{k,n}$ represent the number of spikes of the n-th neuron belonging to the k-th population during the time interval $[0,t]$. The sequence of counting processes $\{(Z_t^{k,n})_{t\geq0}, 1 \leq k \leq K, 1 \leq n \leq N_k\}$ is characterized by the intensity processes $(\lambda^{k,n}(t))_{t\geq0}$, which are formally defined through the relation

$$\mathbb{P}(Z_t^{k,n} \text{ has a jump in } (t, t + dt]|\mathcal{F}_t) = \lambda^{k,n}(t)dt,$$

where $\mathcal{F}_t$ contains the information about the processes $(Z_t^{k,n})_{t\geq0}$ up to time t. The mean-field framework considered here corresponds to intensities $\lambda^{k,n}(t)$ given by

$$\lambda^{k,n}(t) = f_k \left(\sum_{l=1}^{K} \frac{1}{N_l} \sum_{1 \leq m \leq N_l} \int_{(0,t)} h_{kl}(t - s) dZ_s^{l,m} \right), \tag{4.1}$$

where $\{h_{kl} : \mathbb{R}_+ \to \mathbb{R}\}$ is a family of *synaptic weight functions* (also called memory kernels), which model the influence of population l on population k. The function $f_k : \mathbb{R} \to \mathbb{R}_+$ is the *spiking rate function* of population k. The expression "mean-field framework" refers to the fact that the intensity $\lambda^{k,n}(t)$ depends on the whole system only through the "mean-field" behaviour of each population, namely $\frac{1}{N_l} \sum_{1 \leq m \leq N_l} dZ_s^{l,m}$. Furthermore, as $N \to \infty$ we assume that $N_k/N \to p_k > 0$ for all k.

Throughout the chapter we assume that the functions f_k satisfy the following conditions:

(A) The spiking rate functions f_k are positive, Lipschitz-continuous, non-decreasing and such that $0 < f_k \leq f_k^{\max}$ for $k = 1, \ldots, K$.

In this chapter, Erlang-type memory kernels and a cyclic feedback system of interactions are considered. This means that for each k, population k is only influenced by population $k + 1$, where we identify $K + 1$ with 1. In this case, all the memory kernels are null except the ones given by

$$h_{kk+1}(t) = c_k e^{-\nu_k t} \frac{t^{\eta_k}}{\eta_k!}, \tag{4.2}$$

where $c_k = \pm 1$. This constant determines whether the population has an *inhibitory* $(c_k = -1)$ or *excitatory* $(c_k = +1)$ effect. The parameter $\eta_k \geq 1$ is an integer number, determining the memory order for the interaction function from population $k + 1$ to population k.

The parameters η_k and ν_k determine, intuitively, the typical delay of interaction and its time width. The delay of the influence of the population $k+1$ on population k attains its maximum η_{k+1}/ν_{k+1} units back in time, and its mean is $(\eta_{k+1}+1)/\nu_{k+1}$. The larger is this ratio, the more "old" events are important. When the ratio is fixed (equal to τ), but both η_k and ν_k tend to infinity, then h_{kk+1} tends to a Dirac mass in τ. This means that only one specific moment in time is important. The interested reader is referred to Ditlevsen and Löcherbach (2017) and Löcherbach (2019) for more details.

In this chapter we are interested in the processes $\{(\bar{X}_t^{k,1})_{t\geq 0}, 1 \leq k \leq K\}$, which are the arguments of the function f_k in Equation (4.1) and are defined by

$$\bar{X}_t^{k,1} = \frac{1}{N_{k+1}} \sum_{1 \leq m \leq N_{k+1}} \int_{(0,t)} h_{kk+1}(t-s) dZ_s^{k+1,m}. \tag{4.3}$$

When the memory kernels are given in form (4.2), the processes defined in (4.3) can be obtained as marginals of the process $(\bar{X}_t)_{t\geq 0} = \{(\bar{X}_t^{k,j})_{t\geq 0}, 1 \leq k \leq K, 1 \leq j \leq \eta_k + 1\}$ which solves the following system of dimension $\kappa = \sum_{k=1}^K (\eta_k + 1)$:

$$\begin{cases} d\bar{X}_t^{k,j} = \left[-\nu_k \bar{X}_t^{k,j} + \bar{X}_t^{k,j+1}\right] dt, \text{ for } j = 1, \ldots, \eta_k, \\ d\bar{X}_t^{k,\eta_k+1} = -\nu_k \bar{X}_t^{k,\eta_k+1} dt + c_k d\bar{Z}_t^{k+1}, \\ \bar{X}_0 = x_0 \in \mathbb{R}^\kappa, \end{cases} \tag{4.4}$$

where $\bar{Z}_t^{k+1} = \frac{1}{N_{k+1}} \sum_{n=1}^{N_{k+1}} Z_t^{k+1,n}$, each $Z_t^{k+1,n}$ jumping at rate $f(\bar{X}_{t-}^{k+1,1})$, see Ditlevsen and Löcherbach (2017) for more insight. This type of equation is called a Markovian cascade in the literature.

The process $(\bar{X}_t)_{t\geq 0}$ summarizes and averages the influence of the past events. This process, along with the firing rate functions f_k, determine the dynamics of $(Z_t^{k,n})_{t\geq 0}$, described by its intensity (4.1).

From a modelling point of view, the process $(\bar{X}_t^{k,1})_{t\geq 0}$ can be roughly regarded as the voltage membrane potential of any neuron in population k. Then, the probability of a neuron to emit a spike is given as a function of its membrane potential. To summarize, the processes, with coordinates $(k,1)$, defined by (4.3), describe the membrane potential in each population, whereas the other coordinates represent higher levels of memory for the process.

Note that the model presented so far starts with empty memory. The right-hand side of (4.1) is equal to $f_k(0)$ at time $t = 0$ or equivalently $x_0 = 0$. However, one could easily generalize this to any initial condition x_0 in $\mathbb{R}^\kappa$ as it is done in the rest of the chapter. Moreover, the interested reader is referred to Duarte et al. (2019), where a more general model is studied numerically and theoretically for $K = 1$ population.

4.2.2 *Notations*

Now we focus on the case of two interacting populations of neurons ($K = 2$), consisting of N_1 and N_2 neurons, respectively. Taking $K = 2$ allows for an investigation of the interactions between the

populations of different sizes while avoiding heavy notations. Throughout the chapter the following notation is used: $\mathbb{O}_{n \times m}$ denotes a $n \times m$-dimensional zero matrix and 0_n denotes a n-dimensional zero vector. Then, it is convenient to rewrite system (4.4) in the matrix-vector form

$$d\bar{X}_t = A\bar{X}_t dt + \Gamma \, d\bar{Z}_t, \quad \bar{X}_0 = x_0 \in \mathbb{R}^\kappa, \tag{4.5}$$

with

- $A \in \mathbb{R}^{\kappa \times \kappa}$ defined as

$$A = \begin{pmatrix} A_{\nu_1} & \mathbb{O}_{(\eta_1+1) \times (\eta_2+1)} \\ \mathbb{O}_{(\eta_2+1) \times (\eta_1+1)} & A_{\nu_2} \end{pmatrix}, \tag{4.6}$$

  where A_{ν_k} is a $(\eta_k + 1) \times (\eta_k + 1)$ tri-diagonal matrix with lower-diagonal equal to 0_{η_k}, diagonal equal to $(-\nu_k, \ldots, -\nu_k)$ and upper-diagonal equal to $(1, \ldots, 1)$,

- $\Gamma \in \mathbb{R}^{\kappa \times 2}$ having zero coefficients everywhere, except for $\Gamma_{\eta_1+1,2} = c_1$ and $\Gamma_{\kappa,1} = c_2$,

- and $\bar{Z}_t = \left(\bar{Z}_t^1, \bar{Z}_t^2 \right)^T$.

Throughout the chapter the following convention is made. The coordinates of a generic vector x in $\mathbb{R}^\kappa$ are either denoted as $(x_i)_{i=1,\ldots,\kappa}$ or $(x^{k,j})_{k=1,2; \, j=1,\ldots,\eta_k+1}$ with the relation $i = j$ if $k = 1$ and $i = \eta_1 + 1 + j$ if $k = 2$. The second notation is usually preferred since each population is easily identified by the index k. For some generic function $g : \mathbb{R}^\kappa \to \mathbb{R}^\kappa$, the upper indexes are used as follows: $(g(x))^{k,j}$. Moreover, it is sometimes more natural to consider some generic $\mathbb{R}^\kappa$-valued process x_t population-wise. Thus, it is split into two components $x_t^1 = (x_t^{1,1}, \ldots, x_t^{1,\eta_1+1}) \in \mathbb{R}^{\eta_1+1}$ and $x_t^2 = (x_t^{2,1}, \ldots, x_t^{2,\eta_2+1}) \in \mathbb{R}^{\eta_2+1}$, such that $x_t = (x_t^1, x_t^2)^T \in \mathbb{R}^\kappa$.

4.3   THE LIMITING STOCHASTIC DIFFUSION

In Ditlevsen and Löcherbach (2017) it is proved that the limit behaviour of (4.5) can be approximated by the diffusion process $X = (X^1, X^2)^T \in \mathbb{R}^\kappa$, which is obtained as the the unique strong solution of the SDE

$$dX_t = (AX_t + B(X_t))dt + \frac{1}{\sqrt{N}} \sigma(X_t)dW_t, \quad X_0 = x_0, \tag{4.7}$$

where $W = (W^1, W^2)^T$ is a 2-dimensional Brownian motion, and $x_0 \in \mathbb{R}^\kappa$ is a deterministic initial condition. The non-linear part of the drift term $B : \mathbb{R}^\kappa \to \mathbb{R}^\kappa$ is given by

$$B(X) = (B^1(X^2), B^2(X^1))^T, \tag{4.8}$$

where $B^1 : \mathbb{R}^{\eta_2+1} \to \mathbb{R}^{\eta_1+1}$ and $B^2 : \mathbb{R}^{\eta_1+1} \to \mathbb{R}^{\eta_2+1}$ read as $B^1(X^2) = (0, \ldots, 0, c_1 f_2(X^{2,1}))$ and $B^2(X^1) = (0, \ldots, 0, c_2 f_1(X^{1,1}))$. The diffusion component $\sigma : \mathbb{R}^\kappa \to \mathbb{R}^{\kappa \times 2}$ is given by

$$\sigma(X) = \begin{pmatrix} \sigma^1(X^2) \\ \sigma^2(X^1) \end{pmatrix}, \tag{4.9}$$

where $\sigma^1 : \mathbb{R}^{\eta_2+1} \to \mathbb{R}^{(\eta_1+1)\times 2}$ and $\bar{\sigma}^2 : \mathbb{R}^{\eta_1+1} \to \mathbb{R}^{(\eta_2+1)\times 2}$ read as

$$\sigma^1(X^2) = \begin{pmatrix} 0 & 0 \\ \vdots & \vdots \\ 0 & \frac{c_1}{\sqrt{p_2}}\sqrt{f_2(X^{2,1})} \end{pmatrix}, \quad \sigma^2(X^1) = \begin{pmatrix} 0 & 0 \\ \vdots & \vdots \\ \frac{c_2}{\sqrt{p_1}}\sqrt{f_1(X^{1,1})} & 0 \end{pmatrix}.$$

In other words, the jump term $\Gamma\, d\bar{Z}$, determining the dynamics of the Markovian cascade given in (4.5), is replaced by the sum of a non-linear drift and a diffusion term.

As N goes to infinity, the diffusion term in (4.7) vanishes and the SDE transforms into an ODE of the form

$$dU_t = (AU_t + B(U_t))dt, \quad U_0 = x_0. \tag{4.10}$$

The focus of this chapter lies in the theoretical and numerical relations between the PDMP and its stochastic diffusion approximation. Thus, we do not address the properties of ODE (4.10) in this work and refer to Ditlevsen and Löcherbach (2017) for related qualitative features and convergence results.

The rest of this section is organized as follows. First, we investigate how accurately the stochastic diffusion approximates the dynamics of the point process, proving a strong error bound between PDMP (4.5) and SDE (4.7). Then, we study the properties of SDE (4.7), focusing on moment bounds.

4.3.1 *Strong error bound between the limiting diffusion and the piece-wise deterministic Markov process*

Any error bound of the diffusion approximation is determined by two facts, namely the approximation of a compensated Poisson process by a Brownian motion and the approximation of N_k by $p_k N$. We get rid of the second approximation by considering SDE (4.7) with $p_k = N_k/N$ and denote the solution of this equation by Y. By choosing a different notation we stress the fact that, on the contrary to X, it depends on the exact number of neurons N_k and not on its proportion, obtained in the mean-field limit. The same convention is used in Ditlevsen and Löcherbach (2017), where the following weak error bound is proved.

Theorem 4.1 (Ditlevsen and Löcherbach (2017))**.** *Grant assumption (A) and suppose that all spiking functions f_k belong to the space C_b^5 of bounded functions having bounded derivatives up to order 5. Then there exists a constant C depending only on f_1, f_2 and the bounds on their derivatives such that for all $\varphi \in C_b^4(\mathbb{R}^\kappa, \mathbb{R})$ and $\forall x_0 \in \mathbb{R}^\kappa$,*

$$\sup_{x\in\mathbb{R}^k} |\mathbb{E}\varphi(\bar{X}_t) - \mathbb{E}\varphi(Y_t)| \leq Ct\frac{\|\varphi\|_{4,\infty}}{N^2}. \tag{4.11}$$

In the following, we strengthen the above result, allowing for a comparison of trajectories of the PDMP and the diffusion.

Theorem 4.2 (Strong error bound)**.** *Grant assumption (A) and let $\|\cdot\|_\infty$ denote the sup norm on $\mathbb{R}^\kappa$. For all $N > 0$, a solution $\bar{X}$ of (4.5) and a solution Y of (4.7) (with $p_k = N_k/N$) can be*

constructed on the same probability space such that there exists a constant $C > 0$ such that, for all $T > 0$,

$$\sup_{t \leq T} \|\bar{X}_t - Y_t\|_\infty \leq \Theta_N e^{CT} \frac{\log(N)}{N} \tag{4.12}$$

almost surely, where Θ_N is a random variable with exponential moments whose distribution does not depend on N. In particular,

$$\mathbb{E}\left[\sup_{t \leq T} \|\bar{X}_t - Y_t\|_\infty\right] \leq C e^{CT} \frac{\log(N)}{N}. \tag{4.13}$$

The proof of Theorem 4.2 is mainly inspired by Kurtz et al. (1978) and relies on two main ingredients, a strong coupling between the standard Poisson process and the Brownian motion and a sharp result on the modulus of continuity for the Brownian motion. All the material is postponed to Appendix.

When comparing (4.11) and (4.13), one notices that there is an exchange between the expectation sign and the absolute value. There are two prices to pay for such an exchange. First, a slower convergence rate with respect to N. Second, a faster divergence rate with respect to t (the exponential term is coming from a Grönwall type argument). In the following remark we precise the bound on the error which is caused by using directly the parameter p_k instead of N_k/N.

Remark 4.1. *Let Y denote a solution of (4.7) (with parameter p_k equal to N_k/N) and X denote a solution of (4.7) with fixed values p_k. Following the proof of Theorem 4.2, one can show that*

$$\sup_{t \leq T} \|X_t - Y_t\| \leq \Theta_N e^{CT} \left(\frac{\log(N)}{N} + \max_k \left\{ \frac{1}{\sqrt{p_k N}} \left(1 - \sqrt{p_k N / N_k} \right) \right\} \right)$$

so that the strong error bound stated in the theorem also holds for the non-modified SDE if $\sqrt{p_k N / N_k} - 1$ is of order $N^{-1/2}$ or of faster order.

Fortunately, for any fixed N, setting $N_1 = \lfloor p_1 N \rfloor$ and $N_2 = \lceil p_2 N \rceil$ ensures that $\sqrt{p_k N / N_k} - 1$ is of order $N^{-1} < N^{-1/2}$, which grants that Theorem 4.2 holds for SDE (4.7).

Since SDE (4.7) transforms into ODE (4.10) as N goes to infinity, the strong error bound can be used to prove the convergence of the PDMP to the solution of the ODE. However, this is beyond the scope of this chapter.

4.3.2   *Properties of the stochastic diffusion*

The solution process $(X_t)_{t \geq 0}$ of SDE (4.7) is positive Harris recurrent with invariant measure π which is of full support (see Löcherbach (2019)). It means that the trajectories visit all sets in the support of the invariant measure infinitely often almost surely. More precisely, for any initial condition x_0 and measurable set A such that $\pi(A) > 0$, $\limsup_{t \to +\infty} \mathbf{1}_A(X_t) = 1$ almost surely. Besides, by following the arguments in Mattingly et al. (2002), the technical results proven in Löcherbach (2019) can be used to prove geometric ergodicity of $(X_t)_{t \geq 0}$ as stated in Proposition 4.1 below.

In order to state the geometric ergodicity of $(X_t)_{t \geq 0}$, let us first specify the Lyapunov function $G : \mathbb{R}^\kappa \to \mathbb{R}$ introduced in Ditlevsen and Löcherbach (2017):

$$G(x) = \sum_{k=1}^{K} \sum_{j=1}^{\eta_k+1} \frac{j}{\nu_k^{j-1}} J(x^{k,j}), \tag{4.14}$$

where J is some smooth approximation of the absolute value. In particular, $J(x) = |x|$ for all $|x| \geq 1$ and $\max\{|J'(x)|, |J''(x)|\} \leq J_c$ for all x, for some finite constant J_c.

Proposition 4.1 (Geometric ergodicity). *Grant assumption (A). Then the solution of SDE* (4.7) *has a unique invariant measure π on $\mathbb{R}^\kappa$. For all initial conditions x_0 and all $m \geq 1$, there exist $C = C(m) > 0$ and $\lambda = \lambda(m) > 0$ such that, for all measurable functions $g : \mathbb{R}^\kappa \to \mathbb{R}$ such that $|g| \leq G^m$,*

$$\forall t \geq 0, \quad |\mathbb{E}g(X_t) - \pi(g)| \leq CG(x_0)^m e^{-\lambda t}.$$

Proof. The proof closely follows that of Theorem 3.2 in Mattingly et al. (2002) and is based on Lyapunov and minorization conditions (the latter is implied by the existence of a smooth transition density and the irreducibility of the space).

(i) First, we use the fact that G is a Lyapunov function for X (Ditlevsen and Löcherbach, 2017, Proposition 5), i.e., $\exists \alpha, \beta > 0$, s.t.

$$\mathcal{A}^X G(x) \leq -\alpha G(x) + \beta,$$

where $\mathcal{A}^X G(x)$ is the infinitesimal generator of (4.7).

(ii) Then, we note that, from any initial condition x_0, for any time $T > 0$ and any open set O, the probability that X_T belongs to O is positive. It is ensured by the controllability of system (4.7) (see Theorem 4 in Löcherbach (2019)).

(iii) Finally, we note that the process $(X_t)_{t \geq 0}$ possesses a smooth transition density. Its existence is ensured by verifying the Hörmander condition, which is done in Proposition 7 of Ditlevsen and Löcherbach (2017).

The rest of the proof follows as in the proof of (Mattingly et al., 2002, Theorem 3.2.): apply (Mattingly et al., 2002, Theorem 2.5.) to some discrete-time sampling of the process and conclude by interpolation. $\qquad \square$

Also note that the rank of the diffusion matrix $\sigma\sigma^T$ is smaller than the dimension of system (4.7). This means that the system is not elliptic. However, the specific cascade structure of the drift ensures that the noise is propagated through the whole system via the drift term, such that the diffusion is hypoelliptic in the sense of stochastic calculus of variations (Delarue and Menozzi, 2010, Malliavin and Thalmaier, 2006). We also note that SDE (4.7) is semi-linear, with a linear term given by matrix (4.6). Thus, its solution can be written in the form of a convolution equation (see, among others, Mao (2007, Section 3)).

Proposition 4.2. *The unique solution of* (4.7) *satisfies*

$$X_t = e^{At}x_0 + \int_0^t e^{A(t-s)} B(X_s) ds + \frac{1}{\sqrt{N}} \int_0^t e^{A(t-s)} \sigma(X_s) dW_s. \tag{4.15}$$

Proof. Consider the process $Y_t = e^{-At}X_t$. By Itô's formula one obtains

$$
\begin{aligned}
d\left(e^{-At}X_t\right) &= \left(-Ae^{-At}X_t + e^{-At}\left(AX_t + B(X_t)\right)\right)dt + \frac{e^{-At}}{\sqrt{N}}\sigma(X_t)dW_t \\
&= e^{-At}B(X_t)dt + \frac{e^{-At}}{\sqrt{N}}\sigma(X_t)dW_t.
\end{aligned}
$$

Integrating both parts yields

$$
e^{-At}X_t = x_0 + \int_0^t e^{-As}B(X_s)ds + \frac{1}{\sqrt{N}}\int_0^t e^{-As}\sigma(X_s)dW_s.
$$

Multiplying the expression by e^{At} gives the result. □

Note that from this form, it is straightforward to see that the diffusion term is of full rank. Intuitively, this ensures the hypoellipticity. Further, systems of type (4.15) are called stochastic Volterra equations (Jaber et al., 2019).

Now we focus on first and second moment bounds. The following results are needed, in particular, to ensure the accuracy of the approximation scheme in Section 4.4. In the following remark we provide some purely computational results in order to ease the further analysis.

Remark 4.2. *Due to the block-structure of the matrix A introduced in (4.6), its matrix exponential e^{At} can be computed as*

$$
e^{At} = \begin{pmatrix} e^{A_{\nu_1}t} & \mathbb{0}_{(\eta_1+1)\times(\eta_2+1)} \\ \mathbb{0}_{(\eta_2+1)\times(\eta_1+1)} & e^{A_{\nu_2}t} \end{pmatrix},
$$

where $e^{A_{\nu_k}t}$, $k = 1, 2$, is a $(\eta_k + 1) \times (\eta_k + 1)$ upper-triangular matrix given by

$$
e^{A_{\nu_k}t} = e^{-\nu_k t}\begin{pmatrix} 1 & t & \frac{t^2}{2} & \cdots & \frac{t^{\eta_k}}{\eta_k!} \\ 0 & 1 & t & \cdots & \frac{t^{\eta_k-1}}{(\eta_k-1)!} \\ \vdots & \ddots & \ddots & \ddots & \vdots \\ \vdots & \vdots & \ddots & \ddots & \vdots \\ 0 & 0 & 0 & \cdots & 1 \end{pmatrix}. \tag{4.16}
$$

In further computations we will often use the vectors $e^{At}X_s$. The elements of $e^{At}X_s$ are given by the formula

$$
\left(e^{At}X_s\right)^{k,j} = e^{-\nu_k t}\sum_{m=j}^{\eta_k+1}\frac{t^{m-j}}{(m-j)!}X_s^{k,m}. \tag{4.17}
$$

Theorem 4.3 (First moment bounds of the diffusion process)**.** *Grant assumption (**A**). The following bounds hold for the components of $\mathbb{E}[X_t]$:*

$$
\mathcal{I}_{\min}^{k,j} \leq \mathbb{E}[X_t^{k,j}] \leq \mathcal{I}_{\max}^{k,j},
$$

where

$$
\mathcal{I}_{\min}^{k,j} = \left(e^{At}x_0\right)^{k,j} + \left[1 - e^{-t\nu_k}\sum_{l=0}^{\eta_k+1-j}\frac{(t\nu_k)^l}{l!}\right]\min\left\{0, \frac{c_k f_{k+1}^{\max}}{\nu_k^{(\eta_k+2-j)}}\right\},
$$

$$
\mathcal{I}_{\max}^{k,j} = \left(e^{At}x_0\right)^{k,j} + \left[1 - e^{-t\nu_k}\sum_{l=0}^{\eta_k+1-j}\frac{(t\nu_k)^l}{l!}\right]\max\left\{0, \frac{c_k f_{k+1}^{\max}}{\nu_k^{(\eta_k+2-j)}}\right\}.
$$

Proof of Theorem 4.3. From Proposition 4.2 and Remark 4.2, it follows that the convolution-based representation of the k-th population is given by

$$X_t^k = (e^{At}x_0)^k + \int_0^t e^{A\nu_k(t-s)}B^k(X_s^{k+1})ds + \frac{1}{\sqrt{N}}\int_0^t e^{A\nu_k(t-s)}\sigma^k(X_s^{k+1})dW_s.$$

Consequently, the j-th components are given by

$$
\begin{aligned}
X_t^{k,j} &= \underbrace{\left(e^{At}x_0\right)^{k,j}}_{:=T_1(t)} + \underbrace{\int_0^t c_k f_{k+1}(X_s^{k+1,1})\frac{e^{-\nu_k(t-s)}}{(\eta_k+1-j)!}(t-s)^{\eta_k+1-j}ds}_{:=T_2(t)} \\
&+ \underbrace{\frac{1}{\sqrt{N}}\int_0^t \frac{c_k}{\sqrt{p_{k+1}}}\sqrt{f_{k+1}(X_s^{k+1,1})}\frac{e^{-\nu_k(t-s)}}{(\eta_k+1-j)!}(t-s)^{\eta_k+1-j}dW_s^{k+1}}_{:=T_3(t)}.
\end{aligned}
$$

Note that, $\mathbb{E}[T_1(t)] = T_1(t)$ and $\mathbb{E}[T_3(t)] = 0$. It remains to consider $T_2(t)$. The fact that the intensity function is bounded by $0 < f_{k+1} \leq f_{k+1}^{\max}$ implies that

$$\min\{0,c_k\}\frac{f_{k+1}^{\max}}{(\eta_k+1-j)!}I^{k,j} \leq \mathbb{E}[T^2(t)] \leq \max\{0,c_k\}\frac{f_{k+1}^{\max}}{(\eta_k+1-j)!}I^{k,j},$$

where

$$I^{k,j} = \int_0^t e^{-\nu_k(t-s)}(t-s)^{\eta_k+1-j}ds.$$

Now, let us consider the integral $I^{k,j}$:

$$\int_0^t e^{-\nu_k(t-s)}(t-s)^{\eta_k+1-j}ds = t^{\eta_k+1-j}\int_0^t e^{-\nu_k t\frac{t-s}{t}}\left(\frac{t-s}{t}\right)^{\eta_k+1-j}ds.$$

Setting $z = \frac{t-s}{t}$ yields

$$t^{\eta_k+2-j}\int_0^1 e^{-\nu_k t z}z^{\eta_k+1-j}dz = \frac{(\eta_k+1-j)!}{\nu_k^{(\eta_k+2-j)}}\left[1-e^{-\nu_k t}\sum_{l=0}^{\eta_k+1-j}\frac{(\nu_k t)^l}{l!}\right].$$

This gives the result. $\qquad\square$

Remark 4.3. *Recalling* (4.17) *and using that* $\lim_{t\to\infty}e^{-\nu_k t}\sum_{l=0}^{\eta_k+1-j}\frac{(t\nu_k)^l}{l!} = 0$, *it follows from Theorem 4.3 that*

$$\min\left\{0,\frac{c_k f_{k+1}^{\max}}{\nu_k^{(\eta_k+2-j)}}\right\} \leq \lim_{t\to\infty}\mathbb{E}[X_t^{k,j}] \leq \max\left\{0,\frac{c_k f_{k+1}^{\max}}{\nu_k^{(\eta_k+2-j)}}\right\}.$$

The derived moment bounds give some intuition on how the system behaves in the long run. Remarkably, depending on whether c_k is positive or negative, the trajectories of $(X_t^k)_{t\geq 0}$ are on average bounded by 0 from below or above, respectively. This is in agreement with the fact that the sign of c_k defines whether the corresponding neural population is excitatory ($c_k = +1$) or inhibitory ($c_k = -1$). Moreover, we may immediately see the effect of increasing the memory order η_k, depending on the constant ν_k. When $\nu_k = 1$, the bounds for all j components are determined entirely by c_k and the bounds of the intensity functions. When $\nu_k < 1$ and $\eta_k \to \infty$, then the first components, presenting the current state of the process, tend to infinity. Similarly, for $\nu_k > 1$, the trajectories are attracted to 0. Finally, note that the first moment bounds do not depend on the number of neurons in the system.
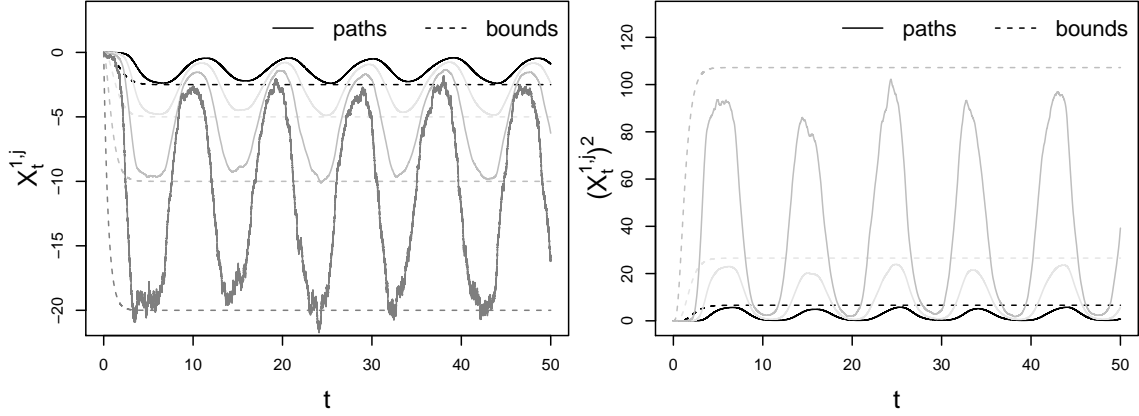
Figure 4.1: First (left panel) and second (right panel) moment bounds with respective trajectories of the inhibitory population $k = 1$. The rate function f_2 is given in Section 4.6. The parameters are $\eta_1 = 3$, $\nu_1 = 2$, $N = 20$ and $p_2 = 1/2$.

Theorem 4.4 (Second moment bounds of the diffusion process). *Grant assumption (A). The following bounds hold for $\mathbb{E}[(X_t^{k,j})^2]$:*

$$
\mathbb{E}[(X_t^{k,j})^2] \leq \left(\left(e^{At} x_0 \right)^{k,j} \right)^2 + 2 \left(e^{At} x_0 \right)^{k,j} \max \left\{ 0, \frac{c_k f_{k+1}^{\max}}{(\eta_k + 1 - j)!} I_1^{k,j}(t) \right\}
$$
$$
+ \quad f_{k+1}^{\max} \left(\frac{c_k}{(\eta_k + 1 - j)!} \right)^2 \left(\sqrt{f_{k+1}^{\max}}\, I_1^{k,j}(t) + \sqrt{\frac{I_2^{k,j}(t)}{N \cdot p_{k+1}}} \right)^2 ,
$$

where $I_u^{k,j}(t)$, $u = 1, 2$, are defined as

$$
I_u^{k,j}(t) \quad := \quad \int_0^t e^{-u\nu_k(t-s)} (t-s)^{u(\eta_k+1-j)} ds
$$
$$
= \quad \frac{(u(\eta_k + 1 - j))!}{(u\nu_k)^{u(\eta_k+1-j)+1}} \left[1 - e^{-ut\nu_k} \sum_{l=0}^{u(\eta_k+1-j)} \frac{(ut\nu_k)^l}{l!} \right].
$$

The proof of Theorem 4.4 is similar to the one of Theorem 4.3 and is postponed to Appendix.

Remark 4.4. *Theorem 4.4 gives the following asymptotic bounds:*

$$
\lim_{t \to \infty} \mathbb{E}[(X_t^{k,j})^2] \qquad \leq \qquad f_{k+1}^{\max} \left(\frac{c_k}{(\eta_k + 1 - j)!} \right)^2 \left(\sqrt{f_{k+1}^{\max}} C_1^{k,j} + \sqrt{\frac{C_2^{k,j}}{N \cdot p_{k+1}}} \right)^2 ,
$$

where

$$
C_u^{k,j} := \lim_{t \to \infty} I_u^{k,j}(t) = \frac{(u(\eta_k + 1 - j))!}{(u\nu_k)^{u(\eta_k+1-j)+1}}.
$$

Note that for $N \to \infty$, the bound obtained in Theorem 4.4 equals the square of the bound for the first moment, derived in Theorem 4.3. This is in agreement with the fact that the stochastic system (4.7) transforms into an ODE as N increases (Ditlevsen and Löcherbach, 2017). In other words, its diffusion coefficient tends to 0 as N tends to infinity.

In Figure 4.1, the first and second moment bounds, derived in Theorem 4.3 and Theorem 4.4, respectively, are illustrated. In the left panel, we plot 4 sample trajectories (solid lines) of an inhibitory

population and their lower first moment bounds (dashed lines). The main variable $X^{k,1}$ and its lower moment bound are depicted in black. The remaining 3 trajectories are auxiliary variables. They (and their corresponding bounds) are depicted in different shades of grey. We see that the trajectories can exceed the theoretical bounds, especially when the effect of noise is large. On average, the trajectories stay within the bounds. In the right panel, we plot the square of the first 3 components of X^k (and their second moment bounds), omitting the 4-th one in order to stay within an easily interpretative scale. We conclude that the bounds are rather precise for the parameter setting under consideration.

4.4 NUMERICAL SPLITTING SCHEMES FOR THE STOCHASTIC DIFFUSION

The solution of system (4.7) cannot be written in an explicit form, and thus a numerical approximation is required. Let $[0, T]$ with $T > 0$ be the time interval of interest and consider the discretization $(t_i)_{i=0,\ldots,i_{\max}}$ given by $t_i = i\Delta$, where $\Delta = T/i_{\max}$. In the following, $\tilde{X}_{t_i}$ denotes a numerical realisation of the diffusion process, evaluated at the discrete time points.

We derive and investigate two numerical schemes based on the splitting approach. The goal of this method is to divide the equation into explicitly solvable subequations and to compose the obtained explicit solutions in a proper way. Usually, the choice of the subsystems is not unique. Here, because of the specific structure of SDE (4.7), we split it into the subsystems

$$
\begin{aligned}
dX_t^{[1]} &= AX_t^{[1]}dt, \\
dX_t^{[2]} &= B(X_t^{[2]})dt + \frac{1}{\sqrt{N}}\sigma(X_t^{[2]})dW_t.
\end{aligned}
$$

Both subsystems are explicitly solvable. The first one is a linear ODE whose flow is given by $\psi_t^{[1]} : x \mapsto e^{At}x$. For the second one, recall that B and σ are given by (4.8) and (4.9), respectively. It is easy to see that all components of $X^{[2]}$, except for two ($X^{[2],1,\eta_1+1}$ and $X^{[2],2,\eta_2+1}$) have null derivative. Moreover, the drift and diffusion coefficients of $X^{[2],1,\eta_1+1}$ only depend on $X^{[2],2,1}$ and vice versa. Hence, the respective explicit (stochastic) flows are given by

$$
\begin{aligned}
\psi_t^{[1]}(x) &:= e^{At}x, \\
\psi_t^{[2]}(x) &:= x + tB(x) + \frac{\sqrt{t}}{\sqrt{N}}\sigma(x)\xi,
\end{aligned}
$$

where $\xi = (\xi^1, \xi^2)^T$ is a 2-dimensional standard normal vector. Then, the Lie-Trotter and the Strang compositions of flows (Mclachlan and Quispel, 2002, Strang, 1968) are given as follows

$$
\tilde{X}_{t_{i+1}}^{LT} = \left(\psi_\Delta^{[1]} \circ \psi_\Delta^{[2]}\right)\left(\tilde{X}_{t_i}^{LT}\right) = e^{A\Delta}\left(\tilde{X}_{t_i}^{LT} + \Delta B(\tilde{X}_{t_i}^{LT}) + \frac{\sqrt{\Delta}}{\sqrt{N}}\sigma(\tilde{X}_{t_i}^{LT})\xi_i\right), \tag{4.18}
$$

$$
\begin{aligned}
\tilde{X}_{t_{i+1}}^{ST} &= \left(\psi_{\frac{\Delta}{2}}^{[1]} \circ \psi_\Delta^{[2]} \circ \psi_{\frac{\Delta}{2}}^{[1]}\right)\left(\tilde{X}_{t_i}^{ST}\right) \\
&= e^{A\Delta}\tilde{X}_{t_i}^{ST} + \Delta e^{A\frac{\Delta}{2}}B(e^{A\frac{\Delta}{2}}\tilde{X}_{t_i}^{ST}) + \frac{\sqrt{\Delta}}{\sqrt{N}}e^{A\frac{\Delta}{2}}\sigma(e^{A\frac{\Delta}{2}}\tilde{X}_{t_i}^{ST})\xi_i,
\end{aligned} \tag{4.19}
$$

respectively, with $\tilde{X}_0^{LT} = \tilde{X}_0^{ST} = x_0$ and $(\xi_i)_{i=1,\ldots,i_{\max}}$ i.i.d. The two splitting schemes (4.18) and (4.19) define numerical solutions of SDE (4.7). Note that by setting $\sigma(x) \equiv 0$, both schemes can be used for simulating ODE (4.10).

For the sake of simplicity, we focus on the Lie-Trotter splitting (4.18) in the subsequent analysis, since its representation is more intuitive. Thus, throughout Section 4.4 we set $\tilde{X} \equiv \tilde{X}^{LT}$. However, similar results can be obtained also for the more evolved Strang approach (4.19).

Remark 4.5. *Note that thanks to the matrix exponential entering the diffusion terms in* (4.18) *and* (4.19), *the noise propagates through all components of the system at each time step. In other words, the conditional variance matrix Σ is of full rank and is given by*

$$\Sigma\left[\tilde{X}_{t_{i+1}} | \tilde{X}_{t_i}\right] := \frac{\Delta}{N} e^{A\Delta} \sigma(\tilde{X}_{t_i}) \sigma^T(\tilde{X}_{t_i}) \left(e^{A\Delta}\right)^T.$$

This can be regarded as a discrete analogue of the hypoellipticity of the continuous process, a property that the approximation methods based on the Itô-Taylor expansion of the infinitesimal generator of (4.7) *(see Kloeden et al. (2003)) do not preserve.*

4.4.1   *Strong convergence in the mean square sense*

Now we focus on the convergence in the mean-square sense and show that the numerical solutions obtained via the splitting approach converge to the process as the time step $\Delta \to 0$ with order 1. The frequently applied Euler-Maruyama scheme usually converges with mean-square order $1/2$ if the noise is multiplicative (Kloeden et al., 2003, Milstein and Tretyakov, 2004), as it is the case for system (4.7). In the following result, thanks to the specific structure of the noise component, we show that the Euler-Maruyama scheme coincides with the Milstein scheme, which is known to converge with mean-square order 1. This result is then used to establish the convergence order of the splitting scheme.

Theorem 4.5 (Mean-square convergence of the splitting scheme)**.** *Grant assumption (A). Let $\tilde{X}_{t_i}$ denote the numerical method defined by* (4.18) *at time point t_i and starting from x_0. Then $\tilde{X}_{t_i}$ is mean-square convergent with order 1, i.e., there exists a constant $C > 0$ such that*

$$\left(\mathbb{E}\left[\left\|X_{t_i} - \tilde{X}_{t_i}\right\|^2\right]\right)^{\frac{1}{2}} \leq C\Delta,$$

for all time points t_i, $i = 1, \ldots, i_{max}$, where $\|\cdot\|$ denotes the Euclidean norm.

Proof of Theorem 4.5. Let us denote by $\tilde{X}^{EM}$ a numerical solution of SDE (4.7) obtained via the Euler-Maruyama method, that is

$$\tilde{X}_{t_{i+1}}^{EM} = \tilde{X}_{t_i}^{EM} + \Delta\left(A\tilde{X}_{t_i}^{EM} + B(\tilde{X}_{t_i}^{EM})\right) + \frac{\sqrt{\Delta}}{\sqrt{N}}\sigma(\tilde{X}_{t_i}^{EM})\xi_i. \tag{4.20}$$

First, we show that the Euler-Maruyama method, when applied to system (4.7), coincides with the Milstein scheme, which is known to converge with mean-square order 1. To do so, we denote the vector x by $x = (x^1, \ldots, x^\kappa)$, where $\kappa = \eta_1 + \eta_2 + 2$. Further, we recall that the j-th component,

$j = 1, \ldots, \kappa$, of the Milstein scheme only differs from the j-th component of the Euler-Maruyama scheme (4.20) by the following additional term

$$\sum_{m_1, m_2 = 1}^{2} \sum_{l=1}^{\kappa} \sigma^{l, m_1} \frac{\partial \sigma^{j, m_2}}{\partial x^l} I(m_1, m_2),$$

where $\sigma^{j, m}$ denotes the value of the element at the j-th row and the m-th column of the diffusion matrix σ at time t_i and

$$I(m_1, m_2) := \int_{t_i}^{t_{i+1}} \int_{t_i}^{s_2} dW_{s_1}^{m_1} dW_{s_2}^{m_2}.$$

Now note that the term $\partial \sigma^{j, m_2} / \partial x^l$ is only different from 0 for $j = \eta_1 + 1$, $m_2 = 1$, $l = \eta_1 + 2$ and for $j = \eta_1 + \eta_2 + 2$, $m_1 = 2$, $l = 1$. However, σ^{l, m_1} equals 0 for those values of l. Thus, the above double sum equals 0 and the Euler-Maruyama method coincides with the Milstein scheme. This implies that

$$\|X_{t_i} - \tilde{X}_{t_i}^{EM}\|_{L^2} \leq C\Delta, \tag{4.21}$$

where $\| \cdot \|_{L^2} := \left(\mathbb{E}[\| \cdot \|^2] \right)^{1/2}$ denotes the L^2-norm and C is some generic constant. For the second part, we provide a proof similar to the one presented in Milstein and Tretyakov (2003). Applying the triangle inequality yields that

$$\|X_{t_i} - \tilde{X}_{t_i}\|_{L^2} \leq \|X_{t_i} - \tilde{X}_{t_i}^{EM}\|_{L^2} + \|\tilde{X}_{t_i}^{EM} - \tilde{X}_{t_i}\|_{L^2}.$$

Given $X_{t_i} := x$, let us denote with $\tilde{X}_{t_{i+1}}^{EM}(x, t_i)$ and $\tilde{X}_{t_{i+1}}(x, t_i)$ the one-step approximation of the Euler-Maruyama and splitting scheme, respectively. For instance, $\tilde{X}_{t_{i+1}}^{EM}(x, t_i)$ is given by Equation (4.20) with $\tilde{X}_{t_i}^{EM}$ replaced by x. By the definition of the matrix exponent, i.e., $e^{A\Delta} := I + \Delta A + \frac{\Delta^2}{2} A^2 + O(\Delta^3)$, and by recalling (4.18), we obtain that

$$\begin{aligned}
\tilde{X}_{t_{i+1}}^{EM}(x, t_i) - \tilde{X}_{t_{i+1}}(x, t_i) &= x + \Delta A x + \Delta B(x) + \frac{\sqrt{\Delta}}{\sqrt{N}} \sigma(x) \xi_i \\
&\quad - e^{A\Delta} \left(x + \Delta B(x) + \frac{\sqrt{\Delta}}{\sqrt{N}} \sigma(x) \xi_i \right) \\
&= x + \Delta A x + \Delta B(x) + \frac{\sqrt{\Delta}}{\sqrt{N}} \sigma(x) \xi_i \\
&\quad - x - \Delta B(x) - \frac{\sqrt{\Delta}}{\sqrt{N}} \sigma(x) \xi_i \\
&\quad - \Delta A x - \Delta^2 A B(x) - \frac{\Delta^{\frac{3}{2}}}{\sqrt{N}} \sigma(x) \xi_i + O(\Delta^3) \\
&= -\Delta^2 A B(x) - \frac{\Delta^{\frac{3}{2}}}{\sqrt{N}} \sigma(x) \xi_i + O(\Delta^3)
\end{aligned}$$

Consequently, we get that

$$\begin{aligned}
\left\| \mathbb{E}\left[\tilde{X}_{t_{i+1}}^{EM}(x, t_i) - \tilde{X}_{t_{i+1}}(x, t_i) \right] \right\| &= O(\Delta^2), \\
\left\| \tilde{X}_{t_{i+1}}^{EM}(x, t_i) - \tilde{X}_{t_{i+1}}(x, t_i) \right\|_{L^2} &= O(\Delta^{\frac{3}{2}}).
\end{aligned}$$

Let us mention that the two bounds above do not depend on x because B and σ are uniformly bounded. Recalling (4.21), the result follows from the fundamental theorem on the mean-square order of convergence, see Theorem 1.1. in Milstein and Tretyakov (2004). □

Theorem 4.5 states that as $\Delta \to 0$, the approximated solution $(\tilde{X}_{t_i})_{i=0,\dots,i_{\max}}$ converges to the true process $(X_t)_{t \geq 0}$ in the mean-square sense. In practice, however, fixed time steps $\Delta > 0$ are required. Thus, there is not yet any guarantee that the constructed numerical solutions share the same properties as the true solution of (4.7). For these reasons, in addition, we study the ability of $(\tilde{X}_{t_i})_{i=0,\dots,i_{\max}}$ to preserve the properties of SDE (4.7).

Note also that, different to ODE systems (Hairer et al., 2006), for stochastic equations the theoretical order of convergence usually cannot be increased by using the Strang composition instead of the Lie-Trotter approach. In practice, however, the Strang splitting often performs better than the Lie-Trotter method, see, e.g., Ableidinger et al. (2017), Buckwar et al. (2019). This is also confirmed by our numerical experiments in Section 4.6.

4.4.2 *Moment bounds of the approximated process*

We are now interested in studying the qualitative properties of the splitting schemes for fixed time steps $\Delta > 0$. We start by illustrating that the constructed splitting schemes preserve the convolution-based structure of the model derived in Proposition 4.2. Using the one-step approximation (4.18) and performing back iteration yields

$$\tilde{X}_{t_i} = e^{At_i}x_0 + \Delta \sum_{l=1}^{i} e^{At_l} B(\tilde{X}_{t_{i-l}}) + \frac{\sqrt{\Delta}}{\sqrt{N}} \sum_{l=1}^{i} e^{At_l} \sigma(\tilde{X}_{t_{i-l}}) \xi_{i-l}. \tag{4.22}$$

Note that the first term on the right side of (4.15) is preserved exactly. Moreover, the sums in (4.22) correspond to approximations of the integrals in (4.15) using the left point rectangle rule. Expression (4.22) allows to derive moment bounds for the numerical process in a similar fashion as presented for the continuous process in the previous section.

Theorem 4.6 (First moment bounds of the approximated process). *Grant assumption (A). The following bounds hold for the components of $\mathbb{E}[\tilde{X}_{t_i}]$:*

$$\tilde{\mathcal{I}}_{\min}^{k,j} \leq \mathbb{E}[\tilde{X}_{t_i}^{k,j}] \leq \tilde{\mathcal{I}}_{\max}^{k,j},$$

where

$$\tilde{\mathcal{I}}_{\min}^{k,j} = \left(e^{At_i}x_0\right)^{k,j} + \Delta \sum_{l=0}^{i} e^{-\nu_k t_l} t_l^{\eta_k+1-j} \min\left\{0, \frac{c_k f_{k+1}^{\max}}{(\eta_k+1-j)!}\right\}$$

$$\tilde{\mathcal{I}}_{\max}^{k,j} = \left(e^{At_i}x_0\right)^{k,j} + \Delta \sum_{l=0}^{i} e^{-\nu_k t_l} t_l^{\eta_k+1-j} \max\left\{0, \frac{c_k f_{k+1}^{\max}}{(\eta_k+1-j)!}\right\}.$$

Proof of Theorem 4.6. From Remark 4.2 and (4.22), it follows that

$$\tilde{X}_{t_i}^k = (e^{At_i}x_0)^k + \Delta \sum_{l=1}^{i} e^{A\nu_k t_l} B^k(\tilde{X}_{t_{i-l}}^{k+1}) + \frac{\sqrt{\Delta}}{\sqrt{N}} \sum_{l=1}^{i} e^{A\nu_k t_l} \sigma^k(\tilde{X}_{t_{i-l}}^{k+1}) \xi_{i-l}.$$

Consequently, the j-th components are given by

$$\tilde{X}_{t_i}^{k,j} = \underbrace{(e^{At_i}x_0)^{k,j}}_{=T_1(t_i)} + \underbrace{\frac{1}{(\eta_k+1-j)!}\Delta\sum_{l=1}^{i}c_k f_{k+1}(\tilde{X}_{t_{i-l}}^{k+1,1})e^{-\nu_k t_l}t_l^{\eta_k+1-j}}_{:=\tilde{T}_2(t)}$$

$$+ \underbrace{\frac{1}{(\eta_k+1-j)!}\frac{\sqrt{\Delta}}{\sqrt{N}}\sum_{l=1}^{i}\frac{c_k}{\sqrt{p_{k+1}}}\sqrt{f_{k+1}(\tilde{X}_{t_{i-l}}^{k+1,1})}e^{-\nu_k t_l}t_l^{\eta_k+1-j}\xi_{i-l}^{k+1}}_{:=\tilde{T}_3(t_i)}.$$

Note that, $\mathbb{E}[T_1(t_i)] = T_1(t_i)$, and $\mathbb{E}[\tilde{T}_3(t)] = 0$. The fact that the intensity function is bounded by $0 < f_{k+1} \leq f_{k+1}^{\max}$ implies the result. $\qquad\square$

Note that the bounds obtained in Theorem 4.6 equal those derived in Theorem 4.3, up to replacing the integrals (calculated in the proof of Theorem 4.3) by left Riemann sums. The accuracy of this approximation depends on the step size Δ. Under reasonably small choices of Δ, the bounds are preserved accurately for all t_i. This is illustrated in the left panel of Figure 4.2, where we plot the first moment bound of the process (main variable of an excitatory population) and the one of the approximated process, derived in Theorem 4.3 and Theorem 4.6, respectively. Different choices of ν_k are compared and for the bound of the approximated process $\Delta = 0.1$ is used.

The following Corollary gives an intuition of the long-time behaviour of the bounds.

Corollary 4.1. *(i) The following bounds hold for the components of $\mathbb{E}[\tilde{X}_{t_i}]$ as $i \to \infty$ (and Δ fixed):*

$$\Delta^{\kappa^{k,j}+1}Li_{-\kappa^{k,j}}\left(e^{-\nu_k\Delta}\right)\min\left\{0,\frac{f_{k+1}^{max}c_k}{\kappa^{k,j}!}\right\} \leq \lim_{i\to\infty}\mathbb{E}[\tilde{X}_{t_i}^{k,j}]$$

$$\leq \Delta^{\kappa^{k,j}+1}Li_{-\kappa^{k,j}}\left(e^{-\nu_k\Delta}\right)\max\left\{0,\frac{f_{k+1}^{max}c_k}{\kappa^{k,j}!}\right\},$$

where $\kappa^{k,j} := \eta_k + 1 - j$ and $Li_{-\kappa^{k,j}}\left(e^{-\nu_k\Delta}\right)$ is a polylogarithm function, which can be written as

$$Li_{-\kappa^{k,j}}\left(e^{-\nu_k\Delta}\right) = (-1)^{\kappa^{k,j}+1}\sum_{l=0}^{\kappa^{k,j}}l!\,S(\kappa^{k,j}+1,l+1)\left(\frac{-1}{1-e^{-\nu_k\Delta}}\right)^{l+1},$$

where $S(\kappa^{k,j}+1,l+1)$ denotes the Stirling numbers of second kind (Rennie and Dobson (1969)).

(ii) The following bounds hold for the components of $\mathbb{E}[\tilde{X}_{t_i}]$ as $i \to \infty$ and $\Delta \to 0$:

$$\min\left\{0,\frac{c_k f_{k+1}^{max}}{\nu_k^{\kappa^{k,j}+1}}\right\} \leq \lim_{\Delta\to 0}\lim_{i\to\infty}\mathbb{E}[\tilde{X}_{t_i}^{k,j}] \leq \max\left\{0,\frac{c_k f_{k+1}^{max}}{\nu_k^{\kappa^{k,j}+1}}\right\}.$$

Proof. **(i)** The zero bound is trivial. Considering

$$\lim_{i\to\infty}\sum_{l=0}^{i}e^{-\nu_k t_l}t_l^{\kappa^{k,j}} = \lim_{i\to\infty}\sum_{l=0}^{i}e^{-\nu_k l\Delta}(l\Delta)^{\kappa^{k,j}}$$

$$= \lim_{i\to\infty}\Delta^{\kappa^{k,j}}\sum_{l=0}^{i}e^{-\nu_k l\Delta}l^{\kappa^{k,j}} = \Delta^{\kappa^{k,j}}Li_{-\kappa^{k,j}}\left(e^{-\nu_k\Delta}\right)$$

gives the result. The explicit form of the function is given in Wood (1992).
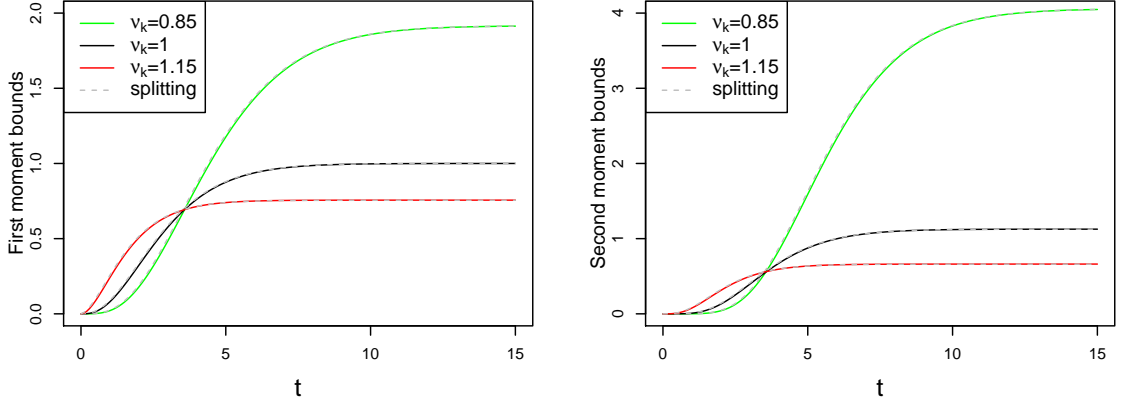
Figure 4.2: First (left panel) and second (right panel) moment bounds of the excitatory population $k = 2$ for different values of ν_2. The moment bounds for the diffusion are in solid lines and the moment bounds for the splitting scheme are in dashed lines. The bound of the rate function is fixed to $f_1^{\max} = 1$. The parameters are $\eta_2 = 3$, $N = 100$, $p_1 = 1/2$ and the time step $\Delta = 0.1$ is used.

(ii) Let us rewrite once again the expression included in the limit:

$$(-1)^{\kappa^{k,j}+1} \lim_{\Delta \to 0} \frac{(\nu_k \Delta)^{\kappa^{k,j}+1}}{\nu_k^{\kappa^{k,j}+1} \kappa^{k,j}!} \sum_{m=0}^{\kappa^{k,j}} m! \, S(\kappa^{k,j}+1, m+1) \left(\frac{-1}{1 - e^{-\nu_k \Delta}} \right)^{m+1}$$

$$= \lim_{\Delta \to 0} \left[\frac{S(\kappa^{k,j}+1, \kappa^{k,j}+1)\kappa^{k,j}!}{\nu_k^{\kappa^{k,j}+1} \kappa^{k,j}!} \left(\frac{\nu_k \Delta}{1 - e^{-\nu_k \Delta}} \right)^{\kappa^{k,j}+1} \right.$$

$$\left. - \Delta \frac{S(\kappa^{k,j}+1, \kappa^{k,j})(\kappa^{k,j}-1)!}{\nu_k^{\kappa^{k,j}} \kappa^{k,j}!} \left(\frac{\nu_k \Delta}{1 - e^{-\nu_k \Delta}} \right)^{\kappa^{k,j}} + O(\Delta^2) \right].$$

Note that $\lim_{\Delta \to 0} \left(\frac{\nu_k \Delta}{1 - e^{-\nu_k \Delta}} \right) = 1$. This implies that in the limit $1/\nu_k^{\kappa^{k,j}+1}$ is the only remaining term, since the rest converges to 0 as $\Delta \to 0$. This gives the result. $\qquad \square$

In the first part of Corollary 4.1, the sums in Theorem 4.6 are calculated explicitly as $i \to \infty$. This limit is described by polylogarithm functions. Note that the zero bounds derived in Remark 4.3, i.e., the upper bounds for the inhibitory population ($c_k = -1$) and the lower bounds for the excitatory population ($c_k = +1$) are preserved exactly by the splitting scheme for all times t_i and for all choices of $\Delta > 0$. Moreover, the lower bounds for the inhibitory population and the upper bounds for the excitatory population are preserved accurately as $i \to \infty$, provided that Δ is reasonably small. Indeed, as $i \to \infty$ and $\Delta \to 0$ (second part of Corollary 4.1), the bounds coincide with the ones obtained in Remark 4.3.

Theorem 4.7 (Second moment bounds of the approximated process). *Grant assumption (A). Each component of $\mathbb{E}[(\tilde{X}_t^k)^2]$ is bounded by*

$$\mathbb{E}[(\tilde{X}_t^{k,j})^2] \leq \left(\left(e^{At} x_0 \right)^{k,j} \right)^2 + 2 \left(e^{At} x_0 \right)^{k,j} \max \left\{ 0, \frac{c_k f_{k+1}^{\max}}{(\eta_k + 1 - j)!} \tilde{I}_1^{k,j}(t) \right\}$$

$$+ f_{k+1}^{\max} \left(\frac{c_k}{(\eta_k + 1 - j)!} \right)^2 \left(\sqrt{f_{k+1}^{\max}} \, \tilde{I}_1^{k,j}(t) + \sqrt{\frac{\tilde{I}_2^{k,j}(t)}{N \cdot p_{k+1}}} \right)^2,$$

where $\tilde{I}_u^{k,j}(t)$, $u = 1, 2$, are defined as

$$\tilde{I}_u^{k,j}(t) := \Delta \sum_{l=0}^{i} e^{-u\nu_k t_l} t_l^{u(\eta_k + 1 - j)}.$$

Proof of Theorem 4.7. The proof repeats the proof of Theorem 4.4, up to replacing integrals $I_u^{k,j}(t)$ by sums $\tilde{I}_u^{k,j}(t)$. $\qquad\square$

Similar to before, the second moment bounds obtained for the splitting scheme equal those derived for the true process in Theorem 4.4, except that the integrals are replaced by corresponding Riemann sums. Using the same arguments as in the proof of Corollary 4.1, we conclude that also the second moment bounds are preserved accurately by the splitting scheme for reasonable choices of the time step Δ. A comparison of the theoretical and discrete second moment bounds is provided in the right panel of Figure 4.2.

4.4.3 *Geometric ergodicity of the approximated process*

Finally, our aim is to prove that the splitting scheme preserves the ergodic property of the underlying process in the spirit of Mattingly et al. (2002), Ableidinger et al. (2017), providing a discrete analogue of Proposition 4.1. The main step is to establish a discrete Lyapunov condition for the approximated solution $(\tilde{X}_{t_i})_{i=0,\dots,i_{\max}}$. It is granted by the following lemma.

Lemma 4.1 (Lyapunov condition for the approximated process)**.** *Grant assumption (A). The functional $\tilde{G}$, given by*

$$\tilde{G}(x) = \sum_{k=1}^{2} \sum_{j=1}^{\eta_k + 1} \frac{j}{\nu_k^{j-1}} \left| x^{k,j} \right|,$$

is a Lyapunov function for $\tilde{X}$, i.e., there exist constants $\alpha \in [0, 1)$ and $\beta \geq 0$, such that

$$\mathbb{E}\left[\tilde{G}(\tilde{X}_{t_{i+1}}) | \tilde{X}_{t_i}\right] \leq \alpha \tilde{G}(\tilde{X}_{t_i}) + \beta.$$

Proof. We bound the approximated solution obtained via (4.18) from above by a sum of three terms, thanks to the triangle inequality:

$$\tilde{G}(\tilde{X}_{t_{i+1}}) = \tilde{G}\left(e^{A\Delta}\tilde{X}_{t_i} + \Delta e^{A\Delta} B(\tilde{X}_{t_i}) + \frac{\sqrt{\Delta}}{\sqrt{N}} e^{A\Delta} \sigma(\tilde{X}_{t_i}) \xi_i\right)$$

$$\leq \underbrace{\tilde{G}\left(e^{A\Delta}\tilde{X}_{t_i}\right)}_{T_1} + \underbrace{\Delta \tilde{G}\left(e^{A\Delta} B(\tilde{X}_{t_i})\right)}_{T_2} + \underbrace{\frac{\sqrt{\Delta}}{\sqrt{N}} \tilde{G}\left(e^{A\Delta} \sigma(\tilde{X}_{t_i}) \xi_i\right)}_{T_3}.$$

Note that the term T_2, as well as the expectation of T_3 is bounded by a constant depending on $f_k^{\max}$, so that $\mathbb{E}[T_2|\tilde{X}_{t_i}] + \mathbb{E}[T_3|\tilde{X}_{t_i}] \leq \beta$, and $\beta > 0$ since we consider the absolute value. Further, using the formulas (4.16)-(4.17), we can expand T_1 as follows.

$$
\begin{aligned}
\tilde{G}\left(e^{A\Delta}\tilde{X}_{t_i}\right) &= \sum_{k=1}^{2} e^{-\nu_k\Delta} \sum_{j=1}^{\eta_k+1} \frac{j}{\nu_k^{j-1}} \left| \sum_{m=j}^{\eta_k+1} \frac{\Delta^{m-j}}{(m-j)!} \tilde{X}_{t_i}^{k,m} \right| \\
&\leq \sum_{k=1}^{2} e^{-\nu_k\Delta} \sum_{j=1}^{\eta_k+1} \frac{j}{\nu_k^{j-1}} \sum_{m=j}^{\eta_k+1} \frac{\Delta^{m-j}}{(m-j)!} \left| \tilde{X}_{t_i}^{k,m} \right| \\
&= \sum_{k=1}^{2} e^{-\nu_k\Delta} \left[\sum_{j=1}^{\eta_k+1} \frac{j}{\nu_k^{j-1}} \left| \tilde{X}_{t_i}^{k,j} \right| + \Delta \sum_{j=2}^{\eta_k+1} \frac{j-1}{\nu_k^{j-2}} \left| \tilde{X}_{t_i}^{k,j} \right| + \cdots + \frac{\Delta^{\eta_k}}{\eta_k!} \left| \tilde{X}_{t_i}^{k,\eta_k+1} \right| \right] \\
&= \sum_{k=1}^{2} e^{-\nu_k\Delta} \left[\sum_{j=1}^{\eta_k+1} \frac{j}{\nu_k^{j-1}} \left| \tilde{X}_{t_i}^{k,j} \right| + \Delta\nu_k \sum_{j=2}^{\eta_k+1} \frac{j-1}{\nu_k^{j-1}} \left| \tilde{X}_{t_i}^{k,j} \right| + \cdots + \frac{(\nu_k\Delta)^{\eta_k}}{\eta_k!} \frac{1}{\nu_k^{\eta_k}} \left| \tilde{X}_{t_i}^{k,\eta_k+1} \right| \right].
\end{aligned}
$$

Note that, since $\nu_k > 0$, for all $m \geq 1$ it holds that

$$
\sum_{j=m}^{\eta_k+1} \frac{(j-m+1)}{\nu_k^{j}} \left| \tilde{X}_{t_i}^{k,j} \right| \leq \sum_{j=1}^{\eta_k+1} \frac{j}{\nu_k^{j}} \left| \tilde{X}_{t_i}^{k,j} \right| = \tilde{G}\left(\tilde{X}_{t_i}^{k}\right).
$$

Thus, we have

$$
\tilde{G}\left(e^{A\Delta}\tilde{X}_{t_i}\right) \leq \sum_{k=1}^{2} \left(e^{-\nu_k\Delta} \sum_{j=0}^{\eta_k} \frac{(\nu_k\Delta)^j}{j!} \right) \tilde{G}\left(\tilde{X}_{t_i}^{k}\right).
$$

Denote $\alpha = \max_k \left(e^{-\nu_k\Delta} \sum_{j=0}^{\eta_k} \frac{(\nu_k\Delta)^j}{j!} \right)$. Since η_k is finite, we get $\alpha < 1$, which implies the result. $\quad\square$

Note that the statement of Lemma 4.1 holds without any assumption on the time step Δ. Also, the Lyapunov function is the same as for the continuous process up to smoothing the absolute value (see (4.14)). Having established a discrete Lyapunov condition, the ergodicity is conditioned on two further technical steps. First, the transition probability of two (or more) consecutive steps, given by the recursive relation (4.18), must have a smooth transition density. This fact is granted by the hypoellipticity of the scheme (see Remark 4.5).

Second, the irreducibility condition must hold. It means that any point $y \in \mathbb{R}^\kappa$ could be reached from any starting point $x \in \mathbb{R}^\kappa$ in a fixed number of steps. In other words, we need a discrete-time analogue of Theorem 4 in Löcherbach (2019), granting the controllability of SDE (4.7). It is the following Lemma, which is proved in Appendix.

Lemma 4.2 (Irreducibility condition). *Grant assumption (A). Denote $\eta^* = \max_k\{\eta_k\}$. Then, for all $x, y \in \mathbb{R}^\kappa$ there exists some sequence of 2-dimensional vectors $(\xi_i)_{i=1,\dots,\eta^*+1}$ such that*

$$
y = \underbrace{(\psi_\Delta[\xi_{\eta^*+1}] \circ \cdots \circ \psi_\Delta[\xi_1])}_{\eta^*+1}(x),
$$

where ψ_Δ denotes one step of the scheme defined by (4.18), where the notation $[\cdot]$ is introduced to stress the dependency on the vectors $(\xi_i)_{i=1,\dots,\eta^*+1}$.

Lemmas 4.1 and 4.2, combined with the hypoellipticity of the scheme gives the following result, which is analogous to Theorem 7.3 in Mattingly et al. (2002).

Theorem 4.8 (Geometric ergodicity). *Grant Assumption* **(A)**. *Then the process* $(\tilde{X}_{t_i})_{i=0,\ldots,i_{\max}}$ *has a unique invariant measure* π^Δ *on* $\mathbb{R}^\kappa$. *For all initial conditions* x_0 *and all* $m \geq 1$, *there exist* $\tilde{C} = C(m, \Delta) > 0$ *and* $\tilde{\lambda} = \tilde{\lambda}(m, \Delta) > 0$ *such that, for all measurable functions* $g : \mathbb{R}^\kappa \to \mathbb{R}$ *such that* $|g| \leq \tilde{G}^m$,

$$\forall i = 0, \ldots, i_{\max}, \quad \left| \mathbb{E}g(\tilde{X}_{t_i}) - \pi^\Delta(g) \right| \leq \tilde{C}\tilde{G}(x_0)^m e^{-\tilde{\lambda}t_i}.$$

4.5 THINNING PROCEDURE FOR THE SIMULATION OF PDMP

In this section we explain the simulation method for the multidimensional point process characterized by the intensities (4.1). This part is motivated by the fact that, on the contrary to the diffusion, the simulation of the PDMP can be exact. By that, we mean that the result of the simulation is a realization of $(\bar{X}_t)_{t \geq 0}$. In comparison, the result of the simulation of the diffusion $(X_t)_{t \geq 0}$ is in fact the discrete time process $(\tilde{X}_{t_i})_{i=0,\ldots,i_{\max}}$. This allows us to compare the PDMP (4.5) with the stochastic diffusion defined through (4.7), which we treat via the property-preserving splitting scheme, We choose the thinning procedure which dates back to Lewis and Shedler (1979) and Ogata (1981). It is based on the rejection principle and relies on the following fact. In order to simulate a point process Z according to the stochastic intensity λ_t, it is sufficient to simulate some (dominating) point process $\tilde{Z}$ with (dominating) predictable piece-wise constant intensity $\tilde{\lambda}$ such that $\lambda_t \leq \tilde{\lambda}_t$. During the simulation of $\tilde{Z}$, each new simulated spiking time $\tilde{T}$ for $\tilde{Z}$ is kept as a point of Z with probability $\lambda_{\tilde{T}}/\tilde{\lambda}_{\tilde{T}}$ (independently from every other point). Otherwise, $\tilde{T}$ is discarded. The efficiency of the thinning procedure is highly related to the sharpness of the upper-bound $\tilde{\lambda}$. The sharper the bound, the less rejections are made and the more efficient is the procedure.

Note that the case $\eta_k = 0$ corresponds to the exponential kernel. The simulation of Hawkes processes with an exponential kernel is widely studied and there exist several implemented packages, e.g., for the software R. Moreover, apart from the thinning procedure, other exact simulation algorithms are available, see, in particular, Dassios et al. (2013). To the best of our knowledge, the only reference for the case when $\eta_k \geq 1$ is Duarte et al. (2019). The aim of the current section is to generalize the algorithm presented in the above mentioned work to the case of multiple populations and to provide a more efficient upper bound $\tilde{\lambda}$. In particular, our approach allows for an efficient handling of rapidly increasing intensity functions.

4.5.1 *Choice of an upper bound for the intensity*

If $\bar{Z}_t = 0$, i.e., in absence of any spike, it follows from (4.5) that $\bar{X}$ evolves as a linear ODE with matrix A so that $\bar{X}_t = e^{At}x_0$. In particular, for all neurons $n = 1, \ldots, N_k$, it follows that

$$\lambda_t^{k,n} = f_k((e^{At}x_0)^{k,1}). \tag{4.23}$$

One possible choice for the dominating intensity $\tilde{\lambda}$ in the thinning procedure is to provide an upper-bound of (4.23) which holds for all $t \geq 0$. A straightforward candidate for such a bound is provided in the following lemma.

Lemma 4.3. *For any $x \in \mathbb{R}^\kappa$, let $\Phi_k(x) = \sup_{t \geq 0}(e^{At}x)^{k,1}$. Then,*

$$\Phi_k(x) \leq \tilde{\Phi}_k(x) = \max_{j=1,\ldots,\eta_k+1} \left\{ 0, \frac{x^{k,j}}{\nu_k^{j-1}} \right\}.$$

Proof. The explicit expression of $(e^{At}x)^{k,1}$ is given in (4.17), that is:

$$(e^{At}x)^{k,1} = e^{-\nu_k t}\left(x^{k,1} + tx^{k,2} + \cdots + \frac{t^{\eta_k}}{\eta_k!}x^{k,\eta_k+1} \right).$$

Setting $y_j = x^{k,j}/(\nu_k)^{j-1}$, one gets

$$(e^{At}x)^{k,1} = e^{-\nu_k t}\left(y_1 + t\nu_k y_2 + \cdots + \frac{(t\nu_k)^{\eta_k}}{\eta_k!}y_{\eta_k+1} \right) \leq \max_k\{0, y_k\}e^{-\nu_k t}g(t).$$

The result follows from the fact that $g(t) = 1 + t\nu_k + \cdots + (t\nu_k)^{\eta_k}/\eta_k! \leq e^{\nu_k t}$. $\quad\square$

Remark 4.6. *Another possible choice of a uniform bound, similar to the one given in Lemma 4.3, is provided in Duarte et al. (2019). Their method, adapted to our case, gives*

$$\Phi_k(x) \leq e\max\left\{ 1, \left(\frac{\eta_k}{e\nu_k} \right)^{\eta_k} \right\} \max_j\{x^{k,j}\},$$

which is larger, and thus less efficient than the bound proposed in Lemma 4.3.

Since the functions f_k are non-decreasing, the upper-bound of $(e^{At}x)^{k,1}$ given in Lemma 4.3 provides the bound $\tilde{f}_k(x) = f_k(\tilde{\Phi}_k(x))$ on the intensity. However, there is no guarantee that this bound is sharp. In most practical cases (especially when the functions f_k are increasing fast), the procedure rejects a vast majority of the simulated points. Hence, a more efficient approach, based on the computation of the critical points of the function $(e^{At}x)^{k,1}$, is proposed. Further, instead of considering a bound for any $t > 0$ we choose a fixed time step $\tilde{\Delta} > 0$ (such that one spike is likely to occur in the interval $[0, \tilde{\Delta}]$) and compute $\Phi_k^{\tilde{\Delta}}(x) = \sup_{0 \leq t \leq \tilde{\Delta}}(e^{At}x)^{k,1}$ instead of $\Phi_k(x)$. This choice has no impact on the precision of the simulation. It only influences the sharpness of the bound used in the method and thus its computational efficiency.

Lemma 4.4. *For any $x \in \mathbb{R}^\kappa$, it holds that*

$$\Phi_k^{\tilde{\Delta}}(x) = \max_{0 < t_c < \tilde{\Delta}}\{x^{k,1}, (e^{At_c}x)^{k,1}, (e^{A\tilde{\Delta}}x)^{k,1}\},$$

where the maximum is taken over the critical points t_c of $t \mapsto (e^{At}x)^{k,1}$, that are the solutions of the equation

$$(-\nu_k x^{k,1} + x^{k,2}) + \cdots + (-\nu_k x^{k,\eta_k} + x^{k,\eta_k+1})\frac{(t_c)^{\eta_k-1}}{(\eta_k-1)!} + (-\nu_k x^{k,\eta_k+1})\frac{(t_c)^{\eta_k}}{(\eta_k)!} = 0.$$

Proof. The result follows from the computation of the time derivative of $(e^{At}x)^{k,1}$. $\quad\square$
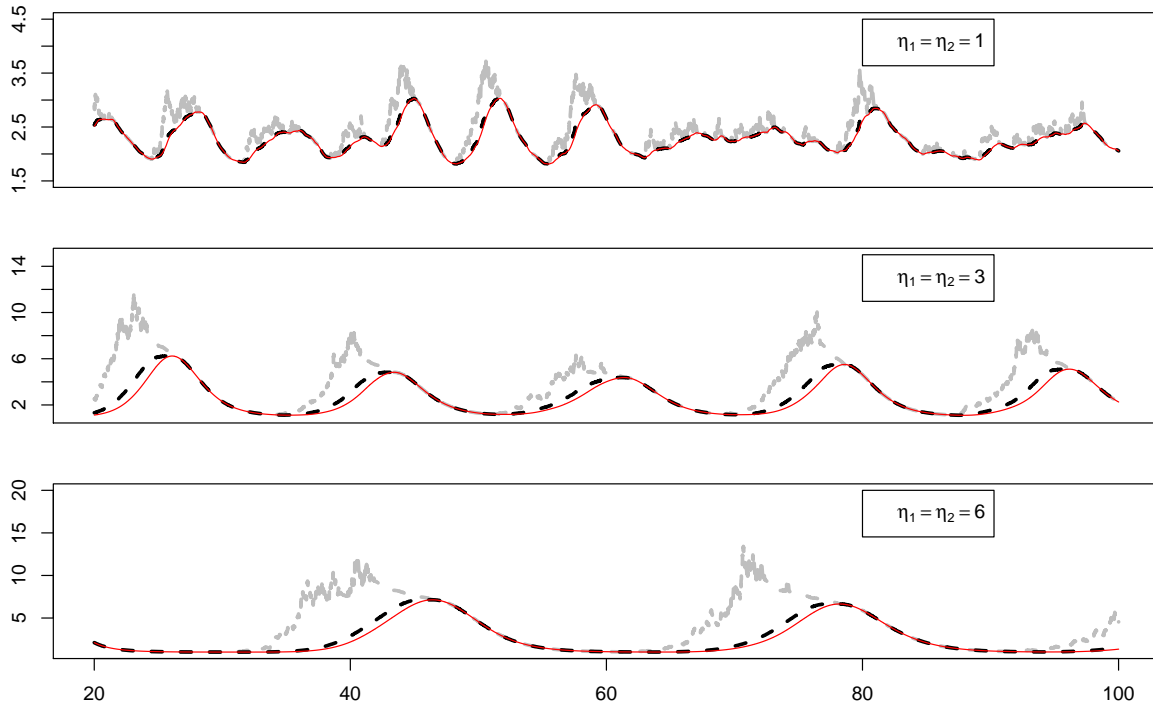
Figure 4.3: Intensity and intensity bounds for the second population (excitatory) $t \in [20, 100]$. Red solid line: true intensity λ_t^2, black dash line: $\tilde{f}_2^{\tilde{\Delta}}(\bar{X}_t)$, grey dash line: $\tilde{f}_2(\bar{X}_t)$. Intensity functions f_1 and f_2 are given by (4.24), $\nu_1 = \nu_2 = 0.9$, $N_1 = N_2 = 50$.

The critical points in Lemma 4.4 are given by polynomial roots, which can be accurately computed numerically. In most practical cases, the computational cost of the polynomial roots is compensated by the efficiency gained in the rejection method. Finally, let us define the upper-bound intensity function by

$$\tilde{f}_k^{\tilde{\Delta}}(x) = f_k(\Phi_k^{\tilde{\Delta}}(x)).$$

Note that when the population is inhibitory ($c_k = -1$), the naive upper-bound $\tilde{f}_k$ is constant with respect to time because all the coordinates of $\bar{X}^1$ are always negative and the bound given by Lemma 4.3 is 0. Thus, $\tilde{f}_k \equiv f_k(0)$. Of course, such a bound is not sharp in general. However, it is interesting to see how the two upper-bounds $\tilde{f}_k$ and $\tilde{f}_k^{\tilde{\Delta}}$ behave for a particular realisation of the intensity process for excitatory populations. Figure 4.3 gives a comparison of the paths of $\tilde{f}_2$ and $\tilde{f}_2^{\tilde{\Delta}}$ for the excitatory population (with $\tilde{\Delta} \equiv 1$). We observe that both bounds are rather precise when the potential $\bar{X}_t^2$ (and, respectively, the intensity process) is decreasing. On these intervals the differences between the three trajectories are negligible. However, the accuracy of $\tilde{f}_2$ drops drastically on the intervals where the intensity grows. In general, the higher is the amplitude of the oscillations, the less performing is the naive bound. This is particularly visible when illustrated on systems with high memory order ($\eta_k = 3$ or 6). For $\eta_k = 1$ both bounds perform good, however, $\tilde{f}_k^{\tilde{\Delta}}$ is clearly closer to the true process. The influence of the bound ($\tilde{f}_2$ or $\tilde{f}_2^{\tilde{\Delta}}$) on the execution time is discussed in Section 4.6.

4.5.2   *Simulation algorithm*

Now let us detail the recursive procedure, which is summarized in Algorithm 3. We choose a discrete time step $\tilde{\Delta}$, a stopping time $t_{\max}$ and fix the initial values $t_0 = 0$ and $\bar{X}_0 = x_0 \in \mathbb{R}^\kappa$. Let us assume that the procedure's current step is i with current time t_i and potential value $\bar{X}_i$. Let us explain how t_{i+1} and $\bar{X}_{i+1}$ are obtained. One simulates two independent exponential variables τ_1 and τ_2 with respective parameters $N_k \tilde{f}_k^{\tilde{\Delta}}(x)$ (one for each population). They represent the waiting times to the next spikes of the dominant process $\tilde{Z}$ for each respective population. Then, two cases may occur.

1. If $\min\{\tau_1, \tau_2\} > \tilde{\Delta}$, no spike occurs in the interval $[t_i, t_i + \tilde{\Delta}]$. We update $t_{i+1} = t_i + \tilde{\Delta}$ and $\bar{X}_{i+1} = e^{A\tilde{\Delta}} \bar{X}_i$.

2. If $\tau = \min\{\tau_1, \tau_2\} \leq \tilde{\Delta}$, then the dominating point process $\tilde{Z}$ emits a spike at time $t^* = t_i + \tau$. Let us denote by k^* the population with the smallest waiting time, that is $\tau = \tau_{k^*}$. It remains to decide whether t^* is also a spiking time for the process Z. If not, this point is discarded. We draw a uniform variable U on $[0, 1]$ and define the threshold R:

$$R := \frac{f_{k^*}\left(e^{A\tau}\bar{X}_i\right)}{\tilde{f}_{k^*}^{\tilde{\Delta}}(\bar{X}_i)}, \quad R \in [0,1] \text{ by the definition of } \tilde{f}_k^{\tilde{\Delta}}(x).$$

   - If $U \geq R$, then t^* is discarded, i.e., no spike occurs in the interval $[t_i, t^*]$. We update $t_{i+1} = t^*$ and $\bar{X}_{i+1} = e^{A\tau} \bar{X}_i$.

   - If $U < R$, then t^* is kept, i.e., we add t^* to the list of one neuron of population k^* chosen uniformly at random. We update $t_{i+1} = t^*$ and $\bar{X}_{i+1} = e^{A\tau} \bar{X}_i + \Gamma \mathbb{1}(k^*)$, where $\mathbb{1}(k^*) = (\mathbb{1}_{k^*=1}, \mathbb{1}_{k^*=2})^T$.

Finally, the execution is stopped once $t_i \geq t_{\max}$, i.e., once the time horizon of interest is reached. As output the algorithm returns a list of the spiking times of each neuron and the values of the processes $\bar{X}$ and λ at the spiking times. On this stage it is clear why it is important to have a sharp upper bound. The closer the threshold R is to 1, the less points are rejected.

Algorithm 3 is most efficient when every iteration of the **while** loop enters condition **(2)**. Of course, that ideal case does not occur in practice. When lowering the value of $\tilde{\Delta}$, the number of loops satisfying condition **(3)** decreases because the dominating intensity $\tilde{\lambda}$ is getting smaller. On the other hand, the number of loops fulfilling condition **(1)** increases because the exponentially distributed times have greater chances of being larger than $\tilde{\Delta}$. The calibration of $\tilde{\Delta}$ is a difficult problem which is not addressed here. In practice, it is observed that the execution time is not very sensitive to the value of $\tilde{\Delta}$. The main bottleneck of the thinning algorithm is the sharpness of the intensity bound. When the intensity functions are exponential, the computational time is more than halved with the bound of Lemma 4.4 compared to the bound of Lemma 4.3. This is illustrated in the right panel of Figure 4.8.

Algorithm 3: Simulation of model (4.1) with $K = 2$ populations.

Input: intensity functions f_1 and f_2; integers N_1, N_2, η_1 and η_2; real numbers c_1, c_2, ν_1, ν_2, $\tilde{\Delta}$ and $t_{\max}$; real vector $x_0 \in \mathbb{R}^\kappa$.

Output: point processes $(Z^{k,n})_{k=1,2;\, n=1,\ldots,N_k}$, Markovian cascade process $\bar{X}$ and intensity processes $(\lambda^k)_{k=1,2}$.

Initialization: $t \leftarrow 0$, $x \leftarrow x_0$;

while $t < t_{\max}$ **do**

$\quad \tilde{\lambda}_k \leftarrow \tilde{f}_k^{\tilde{\Delta}}(x)$ for $k = 1, 2$;

$\quad$ draw $\tau_k \sim \mathcal{E}(N_k \tilde{\lambda}_k)$ for $k = 1, 2$;

$\quad \tau \leftarrow \min_k \tau_k$ and $k^* \leftarrow \arg\min_k \tau_k$;

$\quad$ **if** $\tau > \tilde{\Delta}$ **then**

(1) $\quad\quad t \leftarrow t + \tilde{\Delta}$ and $x \leftarrow e^{A\tilde{\Delta}} x$;

$\quad$ **else**

$\quad\quad t \leftarrow t + \tau$, $x \leftarrow e^{A\tau} x$, $\lambda_{k^*} \leftarrow f_{k^*}(x)$;

$\quad\quad$ draw $U \sim \mathcal{U}([0,1])$;

$\quad\quad$ **if** $U < \lambda_{k^*} / \tilde{\lambda}_{k^*}$ **then**

(2) $\quad\quad\quad$ draw $n \sim \mathcal{U}(\{1, \ldots, N_{k^*}\})$ and add t to the list $Z^{k^*, n}$;

$\quad\quad\quad x \leftarrow x + \Gamma \mathbb{1}(k^*)$;

$\quad\quad\quad$ add x to the list $\bar{X}$ and $\lambda_k = f_k(x)$ to the list λ^k for $k = 1, 2$;

$\quad\quad$ **else**

(3) $\quad\quad\quad$ do nothing;

4.6 NUMERICAL EXPERIMENTS

A simulation study, illustrating the theoretical results discussed in the previous sections, is now provided. It consists in two steps. First, we study the performance of the proposed splitting schemes. More precisely, we compare the Lie-Trotter (4.18) and Strang (4.19) splitting schemes with the Euler-Maruyama approximation. We report sample paths, empirical densities and comment also on the first and second moments. This step follows the numerical study in Ableidinger et al. (2017), and shows that the Strang splitting performs best. Second, we compare the diffusion process (simulated with the property-preserving Strang splitting scheme) to the PDMP, varying the number of neurons N. In particular, when comparing the long-time behaviour of the processes (see Figure 4.9), we show that the diffusion approximation is less and less accurate as $t \to +\infty$. It confirms the results obtained in Theorems 4.1 and 4.2.

Following the work of Ditlevsen and Löcherbach (2017), throughout this section we use the following intensity functions

$$f_1(x) = \begin{cases} 10e^x & \text{if } x < \log(20) \\ \frac{400}{1+400e^{-2x}} & \text{if } x \geq \log(20) \end{cases}, \quad f_2(x) = \begin{cases} e^x & \text{if } x < \log(20) \\ \frac{40}{1+400e^{-2x}} & \text{if } x \geq \log(20) \end{cases}. \tag{4.24}$$

Further, we fix the parameters $c_1 = -1, c_2 = 1$ and consider $N_1 = N_2$. Unless stated differently, throughout this section the initial condition is fixed to $x_0 = 0_\kappa$. The parameter p_k is then defined as N_k/N. The fact that $c_1 c_2 < 0$ ensures that the population shows an oscillatory behaviour, for certain parameters ν_k and η_k (see Ditlevsen and Löcherbach (2017) for further details).

4.6.1 *Comparison of the Euler-Maruyama method and the splitting schemes*

In this section we are interested in comparing the performance of the splitting schemes with that of the frequently applied Euler-Maruyama method (EM), for varying time steps Δ. The parameter values $\nu_1 = \nu_2 = 1$, $\eta_1 = 3$, $\eta_2 = 2$, $N_1 = N_2 = 50$ are used and the dimension of the system is thus $\kappa = 7$. Except for the density and mean-square convergence plots, we consider the time interval $[0, 100]$. Unless stated otherwise, we plot the variables $X_t^{k,1}$ for $k = 1, 2$ in black and the remaining $\eta_1 + \eta_2$ auxiliary memory variables in grey.

4.6.1.1 *Illustration of the mean-square convergence order*

We start our study by comparing the convergence rates of the EM method and the Lie-Trotter (4.18) and Strang (4.19) splitting schemes. The root mean-square error, approximating the left side of the equation in Theorem 4.5, is defined as

$$\text{RMSE}(\Delta) := \left(\frac{1}{M} \sum_{l=1}^{M} \|X_{t^*}^{(l)} - \tilde{X}_{t^*}^{(l)}\|^2 \right)^{1/2},$$

where $X_{t^*}^{(l)}$ and $\tilde{X}_{t^*}^{(l)}$ denote the values at a fixed time t^* of the l-th simulated trajectory of the true process and its numerical approximation, respectively. The integer M is the total number of simulated
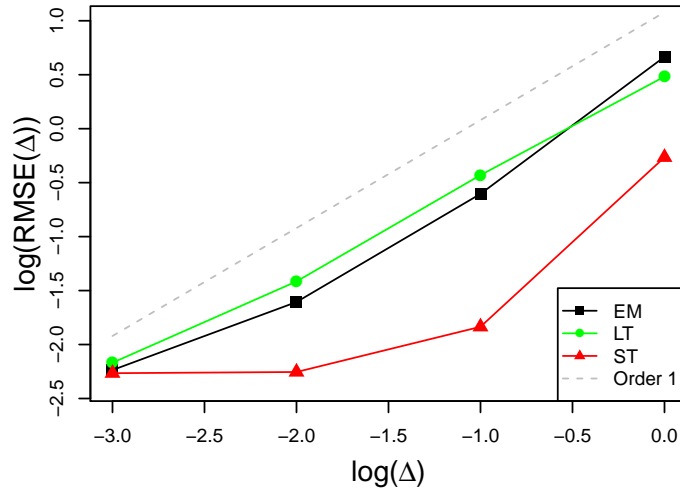
Figure 4.4: Mean-square order of convergence. The reference solution is obtained with the Euler-Maruyama method and the small time step $\Delta = 10^{-4}$. The numerical solutions are calculated for $\Delta = 10^{-3}, 10^{-2}, 10^{-1}, 10^{0}$. The log is with base 10, $t^* = 1$ and $M = 10^3$.

differences. The value of the true process $X_{t^*}^{(l)}$ is obtained from the EM scheme, using the small time step $\Delta = 10^{-4}$. The number of simulations is fixed to $M = 10^3$ and $t^* = 1$.

We report the RMSE in Figure 4.4, where the x-axis corresponds to the logarithm (base 10) of the time step Δ and the y-axis corresponds to the logarithm (base 10) of the RMSE. The theoretical rate of convergence obtained in Theorem 4.5 (all considered schemes converge with order 1) is confirmed empirically. While the Lie-Trotter splitting and the EM scheme show a similar RMSE for varying Δ, the RMSE obtained for the Strang splitting method is significantly smaller for all Δ under consideration, implying a higher efficiency of that scheme. We stress, however, that from the fact that the rate of convergence is the same, it does not follow that they share the same qualitative properties when the step size Δ is fixed.

4.6.1.2 *Illustration of the qualitative properties of the splitting schemes*

Now we illustrate how the proposed splitting schemes preserve the structure (e.g., the moments and the underlying invariant distribution) of the process, even for large values of Δ, while the EM method may fail in doing so. We start with studying sample trajectories (see Figure 4.5). All three methods yield a comparable performance when $\Delta = 0.01$. For $\Delta = 0.5$, the EM scheme preserves the oscillations, but does not preserve the amplitude. The behaviour of the inhibitory population is less accurately approximated than the excitatory one. This problem aggravates as Δ increases further to 0.7. An interesting observation is that, for time steps Δ not "small enough", the Euler-Maruyama scheme may not preserve the mean of the process (see also Figure 4.7). Indeed, it has been observed that the Euler-Maruyama method preserves the first, but not the second moments (see, e.g., Ableidinger et al. (2017), Higham and Strømenn Melbø (2004)). In other words, the amplitude of the oscillations grows, but the main is unchanged. In our case, however, since the trajectories are bounded by 0 from below or above (depending on the sign of c_k), the increased amplitude introduces also a bias in
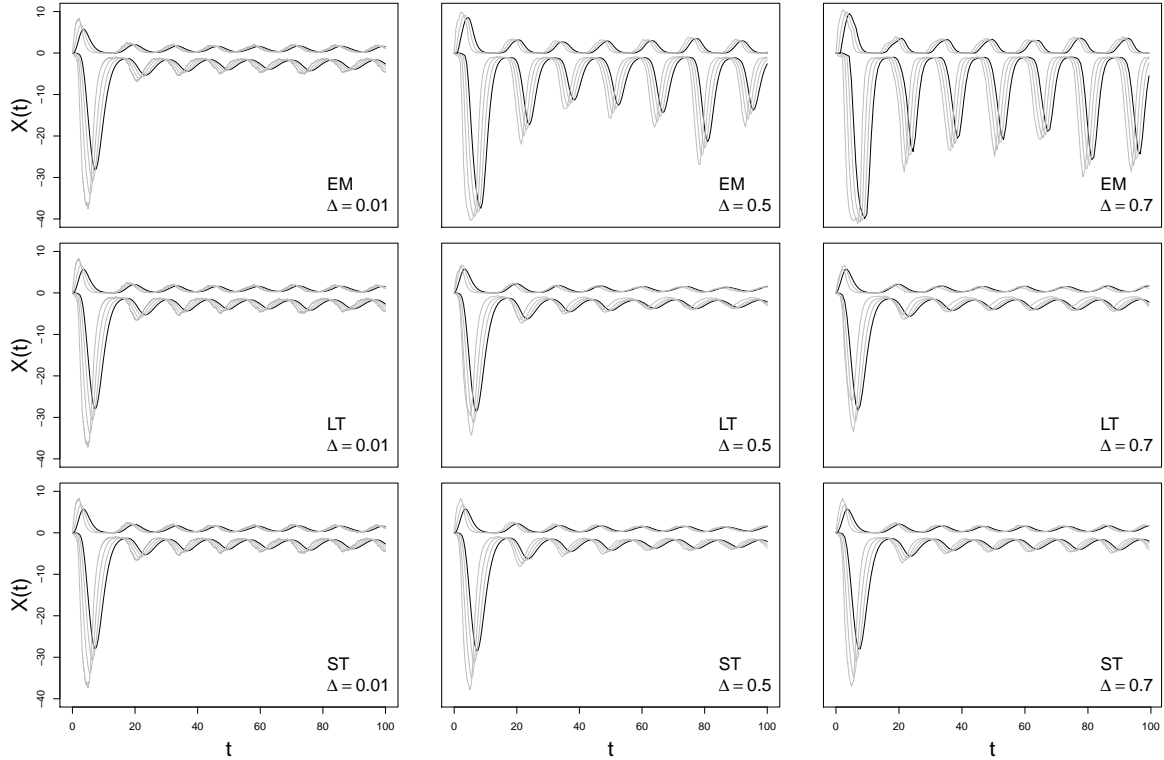
Figure 4.5: Sample trajectories of the system, simulated with the Euler-Maruyama scheme (top), the Lie-Trotter (middle) and the Strang (bottom) splitting scheme for varying Δ.

the first moment. Thus, the Euler-Maruyama approximation of system (4.7) does neither preserve the first nor the second moments. In contrast, the Lie-Trotter and Strang splitting schemes show a comparably good performance. However, the Lie-Trotter splitting is less accurate in reproducing the delay between the current state of the process (black line) and the memory variables (grey lines) in the beginning of the interval, where the amplitude of the oscillations is large (see also Figure 4.7). The difference between the schemes becomes clearer as we look at the phase portrait of the system (Figure 4.6). We observe again that both splitting schemes yield satisfactory approximations (for all Δ under consideration), the Strang approach slighly outperforming the Lie-Trotter method. In contrast, the phase portrait obtained with the EM approximation fails to reproduce the behaviour of the process for $\Delta = 0.5$ or 0.7. Similar conclusions can be drawn from Figure 4.7, where we visualize the marginal densities of the process. Each visualized density is estimated with a standard kernel density estimator, based on a simulated long-time trajectory ($T = 10^5$) of each variable of the process. We observe again that the EM method may not preserve the mean of the process (red dashed vertical lines). Moreover, the EM scheme may even suggest a transition from a unimodal to a bimodal density as Δ increases.

4.6.2 *Comparison of the PDMP and the diffusion*

Now we are interested in comparing the PDMP process $\bar{X}$, simulated with the thinning algorithm detailed in Section 4.5, with the diffusion X, simulated with the property-preserving Strang splitting
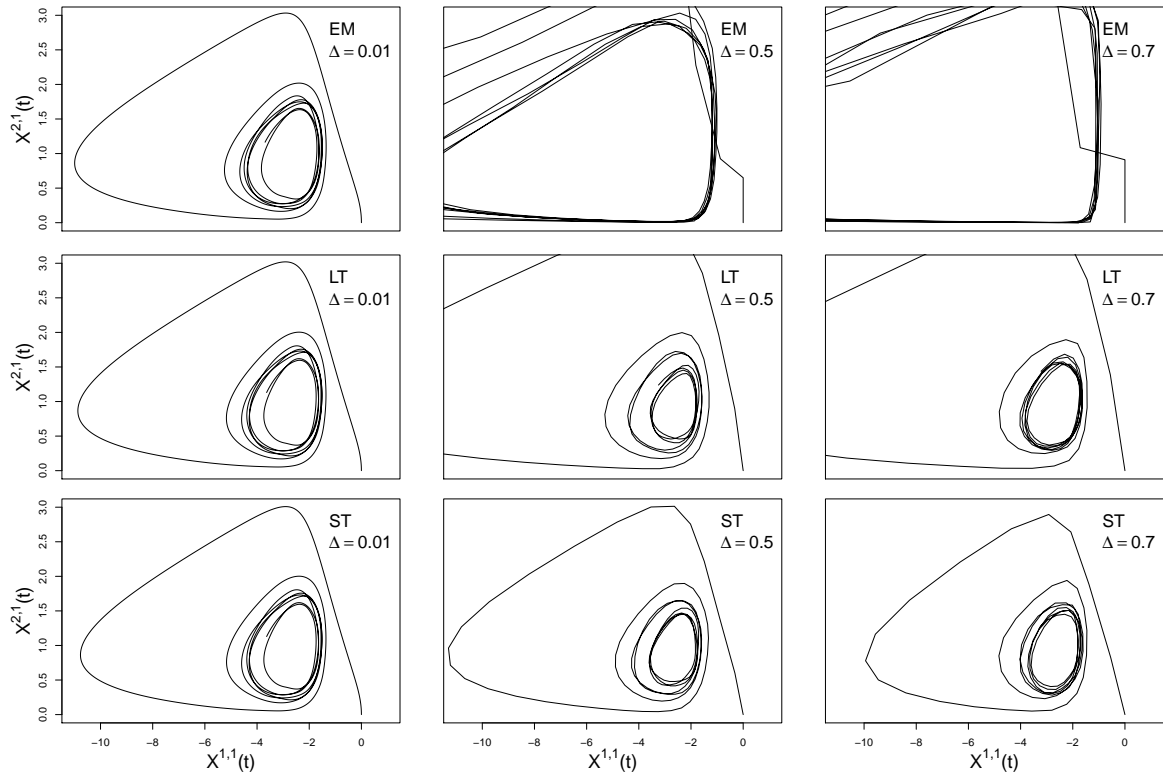
Figure 4.6: Phase portrait of the main variables, simulated with the Euler-Maruyama scheme (top), the Lie-Trotter (middle) and the Strang (bottom) splitting scheme for varying Δ and $x_0 = (0, 0, -3.5, -4, 0, 1.3, 1.1)$.
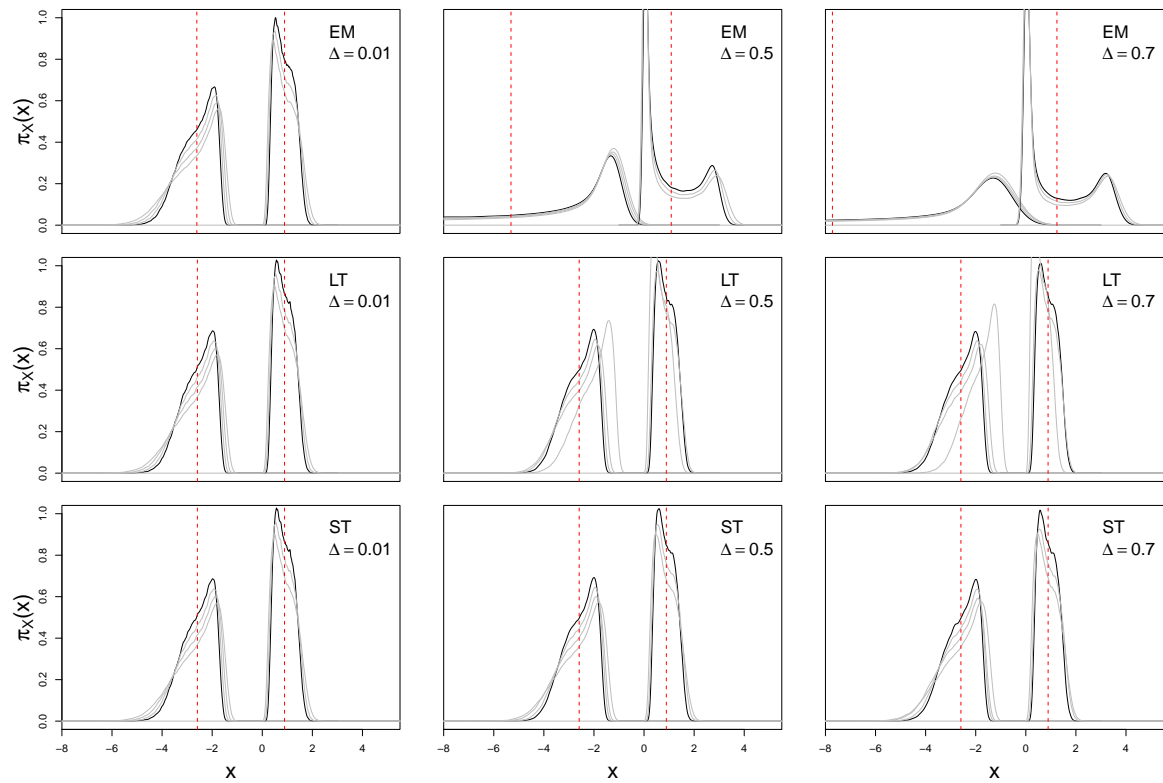
Figure 4.7: Empirical density of the system, simulated with the Euler-Maruyama scheme (top), the Lie-Trotter (middle) and the Strang (bottom) splitting scheme for varying Δ and $T = 10^5$.
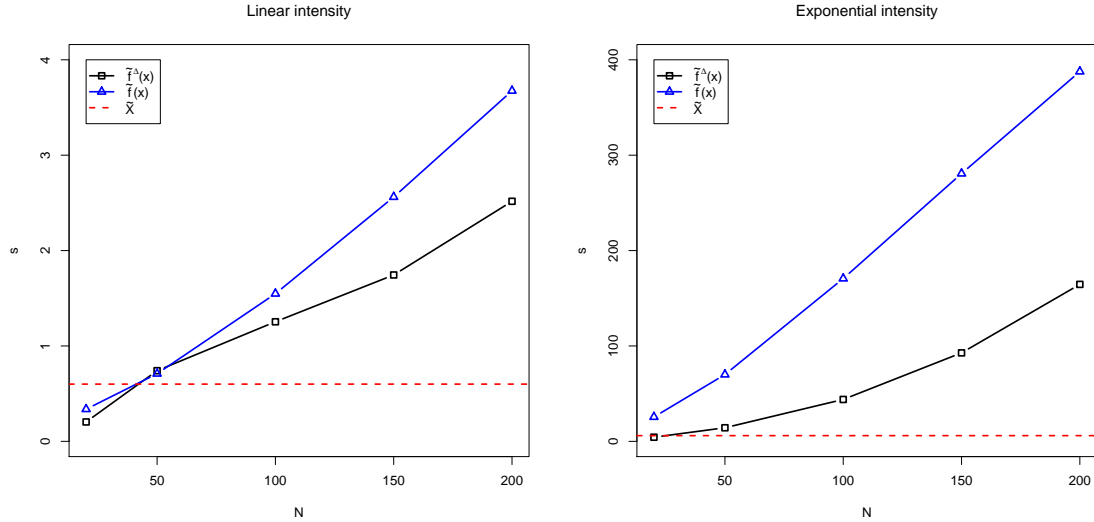
Figure 4.8: Mean execution time for the PDMP (solid line) and diffusion (dashed line) simulation for $t_{\max} = 100$ over 100 realizations. Right panel: $f_1(x) = f_2(x) = \min\{1 + x\mathbb{1}_{[x>0]}, 10\}$. Left panel: f_1 and f_2 are given by (4.24). The rest of the parameters are given in the beginning of Section 4.6.

scheme introduced in Section 4.4. We simulate the trajectories of the diffusion process with the Strang splitting scheme, since it has shown the best performance in the previous section.

4.6.2.1 *Execution time*

As a first step we are interested in the execution time. We compare the numerical cost of the simulation of the process $\bar{X}$ with two different intensity bounds (based on Lemmas 4.3 and 4.4) to the simulation of the diffusion X with the Strang splitting scheme.

We set $t_{\max} = 100$ and vary the total number of neurons, taking $N = 20, 50, 100, 150, 200$ and $N_1 = N_2$. In the case of the diffusion simulation, the parameter N does not influence the computational cost. Thus, we report the execution time for the diffusion simulation only for $N = 200$, taking $\Delta = 0.1$ and report it as a reference value. The time step $\tilde{\Delta}$ for the thinning procedure is defined in an adaptive way within the **while** loop of Algorithm 3. In each step we use the last computed value of the intensities λ_k and set $\tilde{\Delta}$ equal to $(N_1\lambda_1 + N_2\lambda_2)^{-1}$. This choice takes into account the scaling with respect to the number of neurons and the dynamics of the intensities. For instance, $\bar{X}^{2,1}$ roughly belongs to $[0, 2]$ (see Figure 4.9) such that the intensity of population roughly belongs to $[1, 7]$ (with the intensity functions defined in (4.24)).

In Figure 4.8, two different sets of intensity functions, linear ones and exponential ones, are studied. The mean execution time (over 100 realizations) in seconds required to simulate the process on interval $[0, t_{\max}]$, using the bounds $\tilde{f}(x)$ and $\tilde{f}^{\Delta}(x)$ are plotted.

Note that there is almost no difference in the performance of the algorithm with different bounds in the linear case (left panel of Figure 4.8). That means that the bound obtained in Lemma 4.3 is sharp enough. Note also that since $f_k^{\max} = 10$, there occur only a few spikes and the process is simulated very fast. However, in the case of an exponential intensity (right panel of Figure 4.8), the execution

time drastically increases. The process is simulated at least twice faster with the local bound. The main reason is that the local bound $\tilde{f}_k^\Delta(x)$ rejects around 2% of points, while the $\tilde{f}_k(x)$ rejects around 90%. In general, we can conclude that the execution time depends linearly on the number of neurons for both the local and the general bound. Disregarding the bound chosen, both algorithms cannot compete with the time required for simulating the diffusion. For $\Delta = 0.1$ and $T = 100$ the average running time with the exponential firing rate function is equal to 0.598s (with standard deviation 0.12s). For the linear one it is 0.597s (with standard deviation 0.15s). Thus, the execution time for the diffusion approximation does not depend on the firing rates.

Finally, a summary of the performances of both frameworks (diffusion and PDMP), with respect to the parameters of the model, is given below.

- In both cases, the execution time increases as the dimension of the system grows, i.e., as η_k increases.

- For the diffusion, the execution time depends, in a linear manner, on the step size Δ.

- For the PDMP, the execution time mainly depends, in a linear manner, on the number N of neurons. To be precise, it also depends on the temporal mean value of the intensities of the two populations, which in turn depends, in a complex non-linear manner, on the parameters ν_k, η_k and f_k.

- Unless N very small, the simulation of the diffusion requires much less computational cost than that of the PDMP.

4.6.2.2 *Qualitative properties*

It remains to determine if the stochastic diffusion can really catch the behaviour of the underlying PDMP. To get an intuitive idea of how different processes behave when the number of neurons changes we look at some sample trajectories. We take one realisation of the PDMP and the diffusion process on a time interval of length $T = 300$ and plot them on Figure 4.9, cutting the initial part in order to observe the process in its oscillatory regime. For simplicity, we focus only on the second (excitatory) population. The trajectories in the top panel are simulated with $N_2 = 10$, those in the middle panel with $N_2 = 50$ and those in the bottom panel with $N_2 = 100$.

Let us mention that Figure 4.9 is not an illustration of Theorem 4.2. Indeed, the trajectories are not coupled in such a way that (4.12) is satisfied. Up to our knowledge, there is no such result in the literature and the coupling involved in the proof of Theorem 4.2 is not explicit. However, the figure illustrates the fact that the fluctuations of both trajectories vanish as N goes to infinity and that both converge to the solution of the ODE (4.10).

As a final step, we are interested in the long-time behaviour of the processes. We simulate both processes ($\bar{X}$ and X) on a long-time interval, taking $T = 10^5$ and report the respective marginal empirical densities in Figure 4.10. The densities of the PDMP are plotted with solid lines and those of the diffusion with dashed lines. Even for small N, the difference between the densities is negligible
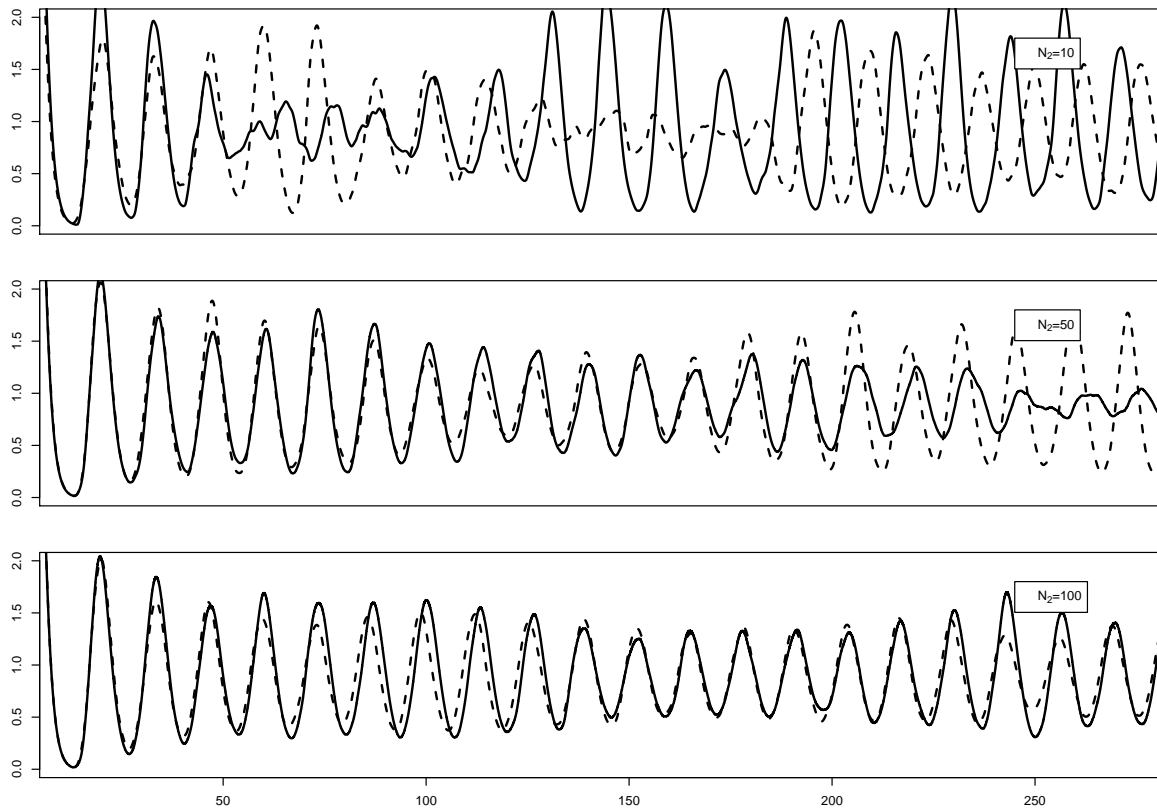
Figure 4.9: Sample trajectories of the PDMP and the diffusion for varying N (excitatory population). Solid line: main variable of $\bar{X}$, dashed line: main variable of X (simulated with the Strang splitting scheme, using $\Delta = 0.01$).
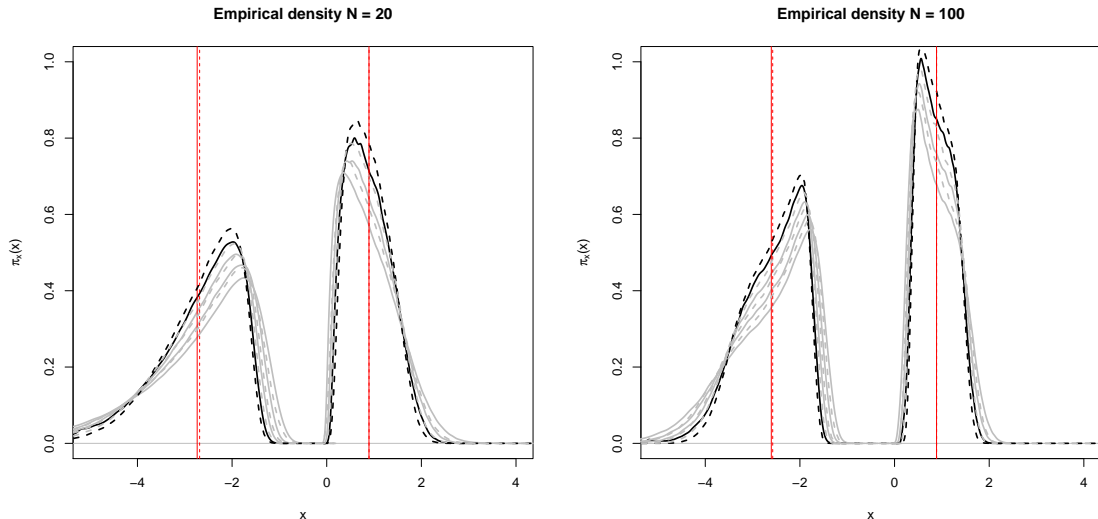
Figure 4.10: Empirical density of the PDMP and the diffusion for $N = 20$ (left) and $N = 100$ (right). Solid line: $\bar{X}$, dashed line: X (simulated with the splitting scheme, $\Delta = 0.1$, $T = 10^5$). The red solid and dashed vertical lines denote the mean of the respective main variables.

and their means are almost overlapping. As the number of neurons N increases, we observe that the empirical densities converge to some compactly supported distribution. Note that the mean-field limit is given by the ODE (4.10) as illustrated in Figure 4.9. Thus we expect that the support of the limit distribution is given by the amplitude of the solution of the ODE.

CONCLUSIONS

This work is thought to complement the papers by Ditlevsen and Löcherbach (2017) and Duarte et al. (2019). First, we bridge the gap between the piece-wise deterministic Markov process (4.5) and the solution of SDE (4.7) by proving a strong error bound on the distance between the two. Second, moment bounds of the diffusion process are derived.

Further, since SDE (4.7) cannot be solved explicitly, two approximation schemes, based on the Lie-Trotter and the Strang splitting approaches, are proposed. They are proved to converge with mean-square order 1 and to preserve the properties of the model. In particular, the advantage of the proposed approximation methods is that they make a full use of the matrix exponential e^{At}, which describes the flow of the Markovian cascade (4.5). Thanks to this we are able to propagate the noise through all components of the system, thus preserving its hypoellipticity. Moreover, we show that the splitting schemes accurately reproduce the derived first and second moment bounds and that they preserve the ergodicity of the continuous process, even for large values of the discretization step Δ.

These properties are particularly important when embedding the numerical scheme, for instance, into a statistical inference procedure. For example, maximum likelihood estimation techniques require the existence of a non-degenerate covariance matrix of the discretized process. For simulation-based inference methods (see Buckwar et al. (2019)), the performance of the Euler-Maruyama method may be

acceptable for "small enough" time steps. However, the use of smaller time steps drastically increases the computational cost, making the inference based on the Euler-Maruyama method computationally infeasible. Moreover, even for arbitrary small time steps there is no guarantee that the Euler-Maruyama scheme preserves the model properties.

In addition, an exact simulation procedure of the Markovian cascade is proposed. A sharp upper bound, in order to get an efficient procedure, is provided and its performance is compared to the one given in Duarte et al. (2019). When the number of neurons increases, the computational cost required for the PDMP simulation rises rapidly and cannot compete with the simulation of the diffusion via the splitting scheme.

The Markovian cascade and the diffusion process show a similar behaviour. In particular, they possess matching empirical densities. Thus, we conclude that the diffusion process describes the behaviour of the original neuronal model at a very good precision and at negligible computational cost, compared to the PDMP.

4.7 PROOFS

4.7.1 *Proof of Theorem 4.2*

The proof of Theorem 4.2 is mainly based on two lemmas which are stated before the proof. The first lemma concerns the coupling between a Poisson process and a Brownian motion. Its proof can be found in Ethier and Kurtz (2009, Section 5.5) (the exponential moments can be deduced from the proof of Corollary 5.5.5).

Lemma 4.5. *A standard Poisson process $(\Pi_t)_{t\geq 0}$ and a standard one-dimensional Brownian motion $(B_t)_{t\geq 0}$ can be constructed on the same probability space such that*

$$\sup_{t\geq 0} \frac{|\Pi_t - t - B_t|}{\log(2\vee t)} \leq \Xi < \infty$$

almost surely, where Ξ is a random variable having exponential moments.

The second lemma concerns the modulus of continuity for the Brownian motion. It is stated in Kurtz et al. (1978) without a proof. Hence, for the sake of completeness, we provide a proof which is an adaptation of the arguments presented in the appendix of Fischer and Nappo (2009).

Lemma 4.6. *Let B be a standard Brownian motion and T a positive time. Then,*

$$M := \sup_{t,s\leq T} \frac{|B_t - B_s|}{\sqrt{|t-s|(1+\log(T/|t-s|))}},$$

is a finite random variable such that M^2 has finite exponential moments.

Proof. Thanks to the scaling properties of Brownian motion, it is sufficient to prove the statement for $T = 1$. According to Fischer and Nappo (2009), let $c > 1$ and define two increasing functions Ψ and μ by

$$\Psi(x) = e^{x^2/2} - 1 \quad \text{and} \quad \mu(x) = \sqrt{cx},$$

for all $x \geq 0$. Let now ξ be the random variable defined by

$$\xi = \int_0^1 \int_0^1 \Psi\left(\frac{|B_t - B_s|}{\mu(|t-s|)}\right) dt ds.$$

The Garsia–Rodemich–Rumsey inequality (Stroock and Varadhan, 2007, Theorem 2.1.3.) implies that

$$|B_t - B_s| \leq 8 \int_0^{|t-s|} \Psi^{-1}\left(\frac{4\xi}{x^2}\right) \mu'(x) dx,$$

with $\Psi^{-1}(y) = \sqrt{2\log(1+y)}$ and $\mu'(x) = (\sqrt{c}/2)x^{-1/2}$. Yet, for $0 < x < 1$,

$$\Psi^{-1}\left(\frac{4\xi}{x^2}\right) = \sqrt{2}\sqrt{\log(4\xi + x^2) + 2\log(1/x)} \leq \sqrt{2}\sqrt{\log(4\xi+1)} + 2\sqrt{\log(1/x)}.$$

Combining the last two equations, one gets for all h,

$$\sup_{|t-s|\leq h} |B_t - B_s| \leq 4\sqrt{2c}\sqrt{\log(4\xi+1)} \int_0^h \frac{dx}{\sqrt{x}} + 8\sqrt{c} \int_0^h \sqrt{\log(1/x)}\frac{dx}{\sqrt{x}}. \qquad (4.25)$$

The second term can be bounded thanks to

$$\int_0^h \sqrt{\log(1/x)}\frac{dx}{\sqrt{x}} = \int_0^h \left(\sqrt{\log(1/x)} - \frac{1}{\sqrt{\log(1/x)}}\right) + \frac{1}{\sqrt{\log(1/x)}}\frac{dx}{\sqrt{x}}$$
$$\leq 2\sqrt{h\log(1/h)} + 4\sqrt{h},$$

using (when $h > e^{-1}$) the fact that

$$\int_{e^{-1}}^h \frac{1}{\sqrt{x}\log(1/x)} dx = \int_{e^{-1}}^h 2\sqrt{x}\frac{1}{x\sqrt{\log(1/x)}} dx \leq 2\sqrt{h}(1 - \sqrt{\log(1/h)}).$$

Going back to Equation (4.25), for some constant C which does not depend on c, one has that

$$\sup_{|t-s|\leq h} |B_t - B_s| \leq C\sqrt{c}\left(\sqrt{\log(4\xi+1)} + 1\right)\sqrt{h(1 + \log(1/h))}.$$

Note that the random variable M defined in the statement of the lemma satisfies

$$M = \sup_{0<h<1} \frac{\sup_{|t-s|\leq h} |B_t - B_s|}{\sqrt{h(1 + \log(1/h))}} \leq C\sqrt{c}\left(\sqrt{\log(4\xi+1)} + 1\right),$$

so that

$$\mathbb{E}\left[e^{\alpha M^2}\right] \leq \mathbb{E}\left[e^{2\alpha c C^2(\log(4\xi+1)+1)}\right] \leq e^{2\alpha c C^2}\mathbb{E}\left[(4\xi+1)^{2\alpha c C^2}\right].$$

To conclude, we refer to the control of the moments of ξ given in the appendix of Fischer and Nappo (2009). It states in particular that $\mathbb{E}[(4\xi+1)^{2\alpha c C^2}]$ is finite as soon as $2\alpha c C^2 < c$ which is granted if we take α small enough. $\qquad \square$

Before going through the proof of the Theorem, let us give some alternative representation of Equation (4.5) and some sketch of the proof. Thanks to the time change property of point processes (see Brémaud (1981, Section II.6.) for instance), there exists two independent standard (i.e., with rate equal to one) Poisson processes Π^1 and Π^2 such that $\bar{Z}_t^k = N_k^{-1}\Pi_{\bar{\Lambda}_t^k}^k$ where $\bar{\Lambda}_t^k$ is the integrated intensity of $\bar{Z}_t^k$, that is

$$\bar{\Lambda}_t^k = N_k \int_0^t f_k(\bar{X}_s^{k+1,1}) ds.$$

This time-change property is an analogous martingale property to the time-change property for diffusions. Then, the integrated form of (4.5) is given by

$$\bar{X}_t = x_0 + \int_0^t A\bar{X}_s ds + c\bar{Z}_t = \int_0^t A\bar{X}_s ds + c \begin{pmatrix} N_1^{-1} \Pi^1_{\bar{\Lambda}^1_t} \\ N_2^{-1} \Pi^2_{\bar{\Lambda}^2_t} \end{pmatrix}. \tag{4.26}$$

In a similar way, the SDE can be written with respect to two time-changed Brownian motions and the general idea of the proof is then to couple the standard Poisson processes Π^k with the Brownian motions.

Proof of Theorem 4.2. It is more convenient to first prescribe the Brownian motions and then couple them with Poisson processes. That is exactly how we proceed below. Let Y be the solution of (4.7) with respect to some two dimensional Brownian motion $W = (W^1, W^2)^T$. Thanks to the time change property of the Brownian motion (see Ethier and Kurtz (2009, Theorem 2.12.) for instance), let B^k be the Brownian motion defined by

$$B^k_t = \int_0^{\tau^k(t)} \sqrt{N_k f_k(Y^{k,1}_s)} dW^k_s,$$

where $\tau^k(t)$ is the stopping time satisfying

$$t = N_k \int_0^{\tau^k(t)} f_k(Y^{k,1}_s) ds.$$

Then, Y can be written as follows

$$Y_t = x_0 + \int_0^t AY_s ds + \int_0^t \Gamma \begin{pmatrix} f_2(Y^{2,1}_s) \\ f_1(Y^{1,1}_s) \end{pmatrix} ds + \Gamma \begin{pmatrix} N_1^{-1} B^1_{\Lambda^1_t} \\ N_2^{-1} B^2_{\Lambda^2_t} \end{pmatrix}, \tag{4.27}$$

where

$$\Lambda^k_t = N_k \int_0^t f_k(Y^{k,1}_s) ds.$$

We are now in the position to use the coupling with Poisson processes. Let Π^k be the Poisson process given by Lemma 4.5 with associated random variable Ξ_k. Now, let $\bar{X}$ be defined as in (4.26). Then,

$$\bar{X}_t = x_0 + \int_0^t A\bar{X}_s ds + \int_0^t \Gamma \begin{pmatrix} f_2(\bar{X}^{2,1}_s) \\ f_1(\bar{X}^{1,1}_s) \end{pmatrix} ds + \Gamma \begin{pmatrix} N_1^{-1} B^1_{\bar{\Lambda}^1_t} + R^1_t \\ N_2^{-1} B^2_{\bar{\Lambda}^2_t} + R^2_t \end{pmatrix}, \tag{4.28}$$

where

$$R^k_t = \frac{1}{N_k} \left(\Pi^k_{\bar{\Lambda}^k_t} - \bar{\Lambda}^k_t - B^k_{\bar{\Lambda}^k_t} \right).$$

Thanks to Lemma 4.5,

$$|R^k_t| \le \frac{1}{N_k} \Xi_k \log(2 \vee \bar{\Lambda}^k_t) \le \Xi_k \left(\frac{\log N_k}{N_k} + \frac{\log t}{N_k} + \frac{1}{N_k} \right),$$

$$\le C \Xi_k \left(\frac{\log N}{N} + \frac{\log t}{N} + \frac{1}{N} \right), \tag{4.29}$$

for some constant C, where we used that $\bar{\Lambda}^k_t \le N_k t f^{max}_k$ and N/N_k is bounded for N and N_k large enough.

Let us denote $G^N(t) = \sup_{s \leq t} N\|\bar{X}_s - Y_s\|$ where $\|\cdot\|$ denotes the sup norm on $\mathbb{R}^\kappa$ here and below. Combining (4.27) and (4.28) as well as using the Lipschitz continuity of f_k (with respect to constant L_k) give

$$\|\bar{X}_t - Y_t\| \leq \int_0^t \|A(\bar{X}_s - Y_s)\| ds + \max\{|c_1|L_2, |c_2|L_1\} \int_0^t \|\bar{X}_s - Y_s\| ds$$
$$+ \max_k \left\{ |c_{k-1}| \left(N_k^{-1} \left| B_{\bar{\Lambda}_t^k}^k - B_{\Lambda_t^k}^k \right| + |R_t^k| \right) \right\}.$$

Then, since the operator norm $\|A\|$ corresponding to the sup norm is finite, Grönwall's lemma yields

$$G^N(T) \leq C_1 \max_k \left\{ \sup_{t \leq T} \left| B_{\bar{\Lambda}_t^k}^k - B_{\Lambda_t^k}^k \right| + N|R_t^k| \right\} e^{C_2 T} \tag{4.30}$$

for two deterministic constants C_1 and C_2 which do neither depend on N nor on T. Hence, it only remains to estimate the Brownian increments. This can be done via the modulus of continuity of Brownian motion. Indeed, for $t \leq T$, $\bar{\Lambda}_t^k$ and Λ_t^k are bounded by NTf_k^{max} so Lemma 4.6 gives

$$\left| B_{\bar{\Lambda}_t^k}^k - B_{\Lambda_t^k}^k \right| \leq M_k \sqrt{\left| \bar{\Lambda}_t^k - \Lambda_t^k \right| (1 + \log(Nf_k^{max}T/|\bar{\Lambda}_t^k - \Lambda_t^k|))},$$

where M_k is some random variable defined in the lemma. For all $a > 0$, the function $x \mapsto \sqrt{x(1 + \log(a/x))}$ is increasing for $0 < x \leq a$ and Lipschitz continuity of f_k gives

$$|\bar{\Lambda}_t^k - \Lambda_t^k| = N \left| \int_0^t f_k(\bar{X}_s^{k,1}) - f_k(Y_s^{k,1}) ds \right| \leq C \int_0^t G^N(s) ds \leq CT G^N(T)$$

so that

$$\left| B_{\bar{\Lambda}_t^k}^k - B_{\Lambda_t^k}^k \right| \leq M_k \sqrt{CTG^N(T)(1 + \log(Nf_k^{max}/CG^N(T)))}.$$

On the event where $G^N(T) < 1$, (4.12) holds. If $G^N(T) \geq 1$ then the equation above implies

$$\left| B_{\bar{\Lambda}_t^k}^k - B_{\Lambda_t^k}^k \right| \leq M_k \sqrt{CTG^N(T)(1 + \log(Nf_k^{max}/C))}$$

and so coming back to (4.30) one has

$$G^N(T) \leq C_1 \left(M\sqrt{CT(1 + \log(Nf^{max}/C))}\sqrt{G^N(T)} \right.$$
$$\left. + N \max_k \sup_{t \leq T} |R_t^k| \right) e^{C_2 T},$$

with $f^{max} = \max\{f_1^{max}, f_2^{max}\}$ and $M = \max\{M_1, M_2\}$. The inequality above is of order 2 with respect to $x = \sqrt{G^N(T)}$. Yet, the positive values of x such that $p(x) = x^2 + bx + c$ is negative are such that $x^2 \leq b^2 - c$. Hence,

$$G^N(T) \leq C \left(M^2 T(1 + \log(Nf^{max}/C)) + N \max_k \sup_{t \leq T} |R_t^k| \right) e^{2C_2 T}.$$

Finally, (4.12) follows from the control of $|R_t^k|$ given by (4.29). $\square$

4.7.2 *Proof of Theorem 4.4*

Recall that the components of the process X^k are given by

$$X_t^{k,j} = \left(e^{At}X_0\right)^{k,j} + \int_0^t c_k f_{k+1}(X_s^{k+1,1}) \frac{e^{-\nu_k(t-s)}}{(\eta_k+1-j)!}(t-s)^{\eta_k+1-j}ds$$
$$+ \frac{1}{\sqrt{N}}\int_0^t \frac{c_k}{\sqrt{p_{k+1}}}\sqrt{f_{k+1}(X_s^{k+1,1})}\frac{e^{-\nu_k(t-s)}}{(\eta_k+1-j)!}(t-s)^{\eta_k+1-j}dW_s^{k+1}.$$

Squaring the above expression yields

$$(X_t^{k,j})^2 = T_1(t) + T_2(t) + T_3(t) + T_4(t) + T_5(t) + T_6(t),$$

where

$$T_1 = \left((e^{At}x_0)^{k,j}\right)^2,$$

$$T_2 = \left(\int_0^t c_k f_{k+1}(X_s^{k+1,1})\frac{e^{-\nu_k(t-s)}}{(\eta_k+1-j)!}(t-s)^{\eta_k+1-j}ds\right)^2,$$

$$T_3 = \left(\frac{1}{\sqrt{N}}\int_0^t \frac{c_k}{\sqrt{p_{k+1}}}\sqrt{f_{k+1}(X_s^{k+1,1})}\frac{e^{-\nu_k(t-s)}}{(\eta_k+1-j)!}(t-s)^{\eta_k+1-j}dW_s^{k+1}\right)^2,$$

$$T_4 = 2(e^{At}x_0)^{k,j}\int_0^t c_k f_{k+1}(X_s^{k+1,1})\frac{e^{-\nu_k(t-s)}}{(\eta_k+1-j)!}(t-s)^{\eta_k+1-j}ds,$$

$$T_5 = 2\int_0^t c_k f_{k+1}(X_s^{k+1,1})\frac{e^{-\nu_k(t-s)}}{(\eta_k+1-j)!}(t-s)^{\eta_k+1-j}ds$$
$$\cdot \frac{1}{\sqrt{N}}\int_0^t \frac{c_k}{\sqrt{p_{k+1}}}\sqrt{f_{k+1}(X_s^{k+1,1})}\frac{e^{-\nu_k(t-s)}}{(\eta_k+1-j)!}(t-s)^{\eta_k+1-j}dW_s^{k+1},$$

$$T_6 = 2(e^{At}x_0)^{k,j}\frac{1}{\sqrt{N}}\int_0^t \frac{c_k}{\sqrt{p_{k+1}}}\sqrt{f_{k+1}(X_s^{k+1,1})}\frac{e^{-\nu_k(t-s)}}{(\eta_k+1-j)!}(t-s)^{\eta_k+1-j}dW_s^{k+1}.$$

First, we note that $\mathbb{E}[T_6(t)] = 0$ and that $\mathbb{E}[T_1(t)] = T_1(t)$. Since the intensity function is bounded by $0 < f_{k+1} \leq f_{k+1}^{\max}$, we have that

$$\mathbb{E}[T_4(t)] \leq \max\left\{0, \frac{c_k f_{k+1}^{\max}}{(\eta_k+1-j)!}\right\}2(e^{At}x_0)^{k,j}\int_0^t e^{-\nu_k(t-s)}(t-s)^{\eta_k+1-j}ds.$$

Further, applying Itô's isometry gives

$$\mathbb{E}[T_3(t)] = \frac{c_k^2}{Np_{k+1}((\eta_k+1-j)!)^2}\int_0^t \mathbb{E}[f_{k+1}(X_s^{k+1,1})]e^{-2\nu_k(t-s)}(t-s)^{2(\eta_k+1-j)}ds.$$

Using again the fact that $f_{k+1} < f_{k+1}^{\max}$ results in

$$\mathbb{E}[T_3(t)] \leq \frac{1}{N}\frac{c_k^2}{p_{k+1}}\frac{f_{k+1}^{\max}}{((\eta_k+1-j)!)^2}\int_0^t e^{-2\nu_k(t-s)}(t-s)^{2(\eta_k+1-j)}ds.$$

Moreover, since f_{k+1} is bounded, also $(T_2(t))^2$ is bounded, and thus it follows from the proof of Theorem 4.3 that

$$\mathbb{E}[T_2(t)] \leq \left(\frac{c_k f_{k+1}^{\max}}{(\eta_k+1-j)!}\right)^2\left(\int_0^t e^{-\nu_k(t-s)}(t-s)^{(\eta_k+1-j)}ds\right)^2.$$

Applying the Cauchy-Schwarz inequality gives that

$$\mathbb{E}[T_6(t)] \leq 2 \left(\mathbb{E}[T_2(t)]\mathbb{E}[T_3(t)] \right)^{1/2}.$$

Combining the above results and using that

$$\int_0^t e^{-2\nu_k(t-s)}(t-s)^{2(\eta_k+1-j)}ds = \frac{(2(\eta_k+1-j))!}{(2\nu_k)^{2(\eta_k+1-j)+1}}\left[1 - e^{-2\nu_k t}\sum_{l=0}^{2(\eta_k+1-j)}\frac{(2\nu_k t)^l}{l!} \right]$$

proves the statement.

4.7.3   Proof of Lemma 4.2

In order to rely on a linear control problem, we decouple the two populations and treat the non-linear interactions in a second step as it is done in Löcherbach (2019) for the continuous-time framework. Let us rewrite the numerical scheme (4.18) as given by the one-step mapping ψ_Δ defined by

$$\psi_\Delta[\xi](x) = e^{A\Delta}\left(x + \Delta B(x) + \frac{\sqrt{\Delta}}{\sqrt{N}}\sigma(x)\xi \right) = \begin{pmatrix} \psi_\Delta[\xi](x)_1 \\ \psi_\Delta[\xi](x)_2 \end{pmatrix},$$

where

$$\psi_\Delta[\xi](x)_k = e^{A_{\nu_k}\Delta}x^k + \left(\Delta c_k f_{k+1}(x^{k+1,1}) + \frac{\sqrt{\Delta}}{\sqrt{N}}\frac{c_k}{\sqrt{p_{k+1}}}\sqrt{f_{k+1}(x^{k+1,1})}\xi^{k+1} \right)b_k,$$

with $b_k = e^{A_{\nu_k}\Delta}(0,\ldots,0,1)^T = \left(\frac{\Delta^{\eta_k}}{\eta_k!}, \frac{\Delta^{\eta_k-1}}{(\eta_k-1)!},\ldots,1 \right)^T \in \mathbb{R}^{\eta_k+1}$. Now let us study the following discrete dynamical systems: $x^k(0) = x^k$ and for all $t \in \mathbb{N}$,

$$x^k(t+1) = e^{A_{\nu_k}\Delta}x^k(t) + b_k u^k(t+1), \tag{4.31}$$

where $(u^k(t))_{t\in\mathbb{N}^*}$ is a sequence of real numbers that will be specified below. This system is controllable as soon as $b_k, e^{A_{\nu_k}\Delta}b_k,\ldots,e^{\eta_k A_{\nu_k}\Delta}b_k$ are linearly independent (see Theorem 6.D1 in Chen (1998)). For all $j = 0,\ldots,\eta_k$, we have

$$e^{jA_{\nu_k}\Delta}b_k = \left(\frac{((j+1)\Delta)^{\eta_k}}{\eta_k!}, \frac{((j+1)\Delta)^{\eta_k-1}}{(\eta_k-1)!},\ldots,1 \right)^T.$$

Yet, $\{1, X,\ldots,X^{\eta_k}/\eta_k!\}$ is a basis of the vector space of polynomials with degree at most η_k which ensures linear independence. The controllability of the system means that for all $x^k, y^k \in \mathbb{R}^{\eta_k+1}$, there exists some sequence of real numbers $(u^k(t))_{t=1,\ldots,\eta^*+1}$ such that $x^k(\eta^* + 1) = y^k$ where x^k is inductively defined by (4.31). In the following, we use the notation $x(t) = (x^1(t), x^2(t))^T$.

Now, let x and y be as in the statement of Lemma 4.2 and denote $x = (x^1, x^2)^T$ and $y = (y^1, y^2)^T$. According to the first step of the proof, let $(u^k(t))_{t=1,\ldots,\eta^*+1}$ be such that $x^k(\eta^* + 1) = y^k$ and define, for all $t = 1,\ldots,\eta^* + 1$,

$$\xi^k(t) = \frac{u^k(t) - \Delta c_{k+1}f_k(x^{k,1}(t))}{\frac{\sqrt{\Delta}}{\sqrt{N}}\frac{c_k}{\sqrt{p_{k+1}}}\sqrt{f_k(x^{k,1}(t))}},$$

in such a way that

$$u^k(t) = \Delta c_{k+1}f_k(x^{k,1}(t)) + \frac{\sqrt{\Delta}}{\sqrt{N}}\frac{c_k}{\sqrt{p_{k+1}}}\sqrt{f_k(x^{k,1}(t))}\xi^k(t).$$

Substituting $u^k(t+1)$ in (4.25) and denoting $\xi_t = \xi(t)$, yields $x^k(t+1) = \psi_\Delta[\xi_{t+1}](x(t))_k$ and thus

$$y = x(\bar{\eta}+1) = \underbrace{(\psi_\Delta[\xi_{\bar{\eta}+1}] \circ \cdots \circ \psi_\Delta[\xi_1])}_{\eta^*+1}(x),$$

which proves the result.

<div style="text-align: right;">5</div>

HORIZONTAL GENE TRANSFER: STOCHASTIC AND DETERMINISTIC APPROACHES. NUMERICAL STUDY.

This chapter is based on the article Calvez, Vincent et al. (2020), written in collaboration with Vincent Calvez, Hélène Hivert, Sylvie Méléard, Susely Figueroa Iglesias and Samuel Nordmann.

Abstract. Horizontal gene Transfer (HT) denotes the transmission of genetic material between two living organisms, while the vertical transmission refers to a DNA transfer from parents to their offspring. Consistent experimental evidence report that this phenomenon plays an essential role in the evolution of certain bacterias. In particular, HT is believed to be the main instrument of developing the antibiotic resistance. In this work, we consider several models which describe this phenomenon: a stochastic jump process (individual-based) and the deterministic nonlinear integrodifferential equation obtained as a limit for large populations. We also consider a Hamilton-Jacobi equation, obtained as a limit of the deterministic model under the assumption of small mutations. The goal of this paper is to compare these models with the help of numerical simulations. More specifically, our goal is to understand to which extent the Hamilton-Jacobi model reproduces the qualitative behavior of the stochastic model and the phenomenon of evolutionary rescue in particular.

Résumé: Le transfert horizontal de gènes (HT) est la transmission de matériel génétique entre deux organismes vivants, contrairement à la transmission verticale qui désigne le transfert d'ADN d'un parent à sa progéniture. Il est prouvé que ce phénomène joue un rôle important dans l'évolution de certaines bactéries, notamment pour le développement d'une résistance aux antibiotiques. Nous considérons ici un processus stochastique à saut individu-centré, et l'équation intégro-differentielle non linéaire obtenue comme limite pour une population de grande taille. En supposant que les mutations sont petites, après un changement de variable et un passage à la limite, nous obtenons une équation d'Hamilton Jacobi. L'objectif de ce travail est de comparer ces differents modèles à l'aide de simulations numériques, et de déterminer si l'équation d'Hamilton-Jacobi parvient à capturer les phénomènes qualitatifs du modèle stochastique, notamment le sauvetage évolutif.

Keywords: Horizontal gene transfer, stochastic individual-based models, integro-differential equations, Hamilton-Jacobi equation, evolution dynamics, resistance to antibiotics.

5.1   INTRODUCTION

Accurate mathematical description of the evolutionary mechanism is an open question in biology, medicine, and industry. In particular, transmission of pathogens, or antibiotic resistance of bacteria is directly linked to the ability of the bacteria population to mutate and exchange genetic material either vertically (from parents to offspring), or horizontally (from the interaction between non-parental individuals).

Horizontal Gene Transfer was first described in bacteria when the antibiotic resistance was discovered. This resistance occurs when one bacterial cell becomes resistant to an antibiotic due to mutation, and then transfers resistance genes to other species of bacteria. However the Horizontal Transfer of biologic information is not restricted to genes, it also describes the transfer of plasmids and endosymbionts, see for example M Henry et al. (2013), Lili et al. (2007). Some artificial applications of horizontal transfer include forms of genetic engineering (Gene Delivery) that result in an organism with its genes changed in some way, and, consequently, possessing new properties or functions (see for instance Kamimura et al. (2011)). These applications are particularly useful for "Gene Therapy", which is an experimental procedure that may help treat or prevent genetic disorders and some types of cancer.

The primary goal of our work is to describe the mechanism of the transfer itself and explain how it affects the population dynamics. Throughout the paper we abbreviate the Horizontal Transfer to HT.

Our study starts with finding a good model of a bacteria population. Several mathematical models for describing a population dynamics were proposed in literature. The first model we consider is a stochastic birth and death process (see, for reference, Billiard et al. (2015), Fournier and Méléard (2004)), which describes the dynamics of reproduction, competition, and exchange of genetic material between individuals in a population. The phenotype of each individual is described by a numerical parameter, called trait. Numerical experiments show that the effect of a unilateral horizontal gene transfer may lead to a cyclic behavior of the population. Roughly speaking, while HT drives individuals towards a non-fit phenotype — and, consequently, to extinction, very few not affected by transfer fit individuals may eventually repopulate the environment, before being driven again to deleterious phenotypes. This phenomenon is called an *evolutionary rescue of a small population.*

However, within a framework of stochastic jump processes, it is hard to define and study the observed cycling phenomena accurately. The second drawback of the stochastic system is that it is costly to compute, especially for a large time scale and population size. Thus, in the case of a large population, it is more convenient to work with a deterministic PDE model, describing the limiting behaviour of a stochastic system when the population size goes to infinity Billiard et al. (2016b,a), Ferrière and Tran (2009). In certain settings, the population dynamics involve concentration phenomena (i.e., the convergence of the population density to singular solutions, such as Dirac masses). In that case, the PDE formulation is not suitable. Thus, applying a limiting procedure for small mutations and time rescaling to the PDE model, we pass to a Hamilton-Jacobi type equation.

The primary goal of our work is thus to conduct a numerical analysis of the population dynamics on a macroscopic individual-based model and to compare it with the deterministic system which is

obtained as a limit for a large population. We are especially interested in determining to which extent the limiting Hamilton-Jacobi equation can grasp qualitative properties of the stochastic model. This framework has already been successfully used to understand the concentration phenomena, and the location of the dominant trait (see for instance Lorz et al. (2011), Perthame and Barles (2008)). We aim to understand if the Hamilton-Jacobi approach is also well suited to describe the evolutionary rescue phenomena which crucially rely on an accurate description of the small populations.

On this step, the choice of an approximation scheme for simulating solutions of the PDE model is of tremendous importance. As we further explain in Section 5.3, classical explicit schemes do not preserve the asymptotic behavior of the solution if the time rescaling step goes to 0. From a numerical point of view, it involves operations with exponentially big values, which lead to non-negligible errors for explicit numerical schemes. We address this question by proposing an asymptotic preserving scheme for a Hamilton-Jacobi equation, adapting an approach proposed in Crandall and Lions (1984). More generally, the numerical approximation problem for solutions of Hamilton-Jacobi equations is treated in Achdou et al. (2013).

This chapter is structured as follows: in Section 5.2 we introduce the model both in a stochastic and deterministic setting, and formally derive the limiting Hamilton-Jacobi equation. Then, we simulate a jump process, describing the bacteria population, and study its properties for different values of parameters. Numerical experiments are gathered in Section 5.3. We aim to numerically determine the critical HT rate, which leads to an almost sure extinction of the whole population. On the next step, we conduct the same analysis for a Hamilton-Jacobi equation with the help of an asymptotic preserving scheme and compare it with the stochastic model on an appropriate timescale, and explain why the classical scheme fails to work. We end our study with conclusions and discussion of yet unsolved numerical and theoretical questions.

5.2 MODEL

5.2.1 *Stochastic model*

We consider a stochastic model describing the evolution of a population structured by phenotype. In a general case it is described at each time t by the point measure

$$\nu_t^K(dx) = \frac{1}{K} \sum_{i=1}^{N_t^K} \delta_{X_i(t)}(dx), \tag{5.1}$$

where the parameter K is a scaling parameter, referred to as the *carrying capacity*. It stands for the maximal number of individuals that the underlying environment is able to host (K can represent, for example, the amount of available resources). $N_t^K = K \int \nu_t^K(dx)$ is the size of the population at time t, and $X_i(t) \in \mathbb{R}^n$ is the trait of i-th individual living at t, which summarizes the phenotype information. In this work we assume $n = 1$, that is, the trait is given by a point on a real line.

The demography of the population is regulated, first of all, by its birth and death rates. An individual with a trait x gives birth to a new individual with rate $b(x)$. The trait y of the offspring is

chosen from a probability distribution $m(x-y)dy$ (by that we mean that $\int_{\mathbb{R}} m(x-y)dy = 1$). We will refer to it as the *mutation kernel*. An individual with a trait x dies according to an intrinsic death rate $d(x)$ plus an additional death rate $C\dfrac{N_t^K}{K}$ (independent of x) which stands for the competition between individuals.

Finally, an individual with a trait x can induce a *unilateral* HT to an individual with trait y at rate $h_K(x, y, \nu)$, such that the pair (x, y) becomes (x, x). In literature this kind of transfer is sometimes referred to as a *conjugation*. For simplicity, we assume $h_K(x, y, \nu)$ to be in the particular form

$$h_K(x, y, \nu) = h_K(x-y, N) = \tau_0 \frac{\alpha(x-y)}{N/K}, \tag{5.2}$$

where $N = K\int_{\mathbb{R}} \nu(dx)$ is the number of individuals, $\tau_0 > 0$ is a constant and α is either a Heaviside, or a smooth bounded function, such that for a small $\delta > 0$:

$$\alpha(z) = \begin{cases} 0 & \text{if } z < -\delta \\ 1 & \text{if } z > +\delta \end{cases}, \quad \alpha'(0) = \frac{1}{2\delta}, \tag{5.3}$$

where δ is the stiffness parameter. We introduce δ to have the advantage of working with a smooth function (which will be useful in the following parts), while mimicking the binary nature of the Heaviside function.

For a population $\nu = \frac{1}{K}\sum_{i=1}^N \delta_{x_i}$ and a generic measurable bounded function F, the generator of the process is then given by:

$$L^K F(\nu) = \sum_{i=1}^N b(x_i) \int_{\mathbb{R}} \left(F\left(\nu + \frac{1}{K}\delta_y\right) - F(\nu) \right) m(x_i, dy)$$

$$+ \sum_{i=1}^N \left(d(x_i) + C\frac{N}{K} \right) \left(F\left(\nu - \frac{1}{K}\delta_{x_i}\right) - F(\nu) \right)$$

$$+ \sum_{i,j=1}^N h_K(x_i, x_j, \nu) \left(F\left(\nu + \frac{1}{K}\delta_{x_i} - \frac{1}{K}\delta_{x_j}\right) - F(\nu) \right).$$

It is standard to construct the measure-valued process ν^K as the solution of a stochastic differential equation driven by Poisson point measures and to derive moment and martingale properties (see for instance Fournier and Méléard (2004)).

5.2.2 *The PDE model*

It is proven (see in particular Billiard et al. (2016b), Champagnat et al. (2008)) that for $K \to +\infty$ the stochastic process defined by a sequence of point measures given by (5.1) converges in probability to the unique solution of a non-linear integro-differential equation. This equation is given by:

$$\begin{cases} \partial_t f(t, x) = -(d(x) + C\rho_1(t))f(t, x) + \int_{\mathbb{R}^n} m(x-y)b(y)f(t, y)dy + \\ \qquad f(t, x) \int_{\mathbb{R}^n} \tau(x-y)\dfrac{f(t, y)}{\rho_1(t)}dy, \text{ in } \mathbb{R}_+ \times \mathbb{R}^n, \\ \rho_1(t) = \int_{\mathbb{R}} f(t, x)dx, \\ f(0, x) = f^0(x) > 0, \end{cases}$$

where $f(t, x)$ is the macroscopic density of the population with trait x at time t and, accordingly to the previous section, $b(x)$, $d(x)$ and C are the birth, death and competition rate respectively, m is the mutation kernel, and

$$\tau(y - x) := \tau_0 \left[\alpha(x - y) - \alpha(y - x) \right] \tag{5.4}$$

is the horizontal transfer flux.

Now our goal is to pass from a micro- to a macroscopic scale with the help of a rescaling. On the one hand, we consider the case of small mutations: for a small parameter $\varepsilon > 0$ we define

$$m_\varepsilon(x - y) = \frac{1}{\varepsilon^n} m\left(\frac{x - y}{\varepsilon}\right).$$

With a change of variable $z = \frac{x-y}{\varepsilon}$ we can rewrite the mutation term at (t, x) as

$$\int_{\mathbb{R}^n} m_\varepsilon(x - y) b(y) f(t, y) dy = \int_{\mathbb{R}^n} m(z) b(x + \varepsilon z) f(t, x + \varepsilon z) dz.$$

On the other hand, when ε is small, the effect of mutations can only be observed in a larger time scale. Thus, we rescale time with $t \mapsto \frac{t}{\varepsilon}$.

We end up with the following system, for $\varepsilon > 0$, and $(t, x) \in \mathbb{R}_+ \times \mathbb{R}^n$:

$$\begin{cases} \varepsilon \partial_t f_\varepsilon(t, x) = -(d(x) + C\rho_\varepsilon(t)) f_\varepsilon(t, x) + \displaystyle\int_{\mathbb{R}^n} m(z) b(x + \varepsilon z) f_\varepsilon(t, x + \varepsilon z) dz + \\ \qquad\qquad f_\varepsilon(t, x) \displaystyle\int_{\mathbb{R}^n} \tau(x - y) \frac{f_\varepsilon(t, y)}{\rho_\varepsilon(t)} dy, \\ \rho_\varepsilon(t) = \displaystyle\int_{\mathbb{R}} f_\varepsilon(t, x) dx, \\ f_\varepsilon(0, x) = f_\varepsilon^0(x) > 0. \end{cases} \tag{5.5}$$

5.2.3 *The Hamilton-Jacobi limit*

We now derive the limiting problem (5.5) when $\varepsilon \to 0$. As we will see, the limiting problem allows us to give a rigorous mathematical framework and to perform useful formal calculations.

Equations in the form of (5.5) often give rise to a concentration phenomenon, i.e the convergence of f_ε towards a Dirac mass when $\varepsilon \to 0$ (see Perthame and Barles (2008), Diekmann et al. (2005)). The usual way to deal with these asymptotics is to perform a Hopf-Cole transformation (or WKB ansatz), i.e to consider

$$u_\varepsilon(t, x) := \varepsilon \ln(f_\varepsilon(t, x)). \tag{5.6}$$

This change of variable comes from the intuition that a Dirac mass is no more than a narrow Gaussian, and more precisely that f_ε should behave like a Gaussian of variance ε when $\varepsilon \to 0$. Accordingly, we expect u_ε to have a non singular limit when $\varepsilon \to 0$. Incidentally, this substitution also gives insights on the convenient scheme to use for numerical simulations, as we will see in the following section.

Now our goal is to identify and derive the asymptotic properties of u_ε when $\varepsilon \to 0$, which will be used for discussions in the sequel. The following computations are only formal, since rigorous proofs are often intricate in this context. Substituting (5.6) into (5.5) we deduce that u_ε satisfies

$$\partial_t u_\varepsilon = -(d(x) + C\rho_\varepsilon(t)) + \int_{\mathbb{R}^n} m(z)b(x + \varepsilon z) \exp\left\{ \frac{u_\varepsilon(t, x + \varepsilon z) - u_\varepsilon(t, x)}{\varepsilon} \right\} dz +$$

$$\int_{\mathbb{R}^n} \tau(x - y) \frac{f_\varepsilon(t, y)}{\rho_\varepsilon(t)} dy. \quad (5.7)$$

Formally, at the limit $\varepsilon \to 0$, u_ε converges to a continuous function u which satisfies the following Hamilton-Jacobi equation in the *"viscosity"* sense:

$$\partial_t u = -(d(x) + C\rho(t)) + b(x) \int_{\mathbb{R}^n} m(z) e^{z \cdot \nabla_x u} dz + \tau(x - \bar{x}(t)), \quad (5.8)$$

where $\rho(t) \geq 0$ is the weak limit of $\rho_\varepsilon(t)$ and

$$\bar{x}(t) = \operatorname{argmax} u(t, \cdot). \quad (5.9)$$

We formally assume here and in the following that the definition of $\bar{x}(t)$ is unambiguous, i.e that u reaches its maximum in a single point. Note that the limiting function u is not expected to be C^1 for all time. We thus need to deal with a generalized notion of solutions, namely *viscosity solution* (see Barles (1994)).

This framework is convenient because most of the information is contained in the dynamics of $\bar{x}(t)$. See the next section for further analysis.

5.2.4   *Formal analysis on the Hamilton-Jacobi equation*

Hamilton-Jacobi equations are particularly known in mathematical biology to be a good model to describe how a population concentrates around the dominant trait(s) when the mutations are small. However, here we are interested to use this model to describe a phenomenon of *evolutionary rescue*. In this subsection we attempt an analysis of the equation (5.8). We point out that the calculations are only formal, since rigorous proofs are intricate and beyond the scope of this paper.

5.2.4.1   *Generality*

From an integration of (5.5) with respect to x and classical computations (under the assumptions of bounded functions for the birth, death and transfer rates), we deduce that our model satisfies a *saturation property*, i.e. $\rho_\varepsilon(t)$ is bounded from above, uniformly in $t \geq 0$ and $\varepsilon > 0$. From this and $\rho_\varepsilon(t) = \int_{\mathbb{R}^n} e^{\frac{u_\varepsilon(t, x)}{\varepsilon}} dx$, we deduce that $\forall t > 0$, $\sup_{x \in \mathbb{R}^n} u(t, x) \leq 0$ and the following constraint holds:

$$\sup_{x \in \mathbb{R}^n} u(t, x) = 0 \quad \text{when} \quad \rho(t) > 0. \quad (5.10)$$

Note that our model allows the population to get extinct, thus we cannot expect ρ to be always positive. As a byproduct, we derive the *concentration property*, i.e the formal weak convergence of measures

$$f_\varepsilon(t, x) \rightharpoonup \rho(t) \delta_{\bar{x}(t)}(dx), \quad \text{when } \varepsilon \to 0,$$

where $\delta_{\bar{x}(t)}$ denotes, as usually, the Dirac measure centered in $\bar{x}(t)$. From (5.10) it is possible to formally derive a formula for ρ. Indeed, either $\rho(t) = 0$ or $\rho(t) > 0$ and

$$\partial_t u(t, \bar{x}(t)) = 0,$$

which implies

$$\rho(t) = \frac{b(\bar{x}(t)) - d(\bar{x}(t)) + \tau(0)}{C} = \frac{b(\bar{x}(t)) - d(\bar{x}(t))}{C}, \tag{5.11}$$

for τ defined in (5.4).

Having the above definitions in hand, we can now perform a formal analysis on the dynamics of $\bar{x}(t)$, defined below in (5.15). Our aim is to show how the behaviour of the system can be analyzed within the framework of a Hamilton-Jacobi equation (5.8). To fix ideas, we fix all constants but τ_0 and we assume (5.12)-(5.14) as follows:

$$b(x) = b_r > 0, \tag{5.12}$$

$$d(x) = d_r x^2, \quad d_r > 0, \tag{5.13}$$

$$m(z) = \frac{1}{\sqrt{2\pi}\sigma} e^{-\frac{z^2}{2\sigma^2}}, \tag{5.14}$$

and the transfer function $h_K(x, y, \nu)$ is defined in (5.2). Moreover we work under the following assumptions:

$$u(t, \cdot) \text{ reaches its maximum on a single point } \bar{x}(t),$$
$$\bar{x}(t) \text{ is a non-degenerate maximum, i.e } \nabla_x^2 u(t, x) < 0, \tag{5.15}$$
$$\bar{x}(t) \text{ is smooth with respect to } t.$$

Finally we assume that the initial condition f^0 is a given function of x which reads:

$$f_\varepsilon^0(x) = \frac{1}{\sqrt{\varepsilon}} e^{-\frac{x^2}{2\varepsilon}}. \tag{5.16}$$

5.2.4.2 Smooth dynamics $\bar{x}(t)$.

The following statement deals with the smooth dynamics of $\bar{x}(t)$, i.e in the regime where no jump occurs in the dynamics of $\bar{x}(t)$.

Statement 5.1. *Under assumptions* (5.12)-(5.15), *the function* $t \mapsto \bar{x}(t)$ *is an increasing function which satisfies the following inequality* $\forall t \geq 0$:

$$0 \leq \bar{x}(t) \leq \frac{\tau_0}{2d\delta}.$$

More precisely, $\bar{x}(t)$ *satisfies the canonical equation*

$$\frac{\mathrm{d}}{\mathrm{d}t}\bar{x}(t) = \left[-\nabla_x^2 u(t, \bar{x}(t))\right]^{-1} \cdot \left(\nabla_x r(\bar{x}(t)) + \nabla_x \tau(0)\right), \tag{5.17}$$

where

$$r(x) := b(x) - d(x), \tag{5.18}$$

and $\nabla_x^2 u$ *denotes the Hessian of* u *with respect to the* x *variable.*

Proof. Under the above assumptions we can derive the dynamics of $\bar{x}(t)$, referred to as the *canonical equation* in the literature (see for instance Mirrahimi and Roquejoffre (2016)). Indeed, starting from

$$\nabla_x u(t, \bar{x}(t)) = 0,$$

a differentiation with respect to t gives (5.17). Equation (5.17) has a unique singular point $x_\star$, which satisfies $r'(x_\star) + \tau'(0) = 0$, with τ defined in (5.2) and r in (5.18). We find

$$x_\star = \frac{\tau_0}{2 d_r \delta}. \tag{5.19}$$

Note that $t \mapsto \bar{x}(t)$ is increasing when $\bar{x}(t) < x_\star$ and decreasing when $\bar{x}(t) > x_\star$. Besides, from the initial condition (5.16), we have $\bar{x}(0) = 0$, and consequently $0 \leq \bar{x}(t) \leq x_\star \quad \forall t$. $\qquad \square$

5.2.4.3 *Evolutionary rescue.*

In general, the canonical equation (5.17) does not hold in every point of time. Indeed, a new maximum of u can arise in a finite time, which would cause a "jump" in the dynamics of $\bar{x}(t)$: this is what we call an *evolutionary rescue*. Formally, this is what happens (periodically in time) in the case of cycles, see Figure 5.5b. We thus expect $\bar{x}(t)$ to possibly jump periodically, and to follow (5.17) between two jumps. We now try to characterize the possible jumps. For $T > 0$, we denote

$$\bar{x}(T^-) := \lim_{\substack{t \to T \\ t < T}} \bar{x}(t), \quad \bar{x}(T^+) := \lim_{\substack{t \to T \\ t > T}} \bar{x}(t).$$

Statement 5.2. *We assume that* (5.12)-(5.15) *hold until a time* $T > 0$*, such that* $u(T, \cdot)$ *reaches its maximum on* $\bar{x}(T^-)$ *and on another point* $\tilde{x}$*. Then* $\tilde{x} = 0$ *and* $\bar{x}(t)$ *will jump towards* 0 *at time* T*, i.e* $\bar{x}(T^+) = 0$*.*

Proof. From assumption (5.15), we have $\forall t \in [0, T]$ that $u(t, \cdot)$ is concave non-degenerate on $[\bar{x}(t) \pm \theta]$, with $\theta > 0$. For simplicity, we further assume $\delta \leq \theta$, where δ is defined in (5.3).

First, let us show that $\tilde{x} = 0$. We define the fitness function of trait x in a population concentrated in $\bar{x}$:

$$F_{\bar{x}}(x) := r(x) + \tau(x - \bar{x}),$$

where r and τ are respectively defined in (5.18) and (5.4). Note that we have $\partial_t u(t, x) = F_{\bar{x}(t)}(x) - C\rho(t)$, for $t < T$. But $\tilde{x} \notin [\bar{x}(t) \pm \delta]$ and the choice of parameters (5.12)-(5.13)-(5.3) implies $\tilde{x}$ must maximize $F_{\bar{x}(T^-)}(\cdot)$, hence $\tilde{x} = 0$.

The second step is to prove that there will be an actual jump towards 0, i.e $\bar{x}(T^+) = 0$. First, note that there exists a small $\eta > 0$ such that $\forall t \in (T - \eta, T)$, $u(t, \bar{x}(t)) = 0$ and $u(t, 0) < 0$. Let us fix $t \in (T - \eta, T)$. We have $F_{\bar{x}(t)}(0) \geq F_{\bar{x}(t)}(\bar{x}(t))$, and we claim that the inequality is strict. Indeed, since $t \mapsto x(t)$ is increasing, $F_{\bar{x}(t)}(\bar{x}(t))$ is decreasing, whereas $F_{\bar{x}(t)}(0)$ is constant (as long as η is small enough such that $\bar{x}(T - \eta) > \delta$). We end up with

$$F_{\bar{x}(t)}(0) > F_{\bar{x}(t)}(\bar{x}(t)).$$

The above inequality expresses the fact that 0 is fitter than $\bar{x}(t)$ in a population with trait $\bar{x}(t)$. In general, this does not allow to conclude that 0 will invade and become the new dominant trait (i.e.,

that the jump will occur) because it does not imply that 0 will remain fitter during all the process of invasion. But the particular form of our problem, especially the fact that τ is an odd function, implies

$$F_0(0) > F_0(\bar{x}(t)).$$

Indeed we have from the definition of $F_{\bar{x}}(x)$ that

$$F_0(0) - F_0(\bar{x}(t)) = r(0) - r(\bar{x}(t)) + \tau(\bar{x} - \bar{x}) - \tau(0) = d_r \bar{x}(t)^2 > 0.$$

Consequently that for all $\lambda \in [0,1]$

$$\lambda F_0(0) + (1 - \lambda)F_{\bar{x}(t)}(0) > \lambda F_0(\bar{x}(t)) + (1 - \lambda)F_{\bar{x}(t)}(\bar{x}(t)).$$

It shows that 0 remains the fittest trait during all the process of invasion, and therefore that 0 will actually invade, i.e that $\bar{x}(t)$ will actually jump towards 0 at time T^+.   □

5.2.4.4   *Threshold for cycles*

In the previous section, we described the possible *evolutionary rescue*, i.e the possible jumps in the dynamics of $\bar{x}(t)$ towards $x = 0$. When a jump occurs, a new cycle begins: it leads to a periodical behavior of $\bar{x}(t)$, hence the cycling phenomenon.

We recall that a jump corresponds to a rescue of the population concentrated at $\bar{x}(t)$ by the small population with trait $x = 0$. It is possible only if $\bar{x}(t) > \delta$ and if 0 is fitter than $\bar{x}(t)$ during a sufficiently large interval of time (which is the time needed for the small population at $x = 0$ to regrow). Note that 0 is fitter than $\bar{x}(t)$ if and only if

$$F_{\bar{x}(t)}(0) \geq F_{\bar{x}(t)}(\bar{x}(t)) \quad \text{iff} \quad b_r - \tau_0 \geq b_r - d_r \bar{x}(t)^2, \tag{5.20}$$
$$\text{iff} \quad \bar{x}(t) \geq x_{resc} := \sqrt{\frac{\tau_0}{d_r}}.$$

But if no jump occurs, $\bar{x}(t)$ formally follows (5.17), thus $\bar{x}(t) < x_\star$ and $\bar{x}(t)$ converges to $x_\star$ when $t \to +\infty$ (with $x_\star$ is defined in (5.19)).

Statement 5.3. *Under assumptions (5.12)-(5.15), the evolutionary rescue phenomena occurs if and only if*

$$\tau_0 > \tau_{cyc} := 4d_r\delta^2. \tag{5.21}$$

Note that the condition $\tau_0 > \tau_{cyc}$ is equivalent to $x_{resc} < x_\star$, which are defined respectively in (5.19) and (5.20).

5.2.4.5   *Threshold for extinction.*

The population is said to be "extinct" at time t if $\rho(t) = 0$. According to (5.11), we define x_{ext} as to solve $r(x_{ext}) = 0$, i.e

$$x_{ext} := \sqrt{\frac{b_r}{d_r}}, \tag{5.22}$$

that is, a population concentrated at trait $\bar{x}$ is extinct iff $\bar{x} \geq x_{ext}$.

The picture is simple in the case of stabilization without cycles, i.e when $\tau_0 \leq \tau_{cyc}$ (see (5.21)). In this case, we recall that $\bar{x}(t)$ formally follows (5.17) for all $t > 0$, thus $\bar{x}(t) < x_\star$ and $\bar{x}(t)$ converges to $x_\star$ when $t \to +\infty$ (where $x_\star$ is defined in (5.19)). Thus, if $x_\star \leq x_{ext}$, we have $\rho(t) > 0$ for all $t > 0$; on the contrary, if $x_\star > x_{ext}$, there exists a time $t_{ext} > 0$ for which $\rho(t) = 0$ for all $t \geq t_{ext}$. It gives a sharp threshold for extinction of the population: indeed, the population eventually gets extinct if and only if $x_\star > x_{ext}$, which naturally leads us to the following statement.

Statement 5.4. *Under assumptions* (5.12)-(5.15), *if $\tau_0 \leq \tau_{cyc}$, then the population eventually gets extinct if and only if*

$$\tau_0 > \tau_{ext} := 2\sqrt{b_r d_r}\delta.$$

We point out that, surprisingly enough, τ_{ext} is an increasing function of the death rate d_r, meaning that under a higher death rate, the population can survive to a higher HT rate. The interpretation we propose is that if d_r is high, the population driven outward $x = 0$ dies rapidly, thus the population that remained closer to 0 undergoes a milder HT, which makes the overall population more resistant to a high HT rate.

Let us now focus on the case where the cycling phenomenon occurs, i.e when $\tau_0 > \tau_{cyc}$. In this case, $\bar{x}(t)$ will follow (5.17) and will periodically jump to $x = 0$. First, note that if $x_\star < x_{ext}$, $\bar{x}(t)$ remains below x_{ext} for all t and the population does not get extinct:

$$\text{if} \quad \tau \leq \tau_{ext}, \quad \text{then} \quad \rho(t) > 0, \quad \forall t > 0.$$

The most intricate case is when $x_\star > x_{ext}$, which contains cases of extinction and non-extinction, depending on whether the jump of $\bar{x}(t)$ towards 0 happens before or after $\bar{x}(t)$ has passed beyond x_{ext}. In other words, extinction can be avoided if the evolutionary rescue happens before the dominant trait is led to extinction, i.e if $\bar{x}(T^-) \leq x_{ext}$, where T is the time where the jump of $\bar{x}(t)$ towards 0 occurs. However, we are not able to give a satisfactory formula or estimate on T.

Besides, when the jump of $\bar{x}(t)$ occurs, it can happen that the trait $x = 0$ is not fit enough to avoid extinction: in this case the evolutionary rescue does not manage to sustain the population. It corresponds to the case $x_{resc} > x_{ext}$. We have the following threshold: the evolutionary rescue is able to sustain the population iff $r(0) + \tau_0 > 0$, which is equivalent to

$$\tau_0 < \tau_{sus} := b_r.$$

If $\tau \geq \tau_{sus}$, the population eventually gets extinct. If $\tau < \tau_{sus}$, the population is effectively rescued by the evolutionary rescue, even in the case where it passed through an episode of extinction during the previous cycle: in some cases the population is able to regrow after being extinct, which can be seen on Figure 5.5c. We think this is an interesting feature that the Hamilton-Jacobi approach is able to grasp. Regarding the stochastic model, an episode of extinction on Hamilton-Jacobi corresponds to an interval of time where the population reaches extremely small values (of order $e^{-\frac{1}{\varepsilon}}$, with ε the variance of the mutation kernel), and the probability that every individual dies is bigger than the survival of the population.

Statement 5.5. *Assume* (5.12)-(5.15) *and* $\tau_0 > \tau_{cyc}$.

- *if* $\tau_0 \leq \tau_{ext}$, *the population never gets extinct.*

- *the evolutionary rescue effectively manages to sustain the population if and only if* $\tau_0 < \tau_{sus} := b_r$.

5.2.4.6 *Characteristics of a Hamilton-Jacobi equation*

Denoting

$$-H(t,x,p) := -(d(x) + C\rho(t)) + b(x)\int_{\mathbb{R}} m(z)e^{pz}dz + \tau(x - \bar{x}(t)),$$

from (5.8) we have $\partial_t u(t,x) + H(t,x,\nabla_x u(t,x)) = 0$. Since H is convex in the p variable, we have the following representation formula (see Lions (1982)).

$$u(t,x) = \inf_{\substack{\gamma \in C^0(\mathbb{R}_+,\mathbb{R}) \\ \gamma(t)=x}} \left[\int_0^t L\left(s,\gamma(s),\dot{\gamma}(s)\right) ds + u^0(\gamma(0)) \right], \tag{5.23}$$

where $L(t,x,v)$ is the Lagrangian of the equation, obtained through a Legendre transform (or a convex conjugate) of H.

Every γ which is admissible as a minimizer in (5.23) is called a *characteristic* of the Hamilton-Jacobi equation (5.8). Note that every characteristic γ formally satisfies the condition

$$\frac{\mathrm{d}}{\mathrm{d}s}\left[\partial_v L\left(s,\gamma,\dot{\gamma}(s)\right)\right] = \partial_x L\left(s,\gamma(s),\dot{\gamma}(s)\right). \tag{5.24}$$

(5.24) holds because γ is a critical point of the functional defined in (5.23). Note that if we replace H by $\tilde{H}(x,p) = -\frac{x^2}{2} + \frac{p^2}{2} + 1$, the Legendre transform of $\tilde{H}$ can be computed explicitly:

$$\tilde{L}(x,v) = \frac{x^2}{2} + \frac{v^2}{2} - 1.$$

Then (5.24) becomes

$$\ddot{\gamma}(s) = \gamma(s).$$

5.3 NUMERICAL STUDY

In this section we perform several numerical tests for the presented models considering different values of parameters, replicating different scenarios: stabilization around an optimal value, cycles (occurring through the evolutionary rescue phenomena) and the extinction.We then compare the numerical results obtained for the stochastic and deterministic approaches, using in particular an asymptotic-preserving scheme which allows us to observe the population dynamics on the passage from the integro-differential equation (5.5) to a limit (5.7). Throughout this section we define the birth, death rates and the mutation kernel to those given in (5.12)-(5.14) respectively, with the parameters fixed throughout all the experiments to $b \equiv 1$, $d_r \equiv 1$, $C \equiv 0.5$ respectively (unless otherwise stated).

5.3.1 *Stochastic model*

5.3.1.1 *The scheme*

Our aim is to simulate the population dynamics over a fixed interval $[0, T]$. We begin by simulating an initial population of size N^0. We assume that the population is normally distributed around the mean trait x^0_{mean} with a standard deviation σ^0 so that the resulting vector $X^0 \in \mathbb{R}^{N^0}$. We know that in a time step Δ, an individual can die, give birth, or be a subject to HT. Each event happens according to a certain probability that we compute from the rates. A more detailed description of the simulations is provided in Algorithm 1.

Note that in our setting it is possible that $1, 2$ or 3 events happen within the same time step. Keeping a discretization time step small helps us to keep a biological sense in our simulation: even if the event of horizontal transfer with an "already dead" individual is possible in our setting (if $T_d \leq T_{HT} \leq \Delta$), this event is extremely rare.

Algorithm 4: Population dynamics on time interval $[0, T]$

Random initialization of a population $X^0 := \mathcal{N}(x^0_{mean}, \sigma^0) \times N^0$;

while $i\Delta \leq T$ **do**

$\quad X^i = X^{i-1}$, $N^{i-1} = size(X^{i-1})$;

$\quad$ **for** $\forall x \in X^i$ **do**

$\quad\quad R_b := b(x)$, $R_d := d(x) + C N^{i-1}$, $R_{HT} := \sum_{y \in X^i} h_K(x - y, N^{i-1})$;

$\quad\quad T_b := \lambda(R_b)$, $T_d := \lambda(R_d)$, $T_{HT} := \lambda(R_{HT})$, where λ denotes an exponential random law;

$\quad\quad$ **if** $T_b \leq \Delta$ **then**

$\quad\quad\quad$ pick up a new trait z from $\mathcal{N}(x, \sigma)$;

$\quad\quad\quad$ add a new individual with trait z to X^i;

$\quad\quad$ **end**

$\quad\quad$ **if** $T_{HT} \leq \Delta$ **then**

$\quad\quad\quad$ pick a trait $y \in X^{i-1}$ according to the law $\frac{h_K(x - y, N^{i-1})}{\sum_{y \in X^i} h_K(x - y, N^{i-1})}$;

$\quad\quad\quad$ remove individual with trait x and add individual with trait y;

$\quad\quad$ **end**

$\quad\quad$ **if** $T_d \leq \Delta$ **then**

$\quad\quad\quad$ remove the individual with trait x from X^i

$\quad\quad$ **end**

$\quad$ **end**

$\quad$ **return** X^i

end

We simulate the population of initial size $N_0 = 10000$ up to time $T = 1000$ with $\Delta = 0.01$, with the parameters being defined at the beginning of the section, and α is a Heaviside function. Even if

a Heaviside function is not the most easy to analyze when we pass to the deterministic limit of the system (see Subsections 5.2.2 and 5.2.3), we use it for the stochastic simulation, since it is the most straightforward model for HT in biological context, and is much faster to compute than a smooth function. We fix all constants but τ_0, which regulates the Horizontal Transfer, and study how it affects the dynamics. Then we plot the density of the population at each moment of time (left side of each Figure): brighter colors on plot mean that there is a big amount of individuals with very similar traits. On the right top and right bottom we plot the normalized population size (ratio between the actual size and the carrying capacity of the system), and the mean trait.

Depending on the parameters we may observe three types of behavior (see Figure 5.1). A first possibility, for small values of τ_0, is stabilization (Figure 5.1a). In this case the population rapidly reaches the equilibrium and concentrates around the optimal trait, which is close to 0.1 (with stochastic fluctuations). Note that in this case, the mean trait is shifted in comparison to the optimal trait without HT (which is $x = 0$).

A second option, for intermediate values of τ_0, is the cycling behavior (Figure 5.1b). Since the transfer rate is sufficiently large, the population is driven towards a deleterious trait, which is eventually less fit than the trait $x = 0$. If the drift is not too strong, the very few individuals which were not affected by HT and remained fit (with x close to 0) manage to regrow and eventually repopulate the environment, which launches the cycle again.

The last possibility, for large values of the horizontal transfer rate τ_0, is the extinction of the population (Figure 5.1c). It occurs because too many individuals were affected by deleterious traits of their neighbors, so that they die faster than is needed for replicating the population.

(a) Stabilization: $\tau_0 = 0.02$ (b) Cycles: $\tau_0 = 0.4$ (c) Extinction: $\tau_0 = 0.9$
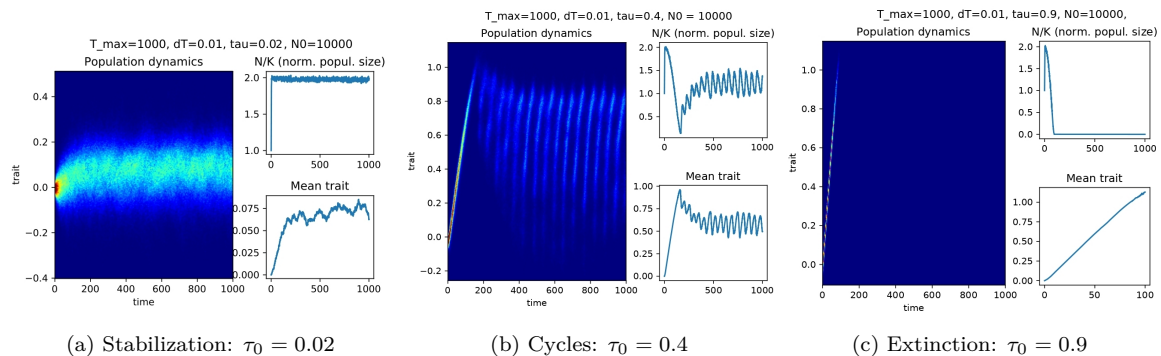
Figure 5.1: Behavior of the population dynamics as the mutation rate τ_0 is changing, ($b_r = d_r = 1$, $\sigma = 10^{-2}$, $K = 10^4$, $\sigma^0 = 10^{-2}$, $x_{mean}^0 = 0$, $N^0 = 10^4$).

To understand better this phenomenon, we have to give a precise definition of what do we actually refer to, when we say "the critical value" of the transfer rate. In the stochastic setting the answer is not trivial, and that is where the individual-based model reaches its limit. What we observe experimentally is the following: when we change the value of the HT rate starting from zero, the cycles in the population dynamics become more clearly visible, the fluctuations of the mean trait and the population size become more ample, until at some point the probability of extinction overweights

the probability of survival and, finally, at the value of τ_0, which we call "critical" we obtain an almost sure extinction.

But since we are working with a point process, giving a strict definition of a "critical value for an extinction" in terms of probability measures seems to be out of reach. Even in the experimental setting this notion is ambiguous: when the value of τ_0 is getting closer to a "critical" value (numerically we observe an almost sure extinction at $\tau_0 = 0.49$), in different repetitions of the same experiment we may observe different types of behavior: either cycles, or extinction, which occurs after several cycles. It is illustrated on Figure 5.2, where the computations, launched with exactly the same set of parameters, give very different results. Furthermore, it is not always clear how to differentiate between the stabilization and cycles, especially when the variance of the mutation kernel is large. To the best of our knowledge, there is no straightforward way to analytically measure the probability of each outcome under given initial conditions, which makes the model difficult to analyse.

This constraint of an individual-based model naturally leads us to studying a limiting system described in Subsection 5.2.2.

(a) Extinction   (b) Cycle and extinction   (c) Cycles
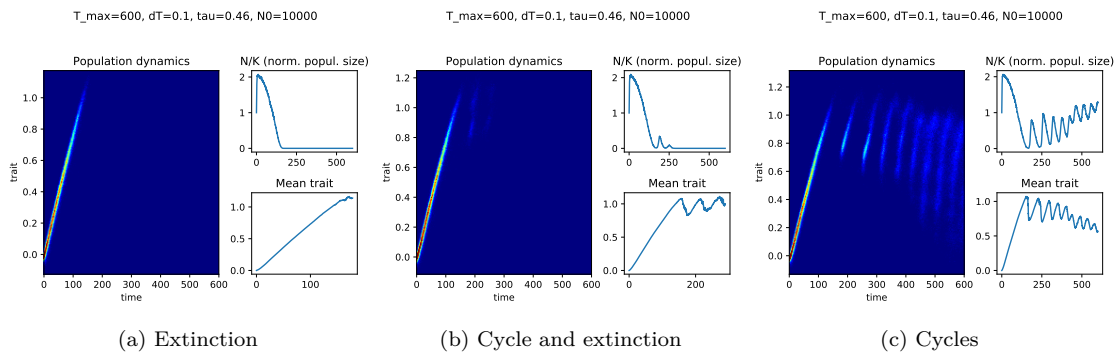
Figure 5.2: Different behaviors for $\tau_0 = 0.46$ (and the other parameters as in Figure 5.1).

5.3.1.2   *Lineages*

With the help of the stochastic model we can keep track of the lineage of an individual i which lives at a final observed time T. More precisely, we are interested in a history of a phenotype which leads to a long-term survival of an individual.

We illustrate some numerical experiments on Figure 5.3. The four simulations are done with the same parameters. In the background, every point with coordinates (t, x) represents an individual with trait x living at time t (as in Figure 1). The solid lines represent the lineages of the individuals that live at the final time. Small fluctuations are the results of birth with mutation, while the large upwards jumps correspond to an occurrence of a HT.

First of all, we can see on the plot that all the lineages are gathered into one line up to $t = 400$. It means that all individuals that live at final time $t = 700$ emanate from one single ancestor of the initial population. This phenomenon is well known and referred to as *coalescence* in the literature (see

for instance Kingman (1982), or Arenas and Posada (2014, 2010) for a mathematical description of a classical population genetics theory).

Besides, we see that the lineages remain centered around $x = 0$ during almost all the observed time. It is explained by the fact that every lineage that goes to a high value of x (corresponding to deleterious phenotype) cannot recover (since the mutations are small), and eventually goes extinct. This illustrates that the population manage to sustain because of the very few individuals that were not affected by HT throughout the history.
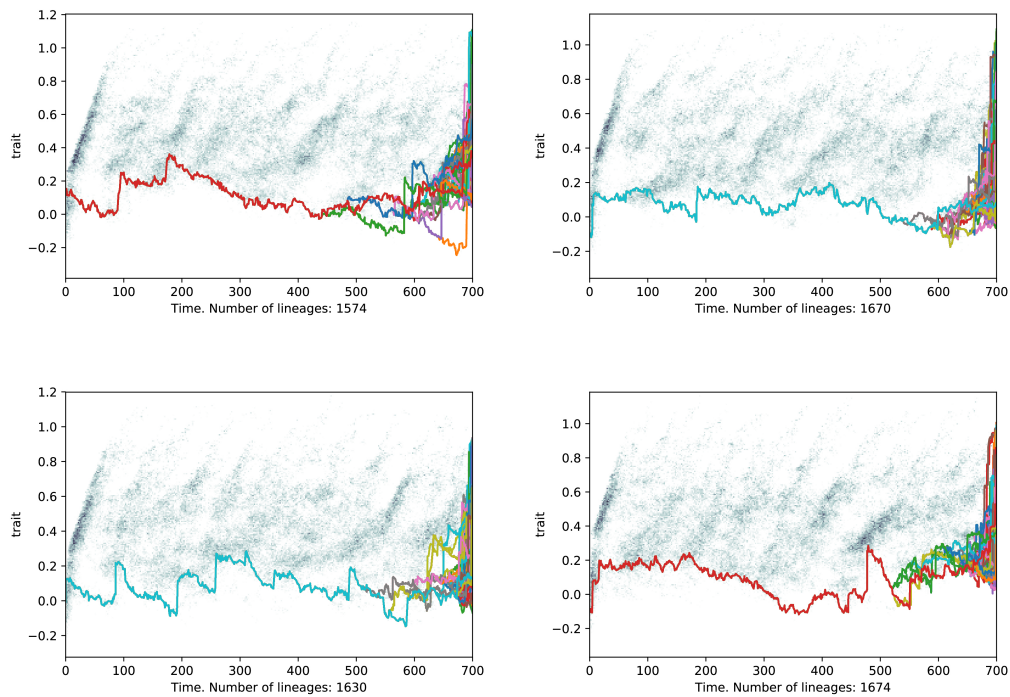
Figure 5.3: Simulations on the stochastic model with lineages. $\tau_0 = 0.4$, $T_{max} = 700$, $dT = 0.1$, $K = N_0 = 1000$ and other parameters as in Figure 5.1.

5.3.2 *Numerical scheme for the PDE model*

In this subsection, a numerical scheme for (5.5) is presented, and its properties are numerically investigated. For the discretization of (5.5), we consider a bounded space of traits $[X_{\min}, X_{\max}]$, discretized with N_x points. Denoting N_x the number of discretization points of the interval $[X_{\min}, X_{\max}]$, we define

$$\Delta x = \frac{X_{\min} - X_{\max}}{N_x - 1},$$

and

$$x_i = X_{\min} + i\Delta x, \ \ 0 \leq i \leq N_x - 1.$$

We consider the time interval $[0, T_{\max}]$, discretized with N_t points $t_n = n\Delta t$, for $0 \leq n \leq N_t - 1$, and where Δt is defined as

$$\Delta t = \frac{T_{\max}}{N_t - 1}.$$

The approximations of the solution f of (5.5) at (t_n, x_i), and of its density ρ at t_n are denoted f_i^n and ρ^n respectively. We recall that the initial condition f^0 is a smooth function of x given in (5.16) and the initial density ρ^0 is computed using a left-point quadrature rule for f^0 as follows:

$$\rho^0 = \Delta x \sum_{i=0}^{N_x - 1} f^0(x_i).$$

The scheme is written with an explicit Euler scheme, in which the integrals are computed with a left-point quadrature rule. For $n \geq 1$ and $0 \leq i \leq N_x - 1$, it reads

$$\varepsilon \frac{f_i^{n+1} - f_i^n}{\Delta t} = (d(x_i) + C\rho^n) f_i^n + [m * (bf)]_i^n + f_i^n \Delta x \sum_{j=0}^{N_x - 1} \tau(x_i - x_j) \frac{f_j^n}{\rho^n}. \qquad (5.25)$$

In (5.25), the convolution product $[m * (bf)]_i^n$ is computed with a left-point quadrature rule, as well as the other integrals. To do so, a grid in the z variable is defined as for the x variable. Let $Z_{\min}$ and $Z_{\max}$, and the number N_z of discretization points be given. The grid in z is defined as

$$\forall 0 \leq k \leq N_z - 1, z_k = Z_{\min} + k\Delta z,$$

where $\Delta z = (Z_{\max} - Z_{\min}) / (N_z - 1)$. When $x_i + \varepsilon z_k \in [X_{\min}, X_{\max}]$, the value of $f(t_n, x_i + \varepsilon z_k)$ is approximated by a linear interpolation of the $(f_i^n)_{0 \leq i \leq N_x - 1}$. When $x_i + \varepsilon z_k < X_{\min}$, or $x_i + \varepsilon z_k > X_{\max}$, it is computed with a linear extrapolation of the $(f_i^n)_{0 \leq i \leq N_x - 1}$, using the slope at the corresponding end of the X domain. Using the notation $f^n(x_i + \varepsilon z_k)$ for the approximation of $f(t_n, x_i + \varepsilon z_k)$, we then define

$$[m * (bf)]_i^n = \Delta z \sum_{k=0}^{N_z - 1} m(z_k) b(x_i + \varepsilon z_k) f^n(x_i + \varepsilon z_k).$$

5.3.2.1   *Case $\varepsilon = 1$: comparison with stochastic model*

A first point that we are interested in is whether under identical parameters and initial conditions we may reproduce the same behavior as in the stochastic model. Thus, we conduct several experiments, fixing the parameter ε to 1 (thus, we do not rescale time, nor the mutation rate), leaving all the other parameters fixed to the same values as in the stochastic simulation case.

As we may see on Figure 5.4, simulations correspond in overall to those of the stochastic model. Indeed, when the HT rate τ_0 is small enough the population rapidly stabilizes around its equilibrium state (see Figure 5.4a), as in the stochastic simulations. A further similarity between the two models is that in both cases the optimal trait is shifted a bit above 0. It is caused by the HT phenomenon.

For larger values of τ_0, where we would expect to have distinguishable cycles, we observe indeed damped oscillations, see Figure 5.4b. We stress that for the stochastic model it is not the case, see Figure 5.1b. The way we understand the damping in the oscillations is that the PDE model and the numerical algorithm that we use are not designed to have a precise grasp on the exponential small

(a) Stabilization: $\tau_0 = 0.02$

(b) Cycles: $\tau_0 = 0.4$

(c) Extinction and cycles: $\tau_0 = 0.9$

(d) Full Extinction $\tau_0 = 1.2$
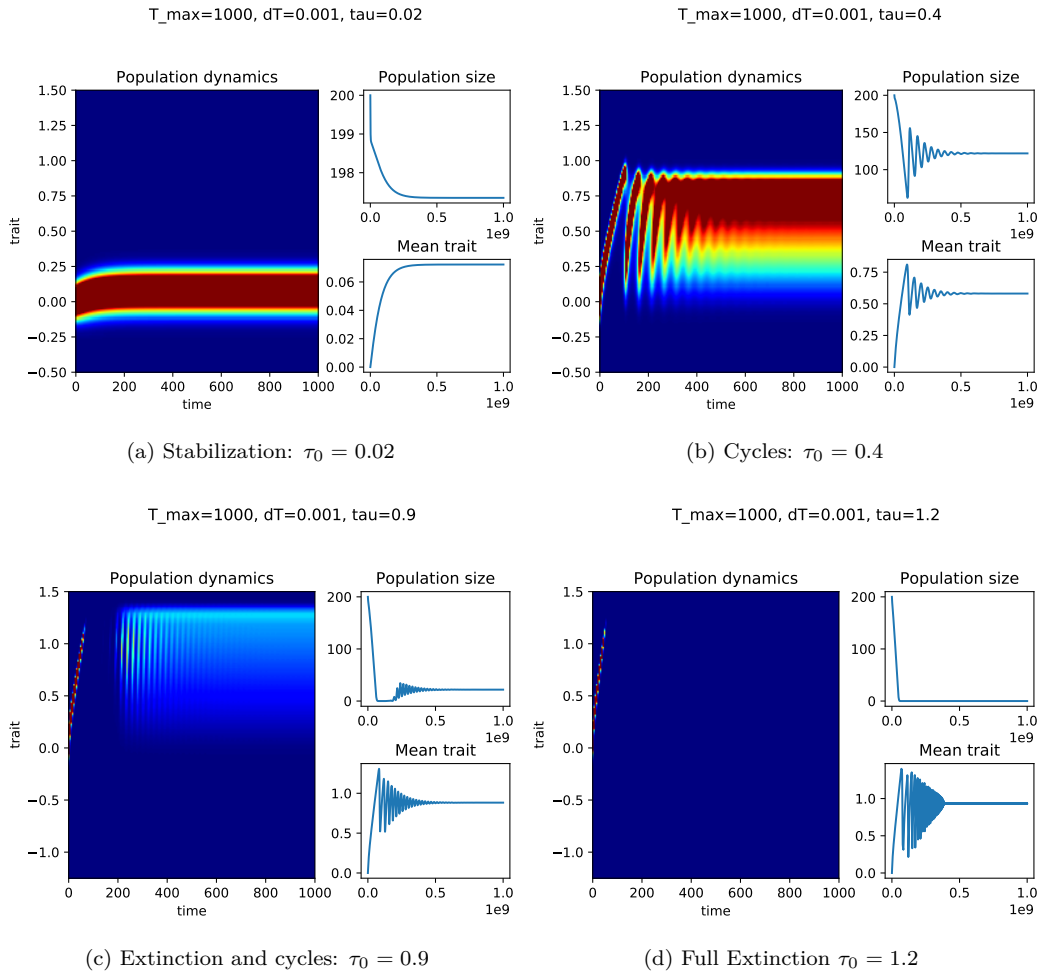
Figure 5.4: Behavior of the population dynamics described by a PDE model as the mutation rate τ_0 is changing, $(b_r = d_r = 1, \sigma = 0.01, \varepsilon = 1)$.

values of f, on which the cycling phenomenon relies. This limitation suggests to perform the change of variable (5.6), and to write a numerical scheme which converges uniformly when $\varepsilon \to 0$. This is what the next subsection is devoted to.

On Figure 5.4c, we observe that as τ_0 becomes larger the population gets extinct, and then, surprisingly enough, "reborns" after a period of extinction. This scenario can only be reproduced on density-based models, since in individual-based model any extinction is definitive. On Figure 5.4d we observe a full extinction of the population without regrowth. We will give further insights on those two cases in the next subsection.

5.3.3 *The scheme for the Hamilton-Jacobi equation*

5.3.3.1 *Case $\varepsilon \to 0$: description of the numerical scheme*

As the rescaling parameter ε goes to 0, the model given by (5.7) gets closer to its limiting state (5.8). However, the numerical approximation of (5.5) for $\varepsilon \ll 1$ is not a trivial task. Indeed, for small ε, the

solution f^ε of (5.5), is expected to concentrate around the dominant trait. To be able to catch its stiffness numerically, one has to refine the grid in x, to ensure enough precision in the computation of f. As a consequence, the computational cost of the numerical simulations increases when $\varepsilon \to 0$, and reaching the asymptotic regime with this scheme is not possible. In this part, we present a numerical scheme for (5.5) which enjoys stability properties in the limit $\varepsilon \to 0$.

To avoid the increase of computational cost when reaching the asymptotics, and to ensure the scheme approaches the limit Hamilton-Jacobi equation for small ε, a scheme for the solution u^ε of (5.7) which enjoys the Asymptotic Preserving (AP) property is proposed here. Such schemes have been introduced in Klar (1998, 1999), Jin (1999), their properties are often summarized by the following diagram:

$$
\begin{array}{ccc}
P_\varepsilon & \xrightarrow{\varepsilon \to 0} & P_0 \\
{\scriptstyle h \to 0} \Big\uparrow & & {\scriptstyle h \to 0} \Big\uparrow \\
S_\varepsilon^h & \xrightarrow{\varepsilon \to 0} & S_0^h
\end{array}
$$

It should be understood as follows: when the parameter $\varepsilon > 0$ is fixed, the scheme S_ε^h is consistent with the ε-dependent problem P_ε. When ε goes to 0, the solution of P_ε converges to the solution of the limit problem P_0. The AP scheme S_ε^h is stable along the transition to the asymptotic regime. It means that, when ε goes to 0 with fixed discretization parameters h, the scheme becomes a limit scheme S_0^h, which is consistent with the limit problem P_0.

As an AP scheme is required to enjoy stability properties when ε is going to 0, one has to ensure that all the quantities that have to be computed enjoy this property. In the case we are considering, the main concerns are the computation of the integral containing the birth term, the computation of the integral containing the transfer term and the computation of ρ. If all of them are correctly defined, the scheme we propose reads

$$
\frac{u_i^{n+1} - u_i^n}{\Delta t} = -(d(x_i) + C\rho^{n+1}) + B_i^n + T_i^n, \tag{5.26}
$$

where B_i^n stands for an approximation of

$$
\int_{\mathbb{R}} m(z) b(x_i + \varepsilon z) e^{(u_\varepsilon(t^n, x_i + \varepsilon z) - u_\varepsilon(t^n, x_i))/\varepsilon} dz, \tag{5.27}
$$

and T_i^n is for

$$
\int_{\mathbb{R}} \tau(x_i - y) \frac{f(t^n, y)}{\rho(t^n)} dy. \tag{5.28}
$$

Here, we used the notations and discretization grids defined in the beginning of Section 5.3.2, and the dependencies in ε are omitted to simplify the notations. In what follows, we present how T_i^n, B_i^n and ρ^{n+1} can be computed in a way that ensures they are consistent with their definition for fixed ε, that they can be computed with a constant computational cost with respect to ε, and that their asymptotic behavior when ε goes to 0 is meeting the continuous one (5.8).

- **Computation of T_i^n.** The direct approximation of (5.28) with a quadrature rule is consistent for $\varepsilon \sim 1$. However, since f is expected to concentrate when $\varepsilon \to 0$, it lacks precision in the

asymptotic regime. Especially, the convergence of f/ρ to a Dirac is not ensured when the integral is approximated directly. Remarking that

$$\frac{f^\varepsilon(t^n,y)}{\rho^\varepsilon(t^n)} = \frac{\mathrm{e}^{u^\varepsilon(t^n,y)/\varepsilon}}{\displaystyle\int_\mathbb{R} \mathrm{e}^{u^\varepsilon(t^n,z)/\varepsilon}\mathrm{d}z} = \frac{\mathrm{e}^{(u^\varepsilon(t^n,y)-\max\limits_x u^\varepsilon(t^n,x))/\varepsilon}}{\displaystyle\int_\mathbb{R} \mathrm{e}^{(u^\varepsilon(t^n,z)-\max\limits_x u^\varepsilon(t^n,x))/\varepsilon}\mathrm{d}z},$$

(5.28) is computed with a left-point quadrature rule in the integrals of the previous expression. It reads

$$T_i^n = \Delta x \sum_{j=1}^{N_x-1} \tau(x_i - y_j)\frac{\mathrm{e}^{(u_j^n-\max\limits_l u_l^n)/\varepsilon}}{\Delta x \displaystyle\sum_{k=0}^{N_x-1} \mathrm{e}^{(u_k^n-\max\limits_l u_l^n)/\varepsilon}} = \frac{\displaystyle\sum_{j=1}^{N_x-1} \tau(x_i - x_j)\mathrm{e}^{(u_j^n-\max\limits_l u_l^n)/\varepsilon}}{\displaystyle\sum_{k=0}^{N_x-1} \mathrm{e}^{(u_k^n-\max\limits_l u_l^n)/\varepsilon}}. \qquad (5.29)$$

For fixed ε, (5.29) is consistent with (5.28). Since all the arguments of the exponentials are nonpositive, the limit of (5.29) for small ε can be read on that expression. Denoting j_0 the index such that

$$u_{j_0}^n = \max_l u_l^n,$$

and supposing that there exists a unique such j_0, the limit of (5.29) for small ε is

$$\tau(x_i - x_{j_0}).$$

This is consistent with the last term in the limit Hamilton-Jacobi equation (5.8).

- **Computation of B_i^n.** Once again, the numerical approximation of (5.27) is done with a quadrature in the integral. Using the notations of Section 5.3.2, a grid in z is defined. The functions m and b are respectively evaluated at z_k and $x_i + \varepsilon z_k$, but the interpolation of u^n at $x_i + \varepsilon z_k$ has to be done with special care to make the scheme enjoy the expected asymptotic behavior. Using a left-point quadrature rule, (5.27) is approximated by

$$\Delta z \sum_{\substack{k=0 \\ \varepsilon|z_k|\leq dx}}^{N_z-1} m(z_k)b(x_i + \varepsilon z_k)\mathrm{e}^{z_k \nabla_{n,i,k}^{\varepsilon,small}} + \Delta z \sum_{\substack{k=0 \\ \varepsilon|z_k|>dx}}^{N_z-1} m(z_k)b(x_i + \varepsilon z_k)\mathrm{e}^{z_k \nabla_{n,i,k}^{\varepsilon,large}},$$

where $\nabla_{n,i,k}^\varepsilon$ stands for an approximation of

$$\frac{u^\varepsilon(t^n,x_i+\varepsilon z_k) - u^\varepsilon(t^n,x_i)}{\varepsilon z_k}.$$

In both cases, it is computed with a linear interpolation of the values u_i^n. Hence, $\nabla_{n,i,k}^{\varepsilon,large}$ is given by

$$\nabla_{n,i,k}^{\varepsilon,large} = \frac{\tilde{u}_{i,k}^n - u_i^n}{\varepsilon z_k},$$

where $\tilde{u}_{i,k}^n$ is computed as the linear interpolation of $(u_i^n)_{1\leq i\leq N_x}$ at $x_i + \varepsilon z_k$. If $x_i + \varepsilon z_k < X_{\min}$ or $x_i + \varepsilon z_k > X_{\max}$, the extrapolation is done linearly using the slope at the first or last point of the interval. Since $\varepsilon z_k > \Delta x$, no stability issue is faced in this computation. Still using a linear interpolation, when $0 < \varepsilon z_k \leq \Delta x$, it is worth noticing that

$$\frac{\tilde{u}_{i,k}^n - u_i^n}{\varepsilon z_k} = \frac{u_{i+1}^n - u_i^n}{\Delta z},$$

and when $0 > \varepsilon z_k \geq -\Delta x$,

$$\frac{\tilde{u}_{i,k}^n - u_i^n}{\varepsilon z_k} = \frac{u_i^n - u_{i-1}^n}{\Delta x}.$$

as a consequence, we define:

$$\nabla_{n,i,k}^{\varepsilon,small} = \begin{cases} \dfrac{u_{i+1}^n - u_i^n}{\Delta x}, & \text{if } 0 < \varepsilon z_k \leq \Delta x \\ \dfrac{u_i^n - u_{i-1}^n}{\Delta x}, & \text{if } -\Delta x \leq \varepsilon z_k < 0 \\ 0, & \text{if } z_k = 0. \end{cases}$$

This definition of B_i^n is consistent with (5.27). Moreover, when ε goes to 0 with fixed numerical parameters, such as $Z_{\min}$ and $Z_{\max}$, the expression $\nabla_{n,i,k}^{\varepsilon,large}$ is not used at all, and

$$B_i^n \underset{\varepsilon \to 0}{=} B_i^{n,0} = \Delta z \sum_{\substack{k=0 \\ z_k < 0}}^{N_z-1} m(z_k)b(x_i)\mathrm{e}^{z_k \frac{u_i^n - u_{i-1}^n}{\Delta x}} + \Delta z m(0)b(x_i) + \Delta z \sum_{\substack{k=0 \\ z_k > 0}}^{N_z-1} m(z_k)b(x_i)\mathrm{e}^{z_k \frac{u_{i+1}^n - u_i^n}{\Delta x}}.$$
(5.30)

- **Computation of ρ^{n+1}.** In (5.26), ρ^{n+1} is considered in an implicit way, to make the limit scheme be consistent with the limit equation (5.8). Since

$$\rho(t) = \int_{\mathbb{R}} \mathrm{e}^{u(t,x)/\varepsilon}\mathrm{d}x,$$

for $\varepsilon > 0$, we define

$$\rho^{n+1} = \Delta x \sum_{i=0}^{N_x-1} \mathrm{e}^{u_i^{n+1}/\varepsilon}.$$

A closed equation on ρ^{n+1} can be deduced from (5.26). Indeed, (5.26) yields

$$\mathrm{e}^{u_i^{n+1}/\varepsilon} = \mathrm{e}^{-\Delta t \rho^{n+1}/\varepsilon}\mathrm{e}^{(u_i^n + \Delta t[-d(x_i)+B_i^n+T_i^n])/\varepsilon},$$

and so

$$\rho^{n+1} = \Delta x \, \mathrm{e}^{-\Delta t \rho^{n+1}/\varepsilon} \sum_{i=0}^{N_x-1} \mathrm{e}^{A_i^n/\varepsilon},$$
(5.31)

where A_i^n denotes $u_i^n + \Delta t\left(-d(x_i) + B_i^n + T_i^n\right)$ to simplify the notations. Eventually, ρ^{n+1} is the solution of $h(y) = 0$, where

$$h(y) = y\mathrm{e}^{\Delta t y/\varepsilon} - \Delta x \mathrm{e}^{A_{i_0}^n/\varepsilon} \sum_{i=0}^{N_x-1} \mathrm{e}^{(A_i^n - A_{i_0}^n)/\varepsilon},$$
(5.32)

where $A_{i_0}^n = \max_i A_i^n$ has been taken apart to get an uniform estimate with respect to ε on the remaining sum. It is also a solution of the equivalent equation $g(y) = 0$, with

$$g(y) = -\varepsilon \ln(y) - \Delta t y + \varepsilon \ln(\Delta x) + A_{i_0}^n + \varepsilon \ln\left(\sum_{i=0}^{N_x-1} \mathrm{e}^{(A_i^n - A_{i_0}^n)/\varepsilon}\right).$$
(5.33)

To find ρ^{n+1}, a Newton's method is applied on expression (5.32) or on (5.33). Both expressions are smooth convex functions of ρ, and are equivalent. Hence, the Newton's method converges whatever is used. Nevertheless, it must be chosen with care. (5.32) is to be chosen when ρ^{n+1} is close to 0 (for large values it becomes less accurate), whereas (5.33) is more adapted when

ρ^{n+1} is not small, since it is more prone to accumulate numerical errors when $\rho^{n+1} \to 0$. In the effective implementation of the method, either one formulation or the other is chosen, depending on the values reached during the iterations of the algorithm. Eventually, to ensure the stability of the numerical resolution of (5.31) when $\varepsilon \to 0$, the inverse of the derivatives of h and g are analytically computed and implemented as

$$\frac{1}{h'(y)} = \frac{\varepsilon}{\varepsilon + \Delta t} e^{-\Delta t y / \varepsilon}, \quad \frac{1}{g'(y)} = -\frac{y}{\varepsilon + \Delta t}.$$

Since $y > 0$, these two expressions are uniformly bounded with respect to ε when Δt is fixed. As a consequence, the cost of the numerical resolution of (5.31) does not increase with ε.

When $\varepsilon > 0$ is fixed, the scheme (5.26) is consistent with (5.7), since only quadrature formula and interpolation methods have been used to write it. The way all the terms are computed, as well as the numerical resolution of the non-linear equation (5.31), ensures the stability of the numerical computations in the small ε regime. Hence, when $\varepsilon \to 0$ with fixed discretization parameters, the scheme (5.26) becomes

$$\frac{u_i^{n+1} - u_i^n}{\Delta t} = -\left(d(x_i) + C\rho^{n+1}\right) + B_i^{n,0} + \tau(x_i - x_{j_0}),$$

where j_0 is such that $u_{j_0}^n = \max_i u_i^n$, and $B_i^{n,0}$ has been defined in (5.30).

We do not give a strict proof of consistency of this scheme with respect to the limiting Hamilton-Jacobi equation (5.8), since it is out of scope of the project. However, we draw the attention to few important points which need to be taken into account while working with the scheme. In particular, the behaviour of the quantity $\rho(t)$ is not well understood in the case of an extinction. The problem is that intuitively $\rho(t)$ must represent the density of the population — so that when it goes to zero, we expect an extinction. However, in a Hamilton-Jacobi case even when the $\rho(t)$ reaches zero, the population can still regrow after some time. This can be explained by the fact that after two limiting procedures (passing first to the infinite system size, and then to the infinite time horizon), the "size" of the population can not be described straightforwardly. Accurate link between the quantities obtained as a result of stochastic and PDE simulation is also a question which requires further investigation when $\rho(t) \ll 1$.

5.3.3.2 *Case $\varepsilon \to 0$: the numerical results*

In this subsection we simulate the dynamics of the population by considering a small value of ε and discuss the obtained results in order to compare them with previous simulations. Note that, in order to compare both, the stochastic and the Hamilton-Jacobi behaviours, the first step to do is to obtain the simulations for the stochastic model also in the case where the HT rate is a smooth function as we do for the Hamilton-Jacobi case. We recall that, in subsection 5.3.1 simulations for the stochastic model are done with a Heaviside function as HT rate since it is a more natural choice for simulation of a jump process.

(a) Stabilization: $\tau_0 = 0.02$

(b) Cycles: $\tau_0 = 0.4$

(c) Cyclic extinction: $\tau_0 = 0.9$

(d) Full extinction: $\tau_0 = 1.2$
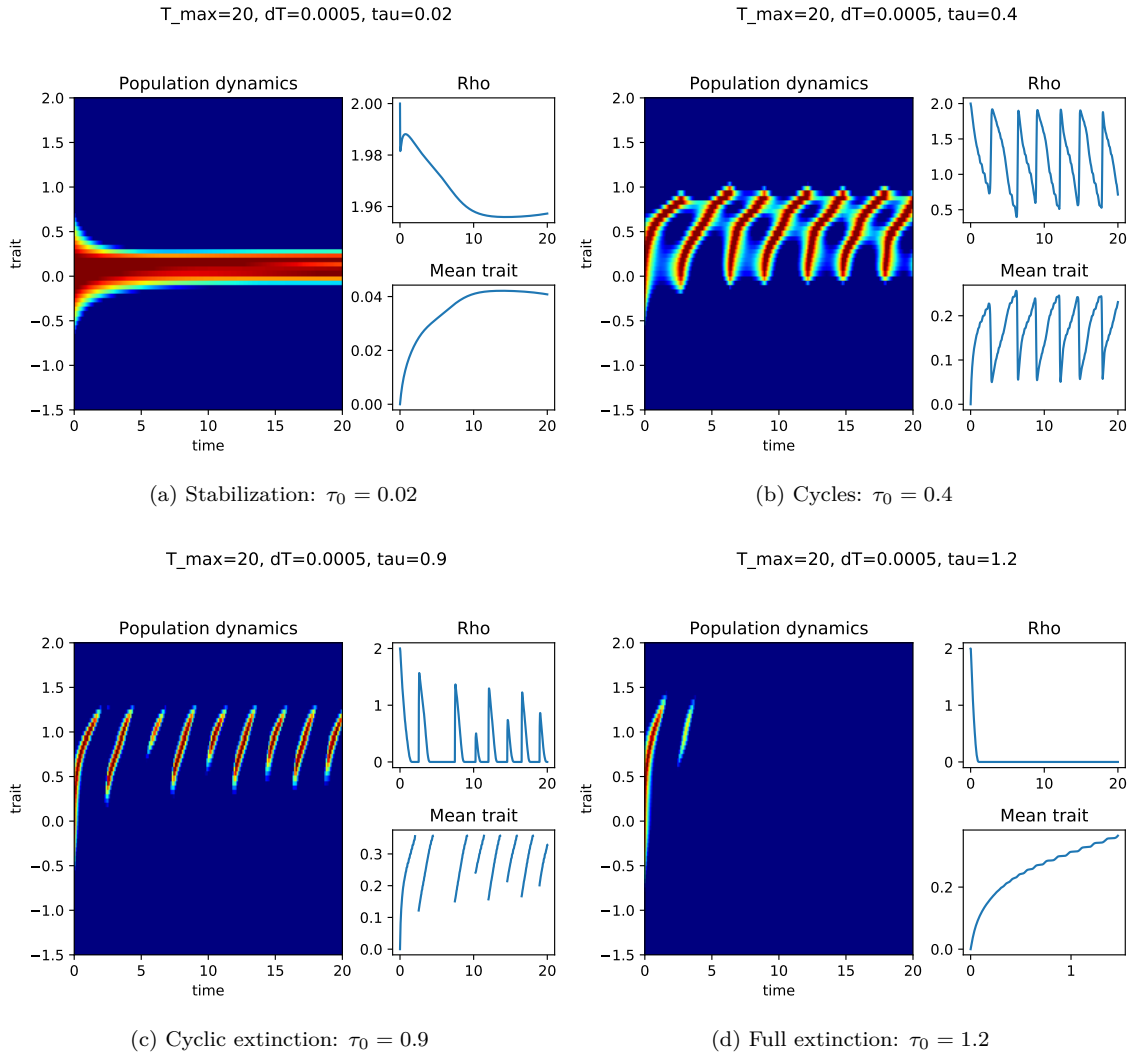
Figure 5.5: Behavior of the population dynamics described by a PDE model for $\varepsilon = 0.01$ as the mutation rate τ is changing, $(b_r = d_r = 1,\ \sigma = 1)$.

On Figure 5.5 we simulate the population dynamics for $\varepsilon = 0.01$. Upon rescaling time (for chosen ε time scale $T = 10$ corresponds, in fact, to $\frac{T}{\varepsilon} = 1000$ in previous simulations) and the variance parameter, we see the same patterns, with few differences.

On Figure 5.5a, we observe a stabilization of the mean trait, as in Figure 5.1a. Similarly, on Figure 5.5b, we observe cycles, but on the contrary to the PDE model oscillations are not damped. Moreover, it is worth pointing out that the duration of a cycle here corresponds to what we observe in the corresponding stochastic plot (on Figure 5.1b) multiplied by $\varepsilon = 0.01$. On Figure 5.5c, we also observe a cycling behavior, but the population goes periodically extinct (i.e the population reaches exponentially small values, of order $e^{1/\varepsilon}$), and then is reborn. In the stochastic model, it corresponds to what is illustrated in Figure 5.2. It is not surprising that this behavior is difficult to observe in the stochastic model, since very small populations are likely to go extinct.

On Figure 5.5d, we can see that the population goes completely extinct. The most interesting case to comment is probably the "partial" extinction seen on 5.5c. Note that despite the fact that ρ

remains at 0 for some time, the population regrows. The point is that, as it was already mentioned above, this numerical parameter has no 1:1 correspondence to the population size parameter $\frac{N_t}{K}$ used in stochastic model. Also note that similar behaviour of stochastic and HJ model are reproduced under a bit different values of parameters. It is caused by the rescaled time and mutation kernel, so that the rigorous link between the two models is still to be developed.

Another interesting thing to comment is that on Figure 5.5b we may notice that, from the dynamics of the mean trait and the density of the population, it is easy to estimate the periods of the system. Indeed, since the system is deterministic, we just have to compute the distances between local maxima on each curve. For the stochastic system this task is more difficult, especially for a small population, because it includes a filtering problem of a noisy signal. To get more accurate results in the stochastic model we have to increase the time scale and number of individuals, which is costly from a computational point of view. However, if our goal is to study numerically the lineages which lead to the evolutionary rescue of the population, it is still more straightforward to use the individual-based model.

To finish with, let us give some flavor on the computational cost of the simulations for each type. In Table 1 we give a short overview of the elapsed time for the same values of parameters, but for different schemes. As expected, individual-based model is the most expensive to compute. All the computations were performed in `numpy` library of Python on MacBook Pro (Intel Core i5 processor, 2,7GHz).

	$\Delta = 0.1,\ T = 10$	$\Delta = 0.01,\ T = 10$
SM ($N = 1000$)	3.883s	38.145s
SM ($N = 10000$)	15.805s	153.255s
PDE ($\varepsilon = 1$)	0.186s	1.673s
HJ ($\varepsilon = 10^{-2}$)	0.191s	1.636s
HJ ($\varepsilon = 10^{-6}$)	0.195s	1.656s

Table 1: Elapsed time for the simulation of population dynamics for different models (other parameters are fixed to values used throughout all the other simulations, $\tau = 0.5$).

5.3.4 *Comparison of the theoretical analysis of the Hamilton-Jacobi equation and the numerical simulations of the stochastic model*

5.3.4.1 *Formal computations*

In this section, we propose some formal computations for the stochastic model, based on the analysis of the Hamilton-Jacobi equation performed in the previous section. To fix ideas, we assume $n = 1$ and (5.3)-(5.12)-(5.13), and we fix all constants but τ_0, as in the previous section. However, we choose the function α as a Heaviside function (this is what has been used in the simulations), which is not a smooth function, and thus will lead to minor modifications compared to the previous section.

We make a strong formal assumption: taking $K \gg 1$, we assume that the population behaves like a normally distributed random variable all the time, i.e

$$\nu_t^K(dx) = \rho(t)\frac{1}{\sqrt{2\pi}s(t)}e^{-\frac{|x-\bar{x}(t)|^2}{2s(t)^2}}\,dx,$$

for some standard deviation $s(t)$ and for $\bar{x}(t)$ defined in (5.9). We expect $s(t)$ to be of the same order as σ, but giving a general estimate for $s(t)$ in function of $\bar{x}(t)$ seems intricate. The normalized size of the population $\rho(t) := \frac{N_t^K}{K}$ is approximately given by (see (5.11))

$$\rho(t) = \frac{1}{C}r(\bar{x}(t)), \tag{5.34}$$

where r is defined in (5.18).

We now formally compute the evolutionary singular state $x_\star$. But as α is a Heaviside function (which formally corresponds to the case when $\delta \to 0$ in (5.19)), our derivations must be slightly adapted. In particular, $\tau(x - \bar{x}(t))$ in (5.8) has to be replaced by

$$\int_{\mathbb{R}} \tau(x-y)\frac{\nu_t^K(dy)}{\rho(t)},$$

and accordingly, recalling that the weak derivative of a Heaviside is a Dirac mass at 0, $\tau'(0)$ in (5.19) has to be replaced by

$$\int_{\mathbb{R}} \tau'(\bar{x}(t)-y)\frac{\nu(dy)}{\rho(t)} = \frac{2\tau_0}{\sqrt{2\pi}s(t)}.$$

We find

$$x_\star = \frac{\tau_0}{\sqrt{2\pi}s_\star d_r}, \tag{5.35}$$

where $s_\star$ is an unknown corresponding to the standard deviation of the population at equilibrium concentrated at $x = x_\star$. Note that it corresponds to (5.19) with $\tilde{\delta} := s_\star\sqrt{\pi/2}$.

We now try to estimate $s_\star$. Formally, $s_\star$ should be such that $u_\star(x) := \frac{-(x-x_\star)^2}{2s_\star^2}$ is a stationary solution of (5.8). Differentiating twice, and applying at $x = x_\star$ we find

$$0 = b_r\sigma^2\left(u_\star''(x_\star)\right)^2 - 2d_r,$$

(with the reasonable assumption $\tau''(0) = 0$), which gives

$$s_\star = \sqrt{\sigma\sqrt{\frac{b_r}{2d_r}}}.$$

Numerically, we find $s_\star = 0.12$. We end up with the following formula:

$$x_\star = \frac{\tau_0}{\sqrt{2\pi}\sigma d_r}\sqrt[4]{\frac{2d_r}{b_r}}. \tag{5.36}$$

5.3.4.2 *Stabilization*

We run a numerical test on the stochastic model corresponding to stabilization, for $\tau_0 = 0.02$, and the other parameters as in Figure (5.1a). In this case, $x_\star$ correspond to the mean trait of the population for large time. From, (5.36) we find $x_\star = 0.067$, and from (5.34), we obtain $\rho_\star = 1.99$, which corresponds to what we can see on Figure (5.1a).

5.3.4.3 *Threshold for cycles*

Since equation (5.20) remains unchanged, we obtain the following threshold for cycles (corresponding to (5.21)):

$$\tau_{cyc} = 2\pi d_r \sigma \sqrt{\frac{b_r}{2d_r}}.$$

With our choice of parameters, we obtain $\tau_{cyc} = 0.09$. This threshold corresponds to the numerical simulations (however, characterizing precisely whether cycles occurs or not on the numerical simulations is not easy when τ_0 is close to the threshold).

5.3.4.4 *Threshold for extinction*

Using (5.22), we can also find a threshold for extinction:

$$\tau_{ext} := \sqrt{2\pi b_r d_r \sigma} \sqrt[4]{\frac{b_r}{2d_r}}.$$

For our choice of parameters, we obtain $\tau_{ext} = 0.30$.

We now compare this formula with numerical experiments on the individual-based model. They are organized as follows: we fix the birth b_r or the death rate d_r, and save the first value of τ_0 under which the extinction occurs. Then, we increase the rate and save the next HT rate under which we have an extinction. The resulting curve for the birth rate is saved on Figure 5.6a (for death rate: Figure 5.6b). Non-concerned parameters remain fixed as in Subsection 5.3.1.

The numerical results, in particular, justify the at the first glance surprising fact that the extinction threshold depends on the birth and death rate in the same manner. It seems logical to assume that while a higher birth rate contributes to a bigger survival probability even with a relatively big horizontal transfer rate, a higher death rate must have an opposite effect. However, in conditions of a very "harsh" environment individuals with non-fit traits die out before they manage to transfer their genetic information to the other individuals. As a consequence, the value of the critical τ increases as the value of the birth (or death) rate constant increases.

(a) Birth dependency   (b) Death dependency
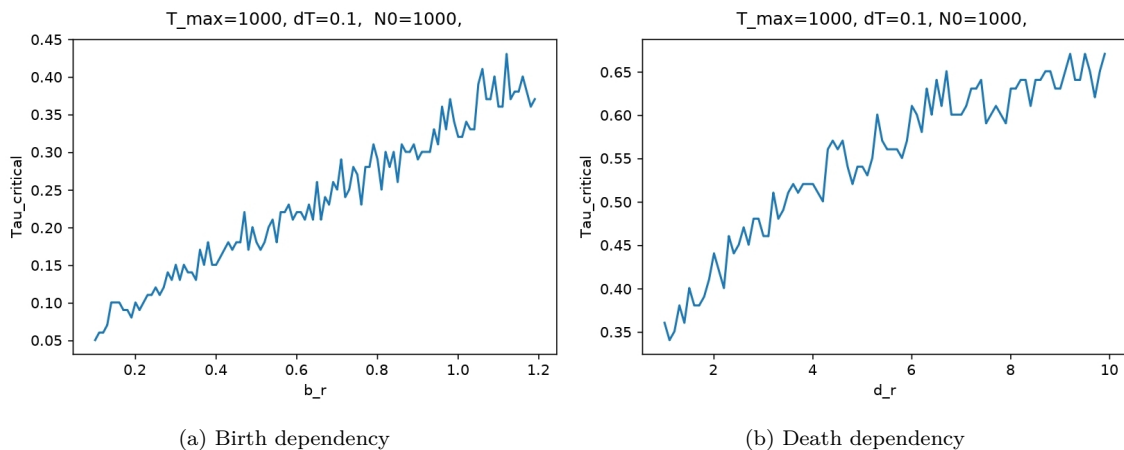
Figure 5.6: Dependency on the threshold for extinction τ_{ext} with respect to the birth rate b_r and death rate d_r

CONCLUSIONS

A first achievement of this chapter consists in an accurate numerical study conducted on the stochastic model given by a point measure (5.1). To the best of our knowledge, in-depth analysis of the influence of the HT rate on the evolutionary dynamics has not been yet attempted. Along with its accuracy, the stochastic model reveals its limitation: an accurate theoretical description of what actually happens in each observed scenario from a mathematical point of view seems to be out of reach. However, we show that this model can be used for tracing back the lineage of the survived individuals through several generations.

In a next step, in a numerical comparative study between the stochastic (individual based) and the PDE (density) model both models exhibit the same behavior for a given set of parameters, which justifies theoretical results from Billiard et al. (2016b, 2015). Minor differences (in particular, the presence of damping oscillations) can be explained by a choice of a numerical scheme. However, further analysis shows that the classical PDE model defined by (5.2.2) leads to instabilities if we try to pass to an asymptotic setting under the small mutation assumption. Those instabilities are then resolved by a transformation of an initial model to a Hamilton-Jacobi type equation and using an asymptotic-preserving scheme. A further advantage of this approach is that the resulting equation (5.7) is easier to analyze from a theoretical point of view than, for example, the stochastic model.

Finally, in a Hamilton-Jacobi setting we manage to numerically replicate the evolutionary rescue of a small population which we observe in the stochastic model. This phenomena is illustrated for stochastic, PDE and HJ simulation on Figure 5.7. On Figures 5.7a-5.7c we trace the moment of the regrowth for different models. Figure 5.7a show the state of the population at a certain moment of time: we see how the individuals are centered around a mean trait. For the PDE and HJ model (red and green line respectively) we simply plot the density function, and on the first (blue) plot we approximate a histogram which describes ratio $\frac{N_t}{K}$ sorted by traits in stochastic model. Stochastic simulations show the evolutionary rescue in a more distinct manner: we see how the very small number of non-mutated individuals rescues the whole population from extinction (transition from 5.7b to 5.7c). On the contrary, the transition on the PDE model is dumped, and the regrowth is not clearly visible. It is due to, again, numerical instability of the PDE scheme for small values of the density function. Finally, HJ explicitly shows how the cycle occurs: the regrow of the "fit" individuals we see in stochastic plot is reproduced by a change of the maximum point (see again 5.7b to 5.7c).

We highlight again that in order to compare the models on a more applied level, we have to give a formal definition of a quantity represented by ρ in a Hamilton-Jacobian case. In this work we have made few steps toward the theoretical analysis of the limiting equation and an accurate description of each event (evolutionary rescue, extinction, etc) in terms of solutions of a PDE. Even though establishing a rigorous mathematical link between the behavior observed in the individual-based model and the Hamilton-Jacobi equation is out of scope of this project, the obtained analytic results already give a flavor of how the analysis of the evolutionary dynamics can be simplified in the future.

(a) $t = 167$ (b) $t = 198$ (c) $t = 216$
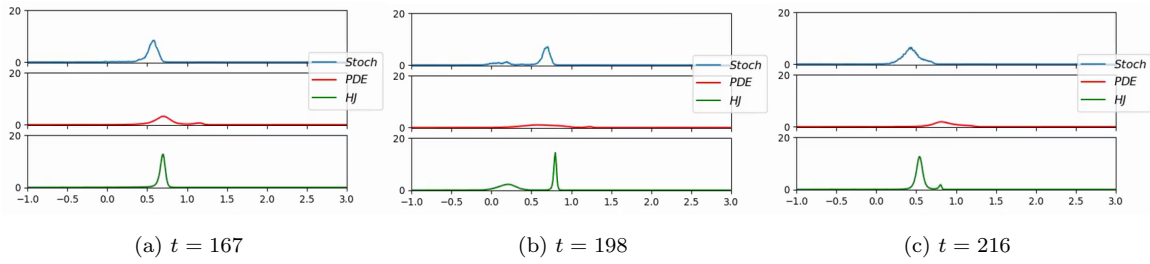
Figure 5.7: Comparison of numerical simulations between the different models. $\tau_0 = 0.4$, $\varepsilon = 0.1$, $\delta = 0.001$ and other parameters as in Figure 5.1. Blue line stands for the stochastic model, red line: for a PDE, green — for a Hamilton-Jacobi PDE

ACKNOWLEDGEMENTS

Part III

STATISTICS

6

PARAMETRIC INFERENCE FOR HYPOELLIPTIC ERGODIC DIFFUSIONS WITH FULL OBSERVATIONS

This Chapter is based on the article Melnykova (2020), published in *Statistical Inference for Stochastic Processes*.

Abstract. Multidimensional hypoelliptic diffusions arise naturally in different fields, for example to model neuronal activity. Estimation in those models is complex because of the degenerate structure of the diffusion coefficient. In this Chapter we consider hypoelliptic diffusions, given as a solution of two-dimensional stochastic differential equations (SDEs), with the discrete time observations of both coordinates being available on an interval of length $T = n\Delta_n$, with Δ_n the time step between the observations. The estimation is studied in the asymptotic setting, with $T \to \infty$ as $\Delta_n \to 0$. We build a consistent estimator of the drift and variance parameters with the help of a discretized log-likelihood of the continuous process. We discuss the difficulties generated by the hypoellipticity and provide a proof of the consistency and the asymptotic normality of the estimator. We test our approach numerically on the hypoelliptic FitzHugh-Nagumo model, which describes the firing mechanism of a neuron.

Résumé. Les diffusions hypoelliptiques multidimensionnelles apparaissent naturellement dans différents domaines, par exemple pour modéliser l'activité neuronale. L'estimation dans ces modèles est complexe en raison de la structure dégénérée du coefficient de diffusion. Nous construisons un estimateur consistent et asymptotiquement normal des paramètres de la dérive et de la variance à l'aide d'une log-vraisemblance discrétisée du processus continu lorsque des observations temporelles discrètes des deux coordonnées sont disponibles sur un intervalle de longueur $T = n\Delta_n$, avec Δ_n le pas de temps entre les observations. Nous discutons des difficultés générées par l'hypoellipticité et apportons une preuve de la consistance et de la normalité asymptotique de l'estimateur dans le cadre asymptotique $T \to \infty$ lorsque $\Delta_n \to 0$. Nous testons notre approche numériquement sur le modèle hypoelliptique de FitzHugh-Nagumo, qui décrit le mécanisme du tir d'un neurone.

6.1 INTRODUCTION

Hypoelliptic diffusions naturally occur in various applications, most notably in neuroscience, molecular physics and mathematical finance. In particular, neuronal activity of one single neuron (Höpfner

et al., 2016a, Leon and Samson, 2018), or a large population of neurons (Ditlevsen and Löcherbach, 2017, Ableidinger et al., 2017), or exotic models of option pricing (Malliavin and Thalmaier, 2006) are described by hypoelliptic diffusions.

The main difference between classical (or *elliptic*) and hypoelliptic systems of stochastic differential equations (SDE) is that in the latter case the rank of the diffusion matrix is lower than the dimension of the system itself. More formally, hypoellipticity can be explained in the following way: though the covariance matrix is singular, smooth transition densities with respect to the Lebesgue measure still exists. That is the case when the noise is propagated to all the coordinates through the drift term.

Hypoelliptic SDEs present a number of extra challenges in comparison to elliptic systems. The most important problem is the degenerate diffusion coefficient. As the explicit form of transition densities of a SDE is often unknown, parametric inference is usually based on discrete approximation with a piece-wise Gaussian processes (see, for example Kessler (1997)). But in the hypoelliptic case this approach cannot be applied directly because the covariance matrix of the approximated transition density is not invertible, since its rank is smaller than the dimension of the system. The second problem is that each coordinate has a variance of different order. It needs to be taken into account when constructing the discretization scheme for approximating the density.

Now let us be more specific. Consider a two-dimensional system of stochastic differential equations of the form:

$$\begin{cases} dX_t = a_1(X_t, Y_t; \theta^{(1)})dt \\ dY_t = a_2(X_t, Y_t; \theta^{(2)})dt + b(X_t, Y_t; \sigma)dW_t, \end{cases} \tag{6.1}$$

where $(X_t, Y_t)^T \in \mathbb{R} \times \mathbb{R}$, $(a_1(X_t, Y_t; \theta^{(1)}), a_2(X_t, Y_t; \theta^{(2)}))^T$ is the drift term, $(0, b(X_t, Y_t; \sigma))^T$ is the diffusion coefficient, W_t is a standard Brownian motion defined on some probability space $(\Omega, (\mathcal{F}_t)_{t \geq 0}, \mathbb{P})$, where $\mathcal{F}_t$ contains the information about all states of the process until time t. $(\theta^{(1)}, \theta^{(2)}, \sigma)$ is the vector of the unknown parameters, taken from some compact set $\Theta_1 \times \Theta_2 \times \Xi$, and (x_0, y_0) is a bounded $\mathcal{F}_0$-measurable random variable, thus independent on (X_t, Y_t).

The goal of this chapter is to estimate the parameters of (6.1) from discrete observations of both coordinates X and Y. It is achieved in two steps: first, we consider a discretization scheme in order to approximate the transition density of the continuous process. Then we propose an estimation technique which maximizes the likelihood function of the discrete approximate model in the asymptotic setting $T = n\Delta_n \to \infty$ and $\Delta_n \to 0$ as $n \to \infty$. Let us first discuss the solutions for hypoelliptic systems proposed by other authors.

Several works treat the parametric inference problem for a particular case of system (6.1), the class of stochastic Damping Hamiltonian systems, also known as Langevin equations (Gardiner and Collett, 1985). These hypoelliptic models arise as the stochastic expansion of 2-dimensional deterministic dynamical systems — for example, the Van der Pol oscillator (Van der Pol, 1920) perturbed by noise. They are defined as the solution of the following SDE:

$$\begin{cases} dX_t = Y_t dt \\ dY_t = a_2(X_t, Y_t; \theta)dt + b(X_t, Y_t; \sigma)dW_t. \end{cases} \tag{6.2}$$

The particular case of Hamiltonian systems with $b(X_t, Y_t; \sigma) \equiv \sigma$ and $a_2(X_t, Y_t; \theta) = g_1(X_t; \theta)X_t + g_2(X_t; \theta)Y_t$ is considered in Ozaki (1989), where the link between the continuous-time solution of (6.2) and the corresponding discrete model is obtained with the so-called local linearization scheme. The idea of this scheme is the following: for a SDE with a non-constant drift and a constant variance, its solution can be interval-wise approximated by the solution of a system with a linear drift (see Biscay et al. (1996), Ozaki (2012), Jimenez and Carbonell (2015)). This scheme allows to construct a quasi Maximum Likelihood Estimator. Consistency of the estimator based on the local linearization scheme for Hamiltonian SDEs is proven in León et al. (2018). Pokern et al. (2007) attempt to solve the problem of the non-invertibility of the covariance matrix for the particular case of (6.2) with a constant variance with the help of Itô-Taylor expansion of the transition density. The parameters are estimated with the Gibbs sampler based on the discretized model with the noise propagated to the first coordinate with order $\Delta_n^{\frac{3}{2}}$. This approach allows to estimate the variance coefficient, but it is not suitable for estimating the parameters of the drift term. In Samson and Thieullen (2012) it is shown that a consistent estimator for fully and partially observed data can be constructed using only the discrete approximation of the second equation of system (6.2). This method can be used in practice even for more general models, under the condition that the system (6.1) can be converted to the simpler form (6.2). However, this transformation of the observations sampled from the continuous model (6.1) often requires the prior knowledge of the parameters involved in the first equation which is often unrealistic. The particular case of (6.1), when $b(X_t, Y_t; \sigma) \equiv \sigma$ and the drift term is linear and thus the transition density is known explicitly, is treated in Le-Breton and Musiela (1985). A consistent maximum likelihood estimator is then constructed in two steps — first, a covariance matrix of the process is estimated from the available continuous-time observations, and then it is used for computing the parameters of the drift term. The resulting estimator is strongly consistent as $T \to \infty$. Few works are devoted to the non-parametric estimation of the drift and the variance terms (Cattiaux et al., 2014, 2016).

To the best of our knowledge for systems (6.1) the only reference is Ditlevsen and Samson (2017). They construct a consistent estimator using a discretization scheme based on a Itô-Taylor expansion. To take into account different variance orders in each variable they construct two separate estimators for the rough and the smooth variables. However, this approach has several limitations. The first problem consists in minimizing two different criteria simultaneously, which is not very natural from a numerical point of view. The second problem is that in order to prove the convergence of the estimator for each variable, the parameters in the other variable need to be fixed to their true values.

In this chapter, we want to avoid these limitations by proposing a single estimation criteria, able to estimate simultaneously all the parameters. This allows to prove the theoretical convergence of the vector of estimators, without any assumption on the knowledge of a set of parameters. Moreover, we illustrate that from a numerical point of view, the estimation of the first coordinate parameters is less biased than the one obtained with the approach proposed by Ditlevsen and Samson (2017). More precisely, we develop a new estimation method, adjusting the local linearization scheme described in Ozaki (1989) developed for the models of type (6.2) to the more general class of SDEs (6.1). Under

the hypoellipticity assumption this scheme propagates the noise to both coordinates of the system and allows to obtain an invertible covariance matrix. We start with describing the discretization scheme, proving the rate of convergence even when only one part of the parameters is fixed at the true value. Then we propose a contrast estimator based on the discretized log-likelihood, estimating the parameters included in the drift and diffusion coefficient simultaneously. We study the convergence of the scheme and prove the consistency and the asymptotic normality of the proposed estimator based on the 2-dimensional contrast. To the best of our knowledge, the proof of this consistency is new in the literature. We finish with numerical experiments, testing the proposed approach on the hypoelliptic FitzHugh-Nagumo model and compare it to the other estimators.

This Chapter is organized as follows: Section 6.2 presents the model and assumptions. The discrete model is introduced in Section 6.3. The estimators are studied in Section 6.4 and illustrated numerically in Section 6.5. We close with Section 6.6, devoted to conclusions and discussions. The proofs are gathered in Appendix.

6.2   MODELS AND ASSUMPTIONS

We assume that both variables of (6.1) are discretely observed at equally spaced periods of time Δ_n on the time interval $[0, T]$. The vector of observations at time $i\Delta_n$ is denoted by $Z_i = (X_i, Y_i)^T$, where Z_i is the value of the process at time $i\Delta_n$, $i \in 0 \ldots n = \frac{T}{\Delta_n}$. We further assume that it is possible to draw a sufficiently large and accurate sample of data, i.e that $T = n\Delta_n \to \infty$, with the partition size $\Delta_n \to 0$ as $n \to \infty$. Let us also introduce the vector notations:

$$dZ_t = A(Z_t; \theta)dt + B(Z_t; \sigma)dW_t, \quad Z_0 = z_0, \quad t \in [0, T] \tag{6.3}$$

where $Z_t = (X_t, Y_t)^T$, W_t is a two-dimensional Brownian motion defined on the filtered probability space, $z_0 = (x_0, y_0)$, and $\theta = (\theta^{(1)}, \theta^{(2)})$ is the vector of drift parameters. The matrices A and B represent, respectively, the drift and the diffusion coefficient, that is $A(Z_t; \theta) = (a_1(X_t, Y_t; \theta^{(1)}), a_2(X_t, Y_t; \theta^{(2)}))^T$ and

$$B(Z_t; \sigma) = \begin{pmatrix} 0 & 0 \\ 0 & b(Z_t; \sigma) \end{pmatrix}.$$

Throughout the Chapter we use the following abbreviations for the partial derivatives (unless the arguments need to be specified): $\partial_{x_i} f \equiv \frac{\partial f}{\partial x_i}(x_1, \ldots, x_p)$, $\partial^2_{x_i, x_j} \equiv \frac{\partial^2 f}{\partial x_i \partial x_j}(x_1, \ldots, x_p) \, \forall i, j \in [1, p]$. We suppress the dependency on the parameters, when their values are clear from the context, otherwise additional indexes are introduced. True values of the parameters are denoted by $\theta_0^{(1)}, \theta_0^{(2)}, \sigma_0$ and P_0 is the probability $P_{\theta_0^{(1)}, \theta_0^{(2)}, \sigma_0}$. We also refer to the variable Y_t which is directly driven by the Gaussian noise as "rough", and to X_t as "smooth".

We are working under the following set of assumptions:

A1 The functions $a_1(Z_t; \theta^{(1)})$, $a_2(Z_t; \theta^{(2)})$ and $b(Z_t; \sigma)$ have bounded partial derivatives of every order, uniformly in θ and σ respectively. Furthermore $\partial_y a_1 \neq 0 \quad \forall (x, y) \in \mathbb{R}^2$.

A2 *Global Lipschitz and linear growth conditions.* $\forall t, s \in [0, \infty) \, \exists K_\theta$ s.t.:

$$\|A(Z_t; \theta) - A(Z_s; \theta)\| + \|B(Z_t; \sigma) - B(Z_s; \sigma)\| \leq K_\theta \|Z_t - Z_s\|$$

$$\|A(Z_t; \theta)\|^2 + \|B(Z_t; \sigma)\|^2 \leq K_\theta^2 (1 + \|Z_t\|^2),$$

where $\| \cdot \|$ is the standard Euclidean norm.

A3 The process $(Z_t)_{t \geq 0}$ is ergodic and there exists a unique invariant probability measure ν_0 with finite moments of any order.

A4 The functions $a_1(Z_t; \theta^{(1)})$, $a_2(Z_t; \theta^{(2)})$ and $b(Z_t; \sigma)$ are identifiable. By the identifiability we mean that $u(Z_t; \theta) \equiv u(Z_t; \theta_0) \Leftrightarrow \theta = \theta_0$. The diffusion coefficient is assumed to be strictly positive with a non-zero derivative with respect to σ, that is $b(Z_t; \sigma) > 0$, $\partial_\sigma b(Z_t; \sigma) \neq 0 \quad \forall t$.

Further, we introduce a rather restrictive assumption, which will be required for the study of the consistency and asymptotic normality of the parameter estimator.

A5 The function $a_1(Z_t; \theta^{(1)})$ can be represented in the following form:

$$a_1(z; \theta^{(1)}) = f(z) + (\theta^{(1)})^T g(x), \tag{6.4}$$

where $g(x)$ is a vector-valued function of the same dimension as the vector $\theta^{(1)}$, $f(z)$ is a continuous function. The functions $f(z)$ and $g(x)$ are such that the assumptions (A1)-(A4) hold everywhere.

The full force of the last assumption will be explained in Section 6.4.1, when the estimator is introduced. The representation (6.4) implies that the derivative $\partial_y a_1$ does not depend on the parameter $\theta^{(1)}$. It will be shown in Section 6.3 that the marginal variance of variable X depends on $\partial_y a_1$. However, condition (A5) ensures that $\theta^{(1)}$ appears only in the drift, which simplifies the analysis. We note however that in practice the estimator shows good results even when ($A5$) does not hold, as it will be shown in the simulation study.

Assumption (A1) ensures that the system is hypoelliptic in the sense of the stochastic calculus of variations (Nualart, 2006, Malliavin and Thalmaier, 2006). In order to prove it we first write the coefficients of the system (6.3) as two vector fields, converting (6.3) from the Itô to the Stratonovich form:

$$A_0(x, y) = \begin{pmatrix} a_1(x, y; \theta^{(1)}) \\ a_2(x, y; \theta^{(2)}) - \frac{1}{2} b(x, y; \sigma) \partial_y b(x, y; \sigma) \end{pmatrix} \qquad A_1(x, y) = \begin{pmatrix} 0 \\ b(x, y; \sigma) \end{pmatrix}.$$

Then their Lie bracket is equal to

$$[A_0, A_1] = \begin{pmatrix} \partial_y a_1(x, y; \theta^{(1)}) \\ \partial_x a_2(x, y; \theta^{(2)}) - \frac{1}{2} \partial_x b(x, y; \sigma) \partial_{xy}^2 b(x, y; \sigma) \end{pmatrix}.$$

By (A1) the first element of this vector is not equal to 0, thus we conclude that A_1 and $[A_0, A_1]$ generate $\mathbb{R}^2$. That means that the weak Hörmander condition is satisfied and as a result the transition density for the system (6.3) exists (even if it is not always possible to write it in an explicit form).

(A2) is a sufficient condition to ensure the existence and uniqueness in law of the strong solution of system (6.3), moreover this solution is Feller (Revuz and Yor, 2013). However, the Feller property and the existence of the strong solution often hold under milder assumptions, thus (A2) can be often relaxed. (A4) is a standard identifiability condition which is needed to prove the consistency of the estimator. (A3) ensures that we can apply the ergodic theorem. That is, for any continuous function f of polynomial growth at infinity:

$$\frac{1}{T}\int_0^T f(Z_s)ds \xrightarrow[T\to\infty]{} \nu_0(f) \quad \text{a.s.,}$$

where $\nu_0(\cdot)$ is the stationary density of the model (6.3). By choosing this notation we highlight that $\nu_0(\cdot) := \nu_{\theta_0^{(1)},\theta_0^{(2)},\sigma_0}(\cdot)$.

We do not investigate the conditions under which the process $(Z_t)_{t\geq 0}$ is ergodic as it is not the main focus of this work. Ergodicity of the stochastic damping Hamiltonian system (6.2) is studied in Wu (2001). Conditions for a wider class of hypoelliptic SDEs can be found in Roynette (1975), Mattingly et al. (2002), Arnold and Kliemann (1987). It is also important to know that if the process $(Z_t)_{t\geq 0}$ is ergodic then its sampling $\{Z_i\}$, $i \in [0,n]$ is also ergodic (Genon-Catalot et al., 2000).

6.3   DISCRETE MODEL

In this section we introduce a Local Linearization scheme, which approximates the solution Z_t of (6.3) by the solution of a piece-wise linear autonomous equation. This solution has a piece-wise Gaussian density. We use the approximated solution to construct a discretization scheme and study its properties.

6.3.1   *Approximation with the Local Linearization scheme*

Local Linearization refers to the family of approximation schemes studied by different authors (Biscay et al., 1996, Ozaki, 2012, Jimenez and Carbonell, 2015). The idea consists in approximating the solution of a general SDE by the solution of an autonomous linear SDE, which can be solved explicitly. Before we proceed to the derivation of the scheme, let us introduce some additional notations. The Jacobian of the drift vector $A(z;\theta)$ is given by

$$\begin{pmatrix} \partial_x a_1(x,y;\theta^{(1)}) & \partial_y a_1(x,y;\theta^{(1)}) \\ \partial_x a_2(x,y;\theta^{(2)}) & \partial_y a_2(x,y;\theta^{(2)}) \end{pmatrix} =: J(z;\theta). \tag{6.5}$$

We also define the Hessian matrix of the j−th coordinate ($j=1,2$) in the drift vector $A(Z_t;\theta)$ as:

$$\begin{pmatrix} \partial_{xx}^2 a_j(x,y;\theta^{(j)}) & \partial_{xy}^2 a_j(x,y;\theta^{(j)}) \\ \partial_{yx}^2 a_j(x,y;\theta^{(j)}) & \partial_{yy}^2 a_j(x,y;\theta^{(j)}) \end{pmatrix} =: H_{a_j}(z;\theta^{(j)}).$$

For further use we also compute the following operator, which corresponds to the cross-term between the diffusion and drift in the Itô-Taylor-expansion for each coordinate:

$$Tr\left[B^T(z;\sigma)H_{a_j}(z;\theta^{(j)})B(z;\sigma) \right] = b^2(z;\sigma)\partial_{yy}^2 a_j(z;\theta^{(j)}).$$

We now consider the Itô-Taylor expansion of the drift term on the interval $t \in [i\Delta_n, (i+1)\Delta_n]$:

$$A(z_t; \theta) \approx A(z_i; \theta) + J(z_i; \theta)(z_t - z_i) + \frac{(t - i\Delta_n)^2}{2} b^2(z_i; \sigma) \partial_{yy}^2 A(z_i; \theta),$$

where $\partial_{yy}^2 A(z; \theta) := (\partial_{yy}^2 a_1(z; \theta^{(1)}), \partial_{yy}^2 a_2(z; \theta^{(2)}))^T$.

This transformation allows us to find an approximate solution of (6.3). We introduce a new process $(\tilde{Z}_t)_{t \in [i\Delta_n, (i+1)\Delta_n]}$ which is the solution of the following linear equation (see Section 5.6 in Karatzas and Shreve (1987)):

$$d\tilde{Z}_t = \left(A(\tilde{Z}_i; \theta) + J(\tilde{Z}_i; \theta)(\tilde{Z}_t - \tilde{Z}_i) + \frac{1}{2} b^2(\tilde{Z}_i; \sigma) \partial_{yy}^2 A(\tilde{Z}_i; \theta)(t - i\Delta_n) \right) dt + B(\tilde{Z}_i; \theta) dW_t.$$

The solution for the above equation is given for $t \in [i\Delta_n, (i+1)\Delta_n]$ by

$$\tilde{Z}_t = \tilde{Z}_i + \int_{i\Delta_n}^t e^{J(\tilde{Z}_i; \theta)(t-s)} \left(A(\tilde{Z}_i; \theta) - J(\tilde{Z}_i; \theta)\tilde{Z}_i + \frac{1}{2} b^2(\tilde{Z}_i; \sigma) \partial_{yy}^2 A(\tilde{Z}_i; \theta)(s - i\Delta_n) \right) ds +$$
$$\int_{i\Delta_n}^t e^{J(\tilde{Z}_i; \theta)(s - i\Delta_n)} B(\tilde{Z}_i; \theta) dW_s. \quad (6.6)$$

Note that conditionally on $\tilde{Z}_i$, $\tilde{Z}_{i+1}$ is a normal variable, whose expectation and variance are given, respectively, by:

$$\mathbb{E}\left[\tilde{Z}_{i+1} | \tilde{Z}_i \right] = \tilde{Z}_i + \int_{i\Delta_n}^{(i+1)\Delta_n} e^{J(\tilde{Z}_i; \theta)((i+1)\Delta_n - s)}.$$
$$\left(A(\tilde{Z}_i; \theta) - J(\tilde{Z}_i; \theta)\tilde{Z}_i + \frac{1}{2} b^2(\tilde{Z}_i; \sigma) \partial_{yy}^2 A(\tilde{Z}_i; \theta)(s - i\Delta_n) \right) ds \quad (6.7)$$

$$\Sigma\left[\tilde{Z}_{i+1} | \tilde{Z}_i \right] = \mathbb{E}\left[\left(\int_{i\Delta_n}^{(i+1)\Delta_n} e^{J(\tilde{Z}_i; \theta)((i+1)\Delta_n - s)} B(\tilde{Z}_i; \sigma) dW_s \right) \cdot \right.$$
$$\left. \left(\int_{i\Delta_n}^{(i+1)\Delta_n} e^{J(\tilde{Z}_i; \theta)((i+1)\Delta_n - s)} B(\tilde{Z}_i; \sigma) dW_s \right)^T \right]. \quad (6.8)$$

The approximation of the solution of (6.3) $(\tilde{Z}_i)_{i \geq 0}$ is then defined recursively as a sum of random variables with mean and variance given by (6.7) and (6.8). However, these expressions are not convenient for the numerical implementation because of the integrals and the matrix exponents. One possible solution is to rely on numerical integration algorithms when implementing the scheme. But we propose to simplify (6.7)-(6.8) in order to obtain the final scheme which is easier to implement and analyze from the theoretical point of view. We use the following propositions, whose proofs are postponed to appendix:

Proposition 6.1. *The component-wise drift approximation for* (6.7) *is given by:*

$$\mathbb{E}\left[\tilde{Z}_{i+1} | \tilde{Z}_i \right] = \begin{pmatrix} \bar{A}_1 \\ \bar{A}_2 \end{pmatrix} + O(\Delta_n^3),$$

where $\bar{A}_1$ and $\bar{A}_2$ are given as follows:

$$\bar{A}_1(\tilde{Z}_i; \theta^{(1)}, \theta^{(2)}, \sigma) := \tilde{X}_i + \Delta_n a_1(\tilde{Z}_i; \theta^{(1)}) +$$

$$\frac{\Delta_n^2}{2} \left(\frac{\partial a_1(\tilde{Z}_i; \theta^{(1)})}{\partial x} \, a_1(\tilde{Z}_i; \theta^{(1)}) + \frac{\partial a_1(\tilde{Z}_i; \theta^{(1)})}{\partial y} a_2(\tilde{Z}_i; \theta^{(2)}) \right) +$$

$$\frac{\Delta_n^2}{4} b^2(\tilde{Z}_i; \sigma) \partial_{yy}^2 a_1(\tilde{Z}; \theta^{(1)})$$

$$\bar{A}_2(\tilde{Z}_i; \theta^{(1)}, \theta^{(2)}, \sigma) := \tilde{Y}_i + \Delta_n a_2(\tilde{Z}_i; \theta^{(2)}) + \tag{6.9}$$

$$\frac{\Delta_n^2}{2} \left(\frac{\partial a_2(\tilde{Z}_i; \theta^{(2)})}{\partial x} \, a_1(\tilde{Z}_i; \theta^{(1)}) + \frac{\partial a_2(\tilde{Z}_i; \theta^{(2)})}{\partial y} a_2(\tilde{Z}_i; \theta^{(2)}) \right) +$$

$$\frac{\Delta_n^2}{4} b^2(\tilde{Z}_i; \sigma) \partial_{yy}^2 a_2(\tilde{Z}; \theta^{(2)}).$$

Proposition 6.2. *The matrix $\Sigma[\tilde{Z}_{i+1}|\tilde{Z}_i]$ defined in (6.8) is approximated by:*

$$b^2(\tilde{Z}_i; \sigma) \begin{pmatrix} (\partial_y a_1)^2 \frac{\Delta_n^3}{3} & (\partial_y a_1)\frac{\Delta_n^2}{2} + (\partial_y a_1)(\partial_y a_2)\frac{\Delta_n^3}{3} \\ (\partial_y a_1)\frac{\Delta_n^2}{2} + (\partial_y a_1)(\partial_y a_2)\frac{\Delta_n^3}{3} & \Delta_n + (\partial_y a_2)\frac{\Delta_n^2}{2} + (\partial_y a_2)^2\frac{\Delta_n^3}{3} \end{pmatrix} + O(\Delta_n^4), \tag{6.10}$$

where the derivatives are computed at time $i\Delta_n$.

Both from the theoretical and computational point of view, it is enough to use only the lower-order terms of (6.10). Thus, we define:

$$\Sigma_{\Delta_n}(\tilde{Z}_{i+1}; \theta, \sigma^2) := b^2(\tilde{Z}_i; \sigma) \begin{pmatrix} \left(\partial_y a_1(\tilde{Z}_i; \theta^{(1)}) \right)^2 \frac{\Delta_n^3}{3} & \partial_y a_1(\tilde{Z}_i; \theta^{(1)}) \frac{\Delta_n^2}{2} \\ \partial_y a_1(\tilde{Z}_i; \theta^{(1)}) \frac{\Delta_n^2}{2} & \Delta_n \end{pmatrix}. \tag{6.11}$$

The inverse of (6.11) is defined by:

$$\Sigma_{\Delta_n}^{-1}(\tilde{Z}_{i+1}; \theta, \sigma^2) = \frac{1}{b^2(\tilde{Z}_i; \sigma)} \begin{pmatrix} \frac{12}{\left(\partial_y a_1(\tilde{Z}_i; \theta^{(1)}) \right)^2 \Delta_n^3} & -\frac{6}{\partial_y a_1(\tilde{Z}_i; \theta^{(1)})\Delta_n^2} \\ -\frac{6}{\partial_y a_1(\tilde{Z}_i; \theta^{(1)})\Delta_n^2} & \frac{4}{\Delta_n} \end{pmatrix}. \tag{6.12}$$

Finally, the element-wise approximation of $\tilde{Z}_{i+1}$ conditionally on $\tilde{Z}_i$ is written as:

$$\tilde{X}_{i+1} = \bar{A}_1(\tilde{Z}_i; \theta^{(1)}, \theta^{(2)}, \sigma) + \xi_{1,i}$$

$$\tilde{Y}_{i+1} = \bar{A}_2(\tilde{Z}_i; \theta^{(1)}, \theta^{(2)}, \sigma) + \xi_{2,i}, \tag{6.13}$$

where $(\xi_{1,i})$ and $(\xi_{2,i})$ are normal random sequences with zero means, independent in i, such that the covariance matrix of vector $(\xi_{1,i}, \xi_{2,i})$ is given by (6.11). Numerically they can be simulated by decomposing the matrix (6.11) with the help of the LU or Cholesky decomposition, i.e. any matrix $\bar{B}(Z_i; \theta, \sigma^2)$ such that $\bar{B}\bar{B}^T = \Sigma(Z_i; \theta, \sigma^2)$, and multiply it by a 2-dimensional vector whose entries are independent standard normal variables. The chosen method of the decomposition does not affect the theoretical properties of the scheme. Note that the approximated diffusion term now depends on the parameters of the drift term. It is proven that the approximated solution $\tilde{Z}_t$ converges weakly to the true solution Z_t with order 2 (see Theorem 2 in Jimenez and Carbonell (2015)).

Now we want to study component-wise the moments of the obtained discretization, built on the observations of the process $(Z_t)_{t\geq 0}$. We will rely on the result of the following Proposition (recall that the true value of the vector of parameters is denoted by θ_0):

Proposition 6.3 (Moments of the discretized process). *The following holds:*

$$\mathbb{E}\left[X_{i+1} - \bar{A}_1(Z_i; \theta_0^{(1)}, \theta_0^{(2)}, \sigma_0)|Z_i\right] = O(\Delta_n^3)$$

$$\mathbb{E}\left[Y_{i+1} - \bar{A}_2(Z_i; \theta_0^{(1)}, \theta_0^{(2)}, \sigma_0)|Z_i\right] = O(\Delta_n^3)$$

$$\mathbb{E}\left[\left(X_{i+1} - \bar{A}_1(Z_i; \theta_0^{(1)}, \theta_0^{(2)}, \sigma_0)\right)^2 |Z_i\right] = (\partial_y a_1)^2_{\theta_0^{(1)}} \frac{\Delta_n^3}{3} b^2(Z_i; \sigma_0) + O(\Delta_n^4)$$

$$\mathbb{E}\left[\left(Y_{i+1} - \bar{A}_2(Z_i; \theta_0^{(1)}, \theta_0^{(2)}, \sigma_0)\right)^2 |Z_i\right] = \Delta_n b^2(Z_i; \sigma_0) + O(\Delta_n^2)$$

$$\mathbb{E}\left[\left(X_{i+1} - \bar{A}_1(Z_i; \theta_0^{(1)}, \theta_0^{(2)}, \sigma_0)\right)\left(Y_{i+1} - \bar{A}_2(Z_i; \theta_0^{(1)}, \theta_0^{(2)}, \sigma_0)\right)|Z_i\right] = (\partial_y a_1)_{\theta_0^{(1)}} \frac{\Delta_n^2}{2} b^2(Z_i; \sigma_0) + O(\Delta_n^3),$$

where $\mathbb{E}$ is taken under $\mathbb{P}_0$ and the derivatives $\partial_y a_1$ are computed at time $i\Delta_n$.

Proof. The moments of the Feller process can be approximated by its generator (Kloeden et al., 2003). That is, for a sufficiently smooth and integrable function $f : \mathbb{R} \times \mathbb{R} \to \mathbb{R}$:

$$\mathbb{E}(f(Z_{t+\Delta_n})|Z_t = z) = \sum_{i=0}^{j} \frac{\Delta_n^i}{i!} L^i f(z) + O(\Delta_n^{j+1}), \tag{6.14}$$

where $L^i f(z)$ is the i times iterated generator of model (6.3) given by

$$Lf(z) = (\partial_z f(z))A(z) + \frac{1}{2} \nabla_B^2 f(z),$$

where $\nabla_B^2(\cdot) = b^2(z; \sigma) \frac{\partial^2}{\partial y^2}(\cdot)$ is a weighted Laplace type operator. Since the process is approximated by (6.9), it coincides with (6.14) up to the terms of order Δ_n^2. $\square$

Further, we need an extension of Proposition 6.3 which gives the order of moments of the increments of the discrete process when parameters are fixed to their true values only partly. By doing that, we loose one order of accuracy in the first two bounds, but the results for the variance remain unchanged. Note however that we cannot obtain the last three terms unless $\theta^{(1)} = \theta_0^{(1)}$. This is the main technical challenge to overcome when constructing an estimator.

Proposition 6.4. *The following holds:*

(i) $\mathbb{E}\left[X_{i+1} - \bar{A}_1(Z_i; \theta_0^{(1)}, \theta^{(2)}, \sigma)|Z_i\right] = O(\Delta_n^2)$

(ii) $\mathbb{E}\left[Y_{i+1} - \bar{A}_2(Z_i; \theta^{(1)}, \theta_0^{(2)}, \sigma)|Z_i\right] = O(\Delta_n^2)$

(iii) $\mathbb{E}\left[\left(X_{i+1} - \bar{A}_1(Z_i; \theta_0^{(1)}, \theta^{(2)}, \sigma)\right)^2 |Z_i\right] = (\partial_y a_1)^2_{\theta_0^{(1)}} \frac{\Delta_n^3}{3} b^2(Z_i; \sigma) + O(\Delta_n^4)$

(iv) $\mathbb{E}\left[(Y_{i+1} - Y_i)^2 |Z_i\right] = \Delta_n b^2(Z_i; \sigma) + O(\Delta_n^2)$

(v) $\mathbb{E}\left[\left(X_{i+1} - \bar{A}_1(Z_i; \theta_0^{(1)}, \theta^{(2)}, \sigma)\right)(Y_{i+1} - Y_i)|Z_i\right] = (\partial_y a_1)_{\theta_0^{(1)}} \frac{\Delta_n^2}{2} b^2(Z_i; \sigma) + O(\Delta_n^3),$

where $\mathbb{E}$ is taken under $\mathbb{P}_0$ and the derivatives $\partial_y a_1$ are computed at time $i\Delta_n$.

Proof. We show the result for (i) and (iii). Start with (i):

$$X_{i+1} - \bar{A}_1(Z_i; \theta_0^{(1)}, \theta^{(2)}, \sigma) = X_{i+1} - \bar{A}_1(Z_i; \theta_0^{(1)}, \theta_0^{(2)}, \sigma_0) +$$

$$\bar{A}_1(Z_i; \theta_0^{(1)}, \theta_0^{(2)}, \sigma_0) - \bar{A}_1(Z_i; \theta_0^{(1)}, \theta^{(2)}, \sigma).$$

The difference $\mathbb{E}\left[X_{i+1} - \bar{A}_1(Z_i; \theta_0^{(1)}, \theta_0^{(2)}, \sigma_0)|Z_i\right] = O(\Delta_n^3)$ by Proposition 6.3 and the assumption (A2). It remains to consider the second part:

$$
\bar{A}_1(Z_i; \theta_0^{(1)}, \theta_0^{(2)}, \sigma_0) - \bar{A}_1(Z_i; \theta_0^{(1)}, \theta^{(2)}, \sigma) =
$$

$$
\frac{\Delta_n^2}{2}\left(\frac{\partial a_1(Z_i; \theta_0^{(1)})}{\partial y}\left(a_2(Z_i; \theta_0^{(2)}) - a_2(Z_i; \theta^{(2)})\right) + \frac{\partial_{yy}^2 a_1(Z; \theta_0^{(1)})}{2}\left(b^2(Z_i; \sigma_0) - b^2(Z_i; \sigma)\right)\right).
$$

Thus, $\mathbb{E}\left[X_{i+1} - \bar{A}_1(Z_i; \theta_0^{(1)}, \theta_0^{(2)}, \sigma_0)|Z_i\right] = O(\Delta_n^2)$. Let us now consider (iii):

$$
\left(X_{i+1} - \bar{A}_1(Z_i; \theta_0^{(1)}, \theta^{(2)}, \sigma)\right)^2 = \left(X_{i+1} - \bar{A}_1(Z_i; \theta_0^{(1)}, \theta_0^{(2)}, \sigma_0)\right)^2 +
$$

$$
\left(\bar{A}_1(Z_i; \theta_0^{(1)}, \theta_0^{(2)}, \sigma_0) - \bar{A}_1(Z_i; \theta_0^{(1)}, \theta^{(2)}, \sigma)\right)^2 +
$$

$$
2\left(X_{i+1} - \bar{A}_1(Z_i; \theta_0^{(1)}, \theta_0^{(2)}, \sigma_0)\right)\left(\bar{A}_1(Z_i; \theta_0^{(1)}, \theta_0^{(2)}, \sigma_0) - \bar{A}_1(Z_i; \theta_0^{(1)}, \theta^{(2)}, \sigma)\right).
$$

Again, by Proposition 6.3 and the previous computations we have the following:

$$
\mathbb{E}\left[\left(X_{i+1} - \bar{A}_1(Z_i; \theta_0^{(1)}, \theta_0^{(2)}, \sigma_0)\right)^2|Z_i\right] = (\partial_y a_1)_{\theta_0}^2 \frac{\Delta_n^3}{3}b^2(Z_i; \sigma) + O(\Delta_n^4)
$$

$$
\mathbb{E}\left[\left(\bar{A}_1(Z_i; \theta_0^{(1)}, \theta_0^{(2)}, \sigma_0) - \bar{A}_1(Z_i; \theta_0^{(1)}, \theta^{(2)}, \sigma)\right)^2|Z_i\right] = O(\Delta_n^4)
$$

$$
\mathbb{E}\left[2\left(X_{i+1} - \bar{A}_1(Z_i; \theta_0^{(1)}, \theta_0^{(2)}, \sigma_0)\right)\left(\bar{A}_1(Z_i; \theta_0^{(1)}, \theta_0^{(2)}, \sigma_0) - \bar{A}_1(Z_i; \theta_0^{(1)}, \theta^{(2)}, \sigma)\right)|Z_i\right] = O(\Delta_n^5).
$$

The rest of the proof follows the same pattern. $\qquad\square$

6.4   PARAMETER ESTIMATION

In this section we propose a contrast estimator based on the pseudo-likelihood function and prove its consistency and asymptotic normality. Then we discuss other already known results for the linear homogeneous SDEs (least squares estimator in particular) and show how it works in the general case.

6.4.1   *Contrast estimator*

Let us introduce the so-called contrast function for the system (6.3). This function is defined as -2 times the log-likelihood of the discretized model (Florens-Zmirou, 1989, Kessler, 1997):

$$
\mathcal{L}_{n,\Delta_n}(\theta, \sigma^2; Z_{0:n}) = \frac{1}{2}\sum_{i=0}^{n-1}(Z_{i+1} - \bar{A}(Z_i; \theta))^T \Sigma_{\Delta_n}^{-1}(Z_i; \theta, \sigma^2)(Z_{i+1} - \bar{A}(Z_i; \theta))
$$

$$
+ \sum_{i=0}^{n-1}\log\det(\Sigma_{\Delta_n}(Z_i; \theta, \sigma^2)), \quad (6.15)
$$

where the inverse matrix $\Sigma_{\Delta_n}^{-1}$ is given by (6.12). Then the local linearization (LL) estimator is defined as:

$$
(\hat{\theta}_{n,\Delta_n}, \hat{\sigma}_{n,\Delta_n}^2) = \arg\min_{\theta,\sigma^2} \mathcal{L}_{n,\Delta_n}(\theta, \sigma^2; Z_{0:n}), \qquad (6.16)
$$

where $\hat{\theta}_{n,\Delta_n} = \hat{\theta}^{(1)}_{n,\Delta_n}, \hat{\theta}^{(2)}_{n,\Delta_n}$.

Before proceeding to the proofs, let us explain how the contrast estimator works in the classical elliptic setting and give a roadmap for the proofs of consistency and asymptotic normality of the estimator (6.16), following Kessler (1997). The first notable difference between the estimator (6.16) and the elliptic case is that in the elliptic case the estimation of the drift and the variance parameters can be separated. For example, the contrast estimator for a 1-dimensional SDE discretized with the Euler-Maruyama scheme is defined as follows:

$$\left(\hat{\theta}, \hat{\sigma}^2\right) = \arg\min_{\theta,\sigma^2} \sum_{i=1}^{n} \left(\frac{1}{2} \frac{(X_{i+1} - X_i - \Delta_n a(X_i; \theta))^2}{\Delta_n b^2(X_i; \sigma)} + \log b^2(X_i; \sigma) \right),$$

where $a(x; \theta)$ is a drift term. Here the estimation of the parameter θ is independent of the value of σ, because the minimization of the criteria boils down to minimizing the expression $(X_{i+1} - X_i - \Delta_n a(X_i; \theta))^2$ and $\hat{\theta}$ converges to θ_0 with a rate $\sqrt{n\Delta_n}$. For the variance term, the estimator of σ converges independently of the value of θ, because $(X_{i+1} - X_i - \Delta_n a(X_i; \theta))^2$ is of order Δ_n for any θ and it is enough to ensure the convergence of the variance parameter. The convergence rate for the variance is $\sqrt{n}$. This property is also shared by the estimator for the Hamiltonian SDE proposed by Samson and Thieullen (2012).

In a general hypoelliptic setting the parametric inference is more complicated. First, the drift parameter θ is contained in the covariance matrix Σ_{Δ_n}. Second, the variance of the first variable is of order Δ_n^3, while for an arbitrary chosen vector of parameters $\theta^{(1)}$ the expression $(X_{i+1} - \bar{A}_1(Z_i; \theta^{(1)}, \theta^{(2)}, \sigma))^2$ is of order Δ_n^2. It is not enough to show the convergence of the diffusion parameter in a standard way. From the practical point of view it means that if we launch the minimization algorithm on (6.16) only with respect to $\theta^{(2)}$ and σ^2, it will not converge to the true value. The inverse, however, is possible: using the Proposition 6.4 the consistency result for $\hat{\theta}^{(1)}$ can be obtained without fixing $\theta^{(2)}$ and σ.

Ditlevsen and Samson (2017) propose to overcome the problem of dependency between the estimators by separating the estimation of the rough and smooth variables. They introduce two separate contrasts, based on the approximate marginal distribution on each variable.

$$\hat{\theta}^{(1)} = \arg\min_{\theta^{(1)}} \sum_{i=1}^{n-1} \left(\frac{3}{2} \frac{\left(X_{i+1} - \bar{A}_1(Z_i; \theta^{(1)}, \theta_0^{(2)}, \sigma_0)\right)^2}{\Delta_n^3 \left(\partial_y a_1(Z_i; \theta^{(1)})\right)^2 b^2(Z_i; \sigma_0)} + \right.$$

$$\left. \log \left(\partial_y a_1(Z_i; \theta^{(1)}) b(Z_i; \sigma_0)\right)^2 \right). \quad (6.17)$$

$$\left(\hat{\theta}^{(2)}, \hat{\sigma}^2\right) = \arg\min_{\theta^{(2)},\sigma^2} \sum_{i=1}^{n-1} \frac{1}{2} \left(\frac{\left(Y_{i+1} - \bar{A}_2(Z_i; \theta_0^{(1)}, \theta^{(2)}, \sigma)\right)^2}{\Delta_n b^2(Z_i; \sigma)} + \log b^2(Z_i; \sigma) \right). \quad (6.18)$$

The estimation is then conducted as follows: first, the parameters of the first equation are estimated from (6.17). Estimator (6.17) is shown to converge with rate $\sqrt{\frac{n}{\Delta_n}}$. Since the parameters of the second equation are contained only in higher order terms, they are shown to have no impact on the convergence of the estimator. We are able to show that thanks to the Proposition 6.4. Then, the

obtained value $\hat{\theta}^{(1)}$ is plugged in (6.18). The contrast is minimized with respect to σ and $\theta^{(2)}$. It is proven that the estimator $\hat{\theta}^{(2)}$ converges with the rate $\sqrt{n\Delta_n}$ and $\hat{\sigma}^2$ — with a rate $\sqrt{n}$. The rates are identical to the rates of convergence obtained in Kessler (1997) for elliptic systems. The weak point of the scheme is that in order to prove the convergence of the estimator (6.18) the value of $\theta^{(1)}$ needs to be fixed to $\theta_0^{(1)}$.

We choose a different approach and focus on the 2-dimensional contrast without splitting the numerical procedure in two parts. We still need to take into account the different rates of convergence and the eventual dependencies between the parameters. Thus, the proof of the consistency and asymptotic normality is splitted in two principal steps. The first step is a proof of the consistency and the convergence rate for $\hat{\theta}_{n,\Delta_n}^{(1)}$ (Theorem 6.1). Except for the unusual convergence rate, the proof repeats the standard techniques from Kessler (1997) and Ditlevsen and Samson (2017), adapted to the unknown value of $\theta^{(2)}$. The second step, however, is more intricate. As in Ditlevsen and Samson (2017), the estimators for $\theta^{(2)}$ and σ^2 do not converge for an arbitrary $\theta^{(1)}$. However, we prove that the consistency and the asymptotic normality still hold for $\hat{\theta}_{n,\Delta_n}^{(2)}$ and $\hat{\sigma}_{n,\Delta_n}^2$, because the sequence of estimators $\hat{\theta}_{n,\Delta_n}^{(1)}$ is tight and converges with rates proven in Theorem 6.1. It is proven at the cost of an additional assumption (A5) on the function $a_1(Z_t; \theta^{(1)})$ in the drift term.

We begin the study of the theoretical properties of the estimator from the following Lemma, on which the consistency of $\hat{\theta}^{(1)}$ crucially relies:

Lemma 6.1. *Under the assumptions (A1)-(A4), and assuming $\Delta_n \to 0$ and $n\Delta_n \to \infty$, the following holds:*

$$\lim_{n\to\infty,\Delta_n\to 0} \frac{\Delta_n}{n} \left[\mathcal{L}_{n,\Delta_n}(\theta^{(1)}, \theta^{(2)}, \sigma^2; Z_{0:n}) - \mathcal{L}_{n,\Delta_n}(\theta_0^{(1)}, \theta^{(2)}, \sigma^2; Z_{0:n}) \right] \xrightarrow{\mathbb{P}_0}$$

$$6 \int \frac{(a_1(z; \theta_0^{(1)}) - a_1(z; \theta^{(1)}))^2}{b^2(z;\sigma)(\partial_y a_1)_\theta^2} \nu_0(dz).$$

Proof is postponed to Appendix. On the next step we obtain the consistency and the asymptotic normality of (6.16) with respect to $\theta^{(1)}$:

Theorem 6.1. *Under the assumptions (A1)-(A5), and assuming $\Delta_n \to 0$, $n\Delta_n \to \infty$ and $n\Delta_n^2 \to 0$, the following holds:*

$$\hat{\theta}_{n,\Delta_n}^{(1)} \xrightarrow{\mathbb{P}_0} \theta_0^{(1)},$$

$$\sqrt{\frac{n}{\Delta_n}}(\hat{\theta}_{n,\Delta_n}^{(1)} - \theta_0^{(1)}) \xrightarrow{\mathcal{D}}$$

$$\mathcal{N}\left(0, 3 \left(\int \frac{(\partial_{\theta^{(1)}} a_1)(\partial_{\theta^{(1)}} a_1)^T}{b^2(z;\sigma)(\partial_y a_1)} \nu_0(dz) \right)^{-1} \left(\int \frac{b^2(z;\sigma_0)}{b^4(z;\sigma)} (\partial_{\theta^{(1)}} a_1)(\partial_{\theta^{(1)}} a_1)^T \left(1 + \frac{1}{(\partial_y a_1)^2} \right) \nu_0(dz) \right) \right),$$

where $\partial_x a_1$ is a simplified notation for $\partial_x a_1(z; \theta_0^{(1)})$

The asymptotic variance of the estimator slightly differs from the one obtained in Ditlevsen and Samson (2017). It is because the 2-dimensional estimator contains the cross-terms of type $(X_{i+1} - \bar{A}_1(Z_i; \theta^{(1)}, \theta^{(2)}, \sigma))(Y_{i+1} - \bar{A}_2(Z_i; \theta^{(1)}, \theta^{(2)}, \sigma))$, not taken into account if the estimator is

splitted in two separate contrasts for rough and smooth variables. The speed of convergence, however, stays the same. Notice also that the assumption (A5) is not used for Lemma 6.1, on which the proof of consistency relies. However, it is needed for the asymptotic normality. However, we do not need $\theta^{(2)}$ and σ^2 to be known, on the contrary to Ditlevsen and Samson (2017).

The idea of the proof of consistency for the diffusion and the rough term parameters follows Gloter and Sørensen (2009). Since we are working in a compact set, we can always find a sequence of estimators $\hat{\theta}^{(1)}_{n,\Delta_n}$ such that the sequence $(\hat{\theta}^{(1)}_{n,\Delta_n} - \theta^{(1)}_0)$ is tight. Then we use the tightness in combination with the rate of convergence obtained in Theorem 6.1 and the continuous mapping theorem for proving the consistency of the remaining terms in a standard way. On this stage we need the additional assumption (A5). The reason for that is when the parameter $\theta^{(1)}$ is included in the derivative $\partial_y a_1$, this parameter is present both in the drift and the variance term, which substantially complicates the study. Also, assuming the linear shape of a_1 with respect to $\theta^{(1)}$, one can fully use the speed of convergence for $\hat{\theta}^{(1)}_{n,\Delta_n}$ obtained in Theorem 6.1. It is rather restrictive, but the idea of the proof can be reused for a more general case. For example, consistency for the parameters of the rough variable can be obtained under the condition of Lipschitz continuity with respect to parameter $\theta^{(1)}$, at the cost of additional technicalities, which are omitted in this work. The consistency follows from the following Lemmas, on which Theorem 6.2 is based (the proofs of both Lemmas and the Theorem are postponed to Appendix):

Lemma 6.2. *Under assumptions (A1)-(A5), and assuming $\Delta_n \to 0$ and $n\Delta_n \to \infty$, the following holds:*

$$\lim_{n\to\infty,\Delta_n\to 0} \frac{1}{n\Delta_n} \left[\mathcal{L}_{n,\Delta_n}(\hat{\theta}^{(1)}_{n,\Delta_n}, \theta^{(2)}, \sigma^2; Z_{0:n}) - \mathcal{L}_{n,\Delta_n}(\hat{\theta}^{(1)}_{n,\Delta_n}, \theta^{(2)}_0, \sigma^2; Z_{0:n}) \right] \xrightarrow{\mathbb{P}_0}$$
$$2 \int \frac{(a_2(z;\theta^{(2)}) - a_2(z;\theta^{(2)}_0))^2}{b^2(z;\sigma)} \nu_0(dz)$$

Lemma 6.3. *Under assumptions (A1)-(A5), and assuming $\Delta_n \to 0$ while $n\Delta_n \to \infty$, the following holds:*

$$\frac{1}{n}\mathcal{L}_{n,\Delta_n}(\hat{\theta}^{(1)}_{n,\Delta_n}, \theta^{(2)}, \sigma^2; Z_{0:n}) \xrightarrow{\mathbb{P}_0} \int \left(\frac{b^2(z;\sigma_0)}{b^2(z;\sigma)} + \log b^2(z;\sigma) \right) \nu_0(dz)$$

Theorem 6.2. *Under assumptions (A1)-(A5), and assuming $\Delta_n \to 0$, $n\Delta_n \to \infty$ and $n\Delta_n^2 \to 0$ the following holds:*

$$\hat{\theta}^{(2)}_{n,\Delta_n} \xrightarrow{\mathbb{P}_0} \theta^{(2)}_0, \quad \hat{\sigma}_{n,\Delta_n} \xrightarrow{\mathbb{P}_0} \sigma_0$$

and

$$\sqrt{n\Delta_n}(\hat{\theta}^{(2)}_{n,\Delta_n} - \theta^{(2)}_0) \xrightarrow{\mathcal{D}} \mathcal{N}\left(0, \left(\int \frac{(\partial_{\theta^{(2)}} a_2(z;\theta^{(2)}_0))(\partial_{\theta^{(2)}} a_2(z;\theta^{(2)}_0))^T}{b^2(z,\sigma)} \nu_0(dz) \right)^{-1} \right)$$

$$\sqrt{n}(\hat{\sigma}_{n,\Delta_n} - \sigma_0) \xrightarrow{\mathcal{D}} \mathcal{N}\left(0, 2\left(\int \frac{(\partial_\sigma b(z,\sigma_0))(\partial_\sigma b(z,\sigma_0))^T}{b^2(z,\sigma_0)} \nu_0(dz) \right)^{-1} \right).$$

The obtained rates coincide with the rates in Ditlevsen and Samson (2017), but with the advantage that we avoid fixing any of the parameters to their true value, instead we work with the estimated sequence $\hat{\theta}^{(1)}_{n,\Delta_n}$.

6.4.2 *Conditional least squares estimator*

For certain applications it is natural to split the estimation of the parameters in the diffusion coefficient and the drift term (see, for example, Le-Breton and Musiela (1985)). First, it reduces the dimension of the optimization problem, and thus spares the computational cost. Second, it is easier to generalize the drift-based least square estimator to high-dimensional hypoelliptic systems, when the approximation of the diffusion matrix is difficult to compute. The idea is to compute the least square estimator of the differences between the discrete observations of $(Z_t)_{t \geq 0}$ and the expectation of this process computed with the LL scheme. For system (6.3) however we should be careful about the order of each difference. In order for the estimator to converge properly we need to renormalize the expression. We do that as follows:

$$\hat{\theta}_{n,\Delta_n}^{LSE} := \left(\hat{\theta}^{(1),LSE}, \hat{\theta}^{(2),LSE} \right)^T \tag{6.19}$$

where

$$\hat{\theta}_{n,\Delta_n}^{LSE,(1)} := \arg\min_{\theta^{(1)}} \sum_{i=0}^{n-1} \frac{\left(X_{i+1} - \bar{A}_1(Z_i; \theta^{(1)}, \theta^{(2)}, \sigma) \right)^2}{\Delta_n^3}$$

$$\hat{\theta}_{n,\Delta_n}^{LSE,(2)} := \arg\min_{\theta^{(2)}} \sum_{i=0}^{n-1} \frac{\left(Y_{i+1} - \bar{A}_2(Z_i; \theta^{(1)}, \theta^{(2)}, \sigma) \right)^2}{\Delta_n},$$

where $\bar{A}_j(Z_i; \theta^{(1)}, \theta^{(2)}, \sigma), j = 1, 2$ are defined in (6.9). Using the same reasoning as for the LL contrast we prove the next Theorem (the proof is postponed to appendix):

Theorem 6.3. *Under the assumptions (A1)-(A4) and the conditions $\Delta_n \to 0$, $n\Delta \to \infty$ and $n\Delta_n^2 \to 0$ the following holds:*

$$\hat{\theta}_{n,\Delta_n}^{LSE} \xrightarrow{\mathbb{P}_0} \theta_0,$$

and

$$\begin{pmatrix} \sqrt{\frac{n}{\Delta_n}} (\hat{\theta}_{n,\Delta_n}^{LSE,(1)} - \theta_0) \\ \sqrt{n\Delta_n} (\hat{\theta}_{n,\Delta_n}^{LSE,(2)} - \theta_0) \end{pmatrix} \xrightarrow{\mathcal{D}} 2\mathcal{N} \left(0, I_2 \cdot \begin{bmatrix} \frac{1}{3} \int b^2(z; \sigma_0)(\partial_y a_1(z; \theta_0^{(1)}))^2 (\partial_{\theta^{(1)}} a_1(z; \theta_0^{(1)}))^2 \nu_0(dz) \\ \int b^2(z; \sigma_0)(\partial_{\theta^{(2)}} a_2(z; \theta_0^{(2)}))^2 \nu_0(dz) \end{bmatrix} \right),$$

where I_2 is a 2×2 identity matrix, $\hat{\theta}_{n,\Delta_n}^{LSE,(j)}$ denote the $j-$th element of the vector $\mathcal{L}_{n,\Delta_n}^{LSE}(\theta; Z_{0:n})$ and

$$C_i = \int (\partial_{\theta^{(i)}} a_i(z; \theta_0^{(i)}))(\partial_{\theta^{(i)}} a_i(z; \theta_0^{(i)}))^T \nu_0(dz)$$

The advantage of this estimator over the LL contrast is that due to the absence of the cross-terms, the estimation of both parameters is independent. For instance, in Theorem 6.3 we prove the consistency of the estimator with respect to $\theta^{(2)}$ without assumption (A5) and fixing $\theta^{(1)}$ to the estimated sequence $\hat{\theta}_{n,\Delta_n}^{(1)}$. Also, since the term $(\partial_y a_1(z; \theta_0^{(1)}))$ is not present in the variance, we do not need (A5) to obtain the asymptotic normality for the estimator of $\theta^{(1)}$. The asymptotic variance differs from that obtained in Theorems 6.1-6.2.Since the terms $\partial_y a_1(z; \theta_0^{(1)})$ and $b(x, y; \sigma)$ were not included in the normalization, they appear in the covariance matrix and influence the performance of the estimator.

Thus, in comparison to the LL estimator defined by (6.16), the conditional least square estimator may perform worse and be prone to outliers when the diffusion coefficient and the value of $(\partial_y a_1(z; \theta_0^{(1)}))^2$ are large.

Note that the result of Theorem 6.3 holds for any σ. However, the diffusion coefficient cannot be estimated from criteria (6.19). One possible way to estimate it would be to plug in the obtained drift parameters in the 2-dimensional criteria (6.15) or in the 1-dimensional criteria from Ditlevsen and Samson (2017), given by (6.18). Analogously, when the noise in SDE (6.1) is additive (i.e., $b \equiv const$, or in a special case when $b(x, y; \sigma) \equiv \sigma f(x, y)$, the parameter σ can be estimated explicitly with the help of the sample covariance matrix. The properties of this approach for the elliptic case are proven in Kessler (1997), Jacod and Protter (2011). For hypoelliptic systems, this approach must be modified, as the discretization of order Δ_n does not allow to compute the terms of order Δ_n^3, which represent the propagated noise. However, the value of σ can still be inferred from the observations of the rough coordinate by computing

$$\tilde{\sigma}_{n,\Delta_n}^2 = \frac{1}{n\Delta_n} \sum_{i=0}^{n-1} \frac{(Y_{i+1} - Y_i)^2}{f^2(X_i, Y_i)}. \tag{6.20}$$

It can be shown that this estimator is consistent and asymptotically normal. In fact, it is a straightforward consequence of point (iv) of Lemma 6.7 (see Appendix), but we do not aim to provide the details here as it only concerns the particular case of model (6.1), that is, when the diffusion term depends linearly on only one unknown parameter. However, we test the performance of the estimator (6.20) in Section 6.5, devoted to the numerical experiments.

6.5 SIMULATION STUDY

6.5.1 *The model*

The two estimators $(\hat{\theta}_{n,\Delta_n}, \hat{\sigma}_{n,\Delta_n}^2)$ and $(\hat{\theta}_{n,\Delta_n}^{LSE}, \tilde{\sigma}_{n,\Delta_n}^2)$ are evaluated on the simulation study with a hypoelliptic stochastic neuronal model called FitzHugh-Nagumo model (Fitzhugh, 1961). It is a simplified version of the Hodgkin-Huxley model (Hodgkin and Huxley, 1952), which describes in a detailed manner activation and deactivation dynamics of a spiking neuron. First it was studied in the deterministic case, then in the stochastic elliptic setting with two sources of noise in both coordinates. However, it is often argued that only ion channels are perturbed by noise, while the membrane potential depends on them in a deterministic way. This idea leads to a 2-dimensional hypoelliptic diffusion. In this Chapter we consider a hypoelliptic SDE with noise only in the second coordinate as studied in Leon and Samson (2018). More precisely, the behaviour of the neuron is defined through the solution of the system

$$\begin{cases} dX_t = \frac{1}{\varepsilon}(X_t - X_t^3 - Y_t - s)dt \\ dY_t = (\gamma X_t - Y_t + \beta)dt + \sigma dW_t, \end{cases} \tag{6.21}$$

where the variable X_t represents the membrane potential of the neuron at time t, and Y_t is a recovery variable, which could represent the channel kinetic. The parameter s is the magnitude of the stimulus

current and is often known in experiments, ε is a time scale parameter and is typically significantly smaller than 1, since X_t moves "faster" than Y_t. Parameters to be estimated are $\theta = (\gamma, \beta, \varepsilon, \sigma)$. For system (6.21) we obtain the following expressions for $\bar{A}$ and Σ_{Δ_n}, which we plug in (6.15):

$$\bar{A}(Z_i; \theta) = \begin{pmatrix} X_i + \frac{\Delta_n}{\varepsilon}(X_i - X_i^3 - Y_i + s) + \frac{\Delta_n^2}{2\varepsilon}\left(\frac{(1-3X_i^2)}{\varepsilon}(X_i - X_i^3 - Y_i + s) - (\gamma X_i - Y_i + \beta)\right) \\ Y_i + \Delta_n(\gamma X_i - Y_i + \beta) + \frac{\Delta_n^2}{2}\left(\frac{\gamma}{\varepsilon}(X_i - X_i^3 - Y_i + s) - (\gamma X_i - Y_i + \beta)\right) \end{pmatrix}$$

$$\Sigma_{\Delta_n}(Z_i; \theta, \sigma) = \sigma^2 \begin{pmatrix} \frac{\Delta_n^3}{3\varepsilon^2} & \frac{\Delta_n^2}{2\varepsilon} \\ \frac{\Delta_n^2}{2\varepsilon} & \Delta_n \end{pmatrix}$$

Hypoellipticity and ergodicity of (6.21) are proven in Leon and Samson (2018). The same problem, but for the hypoelliptic setting is studied in Jensen (2014), Ditlevsen and Samson (2017).

6.5.2   *Experimental design*

We consider two different settings: an excitatory and an oscillatory behaviour. For the first regime, the drift parameters are set to $\gamma = 1.5$, $\beta = 0.3$, $\varepsilon = 0.1$, $s = 0.01$ and the diffusion coefficient $\sigma = 0.6$, and for the second $\gamma = 1.2$, $\beta = 1.3$, $\varepsilon = 0.1$, $s = 0.01$ and $\sigma = 0.4$. The diffusion coefficient does not change the behaviour pattern, only the "noisiness" of the observations. The starting point is $(X_0, Y_0) = (0, 0)$. Sample trajectories for both settings are shown on Figure 6.1.

We organize the trials as follows: first, we generate 100 trajectories using recursive formula (6.13) for each set of parameters with $\Delta_n = 0.0001$ and $n = 500000$. The observed time interval is thus equal to 50. Then we subsample the sequence so that we can vary the discretization step Δ_n and eventually truncate the observed time interval. We estimate the parameters by minimizing the contrast (6.15). We refer to this method as LL contrast. For the least square estimator (LSE) we do the following: we estimate the parameter σ explicitly from the observations of the second variable by (6.20), and then compute the parameters of the drift by minimizing (6.19). In addition, we compare both methods to the 1.5 strong order scheme (Ditlevsen and Samson, 2017), based on two separate estimators for each coordinate, which are defined in (6.17) and (6.18).

The minimization of the criteria is conducted with the `optim` function in **R** with the Conjugate Gradient method. As the initial value of parameters we take $\theta_0 \pm U([0, 1])$, where U stays for the uniform probabilistic law. In Tables 2-3 we present the mean value of the estimated parameters and their standard deviation (in brackets), computed over 100 trajectories for each set of parameters. The reported value of σ is obtained as $\sqrt{\sigma^2}$, since only σ^2 is identifiable. Figures 6.2-6.3 illustrate the estimation densities for $\Delta_n = 0.01$ and the interval of observations being fixed to $T = 5$ or $T = 50$. The LL contrast is depicted in blue, the least square estimator — in red, the 1.5 scheme in green.

The estimation of the diffusion coefficient σ with the LL estimator is slightly biased in both sets of data. This bias does not appear in the one-dimensional criteria and when the value is directly computed from the observations as a mean empirical variance. The performance of the LL contrast improves when we reduce the step size and increase the observed time interval. However, when Δ_n becomes too small the performance of LL contrast with respect to σ is worse than the one-dimensional

estimators for σ given by (6.18) and (6.20). It is slightly biased and its variance is bigger than that of LSE and 1.5 estimator. One possible explanation is that the estimation of σ with the LL contrast, as it is shown in Theorem 6.2, depends heavily on the convergence of the parameters of the first coordinate. Minor inaccuracies in the estimation of the drift parameters lead to non-negligible errors in $\hat{\sigma}$. Note, for example, that the LL scheme scores better on interval $T = 50$ for $\Delta_n = 0.01$ than for $\Delta_n = 0.001$ (see Table 2), while for the other schemes it is not the case. Thus, it is important to ensure that $n \to \infty$ faster than $\Delta_n \to 0$, as required by Theorem 6.2.

Parameters of the second coordinate γ and β are estimated accurately with all three methods once the time interval T is big enough (see the bottom pictures on Figures 6.2-6.3 for $T = 50$). However, when $T = 5$, 1.5 scheme scores considerably worse than the LL and LSE estimator. Also when estimating ε, the 1-dimensional criteria (6.17) does not score better than the LL and LSE estimators. This parameter seems to be underestimated in the case of the 1.5 scheme, and this bias is bigger in the case of the inhibitory setting for $\Delta_n = 0.01$. The problems in the inhibitory setting are anticipated, since the trajectory is more erratic than in the excitatory case. Drift parameters are thus more difficult to estimate: the variance of the estimators is bigger in average. Also, during the simulation study it is observed that ε is the most sensitive to the initial value with which the `optim` function is initialized, since it directly regulates the amount of noise which is propagated to the first coordinate. However, as predicted by Theorems 6.1-6.2, estimators for ε converge indeed faster than for the rest of the parameters.

6.6 CONCLUSIONS

The proposed contrast estimator generalizes parametric inference methods developed for models of type (6.2) to more general class (6.1). Numerical study shows that it can be used with no prior knowledge of the parameters. It is the main advantage of our method over the analogous works, in particular Ditlevsen and Samson (2017), where the convergence of the estimator is proven with the parameters being partly fixed to their true values.

From the theoretical point of view, our estimators reveal good properties. Both the contrast based on the local linearization scheme and the least square estimators are consistent. In the case of the contrast, the estimator of the rough coordinate asymptotically depends on the estimator of the smooth coordinate. Therefore its performance is sensitive to the form of the drift term. The convergence of the smooth coordinate, however, does not depend nor on the diffusion term, nor on the rough coordinate. The question of the asymptotic normality is more intricated. We prove the asymptotic normality under rather restrictive assumptions of the drift term. Nevertheless, the method can be applied to more general models, which is confirmed by the numerical study. The normality of the least squares estimator is studied under no additional assumptions on the drift term. It is noted that the estimation of parameters with LSE in the drift term is mutually independent, that gives an advantage over the classical contrast estimator. However, numerically LSE is rather sensitive to the experiment design and tends to produce outliers if the observation interval is not big enough.

$\Delta_n = 0.01$, T = 5	γ	β	ε	σ
LC	1.501 (0.053)	0.302 (0.055)	0.101 (0.001)	0.592 (0.056)
LSE	1.488 (0.108)	0.311 (0.149)	0.100 (0.000)	0.612 (0.020)
1.5 scheme	1.561 (0.362)	0.324 (0.295)	0.099 (0.000)	0.598 (0.019)

$\Delta_n = 0.01$, T = 10	γ	β	ε	σ
LC	1.504 (0.055)	0.306 (0.053)	0.100 (0.001)	0.562 (0.026)
LSE	1.503 (0.069)	0.299 (0.176)	0.100 (0.000)	0.610 (0.014)
1.5 scheme	1.540 (0.237)	0.301 (0.212)	0.099 (0.000)	0.596 (0.013)

$\Delta_n = 0.01$, T = 50	γ	β	ε	σ
LC	1.500 (0.050)	0.297 (0.052)	0.100 (0.000)	0.560 (0.018)
LSE	1.513 (0.072)	0.302 (0.068)	0.100 (0.000)	0.610 (0.007)
1.5 scheme	1.495 (0.095)	0.301 (0.093)	0.099 (0.000)	0.596 (0.007)

$\Delta_n = 0.001$, T = 5	γ	β	ε	σ
LC	1.505 (0.054)	0.306 (0.051)	0.100 (0.000)	0.699 (0.090)
LSE	1.498 (0.062)	0.290 (0.072)	-47.86 (477.2)	0.599 (0.005)
1.5 scheme	1.497 (0.183)	0.304 (0.169)	0.100 (0.000)	0.598 (0.005)

$\Delta_n = 0.001$, T = 10	γ	β	ε	σ
LC	1.513 (0.049)	0.302 (0.054)	0.100 (0.000)	0.662 (0.096)
LSE	1.501 (0.051)	0.299 (0.052)	0.100 (0.000)	0.600 (0.004)
1.5 scheme	1.513 (0.159)	0.288 (0.161)	0.100 (0.000)	0.599 (0.004)

$\Delta_n = 0.001$, T = 50	γ	β	ε	σ
LC	1.487 (0.054)	0.303 (0.050)	0.100 (0.000)	0.628 (0.098)
LSE	1.493 (0.056)	0.303 (0.052)	0.100 (0.000)	0.601 (0.002)
1.5 scheme	1.488 (0.066)	0.302 (0.068)	0.100 (0.000)	0.600 (0.002)

Table 2: Set 1, $\gamma_0 = 1.5, \beta_0 = 0.3, \varepsilon_0 = 0.1, \sigma_0 = 0.6$.. Value without brackets: mean, value in parentheses: standard deviation.
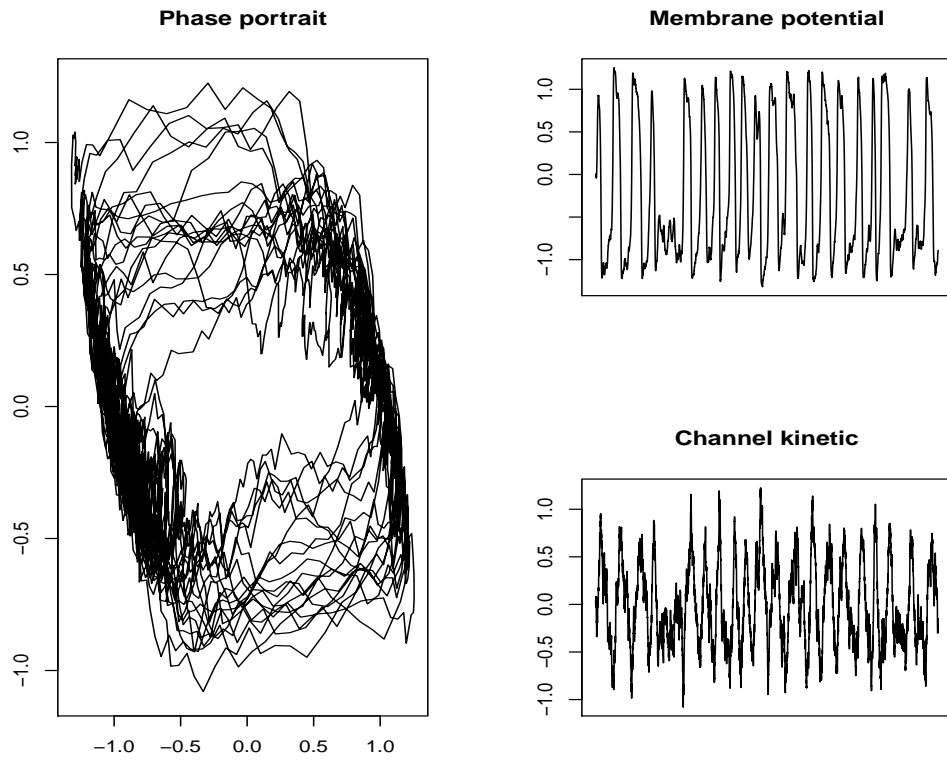
(a) Excitatory set
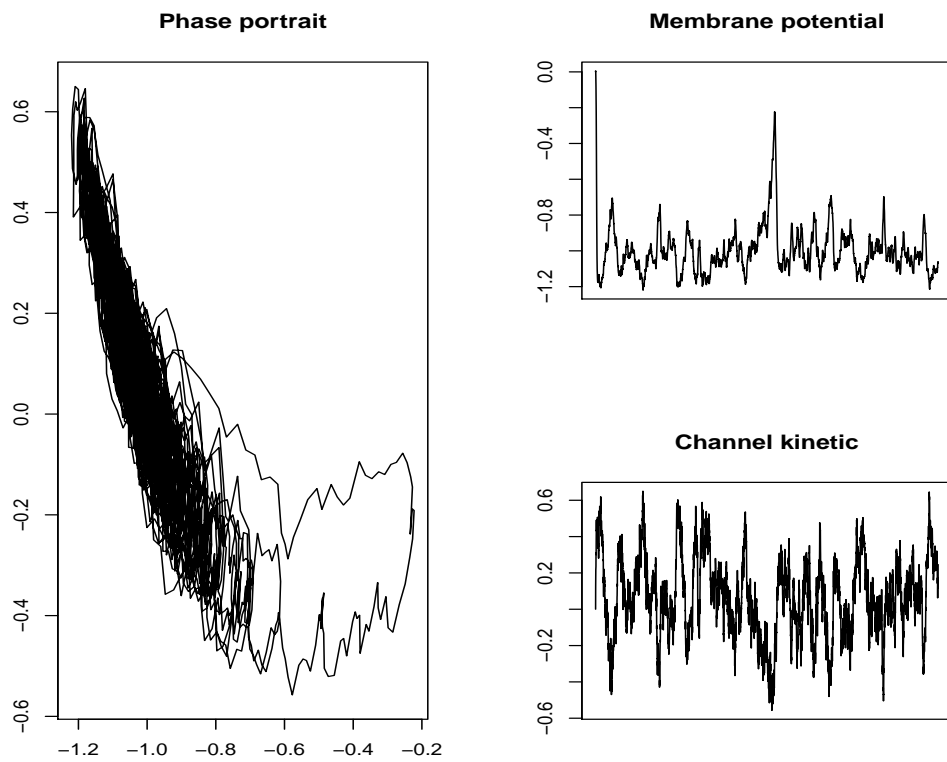
(b) Oscillatory set

Figure 6.1: Trajectories for two sets of parameters

$\Delta_n = 0.01$, T = 5	γ	β	ε	σ
LC	1.205 (0.046)	1.311 (0.053)	0.100 (0.001)	0.357 (0.013)
LSE	1.243 (0.771)	1.592 (0.887)	0.101 (0.002)	0.400 (0.014)
1.5 scheme	1.324 (0.357)	1.415 (0.365)	0.095 (0.002)	0.397 (0.014)

$\Delta_n = 0.01$, T = 10	γ	β	ε	σ
LC	1.201 (0.053)	1.303 (0.053)	0.100 (0.001)	0.356 (0.008)
LSE	1.251 (0.367)	1.507 (0.521)	0.100 (0.001)	0.399 (0.009)
1.5 scheme	1.260 (0.187)	1.354 (0.188)	0.091 (0.003)	0.396 (0.009)

$\Delta_n = 0.01$, T = 50	γ	β	ε	σ
LC	1.200 (0.046)	1.302 (0.048)	0.101 (0.001)	0.357 (0.004)
LSE	1.207 (0.208)	1.374 (0.288)	0.100 (0.001)	0.400 (0.004)
1.5 scheme	1.217 (0.073)	1.304 (0.075)	0.083 (0.009)	0.398 (0.004)

$\Delta_n = 0.001$, T = 5	γ	β	ε	σ
LC	1.206 (0.052)	1.302 (0.050)	0.100 (0.000)	0.370 (0.052)
LSE	1.183 (0.074)	1.330 (0.126)	0.100 (0.000)	0.400 (0.004)
1.5 scheme	1.239 (0.170)	1.327 (0.177)	0.100 (0.000)	0.400 (0.004)

$\Delta_n = 0.001$, T = 10	γ	β	ε	σ
LC	1.193 (0.050)	1.303 (0.050)	0.100 (0.000)	0.345 (0.013)
LSE	1.183 (0.069)	1.328 (0.101)	0.100 (0.000)	0.400 (0.003)
1.5 scheme	1.231 (0.126)	1.328 (0.114)	0.099 (0.000)	0.400 (0.003)

$\Delta_n = 0.001$, T = 50	γ	β	ε	σ
LC	1.201 (0.052)	1.301 (0.053)	0.100 (0.000)	0.344 (0.009)
LSE	1.207 (0.208)	1.374 (0.288)	0.100 (0.001)	0.400 (0.004)
1.5 scheme	1.206 (0.088)	1.295 (0.084)	0.099 (0.000)	0.400 (0.001)

Table 3: Set 2: $\gamma_0 = 1.2, \beta_0 = 1.3, \varepsilon_0 = 0.1, \sigma_0 = 0.4$. Value without brackets: mean, value in parentheses: standard deviation.
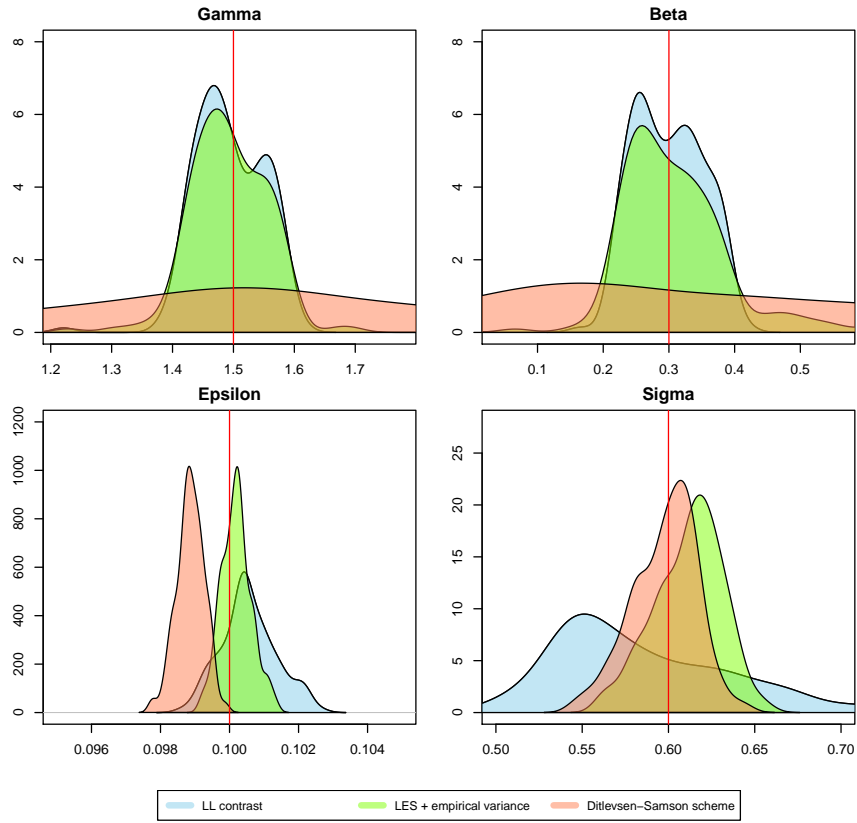
(a) $T = 5$
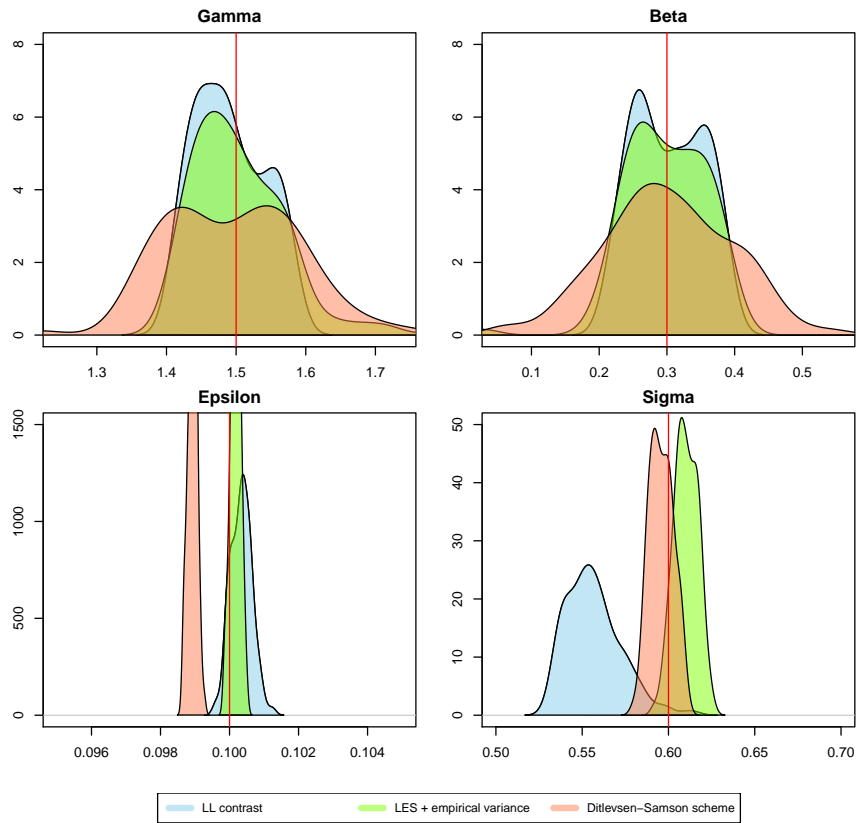
(b) $T = 50$

Figure 6.2: Estimation density for the LL contrast (blue), the LSE (red) and 1.5 scheme (green) estimators for the excitatory set. $\Delta_n = 0.01$

(a) $T = 5$

(b) $T = 50$

Figure 6.3: Estimation density for the LL contrast (blue), the LSE (red) and 1.5 scheme (green) estimators for the inhibitory set. $\Delta_n = 0.01$

The most important direction of the prospective work is the adaptation of the estimation method to the case when only the observations of the first coordinate are available. Under proper conditions it must be possible to couple the contrast minimization with one of the existing filtering methods and estimate the parameters of the system (at least, partially).

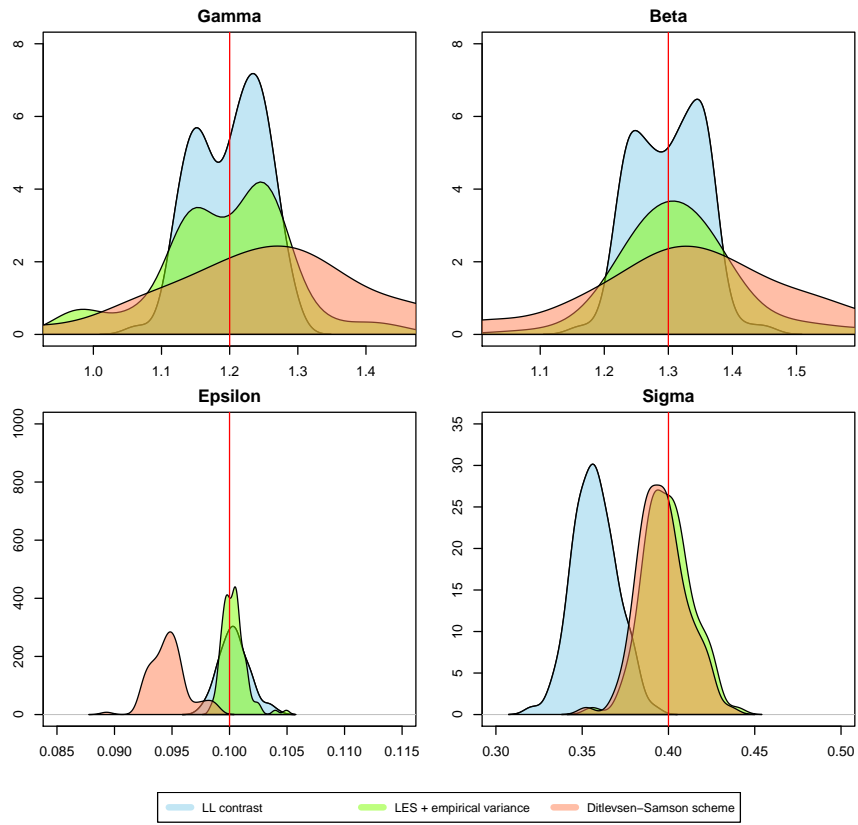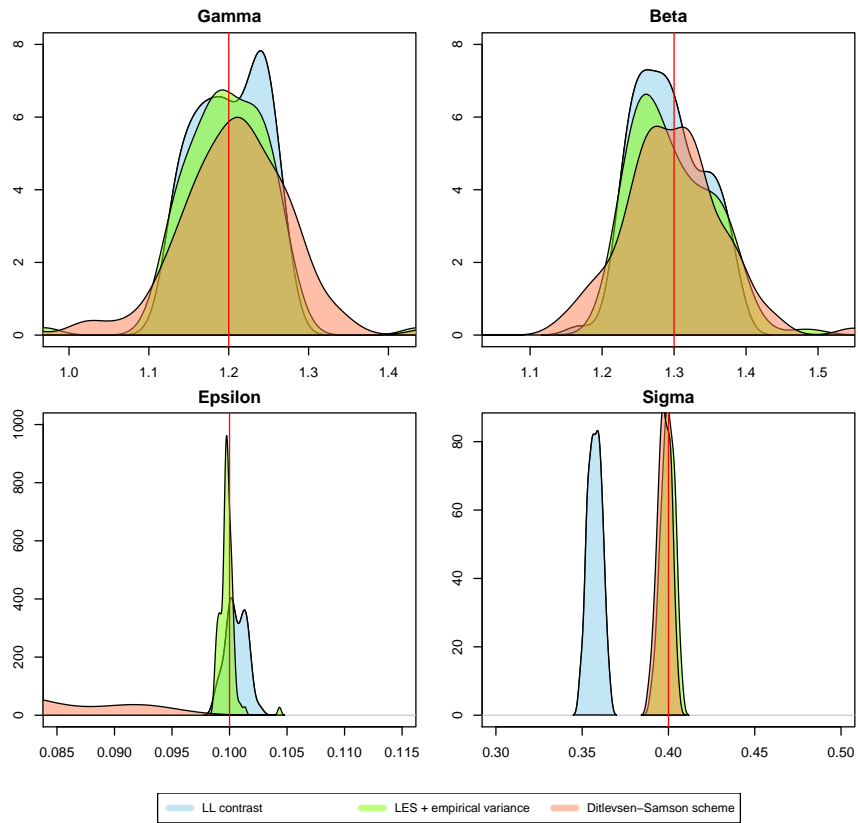Another point is the generalization of the contrast to systems of higher dimension. In practice we often deal with high-dimensional systems with arbitrary number of rough and smooth variables. The general rule which gives the contrast function in that case is not yet established. The most important step here would be to establish the condition of hypoellipticity for such a system. Finally, it is crucial to pair the method with a robust optimization procedure, since the minimization of the contrast is sensitive to choice of the discretization step and initial conditions.

6.7 APPENDIX

6.7.1 *Properties of the scheme*

Proposition 6.1. By integrating (6.6) by parts two times we get the following:

$$\mathbb{E}\left[\tilde{Z}_{i+1}|\tilde{Z}_i\right] = \tilde{Z}_i + J^{-1}(\tilde{Z}_i;\theta)\left(e^{J(\tilde{Z}_i;\theta)\Delta_n} - I\right)A(\tilde{Z}_i;\theta)+$$
$$\frac{1}{2}J^{-2}(\tilde{Z}_i;\theta)\left(e^{J(\tilde{Z}_i;\theta)\Delta_n} - I - J(\tilde{Z}_i;\theta)\Delta_n\right)b^2(\tilde{Z}_i;\sigma)\partial_{yy}^2 A(\tilde{Z}_i;\theta) \quad (6.22)$$

Recall that the matrix exponent for some square matrix M is given by $e^M = \sum_{l=0}^{\infty}\frac{M^l}{l!}$. Then (6.22) can be simplified as:

$$\mathbb{E}\left[\tilde{Z}_{i+1}|\tilde{Z}_i\right] = \tilde{Z}_i + J^{-1}(\tilde{Z}_i;\theta)\left(I + \Delta_n J(\tilde{Z}_i;\theta) + \frac{\Delta_n^2}{2}J^2(\tilde{Z}_i;\theta) - I + O(\Delta_n^3)\right)A(\tilde{Z}_i;\theta)+$$
$$\frac{1}{2}J^{-2}(\tilde{Z}_i;\theta)\left(I + \Delta_n J(\tilde{Z}_i;\theta) + \frac{\Delta_n^2}{2}J^2(\tilde{Z}_i;\theta) - I - \Delta_n J(\tilde{Z}_i;\theta) + O(\Delta_n^3)\right)b^2(\tilde{Z}_i;\sigma)\partial_{yy}^2 A(\tilde{Z}_i;\theta) =$$
$$\tilde{Z}_i + \Delta_n A(\tilde{Z}_i;\theta) + \frac{\Delta_n^2}{2}J(\tilde{Z}_i;\theta)A(\tilde{Z}_i;\theta) + \frac{\Delta_n^2}{4}b^2(\tilde{Z}_i;\sigma)\partial_{yy}^2 A(\tilde{Z}_i;\theta) + O(\Delta_n^3)$$

Writing the above expression component-wise gives the proposition.   □

Proposition 6.2. Let us consider each integral of (6.8) separately. Denote:

$$\mathcal{W}_{(i+1)\Delta_n} = \int_{i\Delta_n}^{(i+1)\Delta_n} e^{J(\tilde{Z}_i;\theta)((i+1)\Delta_n - s)}B(\tilde{Z}_i;\sigma)dW_s.$$

Recall that the Jacobian of system (6.3) is given by (6.5) and the definition of the matrix exponent, we have:

$$
\mathcal{W}_{(i+1)\Delta_n} = \int_{i\Delta_n}^{(i+1)\Delta_n} (I + J(\tilde{Z}_i; \theta)((i+1)\Delta_n - s) + O(\Delta_n^2)) B(\tilde{Z}_i; \sigma) dW_s =
$$

$$
= \int_{i\Delta_n}^{(i+1)\Delta_n} \left[\begin{pmatrix} 1 + \partial_x a_1(\tilde{Z}_i; \theta^{(1)})((i+1)\Delta_n - s) & \partial_y a_1(\tilde{Z}_i; \theta^{(1)})((i+1)\Delta_n - s) \\ \partial_x a_2(\tilde{Z}_i; \theta^{(2)})((i+1)\Delta_n - s) & 1 + \partial_y a_2(\tilde{Z}_i; \theta^{(2)})((i+1)\Delta_n - s) \end{pmatrix} \right.
$$

$$
\left. + O(\Delta_n^2) \right] \begin{pmatrix} 0 & 0 \\ 0 & 1 \end{pmatrix} b(\tilde{Z}_i; \sigma) dW_s =
$$

$$
b(\tilde{Z}_i; \sigma) \begin{bmatrix} 0 & \partial_y a_1(\tilde{Z}_i; \theta^{(1)}) \int_{i\Delta_n}^{(i+1)\Delta_n} ((i+1)\Delta_n - s) dW_s + O(\Delta_n^2) \\ 0 & \int_{i\Delta_n}^{(i+1)\Delta_n} dW_s + \partial_y a_2(\tilde{Z}_i; \theta^{(2)}) \int_{i\Delta_n}^{(i+1)\Delta_n} ((i+1)\Delta_n - s) dW_s + O(\Delta_n^2) \end{bmatrix}
$$

Then we can calculate $\mathbb{E}\left[\mathcal{W}_{(i+1)\Delta_n} \mathcal{W}'_{(i+1)\Delta_n} \right]$:

$$
\mathbb{E}\left[\mathcal{W}_{(i+1)\Delta_n} \mathcal{W}'_{(i+1)\Delta_n} \right] = b^2(\tilde{Z}_i; \sigma) \mathbb{E} \begin{pmatrix} \Sigma_{\Delta_n}^{(1)} & \Sigma_{\Delta_n}^{(12)} \\ \Sigma_{\Delta_n}^{(12)} & \Sigma_{\Delta_n}^{(2)} \end{pmatrix} + O(\Delta_n^4),
$$

where entries are given by:

$$
\Sigma_{\Delta_n}^{(1)} = \left(\partial_y a_1(\tilde{Z}_i; \theta^{(1)}) \right)^2 \left[\int_{i\Delta_n}^{(i+1)\Delta_n} ((i+1)\Delta_n - s) dW_s \right]^2
$$

$$
\Sigma_{\Delta_n}^{(12)} = \left(\partial_y a_1(\tilde{Z}_i; \theta^{(1)}) \int_{i\Delta_n}^{(i+1)\Delta_n} ((i+1)\Delta_n - s) dW_s \right)
$$

$$
\left(\int_{i\Delta_n}^{(i+1)\Delta_n} dW_s + \partial_y a_2(\tilde{Z}_i; \theta^{(2)}) \int_{i\Delta_n}^{(i+1)\Delta_n} ((i+1)\Delta_n - s) dW_s \right)
$$

$$
\Sigma_{\Delta_n}^{(2)} = \left(\int_{i\Delta_n}^{(i+1)\Delta_n} dW_s + \partial_y a_2(\tilde{Z}_i; \theta^{(2)}) \int_{i\Delta_n}^{(i+1)\Delta_n} ((i+1)\Delta_n - s) dW_s \right)^2
$$

The first entry can be easily calculated by the Itô isometry:

$$
\mathbb{E}[\Sigma_{\Delta_n}^{(1)}] = \left(\partial_y a_1(\tilde{Z}_i; \theta^{(1)}) \right)^2 \mathbb{E} \left[\int_{i\Delta_n}^{(i+1)\Delta_n} ((i+1)\Delta_n - s) dW_s \right]^2 =
$$

$$
\left(\partial_y a_1(\tilde{Z}_i; \theta^{(1)}) \right)^2 \int_{i\Delta_n}^{(i+1)\Delta_n} ((i+1)\Delta_n - s)^2 ds = \left(\partial_y a_1(\tilde{Z}_i; \theta^{(1)}) \right)^2 \frac{\Delta_n^3}{3}
$$

Now consider the product of two stochastic integrals in the terms $\Sigma_{\Delta_n}^{(12)}$ and $\Sigma_{\Delta_n}^{(2)}$. Assume for simplicity that $t = 0$. From the properties of the stochastic integrals (Karatzas and Shreve, 1987), it is straightforward to see that:

$$
\mathbb{E} \left[\lim_{n \to \infty} \sum_{t_i, t_{i-1} \in [0, \Delta_n]} (\Delta_n - s)(W_{t_i} - W_{t_{i-1}}) \sum_{t_i, t_{i-1} \in [0, \Delta_n]} (W_{t_i} - W_{t_{i-1}}) \right] =
$$

$$
= \lim_{n \to \infty} \sum_{t_i, t_{i-1} \in [0, \Delta_n]} (\Delta_n - s) \mathbb{E} \left[(W_{t_i} - W_{t_{i-1}})^2 \right] = \int_0^{\Delta_n} (\Delta_n - s) ds = \frac{\Delta_n^2}{2}
$$

That gives the proposition.   □

6.7.2 *Auxiliary results*

We start with an important Lemma which links the sampling and the probabilistic law of the continuous process:

Lemma 6.4 (Kessler (1997)). *Let $\Delta_n \to 0$ and $n\Delta_n \to \infty$, let $f \in \mathbb{R} \times \Theta \to \mathbb{R}$ be such that f is differentiable with respect to z and θ, with derivatives of polynomial growth in z uniformly in θ. Then:*

$$\frac{1}{n}\sum_{i=1}^{n} f(Z_i;\theta) \xrightarrow{\mathbb{P}_0} \int f(z;\theta)\nu_0(dz) \ as \ n \to \infty \ uniformly \ in \ \theta.$$

The Lemma is proven in Kessler (1997) for the one-dimensional case. Its proof is based only on ergodicity of the process and on assumptions analogous to ours, and not on the discretization scheme or dimensionality. So it can be generalized to a multi-dimensional case.

Proposition 6.4 in combination with the continuous ergodic theorem and Lemma 6.4 allow us to establish the following important result:

Lemma 6.5. *Let $f : \mathbb{R}^2 \times \Theta \to \mathbb{R}$ be a function with the derivatives of polynomial growth in x, uniformly in θ. Assume $\Delta_n \to 0$ and $n\Delta_n \to \infty$. Then:*

(i) $\frac{1}{n\Delta_n^3}\sum_{i=0}^{n-1} \frac{f(Z_i;\theta)}{(\partial_y a_1(Z_i;\theta_0^{(1)}))^2}\left(X_{i+1} - \bar{A}_1(Z_i;\theta_0^{(1)},\theta^{(2)},\sigma)\right)^2 \xrightarrow{\mathbb{P}_0} \frac{1}{3}\int f(z;\theta)b^2(z;\sigma_0)\nu_0(dz)$

(ii) $\frac{1}{n\Delta_n}\sum_{i=0}^{n-1} f(Z_i;\theta)\left(Y_{i+1} - Y_i\right)^2 \xrightarrow{\mathbb{P}_0} \int f(z;\theta)b^2(z;\sigma_0)\nu_0(dz)$

(iii) $\frac{1}{n\Delta_n^2}\sum_{i=0}^{n-1} \frac{f(Z_i;\theta)}{\partial_y a_1(Z_i;\theta_0^{(1)})}\left(X_{i+1} - \bar{A}_1(Z_i;\theta_0^{(1)},\theta^{(2)},\sigma)\right)\left(Y_{i+1} - Y_i\right) \xrightarrow{\mathbb{P}_0} \frac{1}{2}\int f(z;\theta)b^2(z;\sigma_0)\nu_0(dz)$

Proof. We consider only the cross-term (iii), since the results for the first and the second term are analogous to Ditlevsen and Samson (2017) (upon replacing the bounds from Proposition 6.3 by 6.4). Thanks to Proposition 6.4 we know that:

$$\mathbb{E}\left[\frac{1}{n\Delta^2}\frac{f(Z_i;\theta)}{\partial_y a_1(Z_i;\theta_0^{(1)})}\left(X_{i+1} - \bar{A}_1(Z_i;\theta_0^{(1)},\theta^{(2)},\sigma)\right)\left(Y_{i+1} - Y_i\right)|\mathcal{F}_i\right] =$$
$$\frac{1}{2n}f(Z_i;\theta)b^2(Z_i;\sigma_0) + O(\Delta_n).$$

Then from Lemma 6.4 it follows that for $n \to \infty$ uniformly in θ:

$$\sum_{i=0}^{n-1}\mathbb{E}\left[\frac{1}{n\Delta^2}\frac{f(Z_i;\theta)}{\partial_y a_1(Z_i;\theta_0^{(1)})}\left(X_{i+1} - \bar{A}_1(Z_i;\theta_0^{(1)},\theta^{(2)},\sigma)\right)\left(Y_{i+1} - Y_i\right)|\mathcal{F}_i\right] \xrightarrow{\mathbb{P}_0}$$
$$\frac{1}{2}\int f(z;\theta)b^2(z;\sigma_0)\nu_0(dz)$$

$\square$

Let us introduce an auxiliary Lemma which establishes the convergence in probability for the first moments:

Lemma 6.6. *Let $f : \mathbb{R}^2 \times \Theta \to \mathbb{R}$ be a function with derivatives of polynomial growth in x, uniformly in θ. Assume $\Delta_n \to 0$ and $n\Delta_n \to \infty$. Then the following convergence results hold:*

(i) $\frac{1}{n\Delta_n} \sum_{i=0}^{n-1} f(Z_i;\theta)(X_{i+1} - \bar{A}_1(Z_i;\theta_0^{(1)},\theta^{(2)},\sigma)) \xrightarrow{\mathbb{P}_0} 0$

(ii) $\frac{1}{n\Delta_n} \sum_{i=0}^{n-1} f(Z_i;\theta)(Y_{i+1} - \bar{A}_2(Z_i;\theta^{(1)},\theta_0^{(2)},\sigma)) \xrightarrow{\mathbb{P}_0} 0$

uniformly in θ.

Proof. Consider (ii). The expectation of the sum tends to zero for $\Delta_n \to 0$ and $n\Delta_n \to \infty$ due to Proposition 6.4. Convergence for $\theta^{(1)}$ is due to Lemma 9 in Genon-Catalot and Jacod (1993) and uniformity in $\theta^{(1)}$ follows the proof of Lemma 10 in Kessler (1997). The second assertion is proven in the same way. For (i) see Lemma 3 in Ditlevsen and Samson (2017). □

We also need the following Lemma for proving the asymptotic normality of the estimators.

Lemma 6.7. *Assume (A1)-(A4) and $n\Delta_n \to \infty$ and $n\Delta_n^2 \to 0$. Then for any bounded function $f(z;\theta) \in \mathbb{R}^2 \times \Theta \to \mathbb{R}$ the following holds:*

(i) $\frac{1}{\sqrt{n\Delta_n^3}} \sum_{i=0}^{n-1} f(Z_i;\theta)(X_{i+1} - \bar{A}_1(Z_i;\theta_0^{(1)},\theta^{(2)},\sigma)) \xrightarrow{\mathcal{D}} \mathcal{N}\left(0, \frac{1}{3}\nu_0\left(b^2(z;\sigma_0)(\partial_y a_1(z;\theta_0^{(1)}))^2 f^2(z;\theta)\right)\right)$

(ii) $\frac{1}{\sqrt{n\Delta_n^3}} \sum_{i=0}^{n-1} f(Z_i;\theta)(X_{i+1} - \bar{A}_1(Z_i;\theta_0^{(1)},\theta^{(2)},\sigma))^2 - \frac{1}{\sqrt{n}} \sum_{i=0}^{n-1} f(Z_i;\theta)\frac{1}{3}b^2(z;\sigma_0)(\partial_y a_1(z;\theta_0^{(1)}))^2 \xrightarrow{\mathcal{D}}$
$\mathcal{N}\left(0, \frac{2}{9}\nu_0\left(b^4(z;\sigma_0)(\partial_y a_1(z;\theta_0^{(1)}))^4 f^2(z;\theta)\right)\right)$

(iii) $\frac{1}{\sqrt{n\Delta_n}} \sum_{i=0}^{n-1} f(Z_i;\theta)(Y_{i+1} - Y_i) \xrightarrow{\mathcal{D}} \mathcal{N}\left(0, \nu_0\left(b^2(z;\sigma_0)f^2(z;\theta)\right)\right)$

(iv) $\frac{1}{\sqrt{n\Delta_n}} \sum_{i=0}^{n-1} f(Z_i;\theta)(Y_{i+1} - Y_i)^2 - \frac{1}{\sqrt{n}} \sum_{i=0}^{n-1} f(Z_i;\theta)b^2(Z_i;\sigma_0) \xrightarrow{\mathcal{D}} \mathcal{N}\left(0, 2\nu_0\left(b^4(z;\sigma_0)f^2(z;\theta)\right)\right)$

(v) $\frac{1}{\sqrt{n}\Delta_n^2} \sum_{i=0}^{n-1} f(Z_i;\theta)(X_{i+1} - \bar{A}_1(Z_i;\theta_0^{(1)},\theta^{(2)},\sigma))(Y_{i+1} - Y_i) -$

$\frac{1}{\sqrt{n}} \sum_{i=0}^{n-1} f(Z_i;\theta)\frac{1}{2}b^2(Z_i;\sigma_0)\partial_y a_1(Z_i;\theta_0^{(1)}) \xrightarrow{\mathcal{D}} \mathcal{N}\left(0, \frac{4}{3}\nu_0\left(f(z;\theta)b^4(z;\sigma_0)(\partial_y a_1(z;\theta_0^{(1)}))^2\right)^2\right)$

Proof. We focus on the proof of (v), since (i)-(iv) closely follow Lemmas 4-5 in Ditlevsen and Samson (2017). To simplify the proof for the cross-term, we recall that the representation (6.13) can be transformed so that the two noise terms are independent. For example, we can use an analogue of such a decomposition proposed in Pokern et al. (2007):

$$X_{i+1} - \bar{A}_1(Z_i;\theta_0^{(1)},\theta^{(2)},\sigma) = b(Z_i;\sigma_0)\partial_y a_1(Z_i;\theta_0^{(1)})\left(\frac{\Delta_n^{\frac{3}{2}}}{\sqrt{12}}\eta_i^1 + \frac{\Delta_n^{\frac{3}{2}}}{2}\eta_i^2\right) + \delta_i^1$$

$$Y_{i+1} - Y_i = \Delta_n a_2(Z_i;\theta^{(2)}) + b(Z_i;\sigma_0)\Delta_n^{\frac{1}{2}}\eta_i^2 + \delta_i^2,$$

where δ_i^1 and δ_i^2 are error terms such that $\mathbb{E}[\delta_i^k|\mathcal{F}_i] = O(\Delta_n^2)$ and $\mathbb{E}[(\delta_i^k)^2|\mathcal{F}_i] = O(\Delta_n^4)$ (see Proposition 6.4), and η_i^1 and η_i^2 are standard independent normal variables.

Then Proposition 6.4 gives that

$$\mathbb{E}\left[\left(X_{i+1} - \bar{A}_1(Z_i;\theta_0^{(1)},\theta^{(2)},\sigma)\right)(Y_{i+1} - Y_i)|\mathcal{F}_i\right] = \frac{\Delta_n^2}{2}b(Z_i;\sigma_0)\partial_y a_1(Z_i;\theta_0^{(1)}) + O(\Delta_n^3),$$

then

$$\mathbb{E}\left[f(Z_i;\theta)\left(\left(X_{i+1} - \bar{A}_1(Z_i;\theta_0^{(1)},\theta^{(2)},\sigma)\right)(Y_{i+1} - Y_i) - \frac{\Delta_n^2}{2}b^2(Z_i;\sigma_0)\partial_y a_1(Z_i;\theta_0^{(1)})\right)|\mathcal{F}_i\right] = 0.$$

With slightly more tedious computations (which are omitted) we get also that

$$\mathbb{E}\left[\left(\left(X_{i+1}-\bar{A}_1(Z_i;\theta_0^{(1)},\theta^{(2)},\sigma)\right)(Y_{i+1}-Y_i)-\frac{\Delta_n^2}{2}b^2(Z_i;\sigma_0)(\partial_y a_1(Z_i;\theta_0^{(1)}))\right)^2\Big|\mathcal{F}_i\right]=$$

$$\frac{4\Delta_n^4}{3}b^4(Z_i;\sigma_0)(\partial_y a_1(Z_i;\theta_0^{(1)}))^2+O(\Delta_n^5)$$

Then we obtain:

$$\frac{1}{\sqrt{n}\Delta_n^2}\sum_{i=0}^{n-1}f(Z_i;\theta)\left(X_{i+1}-\bar{A}_1(Z_i;\theta_0^{(1)},\theta^{(2)},\sigma)\right)(Y_{i+1}-Y_i)-\frac{1}{\sqrt{n}}\sum_{i=0}^{n-1}f(Z_i;\theta)\frac{1}{2}b^2(Z_i;\sigma_0)\partial_y a_1(Z_i;\theta_0^{(1)})$$

$$=\frac{1}{\sqrt{n}\Delta_n^2}\sum_{i=0}^{n-1}f(Z_i;\theta)\left(b(Z_i;\sigma_0)\partial_y a_1(Z_i;\theta_0^{(1)})\left(\frac{\Delta_n^{\frac{3}{2}}}{\sqrt{12}}\eta_i^1+\frac{\Delta_n^{\frac{3}{2}}}{2}\eta_i^2\right)+\delta_i^1\right)$$

$$\left(\Delta_n a_2(Z_i;\theta^{(2)})+b(Z_i;\sigma_0)\Delta_n^{\frac{1}{2}}\eta_i^2+\delta_i^2\right)-\frac{1}{\sqrt{n}}\sum_{i=0}^{n-1}f(Z_i;\theta)\frac{1}{2}b^2(Z_i;\sigma_0)\partial_y a_1(Z_i;\theta_0^{(1)})$$

Since $\frac{\Delta_n}{n}\to 0$ by design we see that

$$\frac{1}{n\Delta_n^4}\mathbb{E}\left[\sum_{i=0}^{n-1}f^2(Z_i;\theta)\left(\left(X_{i+1}-\bar{A}_1(Z_i;\theta_0^{(1)},\theta^{(2)},\sigma)\right)(Y_{i+1}-Y_i)-\right.\right.$$

$$\left.\left.\frac{\Delta_n^2}{2}b(Z_i;\sigma_0)(\partial_y a_1(Z_i;\theta_0^{(1)}))\right)^2\right]\to\frac{4}{3}\nu_0\left(f^2(z;\theta)b^4(z;\sigma_0)(\partial_y a_1(z;\theta_0^{(1)})^2)\right)$$

Further, since $\mathbb{E}\left[f^4(Z_i;\theta)\left(\left(X_{i+1}-\bar{A}_1(Z_i;\theta_0^{(1)},\theta^{(2)},\sigma)\right)(Y_{i+1}-Y_i)-\frac{\Delta_n^2}{2}b^2(Z_i;\sigma_0)(\partial_y a_1(Z_i;\theta_0^{(1)}))\right)^4\Big|\mathcal{F}_i\right]$
is bounded by (A2), we have

$$\frac{1}{n^2\Delta_n^8}\mathbb{E}\left[\sum_{i=0}^{n-1}f^4(Z_i;\theta)\left(\left(X_{i+1}-\bar{A}_1(Z_i;\theta_0^{(1)},\theta^{(2)},\sigma)\right)(Y_{i+1}-Y_i)-\frac{\Delta_n^2}{2}b^2(Z_i;\sigma_0)(\partial_y a_1(Z_i;\theta_0^{(1)}))\right)^4\Big|\mathcal{F}_i\right]\to 0.$$

Therefore, we can apply again the Theorem 3.2 from Hall and Heyde (1980) and obtain the statement (v). □

Remark 6.1. *Note that the results for the convergence in distribution for the increments of the second coordinate hold without any assumption on the parameters of the function $a_2(z;\theta^{(2)})$. It is due to the fact that the order of the noise dominates the order of the drift term (which is not the case in first coordinate, where the noise is propagated with the higher order). As a consequence, the convergence of a functional $\sum_{i=0}^{n-1}f(Z_i;\theta)(Y_{i+1}-\bar{A}_2(Z_i;\theta^{(1)},\theta^{(2)},\sigma))$ holds, with a proper scaling, for any value of θ.*

6.7.3 *Consistency and asymptotic normality of the LL contrast estimator*

Lemma 6.1. **Consistency.** The consistency of the estimator for the parameter $\theta^{(2)}$ is based on Lemma 6.2, with the arguments analogous to the proof of Theorem 6.1. For the diffusion parameter σ, the result follows from Lemma 6.3. Denote $\mathcal{I}(\sigma,\sigma_0):=\frac{b^2(z;\sigma_0)}{b^2(z;\sigma)}+\log b^2(z;\sigma)$. We can choose some subsequence n_k such that $\hat{\sigma}_{n,\Delta_n}$ converges to some σ_∞. By the definition of the estimator we know

that $\mathcal{I}(\sigma_\infty, \sigma_0) \leq \mathcal{I}(\sigma_0, \sigma_0)$. But we also know that $\frac{b^2(z; \sigma_0)}{b^2(z; \sigma)} + \log b^2(z; \sigma) \geq 1 + \log b^2(z; \sigma_0)$ and thus $\mathcal{I}(\sigma_\infty, \sigma_0) \geq \mathcal{I}(\sigma_0, \sigma_0)$, and by the identifiability assumption $\sigma_\infty \equiv \sigma_0$. It proves the consistency of $\hat{\sigma}$.

Asymptotic normality. Consider

$$\frac{\Delta_n}{n} \left[\mathcal{L}_{n,\Delta_n}(\theta^{(1)}, \theta^{(2)}, \sigma^2; Z_{0:n}) - \mathcal{L}_{n,\Delta_n}(\theta_0^{(1)}, \theta^{(2)}, \sigma^2; Z_{0:n}) \right] = T_1 + T_2 + T_3 + T_4,$$

where the terms are given as follows:

$$T_1 = \frac{6\Delta_n}{n\Delta_n^3} \sum_{i=0}^{n-1} \left[\frac{\left(X_{i+1} - \bar{A}_1(Z_i; \theta^{(1)}, \theta^{(2)}, \sigma)\right)^2}{b^2(Z_i; \sigma) \left(\partial_y a_1(Z_i; \theta^{(1)})\right)^2} - \frac{\left(X_{i+1} - \bar{A}_1(Z_i; \theta_0^{(1)}, \theta^{(2)}, \sigma)\right)^2}{b^2(Z_i; \sigma) \left(\partial_y a_1(Z_i; \theta_0^{(1)})\right)^2} \right]$$

$$T_2 = -\frac{6\Delta_n}{n\Delta_n^2} \sum_{i=0}^{n-1} \frac{1}{b^2(Z_i; \sigma)} \left[\frac{\left(X_{i+1} - \bar{A}_1(Z_i; \theta^{(1)}, \theta^{(2)}, \sigma)\right)\left(Y_{i+1} - \bar{A}_2(Z_i; \theta^{(1)}, \theta^{(2)}, \sigma)\right)}{\partial_y a_1(Z_i; \theta^{(1)})} - \right.$$
$$\left. \frac{\left(X_{i+1} - \bar{A}_1(Z_i; \theta_0^{(1)}, \theta^{(2)}, \sigma)\right)\left(Y_{i+1} - \bar{A}_2(Z_i; \theta_0^{(1)}, \theta^{(2)}, \sigma)\right)}{\partial_y a_1(Z_i; \theta_0^{(1)})} \right]$$

$$T_3 = \frac{2\Delta_n}{n\Delta_n} \sum_{i=0}^{n-1} \left[\frac{\left(Y_{i+1} - \bar{A}_2(Z_i; \theta^{(1)}, \theta^{(2)}, \sigma)\right)^2}{b^2(Z_i; \sigma)} - \frac{\left(Y_{i+1} - \bar{A}_2(Z_i; \theta_0^{(1)}, \theta^{(2)}, \sigma)\right)^2}{b^2(Z_i; \sigma)} \right]$$

$$T_4 = \frac{\Delta_n}{n} \sum_{i=0}^{n-1} \log \left(\frac{\partial_y a_1(Z_i; \theta^{(1)})}{\partial_y a_1(Z_i; \theta_0^{(1)})} \right)$$

Consider term T_1:

$$T_1 = \frac{6\Delta_n}{n\Delta_n^3} \sum_{i=0}^{n-1} \frac{1}{b^2(Z_i; \sigma)} \left[\frac{\left(X_{i+1} - \bar{A}_1(Z_i; \theta_0^{(1)}, \theta^{(2)}, \sigma) + \bar{A}_1(Z_i; \theta_0^{(1)}, \theta^{(2)}, \sigma) - \bar{A}_1(Z_i; \theta^{(1)}, \theta^{(2)}, \sigma)\right)^2}{\left(\partial_y a_1(Z_i; \theta^{(1)})\right)^2} - \right.$$
$$\left. \frac{\left(X_{i+1} - \bar{A}_1(Z_i; \theta_0^{(1)}, \theta^{(2)}, \sigma)\right)^2}{\left(\partial_y a_1(Z_i; \theta_0^{(1)})\right)^2} \right] = \frac{6\Delta_n}{n\Delta_n^3} \sum_{i=0}^{n-1} \frac{1}{b^2(Z_i; \sigma)} \left[\left(X_{i+1} - \bar{A}_1(Z_i; \theta_0^{(1)}, \theta^{(2)}, \sigma)\right)^2 \left[\frac{1}{\left(\partial_y a_1(Z_i; \theta^{(1)})\right)^2} - \right. \right.$$
$$\left. \frac{1}{\left(\partial_y a_1(Z_i; \theta_0^{(1)})\right)^2} \right] + \frac{2\Delta_n}{\left(\partial_y a_1(Z_i; \theta^{(1)})\right)^2} \left(X_{i+1} - \bar{A}_1(Z_i; \theta_0^{(1)}, \theta^{(2)}, \sigma)\right) (a_1(Z_i; \theta_0^{(1)}) - a_1(Z_i; \theta^{(1)})) +$$
$$\left. \frac{\Delta_n^2}{(\partial_y a_1(Z_i; \theta^{(1)}))^2} \left(a_1(Z_i; \theta_0^{(1)}) - a_1(Z_i; \theta^{(1)})\right)^2 \right].$$

Recalling Lemmas 6.4, 6.6 and 6.5 we have that:

$$\frac{6}{n\Delta_n^2} \sum_{i=0}^{n-1} \frac{\left(X_{i+1} - \bar{A}_1(Z_i; \theta_0^{(1)}, \theta^{(2)}, \sigma)\right)^2}{b^2(Z_i; \sigma)} \left[\frac{1}{\left(\partial_y a_1(Z_i; \theta^{(1)})\right)^2} - \frac{1}{\left(\partial_y a_1(Z_i; \theta_0^{(1)})\right)^2} \right] \xrightarrow{\mathbb{P}_0} 0$$

$$\frac{6}{n\Delta_n} \sum_{i=0}^{n-1} \frac{1}{b^2(Z_i; \sigma)(\partial_y a_1(Z_i; \theta^{(1)}))^2} \left(X_{i+1} - \bar{A}_1(Z_i; \theta_0^{(1)}, \theta^{(2)}, \sigma)\right) (a_1(Z_i; \theta_0^{(1)}) - a_1(Z_i; \theta^{(1)})) \xrightarrow{\mathbb{P}_0} 0$$

$$\frac{6}{n} \sum_{i=0}^{n-1} \frac{(a_1(Z_i; \theta_0^{(1)}) - a_1(Z_i; \theta^{(1)}))^2}{b^2(Z_i; \sigma)(\partial_y a_1(Z_i; \theta^{(1)}))^2} \xrightarrow{\mathbb{P}_0} 6 \int \frac{(a_1(z; \theta_0^{(1)}) - a_1(z; \theta^{(1)}))^2}{b^2(z; \sigma)(\partial_y a_1(z; \theta^{(1)}))^2} \nu_0(dz).$$

Now consider T_2, which can be rewritten as:

$$-\frac{6}{n\Delta_n}\sum_{i=0}^{n-1}\frac{(Y_{i+1}-Y_i+O(\Delta_n))}{b^2(Z_i;\sigma)}\left[\frac{\left(X_{i+1}-\bar{A}_1(Z_i;\theta_0^{(1)},\theta^{(2)},\sigma)+\bar{A}_1(Z_i;\theta_0^{(1)},\theta^{(2)},\sigma)-\bar{A}_1(Z_i;\theta^{(1)},\theta^{(2)},\sigma)\right)}{\partial_y a_1(Z_i;\theta^{(1)})}-\right.$$

$$\left.\frac{\left(X_{i+1}-\bar{A}_1(Z_i;\theta_0^{(1)},\theta^{(2)},\sigma)\right)}{\partial_y a_1(Z_i;\theta_0^{(1)})}\right]=-\frac{6}{n\Delta_n}\sum_{i=0}^{n-1}\frac{(Y_{i+1}-Y_i+O(\Delta_n))}{b^2(Z_i;\sigma)}\left[\left(X_{i+1}-\bar{A}_1(Z_i;\theta_0^{(1)},\theta^{(2)},\sigma)\right)\right.$$

$$\left.\left[\frac{1}{\partial_y a_1(Z_i;\theta^{(1)})}-\frac{1}{\partial_y a_1(Z_i;\theta_0^{(1)})}\right]+\frac{\Delta_n}{(\partial_y a_1(Z_i;\theta^{(1)}))}(a_1(Z_i;\theta_0^{(1)})-a_1(Z_i;\theta^{(1)}))\right].$$

Then we use the fact that the expectation of $\left(X_{i+1}-\bar{A}_1(Z_i;\theta_0^{(1)},\theta^{(2)},\sigma)\right)$ is of order Δ_n^2 and of increments $Y_{i+1}-Y_i$ is of Δ_n, and by Lemma 6.5 we obtain:

$$-\frac{6}{n\Delta_n}\sum_{i=0}^{n-1}\frac{\left(X_{i+1}-\bar{A}_1(Z_i;\theta_0^{(1)},\theta^{(2)},\sigma)\right)(Y_{i+1}-Y_i+O(\Delta_n))}{b^2(Z_i;\sigma)(\partial_y a_1(Z_i;\theta_0^{(1)}))}\left[\frac{(\partial_y a_1(Z_i;\theta_0^{(1)}))}{(\partial_y a_1(Z_i;\theta^{(1)}))}-1\right]\xrightarrow{\mathbb{P}_0}0.$$

The same holds for T_4. Consider then T_3:

$$\frac{2\Delta_n}{n\Delta_n}\sum_{i=0}^{n-1}\left[2\frac{\left(Y_{i+1}-\bar{A}_2(Z_i;\theta^{(1)},\theta^{(2)},\sigma)\right)^2}{b^2(Z_i;\sigma)}-\frac{\left(Y_{i+1}-\bar{A}_2(Z_i;\theta_0^{(1)},\theta^{(2)},\sigma)\right)^2}{b^2(Z_i;\sigma)}\right]=$$

$$\frac{2}{n}\sum_{i=0}^{n-1}\frac{1}{b^2(Z_i;\sigma)}\left[\left(Y_{i+1}-\bar{A}_2(Z_i;\theta_0^{(1)},\theta^{(2)},\sigma)\right)\left(\bar{A}_2(Z_i;\theta_0^{(1)},\theta^{(2)},\sigma)-\bar{A}_2(Z_i;\theta^{(1)},\theta^{(2)},\sigma)\right)-\right.$$

$$\left.\left(\bar{A}_2(Z_i;\theta_0^{(1)},\theta^{(2)},\sigma)-\bar{A}_2(Z_i;\theta^{(1)},\theta^{(2)},\sigma)\right)^2\right]$$

This term is of order $O(\Delta_n^3)$ (since $\theta^{(1)}$ is contained only in terms of order Δ_n^2), thus it converges to zero as $\Delta_n\to 0$. Thus, we indeed have

$$\lim_{n\to\infty,\Delta_n\to 0}\frac{\Delta_n}{n}\left[\mathcal{L}_{n,\Delta_n}(\theta^{(1)},\theta^{(2)},\sigma^2;Z_{0:n})-\mathcal{L}_{n,\Delta_n}(\theta_0^{(1)},\theta^{(2)},\sigma^2;Z_{0:n})\right]\xrightarrow{\mathbb{P}_0}$$

$$6\int\frac{(a_1(z;\theta_0^{(1)})-a_1(z;\theta^{(1)}))^2}{b^2(z;\sigma)(\partial_y a_1(z;\theta^{(1)}))^2}\nu_0(dz).$$

$\square$

Theorem 6.1 (consistency and asymptotic normality of $\theta^{(1)}$). Throughout the proof we assume that $\theta^{(1)}\in\mathbb{R}$ in order to simplify the notations.

Consistency. It follows essentially from Lemma 6.1. Indeed, the result of the Lemma (and the fact that the parameter space is compact) implies that we can find a subsequence $\hat{\theta}_{n,\Delta_n}^{(1)}$ which converges to some value $\theta_\infty^{(1)}$. However, the minimum of the expression in Lemma 6.1 is attained for $\theta_0^{(1)}$. Then by identifiability of the drift function we have the consistency, that is $\hat{\theta}_{n,\Delta_n}^{(1)}\to\theta_0^{(1)}$.

Asymptotic normality. The proof follows the standard pattern (see Kessler (1997), Genon-Catalot et al. (1999), Ditlevsen and Samson (2017)). First, we write the Taylor expansion of the function (6.15). Then we have:

$$\int\frac{\Delta_n}{n}\frac{\partial^2}{\partial\theta^{(1)}\partial\theta^{(1)}}\mathcal{L}_{n,\Delta_n}\left(\theta_0^{(1)}+u(\hat{\theta}_{n,\Delta_n}^{(1)}-\theta_0),\theta^{(2)},\sigma;z\right)du\cdot\sqrt{\frac{n}{\Delta_n}}(\hat{\theta}_{n,\Delta_n}^{(1)}-\theta_0^{(1)})=$$

$$-\sqrt{\frac{\Delta_n}{n}}\frac{\partial}{\partial\theta^{(1)}}\mathcal{L}_{n,\Delta_n}(\theta_0^{(1)},\theta^{(2)},\sigma;z)$$

Note that the values of $\theta^{(2)}$ and σ may be taken arbitrary. Now we have to compute the first and the second order derivatives of (6.15). We omit the dependency on parameters in the expression for partial derivatives to make it readable and study the convergence of the first order derivative:

$$
\begin{aligned}
\frac{\partial}{\partial \theta^{(1)}} \mathcal{L}_{n,\Delta_n}(\theta_0^{(1)}, \theta^{(2)}, \sigma; z) = \sum_{i=1}^{n-1} & \left[\frac{2\partial_{y,\theta^{(1)}}^2 a_1}{\partial_y a_1} - \frac{6}{b^2(Z_i;\sigma)\partial_y a_1} \right. \\
& \left[\frac{2(X_{i+1} - \bar{A}_1(Z_i;\theta_0^{(1)},\theta^{(2)},\sigma))^2}{\Delta_n^3 (\partial_y a_1)^2} \partial_{y,\theta^{(1)}}^2 a_1 + \frac{2(X_{i+1} - \bar{A}_1(Z_i;\theta_0^{(1)},\theta^{(2)},\sigma))(\partial_{\theta^{(1)}} a_1)}{\Delta_n^2 (\partial_y a_1)} - \right. \\
& \qquad \frac{(Y_{i+1} - \bar{A}_2(Z_i;\theta_0^{(1)},\theta^{(2)},\sigma))(\partial_{\theta^{(1)}} a_1)}{\Delta_n} - \\
& \left. \left. \frac{(X_{i+1} - \bar{A}_1(Z_i;\theta_0^{(1)},\theta^{(2)},\sigma))(Y_{i+1} - \bar{A}_2(Z_i;\theta_0^{(1)},\theta^{(2)},\sigma))(\partial_{y,\theta^{(1)}}^2 a_1)}{\Delta_n^2 (\partial_y a_1)} \right] \right]
\end{aligned}
\tag{6.23}
$$

Under assumption (A5) the only non-zero terms are the following:

$$
\begin{aligned}
\frac{\partial}{\partial \theta^{(1)}} \mathcal{L}_{n,\Delta_n}(\theta_0^{(1)}, \theta^{(2)}, \sigma; z) = \sum_{i=1}^{n-1} & -\frac{6}{b^2(Z_i;\sigma)\partial_y a_1} \left[\frac{2(X_{i+1} - \bar{A}_1(Z_i;\theta_0^{(1)},\theta^{(2)},\sigma))(\partial_{\theta^{(1)}} a_1)}{\Delta_n^2 (\partial_y a_1)} - \right. \\
& \left. \frac{(Y_{i+1} - \bar{A}_2(Z_i;\theta_0^{(1)},\theta^{(2)},\sigma))(\partial_{\theta^{(1)}} a_1)}{\Delta_n} \right]
\end{aligned}
$$

Applying Lemma 6.7, we get:

$$
\frac{1}{\sqrt{n\Delta_n^3}} \sum_{i=1}^{n-1} \left[\frac{12(\partial_{\theta^{(1)}} a_1)}{b^2(Z_i;\sigma)(\partial_y a_1)} (X_{i+1} - \bar{A}_1(Z_i;\theta_0^{(1)},\theta^{(2)},\sigma)) \right] \xrightarrow{\mathcal{D}} \mathcal{N}\left(0, 36\nu_0\left(\frac{b^2(z;\sigma_0)}{b^4(z;\sigma)}(\partial_{\theta^{(1)}} a_1)^2 \right)\right)
$$

$$
\frac{1}{\sqrt{n\Delta_n}} \sum_{i=1}^{n-1} \left[\frac{6(\partial_{\theta^{(1)}} a_1)}{b^2(Z_i;\sigma)} \frac{(Y_{i+1} - \bar{A}_2(Z_i;\theta_0^{(1)},\theta^{(2)},\sigma))}{(\partial_y a_1)} \right] \xrightarrow{\mathcal{D}} \mathcal{N}\left(0, 36\nu_0\left(\frac{b^2(z;\sigma_0)}{b^4(z;\sigma)} \frac{(\partial_{\theta^{(1)}} a_1)^2}{(\partial_y a_1)^2} \right)\right)
$$

Thus, we have the following convergence in law:

$$
\sqrt{\frac{\Delta_n}{n}} \frac{\partial}{\partial \theta^{(1)}} \mathcal{L}_{n,\Delta_n}(\theta_0^{(1)}, \theta^{(2)}, \sigma; z) \xrightarrow{\mathcal{D}} \mathcal{N}\left(0, 36\nu_0\left(\frac{b^2(z;\sigma_0)}{b^4(z;\sigma)}(\partial_{\theta^{(1)}} a_1)^2 \left(1 + \frac{1}{(\partial_y a_1)^2}\right) \right)\right)
$$

For the second order derivative we split again the expression (6.23) in several parts and study their convergence:

$$
T_1 := \frac{\Delta_n}{n} \sum_{i=1}^{n-1} -\frac{12\Delta_n}{\Delta_n^2 b^2(Z_i;\sigma)(\partial_y a_1)^2} \left[(\partial_{\theta^{(1)}} a_1)^2 + (X_{i+1} - \bar{A}_1(Z_i;\theta_0^{(1)},\theta^{(2)},\sigma)) \frac{(\partial_{\theta^{(1)}\theta^{(1)}}^2 a_1)(\partial_y a_1)}{(\partial_y a_1)^2} \right]
$$

$$
T_2 := \frac{\Delta_n}{n} \sum_{i=1}^{n-1} \frac{6(Y_{i+1} - \bar{A}_2(Z_i;\theta^{(1)},\theta^{(2)},\sigma))}{\Delta_n b^2(Z_i;\sigma)} \frac{(\partial_y a_1)^2 \partial_{\theta^{(1)}\theta^{(1)}}^2 a_1}{(\partial_y a_1)^4}
$$

It is easy to see that the terms T_2 converges to 0 by Lemmas 6.6 and 6.5. T_1, according to the Lemma 6.4 and Lemma 6.6, converges to $12 \int \frac{(\partial_{\theta^{(1)}} a_1)^2}{b^2(z;\sigma)(\partial_y a_1)} \nu_0(dz)$. That gives the result. $\qquad \square$

Lemma 6.2. Note that we cannot infer the value of $\theta^{(2)}$ with the same scaling as the parameter of the smooth coordinate because the estimator for each variable converges with different speed. Thus, we fix the parameter $\theta^{(1)}$ to its estimated value $\hat{\theta}_{n,\Delta_n}^{(1)}$ and consider the same sum, but with a different scaling, namely :

$$
\lim_{n\to\infty,\Delta_n\to 0} \frac{1}{n\Delta_n} \left[\mathcal{L}_{n,\Delta_n}(\hat{\theta}_{n,\Delta_n}^{(1)}, \theta^{(2)}, \sigma^2; Z_{0:n}) - \mathcal{L}_{n,\Delta_n}(\hat{\theta}_{n,\Delta_n}^{(1)}, \theta_0^{(2)}, \sigma^2; Z_{0:n}) \right] = T_1 + T_2 + T_3
$$

where the terms are given as follows:

$$T_1 = \frac{6}{n\Delta_n^4} \sum_{i=0}^{n-1} \frac{1}{b^2(Z_i;\sigma)\left(\partial_y a_1(Z_i;\hat{\theta}_{n,\Delta_n}^{(1)})\right)^2} \left[\left(X_{i+1} - \bar{A}_1(Z_i;\hat{\theta}_{n,\Delta_n}^{(1)},\theta^{(2)},\sigma)\right)^2 - \right.$$
$$\left. \left(X_{i+1} - \bar{A}_1(Z_i;\hat{\theta}_{n,\Delta_n}^{(1)},\theta_0^{(2)},\sigma)\right)^2\right]$$

$$T_2 = -\frac{6}{n\Delta_n^3} \sum_{i=0}^{n-1} \frac{1}{b^2(Z_i;\sigma)} \left[\frac{\left(X_{i+1} - \bar{A}_1(Z_i;\hat{\theta}_{n,\Delta_n}^{(1)},\theta^{(2)},\sigma)\right)\left(Y_{i+1} - \bar{A}_2(Z_i;\hat{\theta}_{n,\Delta_n}^{(1)},\theta^{(2)},\sigma)\right)}{\partial_y a_1(Z_i;\hat{\theta}_{n,\Delta_n}^{(1)})} - \right.$$
$$\left. \frac{\left(X_{i+1} - \bar{A}_1(Z_i;\hat{\theta}_{n,\Delta_n}^{(1)},\theta_0^{(2)},\sigma)\right)\left(Y_{i+1} - \bar{A}_2(Z_i;\hat{\theta}_{n,\Delta_n}^{(1)},\theta_0^{(2)},\sigma)\right)}{\partial_y a_1(Z_i;\hat{\theta}_{n,\Delta_n}^{(1)})}\right]$$

$$T_3 = \frac{2}{n\Delta_n^2} \sum_{i=0}^{n-1} \frac{\left[(Y_{i+1} - \bar{A}_2(Z_i;\hat{\theta}_{n,\Delta_n}^{(1)},\theta^{(2)},\sigma))^2 - (Y_{i+1} - \bar{A}_2(Z_i;\hat{\theta}_{n,\Delta_n}^{(1)},\theta_0^{(2)},\sigma))^2\right]}{b^2(Z_i;\sigma)}$$

We start with T_1:

$$T_1 = \frac{6}{n\Delta_n^4} \sum_{i=0}^{n-1} \frac{1}{b^2(Z_i;\sigma)\left(\partial_y a_1(Z_i;\hat{\theta}_{n,\Delta_n}^{(1)})\right)^2} \left[\left(\bar{A}_1(Z_i;\hat{\theta}_{n,\Delta_n}^{(1)},\theta_0^{(2)},\sigma) - \bar{A}_1(Z_i;\hat{\theta}_{n,\Delta_n}^{(1)},\theta^{(2)},\sigma)\right)\right.$$
$$\left.\left(X_{i+1} - \bar{A}_1(Z_i;\hat{\theta}_{n,\Delta_n}^{(1)},\theta_0^{(2)},\sigma)\right) - \left(\bar{A}_1(Z_i;\hat{\theta}_{n,\Delta_n}^{(1)},\theta_0^{(2)},\sigma) - \bar{A}_1(Z_i;\hat{\theta}_{n,\Delta_n}^{(1)},\theta^{(2)},\sigma)\right)^2\right] =$$
$$\frac{6}{n\Delta_n^4} \sum_{i=0}^{n-1} \frac{1}{b^2(Z_i;\sigma)\left(\partial_y a_1(Z_i;\hat{\theta}_{n,\Delta_n}^{(1)})\right)^2} \left[\frac{\Delta_n^2}{2}\left(\partial_y a_1(Z_i;\hat{\theta}_{n,\Delta_n}^{(1)})\right)\left(a_2(Z_i;\theta_0^{(2)}) - a_2(Z_i;\theta^{(2)})\right)\right.$$
$$\left(X_{i+1} - \bar{A}_1(Z_i;\theta_0^{(1)},\theta_0^{(2)},\sigma)\right) + \frac{\Delta_n^3}{2}\left(\partial_y a_1(Z_i;\hat{\theta}_{n,\Delta_n}^{(1)})\right)\left(a_2(Z_i;\theta_0^{(2)}) - a_2(Z_i;\theta^{(2)})\right)$$
$$\left(a_1(Z_i;\theta_0^{(1)}) - a_1(Z_i;\hat{\theta}_{n,\Delta_n}^{(1)})\right) + \frac{\Delta_n^4}{4}\left(\partial_y a_1(Z_i;\hat{\theta}_{n,\Delta_n}^{(1)})\right)^2\left(a_2(Z_i;\theta_0^{(2)}) - a_2(Z_i;\theta^{(2)})\right)^2 -$$
$$\left. \frac{\Delta_n^4}{4}\left(\partial_y a_1(Z_i;\hat{\theta}_{n,\Delta_n}^{(1)})\right)^2\left(a_2(Z_i;\theta_0^{(2)}) - a_2(Z_i;\theta^{(2)})\right)^2\right]$$

Recall that $\left(X_{i+1} - \bar{A}_1(Z_i;\theta_0^{(1)},\theta_0^{(2)},\sigma)\right)$ is of $O(\Delta_n^3)$ by Proposition 6.3. Thus, the first summand of the T_1 is of order Δ_n^5 and converges to 0. The second summand, under assumption $(A5)$, can be rewritten as

$$\frac{3}{n\Delta_n^4} \sum_{i=0}^{n-1} \frac{\Delta_n^3\left(\theta_0^{(1)} - \hat{\theta}_{n,\Delta_n}^{(1)}\right)^T g(X_i)\left(a_2(Z_i;\theta_0^{(2)}) - a_2(Z_i;\theta^{(2)})\right)}{b^2(Z_i;\sigma)\left(\partial_y a_1(Z_i;\hat{\theta}_{n,\Delta_n}^{(1)})\right)} =$$
$$\frac{3}{\sqrt{n\Delta_n}n} \sum_{i=0}^{n-1} \frac{\sqrt{\frac{n}{\Delta_n}}\left(\theta_0^{(1)} - \hat{\theta}_{n,\Delta_n}^{(1)}\right)^T g(X_i)\left(a_2(Z_i;\theta_0^{(2)}) - a_2(Z_i;\theta^{(2)})\right)}{b^2(Z_i;\sigma)\left(\partial_y a_1(Z_i;\hat{\theta}_{n,\Delta_n}^{(1)})\right)}.$$

$\sqrt{\frac{n}{\Delta_n}} \left(\theta_0^{(1)} - \hat{\theta}_{n,\Delta_n}^{(1)} \right)^T$ converges to a normal variable with zero mean due to Theorem 6.1, and the whole expression converges to 0, because $n\Delta_n \to \infty$. Thus T_1 converges to 0. Consider T_2:

$$T_2 = -\frac{6}{n\Delta_n^3} \sum_{i=0}^{n-1} \left[\frac{\Delta_n \left(X_{i+1} - \bar{A}_1(Z_i; \theta_0^{(1)}, \theta^{(2)}, \sigma) \right) (a_2(Z_i; \theta^{(2)}) - a_2(Z_i; \theta_0^{(2)}))}{\partial_y a_1(Z_i; \hat{\theta}_{n,\Delta_n}^{(1)}) b^2(Z_i; \sigma)} + \right.$$
$$\left. \frac{\Delta_n^2 (a_1(Z_i; \theta_0^{(1)}) - a_1(Z_i; \hat{\theta}_{n,\Delta_n}^{(1)}))(a_2(Z_i; \theta^{(2)}) - a_2(Z_i; \theta_0^{(2)}))}{\partial_y a_1(Z_i; \hat{\theta}_{n,\Delta_n}^{(1)}) b^2(Z_i; \sigma)} \right]$$

Then, the first part of the sum converges to zero in probability after applying Lemma 6.6. The second part of the sum also converges to zero because $n\Delta_n \to \infty$ by design, and $\hat{\theta}_{n,\Delta_n}^{(1)} \xrightarrow{\mathbb{P}_0} \theta_0^{(1)}$. So that, recalling (A5), and applying the arguments used above for T_1 to $a_1(Z_i; \theta_0^{(1)}) - a_1(Z_i; \hat{\theta}_{n,\Delta_n}^{(1)}) = \left(\theta_0^{(1)} - \hat{\theta}_{n,\Delta_n}^{(1)} \right) g(X_i)$, we prove that T_2 also converges to 0. So we just have to consider the remaining term T_3:

$$T_3 = \frac{2}{n\Delta_n^2} \sum_{i=0}^{n-1} \frac{1}{b^2(Z_i; \sigma)} \left[(Y_{i+1} - \bar{A}_2(Z_i; \hat{\theta}_{n,\Delta_n}^{(1)}, \theta_0^{(2)}, \sigma))^2 + \right.$$
$$(Y_{i+1} - \bar{A}_2(Z_i; \hat{\theta}_{n,\Delta_n}^{(1)}, \theta_0^{(2)}, \sigma))(\bar{A}_2(Z_i; \hat{\theta}_{n,\Delta_n}^{(1)}, \theta_0^{(2)}, \sigma) - \bar{A}_2(Z_i; \hat{\theta}_{n,\Delta_n}^{(1)}, \theta^{(2)}, \sigma)) +$$
$$\left. (\bar{A}_2(Z_i; \hat{\theta}_{n,\Delta_n}^{(1)}, \theta_0^{(2)}, \sigma) - \bar{A}_2(Z_i; \hat{\theta}_{n,\Delta_n}^{(1)}, \theta^{(2)}, \sigma))^2 - (Y_{i+1} - \bar{A}_2(Z_i; \hat{\theta}_{n,\Delta_n}^{(1)}, \theta_0^{(2)}, \sigma))^2 \right] =$$
$$\frac{2}{n\Delta_n^2} \sum_{i=0}^{n-1} \frac{1}{b^2(Z_i; \sigma)} \left[\Delta_n (Y_{i+1} - \bar{A}_2(Z_i; \hat{\theta}_{n,\Delta_n}^{(1)}, \theta_0^{(2)}, \sigma))(a_2(Z_i; \theta_0^{(2)}) - a_2(Z_i; \theta^{(2)})) + \right.$$
$$\left. \Delta_n^2 (a_2(Z_i; \theta_0^{(2)}) - a_2(Z_i; \theta^{(2)}))^2 \right]$$

The first part of the sum converges to 0 due to Lemma 6.6. Then we apply Lemma 6.5 and get the convergence:

$$\lim_{n\to\infty, \Delta_n \to 0} \frac{1}{n\Delta_n} \left[\mathcal{L}_{n,\Delta_n}(\hat{\theta}_{n,\Delta_n}^{(1)}, \theta^{(2)}, \sigma^2; Z_{0:n}) - \mathcal{L}_{n,\Delta_n}(\hat{\theta}_{n,\Delta_n}^{(1)}, \theta_0^{(2)}, \sigma_0^2; Z_{0:n}) \right] \xrightarrow{\mathbb{P}_0}$$
$$2 \int \frac{(a_2(z; \theta_0^{(2)}) - a_2(z; \theta^{(2)}))^2}{b^2(z; \sigma)} \nu_0(dz)$$

$\square$

Lemma 6.3. We can split the contrast in the following sum:

$$\lim_{n\to\infty, \Delta_n \to 0} \frac{1}{2n} \mathcal{L}_{n,\Delta_n}(\hat{\theta}_{n,\Delta_n}^{(1)}, \theta^{(2)}, \sigma^2; Z_{0:n}) = \lim_{n\to\infty, \Delta_n \to 0} [3T_1 - 3T_2 + T_3 + T_4]$$

where terms are given by follows:

$$T_1 = \frac{1}{n} \sum_{i=0}^{n-1} \frac{(X_{i+1} - \bar{A}_1(Z_i; \hat{\theta}_{n,\Delta_n}^{(1)}, \theta^{(2)}, \sigma))^2}{\Delta_n^3 b^2(Z_i; \sigma)(\partial_y a_1(Z_i; \hat{\theta}_{n,\Delta_n}^{(1)}))^2}$$

$$T_2 = \frac{1}{n} \sum_{i=0}^{n-1} \frac{(X_{i+1} - \bar{A}_1(Z_i; \hat{\theta}_{n,\Delta_n}^{(1)}, \theta^{(2)}, \sigma))(Y_{i+1} - \bar{A}_2(Z_i; \hat{\theta}_{n,\Delta_n}^{(1)}, \theta^{(2)}, \sigma))}{\Delta_n^2 b^2(Z_i; \sigma)(\partial_y a_1(Z_i; \hat{\theta}_{n,\Delta_n}^{(1)}))}$$

$$T_3 = \frac{1}{n} \sum_{i=0}^{n-1} \frac{(Y_{i+1} - \bar{A}_2(Z_i; \hat{\theta}_{n,\Delta_n}^{(1)}, \theta^{(2)}, \sigma))^2}{\Delta_n b^2(Z_i; \sigma)}$$

$$T_4 = \frac{1}{n} \sum_{i=0}^{n-1} \log b^2(Z_i; \sigma)$$

For the term T_1 we have:

$$T_1 = \frac{1}{n\Delta_n^3} \sum_{i=0}^{n-1} \frac{1}{b^2(Z_i;\sigma)} \frac{\left(X_{i+1} - \bar{A}_1(Z_i;\hat{\theta}_{n,\Delta_n}^{(1)}, \theta^{(2)}, \sigma)\right)^2}{(\partial_y a_1(Z_i;\hat{\theta}_{n,\Delta_n}^{(1)}))^2} =$$

$$\frac{1}{n} \sum_{i=0}^{n-1} \frac{1}{b^2(Z_i;\sigma)} \frac{\left(X_{i+1} - \bar{A}_1(Z_i;\theta_0^{(1)}, \theta^{(2)}, \sigma) + \bar{A}_1(Z_i;\theta_0^{(1)}, \theta^{(2)}, \sigma) - \bar{A}_1(Z_i;\hat{\theta}_{n,\Delta_n}^{(1)}, \theta^{(2)}, \sigma)\right)^2}{\Delta_n^3(\partial_y a_1(Z_i;\hat{\theta}_{n,\Delta_n}^{(1)}))^2} =$$

$$= \frac{1}{n} \sum_{i=0}^{n-1} \frac{1}{b^2(Z_i;\sigma)} \left[\frac{\left(X_{i+1} - \bar{A}_1(Z_i;\theta_0^{(1)}, \theta^{(2)}, \sigma)\right)^2}{\Delta_n^3(\partial_y a_1(Z_i;\hat{\theta}_{n,\Delta_n}^{(1)}))^2} \frac{(\partial_y a_1(Z_i;\theta_0^{(1)}))^2}{(\partial_y a_1(Z_i;\theta_0^{(1)}))^2} + \right.$$

$$\left. \frac{2\Delta_n \left(X_{i+1} - \bar{A}_1(Z_i;\theta_0^{(1)}, \theta^{(2)}, \sigma)\right) \left(a_1(Z_i;\theta_0^{(1)}) - a_1(Z_i;\hat{\theta}_{n,\Delta_n}^{(1)})\right)}{\Delta_n^3(\partial_y a_1(Z_i;\hat{\theta}_{n,\Delta_n}^{(1)}))^2} + \frac{\Delta_n^2}{\Delta_n^3} \frac{\left(a_1(Z_i;\theta_0^{(1)}) - a_1(Z_i;\hat{\theta}_{n,\Delta_n}^{(1)})\right)^2}{b^2(Z_i;\sigma)(\partial_y a_1(Z_i;\hat{\theta}_{n,\Delta_n}^{(1)}))^2} \right]$$

Thanks to the Lemmas 6.5 and 6.6, we know that the second term of the sum converges to 0 in probability, and for the first one we have:

$$\frac{1}{n} \sum_{i=0}^{n-1} \frac{1}{b^2(Z_i;\sigma)} \frac{\left(X_{i+1} - \bar{A}_1(Z_i;\theta_0^{(1)}, \theta^{(2)}, \sigma)\right)^2}{\Delta_n^3(\partial_y a_1(Z_i;\hat{\theta}_{n,\Delta_n}^{(1)}))^2} \frac{(\partial_y a_1(Z_i;\theta_0^{(1)}))^2}{(\partial_y a_1(Z_i;\theta_0^{(1)}))^2} \xrightarrow{\mathbb{P}_0} \int \frac{b^2(z;\sigma_0)}{b^2(z;\sigma)} \frac{(\partial_y a_1(z;\theta_0^{(1)}))^2}{(\partial_y a_1(z;\hat{\theta}_{n,\Delta_n}^{(1)}))^2} \nu_0(dz)$$

For the third term, we use the assumption (A5), and then obtain the convergence to 0 in probability thanks to Theorem 6.1, the continuous mapping theorem and Lemma 6.4:

$$\frac{2}{n} \sum_{i=0}^{n-1} \frac{\Delta_n^2}{\Delta_n^3} \frac{\left(a_1(Z_i;\theta_0^{(1)}) - a_1(Z_i;\hat{\theta}_{n,\Delta_n}^{(1)})\right)^2}{b^2(Z_i;\sigma)(\partial_y a_1(Z_i;\hat{\theta}_{n,\Delta_n}^{(1)}))^2} = \frac{2}{n^2} \sum_{i=0}^{n-1} \frac{\left(\sqrt{\frac{n}{\Delta_n}}(\theta_0^{(1)} - \hat{\theta}_{n,\Delta_n}^{(1)})\right)^2 g^2(X_i)}{b^2(Z_i;\sigma)(\partial_y a_1(Z_i;\hat{\theta}_{n,\Delta_n}^{(1)}))^2} \xrightarrow{\mathbb{P}_0} 0.$$

Then, T_2 decomposes as:

$$\frac{1}{n} \sum_{i=0}^{n-1} \frac{(X_{i+1} - \bar{A}_1(Z_i;\hat{\theta}_{n,\Delta_n}^{(1)}, \theta^{(2)}, \sigma))(Y_{i+1} - \bar{A}_2(Z_i;\hat{\theta}_{n,\Delta_n}^{(1)}, \theta^{(2)}, \sigma))}{\Delta_n^2 b^2(Z_i;\sigma)(\partial_y a_1(Z_i;\hat{\theta}_{n,\Delta_n}^{(1)}))} = \frac{1}{n} \sum_{i=0}^{n-1} \frac{(\partial_y a_1(Z_i;\theta_0^{(1)}))}{b^2(Z_i;\sigma)(\partial_y a_1(Z_i;\hat{\theta}_{n,\Delta_n}^{(1)}))}$$

$$\left[\frac{(X_{i+1} - \bar{A}_1(Z_i;\theta_0^{(1)}, \theta^{(2)}, \sigma))(Y_{i+1} - \bar{A}_2(Z_i;\hat{\theta}_{n,\Delta_n}^{(1)}, \theta_0^{(2)}, \sigma))}{\Delta_n^2(\partial_y a_1(Z_i;\theta_0^{(1)}))} + \right.$$

$$\frac{\Delta_n(X_{i+1} - \bar{A}_1(Z_i;\theta_0^{(1)}, \theta^{(2)}, \sigma))(a_2(Z_i;\theta_0^{(2)}) - a_2(Z_i;\theta^{(2)}))}{\Delta_n^2(\partial_y a_1(Z_i;\theta_0^{(1)}))} +$$

$$\frac{\Delta_n(Y_{i+1} - \bar{A}_2(Z_i;\hat{\theta}_{n,\Delta_n}^{(1)}, \theta_0^{(2)}, \sigma))(a_1(Z_i;\theta_0^{(1)}) - a_1(Z_i;\hat{\theta}_{n,\Delta_n}^{(1)}))}{\Delta_n^2(\partial_y a_1(Z_i;\theta_0^{(1)}))} +$$

$$\left. \frac{\Delta_n^2(a_1(Z_i;\theta_0^{(1)}) - a_1(Z_i;\hat{\theta}_{n,\Delta_n}^{(1)}))(a_2(Z_i;\theta_0^{(2)}) - a_2(Z_i;\theta^{(2)}))}{\Delta_n^2(\partial_y a_1(Z_i;\theta_0^{(1)}))} \right]$$

Again, using Lemma 6.6, we know that the second and the third terms are converging to 0 in probability.

For the first term, thanks to Lemma 6.5 we have the following convergence:

$$\frac{1}{n} \sum_{i=0}^{n-1} \frac{(X_{i+1} - \bar{A}_1(Z_i;\theta_0^{(1)}, \theta^{(2)}, \sigma))(Y_{i+1} - \bar{A}_2(Z_i;\hat{\theta}_{n,\Delta_n}^{(1)}, \theta_0^{(2)}, \sigma))(\partial_y a_1(Z_i;\theta_0^{(1)}))}{\Delta_n^2 b^2(Z_i;\sigma)(\partial_y a_1(Z_i;\theta_0^{(1)}))(\partial_y a_1(Z_i;\hat{\theta}_{n,\Delta_n}^{(1)}))} \xrightarrow{\mathbb{P}_0}$$

$$\int \frac{b^2(z;\sigma_0)}{b^2(z;\sigma)} \frac{\partial_y a_1(z;\theta_0^{(1)})}{\partial_y a_1(z;\hat{\theta}_{n,\Delta_n}^{(1)})} \nu_0(dz)$$

Finally, we treat the last term:

$$\frac{1}{n}\sum_{i=0}^{n-1}\frac{\Delta_n^2(a_1(Z_i;\theta_0^{(1)})-a_1(Z_i;\hat{\theta}_{n,\Delta_n}^{(1)}))(a_2(Z_i;\theta_0^{(2)})-a_2(Z_i;\theta^{(2)}))}{\Delta_n^2 b^2(Z_i;\sigma)(\partial_y a_1(Z_i;\hat{\theta}_{n,\Delta_n}^{(1)}))}$$

Using again the Lipschitz continuity of a_1, Theorem 6.1 and the Slutsky's theorem, we obtain a convergence to zero in probability for this term. T_4 converges in probability to $\int \log b^2(z;\sigma)\nu_0(dz)$ due to Lemma 6.4. Consider T_3:

$$T_3 = \frac{1}{n\Delta_n}\sum_{i=0}^{n-1}\frac{1}{b^2(Z_i;\sigma)}\left[(Y_{i+1}-\bar{A}_2(Z_i;\hat{\theta}_{n,\Delta_n}^{(1)},\theta_0^{(2)},\sigma))^2+\right.$$

$$2(Y_{i+1}-\bar{A}_2(Z_i;\hat{\theta}_{n,\Delta_n}^{(1)},\theta_0^{(2)},\sigma))(\bar{A}_2(Z_i;\hat{\theta}_{n,\Delta_n}^{(1)},\theta_0^{(2)},\sigma)-\bar{A}_2(Z_i;\hat{\theta}_{n,\Delta_n}^{(1)},\theta^{(2)},\sigma))+$$

$$\left.(\bar{A}_2(Z_i;\hat{\theta}_{n,\Delta_n}^{(1)},\theta_0^{(2)},\sigma)-\bar{A}_2(Z_i;\hat{\theta}_{n,\Delta_n}^{(1)},\theta^{(2)},\sigma))^2\right]=\frac{1}{n\Delta_n}\sum_{i=0}^{n-1}\frac{(Y_{i+1}-\bar{A}_2(Z_i;\hat{\theta}_{n,\Delta_n}^{(1)},\theta_0^{(2)},\sigma))^2}{b^2(Z_i;\sigma)}+$$

$$2\frac{\Delta_n}{n\Delta_n}\sum_{i=0}^{n-1}\frac{(Y_{i+1}-\bar{A}_2(Z_i;\hat{\theta}_{n,\Delta_n}^{(1)},\theta_0^{(2)},\sigma))(a_2(Z_i;\theta_0^{(2)})-a_2(Z_i;\theta^{(2)}))}{b^2(Z_i;\sigma)}+$$

$$\frac{\Delta_n^2}{n\Delta_n}\sum_{i=0}^{n-1}\frac{(a_2(Z_i;\theta_0^{(2)})-a_2(Z_i;\theta^{(2)}))^2}{b^2(Z_i;\sigma)}$$

Thanks to Lemma 6.5 and 6.6 we conclude that

$$T_3 \xrightarrow{\mathbb{P}_0} \int\frac{b^2(z;\sigma_0)}{b^2(z;\sigma)}\nu_0(dz)+0+0$$

Finally, we obtain

$$\frac{1}{n}\mathcal{L}_{n,\Delta_n}(\theta,\sigma^2;Z_{0:n})\xrightarrow{\mathbb{P}_0}$$

$$\int\left(\frac{b^2(z;\sigma_0)}{b^2(z;\sigma)}\left[3\left(\frac{\partial_y a_1(z;\theta_0^{(1)})}{\partial_y a_1(z;\hat{\theta}_{n,\Delta_n}^{(1)})}\right)^2-3\frac{\partial_y a_1(z;\theta_0^{(1)})}{\partial_y a_1(z;\hat{\theta}_{n,\Delta_n}^{(1)})}+1\right]+\log b^2(z;\sigma)\right)\nu_0(dz)$$

By assumption (A5) $\partial_y a_1(\cdot)$ does not depend on $\theta^{(1)}$, thus $\frac{\partial_y a_1(z;\theta_0^{(1)})}{\partial_y a_1(z;\hat{\theta}_{n,\Delta_n}^{(1)})}=1$. It gives the Lemma. $\square$

Theorem 6.2. The proof follows the standard pattern. Throughout the proof we assume that $\theta^{(2)}$ and $\sigma \in \mathbb{R}$ in order to simplify the notations. We write the Taylor expansion of the contrast function defined in (6.15) and apply an appropriate scaling

$$\int C_{n,\Delta_n}\left(\varphi_0+u(\hat{\varphi}_{n,\Delta_n}-\varphi_0);z\right)du\,E_{n,\Delta_n}=-D_{n,\Delta_n}(\varphi_0),$$

where by φ we now denote $(\theta^{(2)},\sigma)$ and the parameter $\theta^{(1)}$ is fixed to its estimate $\hat{\theta}_{n,\Delta_n}^{(1)}$ throughout the proof, and

$$C_{n,\Delta_n}(\theta):=\begin{bmatrix}\frac{1}{n\Delta_n}\frac{\partial^2}{\partial\theta^{(2)}\partial\theta^{(2)}}\mathcal{L}_{n,\Delta_n}(\hat{\theta}_{n,\Delta_n}^{(1)},\theta^{(2)},\sigma;Z_{0:n}) & \frac{1}{n\sqrt{\Delta_n}}\frac{\partial^2}{\partial\sigma\partial\theta^{(2)}}\mathcal{L}(\hat{\theta}_{n,\Delta_n}^{(1)},\theta^{(2)},\sigma;Z_{0:n})\\ \frac{1}{n\sqrt{\Delta_n}}\frac{\partial^2}{\partial\theta^{(2)}\partial\sigma}\mathcal{L}_{n,\Delta_n}(\hat{\theta}_{n,\Delta_n}^{(1)},\theta^{(2)},\sigma;Z_{0:n}) & \frac{1}{n}\frac{\partial^2}{\partial\sigma\partial\sigma}\mathcal{L}_{n,\Delta_n}(\hat{\theta}_{n,\Delta_n}^{(1)},\theta^{(2)},\sigma;Z_{0:n})\end{bmatrix},$$

$$E_{n,\Delta_n}:=\begin{bmatrix}\sqrt{n\Delta_n}(\hat{\theta}_n^{(2)}-\theta_0^{(2)})\\ \sqrt{n}(\hat{\sigma}_n-\sigma_0)\end{bmatrix},\quad D_{n,\Delta_n}=\begin{bmatrix}\frac{1}{\sqrt{n\Delta_n}}\frac{\partial}{\partial\theta^{(2)}}\mathcal{L}_{n,\Delta_n}(\hat{\theta}_{n,\Delta_n}^{(1)},\theta^{(2)},\sigma;Z_{0:n})\\ \frac{1}{\sqrt{n}}\frac{\partial}{\partial\sigma}\mathcal{L}_{n,\Delta_n}(\hat{\theta}_{n,\Delta_n}^{(1)},\theta^{(2)},\sigma;Z_{0:n})\end{bmatrix}.$$

First, we compute the higher-order terms of the partial derivatives of first and second order with respect to $\theta^{(2)}$ and σ:

$$\frac{\partial}{\partial\theta^{(2)}}\mathcal{L}_{n,\Delta_n}(\cdot) = \sum_{i=1}^{n-1}\left[-6\frac{\Delta_n(\partial_{\theta^{(2)}}a_2)(X_{i+1}-\bar{A}_1(Z_i;\hat{\theta}^{(1)}_{n,\Delta_n},\theta^{(2)},\sigma))}{\Delta_n^2 b^2(Z_i;\sigma)(\partial_{\hat{\theta}^{(1)}_{n,\Delta_n}}a_1)}+\right.$$
$$\left.2\frac{\Delta_n(\partial_{\theta^{(2)}}a_2)(Y_{i+1}-\bar{A}_2(Z_i;\hat{\theta}^{(1)}_{n,\Delta_n},\theta^{(2)},\sigma))}{\Delta_n b^2(Z_i;\sigma)}\right] =: D^1_{n,\Delta_n}$$

$$\frac{\partial}{\partial\sigma}\mathcal{L}_{n,\Delta_n}(\cdot) = -\sum_{i=1}^{n-1}\frac{\partial_\sigma b}{b^3(Z_i;\sigma)}\left[6\frac{(X_{i+1}-\bar{A}_1(Z_i;\hat{\theta}^{(1)}_{n,\Delta_n},\theta^{(2)},\sigma))^2}{\Delta_n^3(\partial_{\hat{\theta}^{(1)}_{n,\Delta_n}}a_1)^2}-\right.$$
$$6\frac{(X_{i+1}-\bar{A}_1(Z_i;\hat{\theta}^{(1)}_{n,\Delta_n},\theta^{(2)},\sigma))(Y_{i+1}-\bar{A}_2(Z_i;\hat{\theta}^{(1)}_{n,\Delta_n},\theta^{(2)},\sigma))}{\Delta_n^2(\partial_{\hat{\theta}^{(1)}_{n,\Delta_n}}a_1)}+$$
$$\left.2\frac{(Y_{i+1}-\bar{A}_2(Z_i;\hat{\theta}^{(1)}_{n,\Delta_n},\theta^{(2)},\sigma))^2}{\Delta_n}\right] + \frac{\partial_\sigma b}{b(Z_i;\sigma)} =: D^2_{n,\Delta_n}$$

$$\frac{\partial^2}{\partial\theta^{(2)}\partial\theta^{(2)}}\mathcal{L}_{n,\Delta_n}(\cdot) = \sum_{i=1}^{n-1}\left[-6\frac{\Delta_n(\partial^2_{\theta^{(2)}\theta^{(2)}}a_2)(X_{i+1}-\bar{A}_1(Z_i;\hat{\theta}^{(1)}_{n,\Delta_n},\theta^{(2)},\sigma))}{\Delta_n^2 b^2(Z_i;\sigma)(\partial_{\theta^{(1)}}a_1)}+\right.$$
$$\left.2\frac{\Delta_n(\partial^2_{\theta^{(2)}\theta^{(2)}}a_2)(Y_{i+1}-\bar{A}_2(Z_i;\hat{\theta}^{(1)}_{n,\Delta_n},\theta^{(2)},\sigma))}{\Delta_n b^2(Z_i;\sigma)} + \frac{\Delta_n^2(\partial_{\theta^{(2)}}a_2)^2}{\Delta_n b^2(Z_i;\sigma)}\right] =: C^{11}_{n,\Delta_n}$$

$$\frac{\partial^2}{\partial\theta^{(2)}\partial\sigma}\mathcal{L}_{n,\Delta_n}(\cdot) = \sum_{i=1}^{n-1}\frac{\partial_\sigma b}{b^2(Z_i;\sigma)}\left[12\frac{\Delta_n(\partial_{\theta^{(2)}}a_2)(X_{i+1}-\bar{A}_1(Z_i;\hat{\theta}^{(1)}_{n,\Delta_n},\theta^{(2)},\sigma))}{\Delta_n^2 b(Z_i;\sigma)(\partial_{\theta^{(1)}}a_1)}+\right.$$
$$\left.4\frac{\Delta_n(\partial_{\theta^{(2)}}a_2)(Y_{i+1}-\bar{A}_2(Z_i;\hat{\theta}^{(1)}_{n,\Delta_n},\theta^{(2)},\sigma))}{\Delta_n b(Z_i;\sigma)}\right] =: C^{12}_{n,\Delta_n} = C^{21}_{n,\Delta_n}$$

$$\frac{\partial^2}{\partial\sigma^2}\mathcal{L}_{n,\Delta_n}(\cdot) = -\sum_{i=1}^{n-1}\frac{6(\partial_\sigma b)^2 - 2b(Z_i;\sigma)(\partial^2_{\sigma\sigma}b)}{b^4(Z_i;\sigma)}\left[6\frac{(X_{i+1}-\bar{A}_1(Z_i;\hat{\theta}^{(1)}_{n,\Delta_n},\theta^{(2)},\sigma))^2}{\Delta_n^3(\partial_{\theta^{(1)}}a_1)^2}-\right.$$
$$6\frac{(X_{i+1}-\bar{A}_1(Z_i;\hat{\theta}^{(1)}_{n,\Delta_n},\theta^{(2)},\sigma))(Y_{i+1}-\bar{A}_2(Z_i;\hat{\theta}^{(1)}_{n,\Delta_n},\theta^{(2)},\sigma))}{\Delta_n^2(\partial_{\theta^{(1)}}a_1)} + 2\frac{(Y_{i+1}-\bar{A}_2(Z_i;\hat{\theta}^{(1)}_{n,\Delta_n},\theta^{(2)},\sigma))^2}{\Delta_n}\Bigg] +$$
$$2\frac{b(Z_i;\sigma)(\partial^2_{\sigma\sigma}b)-(\partial_\sigma b)^2}{b^2(Z_i;\sigma)} =: C^{22}_{n,\Delta_n}$$

We start with proving the convergence for the terms C_{n,Δ_n}. Then we can obtain a convergence in probability after few technical steps. We start with C_{n,Δ_n}^{11}:

$$\frac{1}{n\Delta_n}C_{n,\Delta_n}^{11} = \frac{1}{n\Delta_n}\sum_{i=1}^{n-1}\left[-6\frac{\Delta_n(\partial_{\theta^{(2)}\theta^{(2)}}^2 a_2)(X_{i+1}-\bar{A}_1(Z_i;\hat{\theta}_{n,\Delta_n}^{(1)},\theta^{(2)},\sigma))}{\Delta_n^2 b^2(Z_i;\sigma)(\partial_{\theta^{(1)}}a_1)}+\right.$$

$$\left. 2\frac{\Delta_n(\partial_{\theta^{(2)}\theta_0^{(2)}}^2 a_2)(Y_{i+1}-\bar{A}_2(Z_i;\hat{\theta}_{n,\Delta_n}^{(1)},\theta^{(2)},\sigma))}{\Delta_n b^2(Z_i;\sigma)}+\frac{\Delta_n^2(\partial_{\theta^{(2)}}a_2)^2}{\Delta_n b^2(Z_i;\sigma)}\right] =$$

$$\frac{1}{n\Delta_n}\sum_{i=1}^{n-1}\left[-6\frac{\Delta_n(\partial_{\theta^{(2)}\theta^{(2)}}^2 a_2)(X_{i+1}-\bar{A}_1(Z_i;\theta_0^{(1)},\theta^{(2)},\sigma))}{\Delta_n^2 b^2(Z_i;\sigma)(\partial_{\theta^{(1)}}a_1)}-6\frac{\Delta_n^2(\partial_{\theta^{(2)}\theta^{(2)}}^2 a_2)(a_1(Z_i;\theta_0^{(1)})-a_1(Z_i;\hat{\theta}_{n,\Delta_n}^{(1)}))}{\Delta_n^2 b^2(Z_i;\sigma)(\partial_{\theta^{(1)}}a_1)}\right.$$

$$\left. 2\frac{\Delta_n(\partial_{\theta^{(2)}\theta^{(2)}}^2 a_2)(Y_{i+1}-\bar{A}_2(Z_i;\hat{\theta}_{n,\Delta_n}^{(1)},\theta^{(2)},\sigma))}{\Delta_n b^2(Z_i;\sigma)}+\frac{\Delta_n^2(\partial_{\theta^{(2)}}a_2)^2}{\Delta_n b^2(Z_i;\sigma)}\right]$$

Note that thanks to Lemma 6.6 we know that

$$\frac{1}{n\Delta_n}\sum_{i=1}^{n-1}\left[-6\frac{\Delta_n(\partial_{\theta^{(2)}\theta^{(2)}}^2 a_2)(X_{i+1}-\bar{A}_1(Z_i;\theta_0^{(1)},\theta^{(2)},\sigma))}{\Delta_n^2 b^2(Z_i;\sigma)(\partial_{\theta^{(1)}}a_1)}+\right.$$

$$2\frac{\Delta_n(\partial_{\theta^{(2)}\theta^{(2)}}^2 a_2)(Y_{i+1}-\bar{A}_2(Z_i;\hat{\theta}_{n,\Delta_n}^{(1)},\theta^{(2)},\sigma))}{\Delta_n b^2(Z_i;\sigma)}+$$

$$\left.\frac{\Delta_n^2(\partial_{\theta^{(2)}}a_2)^2}{\Delta_n b^2(Z_i;\sigma)}\right]\xrightarrow{\mathbb{P}_0}\int\frac{(\partial_{\theta^{(2)}}a_2)^2}{b^2(z;\sigma)}\nu_0(dz)$$

What about the remaining term, thanks to the assumption (A5) we have:

$$-\frac{6}{n\Delta_n}\sum_{i=1}^{n-1}\frac{(\partial_{\theta^{(2)}\theta^{(2)}}^2 a_2)(a_1(Z_i;\theta_0^{(1)})-a_1(Z_i;\hat{\theta}_{n,\Delta_n}^{(1)}))}{b^2(Z_i;\sigma)(\partial_{\theta^{(1)}}a_1)} = -\frac{6}{\sqrt{n\Delta_n}}\frac{1}{n}\sum_{i=1}^{n-1}\frac{(\partial_{\theta^{(2)}\theta^{(2)}}^2 a_2)a_1(Z_i;\sqrt{\frac{n}{\Delta_n}}\left(\theta_0^{(1)}-\hat{\theta}_{n,\Delta_n}^{(1)}\right))}{b^2(Z_i;\sigma)(\partial_{\theta^{(1)}}a_1)}$$

We know that $\left(\theta_0^{(1)}-\hat{\theta}_{n,\Delta_n}^{(1)}\right)\sqrt{\frac{n}{\Delta_n}}$ is normally distributed by Theorem 6.1, and $\frac{1}{n}\sum_{i=1}^{n-1}\frac{(\partial_{\theta^{(2)}\theta^{(2)}}^2 a_2)}{b^2(Z_i;\sigma)(\partial_{\theta^{(1)}}a_1)}$ converges to its invariant density by Lemma 6.4. Then by Slutsky's and the continuous mapping theorem the product also converges in distribution to a normal variable, which is, divided by $\sqrt{n\Delta_n}$ converges to zero since $n\Delta_n\to\infty$ by design. However, as $n\Delta_n\to\infty$, this term converges to 0 in probability. As a result,

$$\frac{1}{n\Delta_n}C_{n,\Delta_n}^{11}\xrightarrow{\mathbb{P}_0}\int\frac{(\partial_{\theta^{(2)}}a_2)^2}{b^2(z;\sigma)}\nu_0(dz)$$

With the same arguments we prove that $\frac{1}{n\sqrt{\Delta_n}}C_{n,\Delta_n}^{12}=\frac{1}{n\sqrt{\Delta_n}}C_{n,\Delta_n}^{21}\xrightarrow{\mathbb{P}_0}0$ and that

$$\frac{1}{n}C_{n,\Delta_n}^{22}\xrightarrow{\mathbb{P}_0}-4\int\frac{(\partial_\sigma b)^2}{b^2(z;\sigma_0)}\nu_0(dz)$$

Then we consider the remaining term, recalling the assumption (A5): We start with the term

$$
\frac{1}{\sqrt{n\Delta_n}}D^1_{n,\Delta_n} = \frac{1}{\sqrt{n\Delta_n}}\sum_{i=1}^{n-1}\left[-6\frac{\Delta_n(\partial_{\theta^{(2)}}a_2)(X_{i+1}-\bar{A}_1(Z_i;\hat{\theta}^{(1)}_{n,\Delta_n},\theta^{(2)},\sigma))}{\Delta_n^2 b^2(Z_i;\sigma)(\partial_{\theta^{(1)}}a_1)}+\right.
$$

$$
\left. 2\frac{\Delta_n(\partial_{\theta^{(2)}}a_2)(Y_{i+1}-\bar{A}_2(Z_i;\hat{\theta}^{(1)}_{n,\Delta_n},\theta^{(2)},\sigma))}{\Delta_n b^2(Z_i;\sigma)}\right] = \frac{1}{\sqrt{n\Delta_n}}\sum_{i=1}^{n-1}\left[-6\frac{(\partial_{\theta^{(2)}}a_2)(X_{i+1}-\bar{A}_1(Z_i;\theta^{(1)}_0,\theta^{(2)},\sigma))}{\Delta_n b^2(Z_i;\sigma)(\partial_{\theta^{(1)}}a_1)}-\right.
$$

$$
\left. 6\frac{(\partial_{\theta^{(2)}}a_2)a_1(Z_i;\hat{\theta}^{(1)}_{n,\Delta_n}-\theta^{(1)}_0)}{b^2(Z_i;\sigma)(\partial_{\theta^{(1)}}a_1)}+2\frac{(\partial_{\theta^{(2)}}a_2)(Y_{i+1}-\bar{A}_2(Z_i;\hat{\theta}^{(1)}_{n,\Delta_n},\theta^{(2)},\sigma))}{b^2(Z_i;\sigma)}\right]
$$

For the first and the third term we simply apply Lemma 6.7 and obtain convergence in distribution to $\mathcal{N}\left(0,\nu_0\left(\frac{(\partial_{\theta^{(2)}}a_2)^2}{b^2(z;\sigma_0)}\right)\right)$. For the second term we apply the result of Theorem 6.1, as well as the continuous mapping and Slutsky's theorem we may state that:

$$
-6\sum_{i=1}^{n-1}\frac{(\partial_{\theta^{(2)}}a_2)\,a_1(Z_i;\sqrt{\frac{n}{\Delta_n}}(\hat{\theta}^{(1)}_{n,\Delta_n}-\theta^{(1)}_0))}{b^2(Z_i;\sigma)(\partial_{\theta^{(1)}}a_1)}\xrightarrow{\mathcal{D}}-6\int\frac{(\partial_{\theta^{(2)}}a_2)}{b^2(z;\sigma)(\partial_{\theta^{(1)}}a_1)}a_1(z;\tilde{\eta})\nu_0(dz),
$$

where $\tilde{\eta}$ is distributed as stated in Theorem 6.1. Then as $n\to 0$,

$$
-\frac{6}{n}\sum_{i=1}^{n-1}\frac{(\partial_{\theta^{(2)}}a_2)\,a_1(Z_i;\sqrt{\frac{n}{\Delta_n}}(\hat{\theta}^{(1)}_{n,\Delta_n}-\theta^{(1)}_0))}{b^2(Z_i;\sigma)(\partial_{\hat{\theta}^{(1)}_{n,\Delta_n}}a_1)}\xrightarrow{\mathbb{P}_0}0
$$

By analogy, we prove the convergence for the term D^2_{n,Δ_n}, obtaining:

$$
\frac{1}{\sqrt{n}}D^2_{n,\Delta_n}\xrightarrow{\mathcal{D}}\mathcal{N}\left(0,32\nu_0\left(\frac{(\partial_\sigma b)^2}{b^2(z;\sigma_0)}\right)\right)
$$

That gives the result. □

6.7.4   *Consistency and asymptotic normality of the least squares contrast*

Theorem 6.3. The proof will follow the one of the classical contrast. First, we define the following quantities:

$$
\mathcal{L}^{(1),LSE}_{n,\Delta_n}(\theta^{(1)},\theta^{(2)},\sigma;Z_{0:n}) = \frac{1}{n}\sum_{i=0}^{n-1}\frac{(X_{i+1}-\bar{A}_1(Z_i;\theta^{(1)},\theta^{(2)},\sigma))^2}{\Delta_n^3}
$$

$$
\mathcal{L}^{(2),LSE}_{n,\Delta_n}(\theta^{(1)},\theta^{(2)},\sigma;Z_{0:n}) = \frac{1}{n}\sum_{i=0}^{n-1}\frac{(Y_{i+1}-\bar{A}_2(Z_i;\theta^{(1)},\theta^{(2)},\sigma))^2}{\Delta_n}
$$

Consistency of $\hat{\theta}^{(1)}$. First, consider:

$$
\Delta_n\left[\mathcal{L}^{LSE}_{n,\Delta_n}(\theta^{(1)},\theta^{(2)};Z_{0:n})-\mathcal{L}^{LSE}_{n,\Delta_n}(\theta^{(1)}_0,\theta^{(2)};Z_{0:n})\right] =
$$

$$
\frac{\Delta_n}{n\Delta_n^3}\sum_{i=0}^{n-1}\left[(X_{i+1}-\bar{A}_1(Z_i;\theta^{(1)}_0,\theta^{(2)},\sigma)+\bar{A}_1(Z_i;\theta^{(1)}_0,\theta^{(2)},\sigma)-\right.
$$

$$
\bar{A}_1(Z_i;\theta^{(1)},\theta^{(2)},\sigma))^2-(X_{i+1}-\bar{A}_1(Z_i;\theta^{(1)}_0,\theta^{(2)},\sigma))^2\Big] =
$$

$$
\frac{\Delta_n^2}{n\Delta_n^3}\sum_{i=0}^{n-1}\left[2(X_{i+1}-\bar{A}_1(Z_i;\theta^{(1)}_0,\theta^{(2)},\sigma))(a_1(Z_i;\theta^{(1)}_0)-a_1(Z_i;\theta^{(1)}))+\right.
$$

$$
\Delta_n(a_1(Z_i;\theta^{(1)}_0)-a_1(Z_i;\theta^{(1)}))^2+O(\Delta_n^2)\Big]
$$

Then we have from Lemmas 6.5, 6.6:

$$\frac{2}{n\Delta_n}\sum_{i=0}^{n-1}(X_{i+1}-\bar{A}_1(Z_i;\theta_0^{(1)},\theta^{(2)},\sigma))(a_1(Z_i;\theta_0^{(1)})-a_1(Z_i;\theta^{(1)}))\xrightarrow{\mathbb{P}_0}0$$

$$\frac{1}{n}\sum_{i=0}^{n-1}(a_1(Z_i;\theta_0^{(1)})-a_1(Z_i;\theta^{(1)}))^2\xrightarrow{\mathbb{P}_0}\int(a_1(z;\theta_0^{(1)})-a_1(z;\theta^{(1)}))^2\nu_0(dz)$$

We conclude that there exists a subsequence $\hat{\theta}_{n,\Delta_n}^{(1)}=\arg\min_\theta\mathcal{L}_{n,\Delta_n}^{LSE}(\theta;Z_{0:n})$ that tends to θ_∞. Since the minimum is attained at the point θ_0 and from (A4), we conclude that $\theta_\infty=\theta_0$. Hence the estimator is consistent.

Consistency of $\hat{\theta}^{(2)}$. Consider:

$$\frac{1}{\Delta_n}\left[\mathcal{L}_{n,\Delta_n}^{LSE}(\theta^{(1)},\theta^{(2)};Z_{0:n})-\mathcal{L}_{n,\Delta_n}^{LSE}(\theta^{(1)},\theta_0^{(2)};Z_{0:n})\right]=$$

$$\left[\frac{1}{n\Delta_n^2}\sum_{i=0}^{n-1}(Y_{i+1}-\bar{A}_2(Z_i;\theta^{(1)},\theta_0^{(2)},\sigma)+\bar{A}_2(Z_i;\theta^{(1)},\theta_0^{(2)},\sigma)-\bar{A}_2(Z_i;\theta^{(1)},\theta^{(2)},\sigma))^2-\right.$$

$$\left(Y_{i+1}-\bar{A}_2(Z_i;\theta^{(1)},\theta_0^{(2)},\sigma))^2\right]=\frac{\Delta_n}{n\Delta_n^2}\sum_{i=0}^{n-1}\left[2(Y_{i+1}-\bar{A}_2(Z_i;\theta^{(1)},\theta_0^{(2)},\sigma))(a_2(Z_i;\theta_0^{(2)})-a_2(Z_i;\theta^{(2)}))+\right.$$

$$\left.\Delta_n(a_2(Z_i;\theta_0^{(2)})-a_2(Z_i;\theta^{(2)}))^2+O(\Delta_n^2)\right]$$

Thanks to Lemmas 6.4, 6.5:

$$\frac{2\Delta_n}{n\Delta_n^2}\sum_{i=0}^{n-1}(Y_{i+1}-\bar{A}_2(Z_i;\theta^{(1)},\theta_0^{(2)},\sigma))(a_2(Z_i;\theta_0^{(2)})-a_2(Z_i;\theta^{(2)}))\xrightarrow{\mathbb{P}_0}0$$

$$\frac{\Delta_n^2}{n\Delta_n^2}\sum_{i=0}^{n-1}(a_2(Z_i;\theta_0^{(2)})-a_2(Z_i;\theta^{(2)}))^2\xrightarrow{\mathbb{P}_0}\int(a_2(z;\theta_0^{(2)})-a_2(z;\theta^{(2)}))^2\nu_0(dz)$$

The consistency is concluded following the same arguments as in the case of $\theta^{(1)}$.

Asymptotic normality. We apply again a Taylor formula for a function (6.19):

$$\int C_n\left(\theta_0+u(\hat{\theta}_n-\theta_0)\right)du\,E_n=D_n(\theta_0),$$

where we define

$$C_n(\theta):=\begin{bmatrix}\frac{\Delta_n}{n}\frac{\partial^2}{\partial\theta^{(1)}\partial\theta^{(1)}}\mathcal{L}_{n,\Delta_n}^{LSE}(\theta;Z_{0:n}) & \frac{1}{n}\frac{\partial^2}{\partial\theta^{(1)}\partial\theta^{(2)}}\mathcal{L}_{n,\Delta_n}^{LSE}(\theta;Z_{0:n})\\\frac{1}{n}\frac{\partial^2}{\partial\theta^{(1)}\partial\theta^{(2)}}\mathcal{L}_{n,\Delta_n}^{LSE}(\theta;Z_{0:n}) & \frac{1}{n\Delta_n}\frac{\partial^2}{\partial\theta^{(2)}\partial\theta^{(2)}}\mathcal{L}_{n,\Delta_n}^{LSE}(\theta;Z_{0:n})\end{bmatrix},$$

$$E_n:=\begin{bmatrix}\sqrt{\frac{n}{\Delta_n}}(\hat{\theta}_{n,\Delta_n}^{(1)}-\theta_0^{(1)})\\\sqrt{n\Delta_n}(\hat{\theta}_n^{(2)}-\theta_0^{(2)})\end{bmatrix},\quad D_n(\theta)=\begin{bmatrix}\frac{\sqrt{\Delta_n}}{n}\frac{\partial}{\partial\theta^{(1)}}\mathcal{L}_{n,\Delta_n}^{LSE}(\theta;Z_{0:n})\\\frac{1}{n\sqrt{\Delta_n}}\frac{\partial}{\partial\theta^{(2)}}\mathcal{L}_{n,\Delta_n}^{LSE}(\theta;Z_{0:n})\end{bmatrix}.$$

Using Lemma 6.7 we get:

$$D_n(\theta_0)\xrightarrow{\mathcal{D}}-2\mathcal{N}\left(0,I_2\cdot\begin{bmatrix}\frac{1}{3}\int b^2(z;\sigma_0)(\partial_y a_1(z;\theta_0^{(1)}))^2(\partial_{\theta^{(1)}}a_1(z;\theta_0^{(1)}))^2\nu_0(dz)\\\int b^2(z;\sigma_0)(\partial_{\theta^{(2)}}a_2(z;\theta_0^{(2)}))^2\nu_0(dz)\end{bmatrix}\right),$$

where I_2 is 2×2 identity matrix. And by Lemmas 6.5, 6.4 we have the result for $C_n(\theta)$:

$$C_n(\theta_0)\xrightarrow{\mathbb{P}_0}-2\begin{bmatrix}\int(\partial_{\theta^{(1)}}a_1(z;\theta_0^{(1)}))^2\nu_0(dz) & 0\\0 & \int(\partial_{\theta^{(2)}}a_2(z;\theta_0^{(2)}))^2\nu_0(dz)\end{bmatrix}.$$

That, in the combination with the consistency result, gives the theorem. $\square$

<div style="text-align: right; font-size: 3em;">7</div>

NON-ASYMPTOTIC STATISTICAL TEST OF COVARIANCE MATRIX RANK

This chapter is based on the ongoing work in collaboration with Adeline Samson (Université Grenoble Alpes) and Patricia Reynaud-Bouret (Université de Nice).

Abstract. The aim of this work is to develop a testing procedure which determines the rank of the noise in a multidimensional stochastic process from discrete observations of this process on a fixed time interval $[0, T]$ sampled with a time step Δ. More precisely, we are focused on evaluating the probability that some diffusion coefficients of the process are negligible, where the "negligibility" is determined by a numerical value, set by the experimenter. As first step, we consider the 1- and 2-dimensional case with a known constant drift. In these cases the density of the test statistics can be written explicitly. We construct the test and give conditions, under which the Type I and Type II errors can be controlled. Further, we consider a general $d-$dimensional case and study the probabilistic properties of the test statistics.

Résume. Le but de ce travail est de développer une procédure de test qui détermine le rang du bruit dans un processus stochastique multidimensionnel à partir d'observations discrètes de ce processus sur un intervalle de temps fixe $[0, T]$ échantillonné avec un pas de temps Δ. Plus précisément, nous nous concentrons sur l'évaluation de la probabilité que certains coefficients de diffusion du processus soient négligeables, où la «négligibilité» est déterminée par une valeur numérique, fixée par l'expérimentateur. Dans un premier temps, nous considérons un cas de dimension 1 et 2 avec une dérive constante connue. Dans ce cas, la loi des statistiques de test peut être écrite explicitement. Nous construisons le test et donnons les conditions sous lesquelles les erreurs de type I et de type II peuvent être contrôlées. De plus, nous considérons un cas général de dimension d et étudions les propriétés probabilistes des statistiques de test.

Keywords. Statistical tests, concentration inequalities, non-asymptotic statistics, computational statistics

7.1 INTRODUCTION

Stochastic diffusions became a classical tool for describing a neuronal activity, either of a one single neuron (Ditlevsen and Samson, 2012, Höpfner et al., 2016a, Leon and Samson, 2018), or a large network of neurons (Ditlevsen and Löcherbach, 2017, Ableidinger et al., 2017). However, the techniques which

would allow us to establish a rigorous link between a specific model and available neurophysiological data is often missing. The open question is the source of stochasticity in spiking activity. One point of view is that both the membrane and the ion channels of the neuron cell are affected by noise. Another position is that only the ion channels have a stochastic behaviour and that their concentration in the cell explicitly defines the membrane potential. The question is then how to test both hypotheses with extracellular recordings of the membrane potential, i.e. discrete observations of the stochastic process.

Consider a filtered probability space $(\Omega, \mathcal{F}, (\mathcal{F}_t)_{t \geq 0}, \mathbb{P})$. In this chapter we study the covariance matrix of a $d-$dimensional process X, which is a solution of the following Stochastic Differential Equation (SDE):

$$dX_t = b_t dt + \sigma_t dW_t, \tag{7.1}$$

$b_t : \mathbb{R} \to \mathbb{R}^d, \sigma_t : \mathbb{R} \to \mathbb{R}^{d \times q}$, and W is a q-dimensional Brownian motion. We assume that the discrete equidistant observations of X on a fixed time interval $[0, T]$ are available, we denote them by $\{X_{i\Delta}\}_{i \in \mathbb{N}}$. The central object of our study is $rank(\sigma\sigma^T)$. One of the main difficulties is that we assume the time step Δ being fixed, which places us in a non-asymptotic setting.

Two main works dealing with the problem of the diffusion matrix rank estimation are the papers Jacod et al. (2008), Jacod and Podolskij (2013). Jacod et al. (2008) has proposed to study the determinant of r-dimensional minors of the given matrix by comparing them to a sequence of thresholds. The rank is then estimated basing on the dimension r of the first non-vanishing minors. Jacod and Podolskij (2013) has improved the procedure by computing the statistics with a varying time step. They propose a statistical test which permits to test a hypothesis $rank(\sigma\sigma^T) = r_0$ against an alternative $rank(\sigma\sigma^T) \neq r_0$.

Asymptotically, both approaches reveal good properties, but they are difficult to apply in a non-asymptotic setting. The main problem is that when the discretization step Δ is fixed, one cannot always compute the true rank of the matrix $\sigma\sigma^T$. In other words, one can never be sure that some of the diffusion coefficients are truly zero. However, from a practical point of view, we do not necessarily seek for the perfect answer. What we are rather interested in is whether the influence of noise is negligible at a given precision (determined by the step size of observations Δ). By "negligibility" we mean a hard-set threshold (often linked to the value of Δ).

We proceed with the study as follows. First, we start by introducing the core statistics analogous to Jacod et al. (2008). Our aim is to recycle the idea of "thresholds" which aim to quantify the degeneracy of a given matrix. However, instead of focusing on an integer value of the rank, our aim is to quantify the probability that some of the diffusion coefficients are negligible. The exact definition of "neglibility" is, of course, dictated by a specific application. Thus, we restrict ourselves to some threshold δ which can be deliberately calibrated.

Then, we consider a Brownian motion with a known drift and construct a non-asymptotic test which determines if its diffusion coefficient σ^2 is negligible (i.e., $\sigma^2 \leq \delta$) or not. In one dimensional case, the distribution of the statistics is chi-squared, so that the Type I and Type II errors can be evaluated with a high precision. In a 2-dimensional case, even with a constant variance and known drift, the task is more difficult. However, a statistical test based on the exact distribution of the

statistics, can still be proposed. In 2-dimensional case we obtain a non-asymptotic control of Type I and Type II errors.

Finally, when the dimension of the process is $d > 2$, and the drift and variance coefficients are given by time-dependent functions, the problem is even more complicated. The distribution of the random determinants, which are the key objects in developing the test, are rather well studied when the dimension of the matrix is very large. Some asymptotic results are available in this case (see for example Nguyen and Vu (2014)). However, they cannot be applied in a non-asymptotic setting. Thus, our first goal is to study the distribution of the test statistics. For that, we are using recent results from random matrix theory and quadratic forms of random variables (Nyquist et al., 1954, Girko, 1990, Mathai and Provost, 1992). We evaluate the tail distribution and give the lower and upper concentration bounds. Then, we discuss how the test can be constructed and what can be potentially inferred from the statistics into consideration.

This Chapter is organized as follows. First, we set the notations and present the main statistics in Section 7.2. The respective subsections (7.3.1 and 7.3.2) are devoted to the study of simplified 1- and 2-dimensional models in the case when the drift is known. In each subsection we present the hypothesis of interest and then proceed to evaluating the risks of the test. We obtain the control of the Type I and II errors in both cases. The last Section 7.4 is devoted to the general case, where we do not put additional assumptions on the solution of (7.1) (such as constant drift, variance and a low dimension). The primal goal is to study the distribution of the statistics and its probabilistic properties in a non-asymptotic case. We conclude with discussion and perspectives.

7.2   NOTATIONS AND THE LAYOUT OF THE CHAPTER

Let us define the statistics which will be the main object of a study throughout the paper. We denote by $mat(a^1, a^2, \ldots, a^d)$ a matrix which is defined by its vector-columns $a^1, a^2, \ldots, a^d$. Consider a $d \times d$-dimensional matrix Ξ_i, given by

$$\Xi_i = mat(\xi_i^1, \xi_i^2, \ldots, \xi_i^d), \tag{7.2}$$

where ξ_i^j are given by the increments of the process X, defined in (7.1) as follows:

$$\xi_i^j := \frac{X_{(di+j)\Delta} - X_{(di+j-1)\Delta}}{\sqrt{\Delta}} \quad j = 1, \ldots, d, \quad i = 1, \ldots, n. \tag{7.3}$$

In other words, to construct the first matrix Ξ_1 we take first d increments of the process and write them column-wise (thus, obtaining a aquare $d \times d$ matrix), for the next matrix we start with the $d + 1$-th increment and so on, until we reach the end of the observed interval (so that $n \triangleq \left[\frac{T}{d\Delta}\right]$). The main assumption of the chapter is the following:

(A) ξ_i^j are independent in i and j.

This assumption is satisfied, when the drift and the variance term depend on time but do not depend on the process X itself. Of course, it is rather restrictive, as it is not satisfied by autonomous diffusion

processes. In this chapter we restrict ourselves to this setting, as it allows us to work in a direct continuation of Jacod et al. (2008), Jacod and Podolskij (2013). We believe that most of the results can be carried over to a more general setting at the expense of more complicated computations. Also, some of the presented results (notably in a high-dimensional setting) do not require an independency of rows, only of columns. Nevertheless, we keep the assumption (A) for the whole Chapter to avoid confusions.

Note that the vectors ξ_i^j are distributed according to a normal law, i.e. $\xi_i^j \sim \mathcal{N}\left(\mu_i^j, \Sigma_i^j\right)$, where μ_i^j and Σ_i^j can be approximated, for example, by the Euler-Maruyama scheme as follows:

$$\mu_i^j \approx \sqrt{\Delta} b_{(di+j-1)\Delta} \tag{7.4}$$

$$\Sigma_i^j \approx \sigma_{(di+j-1)\Delta} \sigma_{(di+j-1)\Delta}^T \tag{7.5}$$

We then define the main quantity of interest as follows:

$$S = \frac{1}{n} \sum_{i=1}^{n} \det(\Xi_i^2), \tag{7.6}$$

where Ξ_i is given by (7.2). The distribution of the statistics S given in (7.6) is well studied in Jacod et al. (2008), Jacod and Podolskij (2013) in the asymptotic case, as $\Delta \to 0$. In this setting the influence of the drift is negligible, since it is of order $O(\Delta)$. In the non-asymptotic case, the drift must be taken into account. We note however that a lot of non-parametric drift estimators are available in the literature (see, for example, book Kutoyants (2013)). Plugging the estimator would allow to work with centered statistics, which are easier to analyze.

7.3   STATISTICAL TESTS OF THE MATRIX RANK

In this Section we consider a special 1- and 2-dimensional process with constant diffusion coefficients and a known drift. The specificity of this Section is that the distribution of the main statistics (7.6) can be written explicitly, if it is centered. Both in 1- and 2-dimensional case we first center the statistics, then we write their distribution in explicit form, and then we evaluate the power of the test.

7.3.1   *1-dimensional case*

We start with a simple 1-dimensional process, which is called the Brownian motion with drift:

$$dX_t = bdt + \sigma dW_t, \quad X_0 = x_0, \quad t > 0,$$

where $b \in \mathbb{R}$, $\sigma \in \mathbb{R}$. Recall that the process $(X)_{t \geq 0}$ is discretely observed on a time interval $[0, T]$ at equidistant time steps Δ. Our aim is to construct the following test:

$$H_0 : \sigma^2 < \delta$$

$$H_1 : \sigma^2 \geq \delta,$$

where δ is a pre-chosen parameter, possibly depending on a chosen step size Δ. Further, we will use notations $\mathbb{P}_0$ and $\mathbb{P}_1$ to distinguish the cases when we evaluate the probability under the null or the alternative hypothesis.

Note that in a 1-dimensional case the degeneracy of the diffusion matrix is equivalent to the fact that the solution of (7.1) is a deterministic process. Thus, the aim of the procedure is to help to decide whether the diffusion coefficient is small enough to consider X as a deterministic process. The main statistics (7.6) of the test is given by $\frac{1}{n} \sum_{i=1}^{n} \xi_i^2$, where ξ_i are defined by (7.3). Note that $\xi_i \sim \sigma \left(\eta_i + \Delta \frac{b}{\sigma} \right)$, where η_i are i.i.d. distributed standard normal variables. In other words, $\|\xi\|^2 \sim \sigma^2 \chi_n^2(\lambda)$, where $\chi_n^2(\lambda)$ is a chi-squared distributed random variable with a non-centrality parameter λ, defined as follows:

$$\lambda(\sigma) = \frac{\Delta^2 b^2}{n\sigma^2}.$$

Note that the non-centrality parameter is of order $O(\Delta^2)$. It means that as $\Delta \to 0$, the law of $\|\xi\|^2$ transforms in a standard chi-squared law. Also, it means that even in the case when the drift b is not known, the approximation of the statistics distribution should not be sensitive to the plugged-in estimator of b. Now let us define a α-quantile under H_0. Note that

$$\mathbb{P}\left(S \leq \varepsilon\right) = 1 - Q_{n/2}\left(\sqrt{\lambda(\delta)}, \sqrt{\frac{\varepsilon}{\delta}}\right),$$

where $Q_m(a,b)$ is a Markum Q-function, defined as:

$$Q_m(a,b) = \int_b^\infty x \left(\frac{x}{a}\right)^{m-1} \exp\left(-\frac{x^2 + a^2}{2}\right) I_{m-1}(ax)dx,$$

where I_{m-1} is a modified Bessel function of the first kind. Alternatively, $Q_m(a,b)$ may be also defined as

$$Q_m(a,b) = \exp\left(-\frac{a^2 + b^2}{2}\right) \sum_{k=1-m}^{\infty} \left(\frac{a}{b}\right)^k I_k(ab).$$

Then, H_0 hypothesis is rejected if $S \geq z_\alpha$, where z_α is such that $Q_{n/2}\left(\sqrt{\lambda(\delta)}, \sqrt{\frac{z_\alpha}{\delta}}\right) = \alpha$. To the best of our knowledge, the closed-form expression for the quantile of the non-central chi-squared distribution does not exist. In practice, it can be approximated numerically with the help of built-in methods in most statistical programming languages (such as **R**). However, by centering the statistics we can obtain a closed-form expression for the rejection zone of the test.

Let us assume that the drift b is known or, at least, it can be estimated from discrete observations (for example, by taking an empirical mean). As we have mentioned previously, since the drift is only included in the non-centrality parameter with an order $O(\Delta^2)$, we expect that the law of the statistics is not sensitive to the non-centrality parameter. We can then modify the entries ξ_i of the main statistics as follows:

$$\dot{\xi}_i = \xi_i - b.$$

Then, we build the statistics S defined in (7.6) using $\dot{\xi}_i$, which we denote by $\dot{S}$. Note that the distribution of $\dot{S}$ is a centered chi-squared, in other words, $\dot{S} \sim \sigma^2 \chi_n^2(0)$. Then, under H_0, the following holds:

$$\mathbb{P}_0\left(\dot{S} \geq \delta q_{1-\alpha}\right) = \alpha, \tag{7.7}$$

where $q_{1-\alpha}$ is a respective quantile of a chi-squared distribution. We then define the α quantile of the test as follows:

$$z_\alpha = \delta q_{1-\alpha}.$$

The above equation gives the control of the Type I error and the rejection interval: H_0 is rejected if $\dot{S}$ is in the interval $[z_\alpha, \infty)$. Next, we want to determine the conditions under which the Type II error can be controlled: in other words, how large should be the difference between the diffusion parameter σ and δ, so that the alternative hypothesis would not be mistaken for H_0 with high probability. The control over Type II error can be obtained as follows:

$$\mathbb{P}_1\left(\dot{S} \leq z_\alpha\right) = \mathbb{P}_1\left(\sigma^2 \chi_n^2(0) \leq z_\alpha\right) = \mathbb{P}_1\left(\chi_n^2(0) \leq \frac{z_\alpha}{\sigma^2}\right).$$

It implies that $\mathbb{P}_1\left(\dot{S} \leq z_\alpha\right) \leq \beta$ when $\frac{z_\alpha}{\sigma^2} \leq q_\beta$. Thus, Type II error is bounded by a fixed risk level $\beta \in (0,1)$ when

$$\sigma^2 \geq \frac{z_\alpha}{q_\beta}. \tag{7.8}$$

Equations (7.7)-(7.8) give the control over the Type I and Type II error of the test.

7.3.2   *2-dimensional case*

Now let us consider a 2-dimensional case. Analogously to the previous section, we are interested in constructing a test which helps to determine the order of smallness of the diffusion coefficients. To begin with, we focus on the case where the drift is known and constant. Consider a 2-dimensional process, defined by the solution of:

$$dX_t = b\,dt + \sigma\,dW_t,$$

where $b = (b_1, b_2)^T$ is a drift vector and σ is a diagonal diffusion matrix with constant coefficients σ_1 and σ_2 on the main diagonal, W is a 2-dimensional Brownian motion. The goal is to construct the test of the following hypothesis:

$$H_0 : \sigma_1^2 \sigma_2^2 = \delta$$
$$H_1 : \sigma_1^2 \sigma_2^2 \geq \delta,$$

where δ is some chosen "sensitivity" threshold. H_0 and H_1 correspond roughly to the case of the covariance matrix being of a full rank or not, as δ can be arbitrarily close to 0.

The vectors ξ_i^1 and ξ_i^2 defined in (7.3) consist of the successive increments of a Gaussian process with a given mean and a constant (unknown) variance, so that the corresponding column-vectors are identically distributed as follows $\forall j \in \{1,2\}, \quad i \in \{1, \ldots, n\}$:

$$\xi_i^j := \frac{X_{(2i+j)\Delta} - X_{(2i+j-1)\Delta}}{\sqrt{\Delta}} \sim \mathcal{N}\left((\sqrt{\Delta}b_1, \sqrt{\Delta}b_2)^T, \begin{pmatrix} \sigma_1^2 & 0 \\ 0 & \sigma_2^2 \end{pmatrix}\right).$$

We then define the centered statistics as follows:

$$\dot{S} = \frac{1}{n}\sum_{i=1}^n \det\left(mat\left(\xi_i^1 - \sqrt{\Delta}b, \xi_i^2 - \sqrt{\Delta}b\right)\right)^2.$$

This choice corresponds to the matrix rank estimator proposed by Jacod et al. (2008), Jacod and Podolskij (2013), observed with a time step Δ on the interval $T = n\Delta$, but centered around 0. Centering the statistics gives an immediate advantage of the cumulative distribution function being explicitly known. In particular, the following proposition holds:

Proposition 7.1. *Denote* $\dot{s}_i := \det\left(mat\left(\xi_i^1 - \sqrt{\Delta}b, \xi_i^2 - \sqrt{\Delta}b\right)\right)^2$. *The following holds for all i:*

$$\mathbb{P}\left(\dot{s}_i \leq x\right) = 1 - \left(\sqrt{\frac{x}{\sigma_1^2\sigma_2^2}} + 1\right)e^{-\sqrt{\frac{x}{\sigma_1^2\sigma_2^2}}}$$

Proof. First, note that by Theorem 4.1.1. in Girko (1990) $\dot{s}_i \sim \sigma_1^2\sigma_2^2\chi_{i,1}^2\chi_{i,2}^2$, where by $\chi_{i,k}^2$ we denote a variable distributed according to a chi-squared distribution with k degrees of freedom, all variables being independent in i. Here we use the advantage that the covariance matrix of each vector-column is the same.

Then, we need to write the distribution of $\chi_{i,1}^2\chi_{i,2}^2$. We use the result from Wells et al. (1962) . Generally, the PDF of a product $\chi_{i,1}^2\chi_{i,2}^2$ is written as follows:

$$f(\omega) = \frac{\omega^{1/2}K_{1/2}(\omega^{1/2})}{\sqrt{2}\Gamma(1)\Gamma(1/2)}, \tag{7.9}$$

where $K_v(x)$ is the modified Bessel function of the second kind. Further, we can use the fact that in our specific case, $K_{1/2}(\omega^{1/2}) = \frac{1}{2}\sqrt{2\pi}e^{-\sqrt{\omega}}\omega^{-1/2}$, and simplify (7.9), obtaining:

$$f(\omega) = \frac{1}{2}\frac{\omega^{1/2}\sqrt{2\pi}e^{-\sqrt{\omega}}\omega^{-1/2}}{\sqrt{2\pi}} = \frac{1}{2}e^{-\sqrt{\omega}}.$$

Finally, note that

$$\mathbb{P}\left(\dot{s}_i \leq x\right) = \mathbb{P}\left(\sigma_1^2\sigma_2^2\chi_{i,1}^2\chi_{i,2}^2 \leq x\right) = \mathbb{P}\left(\chi_{i,1}^2\chi_{i,2}^2 \leq \frac{x}{\sigma_1^2\sigma_2^2}\right) = \frac{1}{2}\int_0^{\frac{x}{\sigma_1^2\sigma_2^2}} e^{-\sqrt{\omega}}d\omega.$$

Computing the integral, we obtain the result. $\qquad\square$

Now, we will compute a confidence interval under which H_0 holds with probability $1 - \alpha$. It will give us an α-quantile. Then, the following holds:

Proposition 7.2. *Under H_0 the following bound holds:*

$$\mathbb{P}_0\left(\dot{S} \geq \delta\left(1 + W\left(-\frac{\alpha^{1/n}}{e}\right)\right)^2\right) \leq \alpha,$$

where W denotes Lambert W function[1].

Proof. Note that under H_0, $\mathbb{E}\left[\dot{S}\right] = 2\sigma_1^2\sigma_2^2 = 2\delta\ \forall i$. Then, using the Proposition 7.1, we obtain:

$$\mathbb{P}_0\left(\dot{S} \geq \varepsilon\right) = 1 - \mathbb{P}_0\left(\frac{1}{n}\sum_{i=1}^n \dot{s}_i \leq \varepsilon\right) \leq 1 - \prod_{i=1}^n \mathbb{P}_0\left(\dot{s}_i \leq \varepsilon\right)$$

$$= 1 - \left(1 - \left(\sqrt{\frac{\varepsilon}{\delta}} + 1\right)e^{-\sqrt{\frac{\varepsilon}{\delta}}}\right)^n \leq \left(\sqrt{\frac{\varepsilon}{\delta}} + 1\right)^n e^{-n\sqrt{\frac{\varepsilon}{\delta}}}$$

---

1 Definition and some of the properties of the Lambert W function are available in Appendix.

Now we have to find ε such that

$$\left(\sqrt{\frac{\varepsilon}{\delta}} + 1\right)^n e^{-n\sqrt{\frac{\varepsilon}{\delta}}} \leq \alpha$$

Denote $c := \frac{\varepsilon}{\delta}$. Then, we need to solve the following equation:

$$\left(\sqrt{c} + 1\right)^n e^{-n\sqrt{c}} \leq \alpha.$$

Note that the function $\left(\sqrt{c} + 1\right)^n e^{-n\sqrt{c}}$ is decreasing. Thus, one needs to set $c \geq c_0$, where c_0 is a root of the following equation:

$$\left(\sqrt{c} + 1\right)^n e^{-n\sqrt{c}} = \alpha. \tag{7.10}$$

Note that (7.10) can be transformed as follows:

$$n \ln\left(\sqrt{c} + 1\right) - n\sqrt{c} = \ln \alpha$$

$$\ln\left(\sqrt{c} + 1\right) = \frac{\ln \alpha}{n} + \sqrt{c}$$

$$\sqrt{c} = \exp\left(\frac{\ln \alpha}{n} + \sqrt{c}\right) - 1$$

The solution of such equation is given by a Lambert W function:

$$\sqrt{c} = -W\left(-e^{\left(\frac{\ln \alpha}{n} - 1\right)}\right) - 1 = -W\left(-\frac{\alpha^{1/n}}{e}\right) - 1$$

Finally, we obtain the following constraint:

$$\frac{\varepsilon}{\delta} \geq \left(W\left(-\frac{\alpha^{1/n}}{e}\right) + 1\right)^2.$$

$\square$

Now, let us denote the quantile

$$z_\alpha := \delta \left(1 + W\left(-\frac{\alpha^{1/n}}{e}\right)\right)^2. \tag{7.11}$$

The dependency of z_α is illustrated on the left panel of Figure 7.1, where the function $\left(1 + W\left(-\frac{\alpha^{1/n}}{e}\right)\right)^2$ is plotted. Proposition 7.2 gives us the following rejection rule of the test:

$$H_0 \text{ is rejected if } \dot{S} \geq z_\alpha,$$

where z_α is defined in (7.11). We are now interested in Type II error. For that, we need to evaluate the probability to not reject H_0 if H_1 holds and see under which conditions it does not overpass the fixed level β.

Proposition 7.3. *For fixed levels of Type I and Type II risks α and β respectively and if*

$$\sigma_1^2 \sigma_2^2 \geq \delta \left(\frac{1 + W\left(-\frac{\alpha^{1/n}}{e}\right)}{1 + W\left(-\frac{(1-\beta)^{1/n}}{e}\right)}\right)^2,$$

the following inequality holds:

$$\mathbb{P}_1\left(\dot{S} \leq z_\alpha\right) \leq \beta,$$
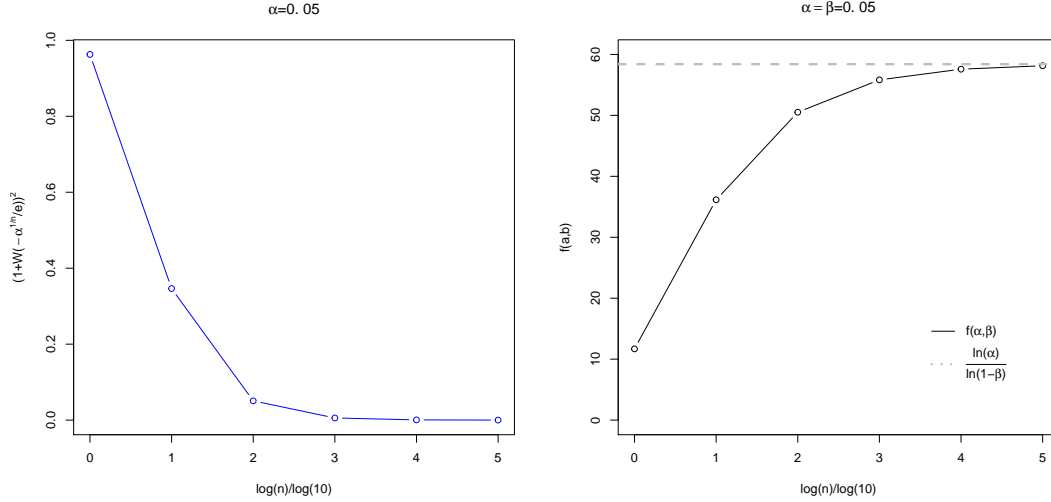
Figure 7.1: Left panel: evolution of the function $\left(1 + W\left(-\frac{\alpha^{1/n}}{e}\right)\right)^2$ as n grows, for $\alpha = 0.05$. Right panel: evolution of the function $f(\alpha, \beta) = \left(\frac{1 + W\left(-\frac{\alpha^{1/n}}{e}\right)}{1 + W\left(-\frac{(1-\beta)^{1/n}}{e}\right)}\right)^2$ as n grows and its limit value, for $\alpha = \beta = 0.05$.

Proof. Using Proposition 7.1, we obtain:

$$\mathbb{P}_1\left(\acute{S} \geq z_\alpha\right) \geq \prod_{i=1}^{n}\left(\acute{s}_i \geq z_\alpha\right) = \left(\sqrt{\frac{z_\alpha}{\sigma_1^2\sigma_2^2}} + 1\right)^n e^{-n\sqrt{\frac{z_\alpha}{\sigma_1^2\sigma_2^2}}}$$

Our goal is to lower-bound the expression on the left by $1 - \beta$, where β denotes the accepted Type II risk. Thus, we need to solve the following inequality:

$$\left(\sqrt{\frac{z_\alpha}{\sigma_1^2\sigma_2^2}} + 1\right)^n e^{-n\sqrt{\frac{z_\alpha}{\sigma_1^2\sigma_2^2}}} \geq 1 - \beta \tag{7.12}$$

Denote $c := \frac{z_\alpha}{\sigma_1^2\sigma_2^2}$. Inequality (7.12) then holds for all $c \leq c_0$, where c_0 is the root of the following equation:

$$\left(\sqrt{c} + 1\right)^n e^{-n\sqrt{c}} = 1 - \beta.$$

The solution of this equation (see more detailed computations in the proof of Proposition 7.2) is given as:

$$c = \left(W\left(-\frac{(1-\beta)^{1/n}}{e}\right) + 1\right)^2.$$

Then, $\mathbb{P}_1\left(\acute{S} \geq z_\alpha\right) \geq 1 - \beta$ or, equivalently, $\mathbb{P}_1\left(\acute{S} \leq z_\alpha\right) \leq \beta$, when the following condition holds:

$$\frac{z_\alpha}{\sigma_1^2\sigma_2^2} \leq \left(W\left(-\frac{(1-\beta)^{1/n}}{e}\right) + 1\right)^2.$$

Recalling the definition of z_α, we obtain:

$$\frac{\delta\left(1 + W\left(-\frac{\alpha^{1/n}}{e}\right)\right)^2}{\sigma_1^2\sigma_2^2} \leq \left(1 + W\left(-\frac{(1-\beta)^{1/n}}{e}\right)\right)^2$$

$$\sigma_1^2\sigma_2^2 \geq \delta\left(\frac{1 + W\left(-\frac{\alpha^{1/n}}{e}\right)}{1 + W\left(-\frac{(1-\beta)^{1/n}}{e}\right)}\right)^2.$$

□

On Figure 7.1 we track the dependency of the limit conditions on the sample size n. Denote

$$f(\alpha, \beta) = \left(\frac{1 + W\left(-\frac{\alpha^{1/n}}{e}\right)}{1 + W\left(-\frac{(1-\beta)^{1/n}}{e}\right)} \right)^2. \tag{7.13}$$

For simplicity, we assume both Type I and Type II error levels to be fixed and equal to 0.05. Note that when $n = 1$, meaning that we have only one observation on the interval $[0, T]$, the Type II risk is controlled when the product $\sigma_1^2 \sigma_2^2$ is equal at least 10δ. As $n \to \infty$, then $\sigma_1^2 \sigma_2^2$ must be at least around 60δ. The obtained numerical result is backed up by Proposition (7.4). Indeed, for $\alpha = \beta = 0.05$, $f(\alpha, \beta) \to \frac{\ln \alpha}{\ln(1-\beta)} \approx 58.4$, which coincides with the limit obtained on Figure 7.1. This result may seem counter-intuitive, as the bound becomes more restrictive as n grows. It can be explain by the fact that the rejection interval shrinks as $n \to 0$, as it is seen on the left panel of Figure 7.1.

Let us now explain the practical meaning of the results obtained in Proposition 7.3. Evaluating the Type II error gives us an idea about how "far" from the null hypothesis should be the value of the product $\sigma_1^2 \sigma_2^2$ in order to be interpreted as corresponding to H_1. Now our goal is to show how this condition evolves as $n \to \infty$. The following proposition holds:

Proposition 7.4. *For $\alpha, \beta \in (0, 1)$, the following holds:*

$$\lim_{n \to \infty} f(\alpha, \beta) = \frac{\ln \alpha}{\ln(1 - \beta)},$$

where $f(\alpha, \beta)$ is defined in (7.13).

Proof. As the first step, we need to find an asymptotic expansion of $W(x)$. In our case both expressions $-\frac{\alpha^{1/n}}{e}$ and $-\frac{(1-\beta)^{1/n}}{e}$ take their values on the interval $(-1/e, 0)$ and converge to $-1/e$ as $n \to \infty$. The interval $x \in (-1/e, 0)$ corresponds to a W_{-1} branch of a Lambert function, and the function $W(x)$ is real-valued and monotone decreasing on this interval. However, the function $W(x)$ is not analytic at $x = 1/e$, since it is the branching point of two branches W_0 and W_{-1}. Thus, the derivative in this point does not exist and $W(x)$ cannot be expressed in the terms of its Taylor expansion. However, several numerical approximations exist. For instance, when $x \geq -1/e$, the following approximation holds for the branch W_{-1} (Corless et al., 1996):

$$W(x) = \sum_{m=0}^{\infty} \theta_l p^l = -1 + p - \frac{1}{3}p^2 + \frac{11}{72}p^3 + \dots, \tag{7.14}$$

where $p = -\sqrt{2(ex + 1)}$ and

$$\theta_l = \frac{l-1}{l+1}\left(\frac{\theta_{l-2}}{2} + \frac{\gamma_{l-2}}{4}\right) - \frac{\gamma_{l-2}}{2} - \frac{\theta_{l-1}}{l+1}, \quad \theta_0 = -1, \theta_1 = 1,$$

$$\gamma_l = \sum_{s=2}^{l-1} \theta_s \theta_{l+1-s}, \quad \gamma_0 = 2, \gamma_1 = -1.$$

Series (7.14) converge for $|p| < \sqrt{2}$. This condition holds for $x \in (-1/e, 0)$, with p being in an interval $(-\sqrt{2}, 0)$. Applying this result to the function $f(\alpha, \beta)$, given in (7.13), we obtain:

$$f^{\frac{1}{2}}(\alpha, \beta) \approx \frac{-\sqrt{2(1 - \alpha^{1/n})} + \frac{2}{3}\left(1 - \alpha^{1/n}\right) - \frac{11}{72}\left(2(1 - \alpha^{1/n})\right)^{3/2} + O\left((1 - \alpha^{1/n})^{5/2}\right)}{-\sqrt{2(1 - (1 - \beta)^{1/n})} + \frac{2}{3}\left(1 - (1 - \beta)^{1/n}\right) - \frac{11}{72}\left(2(1 - (1 - \beta)^{1/n})\right)^{3/2} + O\left((1 - \alpha^{1/n})^{5/2}\right)}$$

$$= \sqrt{\frac{1 - \alpha^{1/n}}{1 - (1 - \beta)^{1/n}}}\left(1 + O\left((1 - \alpha^{1/n})^{1/2}\right)\right)$$

In other words, the value of $f(\alpha, \beta)$ is primarily determined by the ratio $\frac{1 - \alpha^{1/n}}{1 - (1 - \beta)^{1/n}}$. Now we can find the limit of this function for $n \to \infty$:

$$\lim_{n \to \infty} f(\alpha, \beta) = \lim_{n \to \infty} \frac{1 - \alpha^{1/n}}{1 - (1 - \beta)^{1/n}} = \lim_{n \to \infty} \frac{\frac{1}{n}\left(1 - \alpha^{1/n}\right)}{\frac{1}{n}\left(1 - (1 - \beta)^{1/n}\right)}$$

Limits of the numerator and denominator for $n \to \infty$ exist and are equal to $-\ln(\alpha)$ and $-\ln(1 - \beta)$ respectively. Thus, the limit of $f(\alpha, \beta)$ is determined as their ratio:

$$\lim_{n \to \infty} f(\alpha, \beta) = \frac{\ln \alpha}{\ln(1 - \beta)}$$

$\square$

Note that it can be tempting to replace a bulky expression (7.13) by its limit, obtained in the Proposition 7.4. However, as illustrated on Figure 7.1, the limit is not sharp.

7.3.3 *Summary of the obtained results*

In this Section we consider the case when the distribution of the test statistics is explicitly known. In order to apply it to a real data, one needs to couple the test with the drift estimator in order to center the statistics. For example, if the drift is known to be constant, the empirical mean can be used as an estimator. Of course, the assumption of constant drift is rather bold, especially in the case of neuronal models. Analogously, one can apply non-parametric drift estimation and use the obtained process for centering. However, most of the estimators require either the prior knowledge of the structure of the diffusion coefficient, or at least some prior information about the distribution of the process. In addition, the estimation error must be taken into account when deriving the distribution of the test statistics. The accuracy of the obtained estimation can play a pivotal role in controlling the power of the test.

7.4   DISTRIBUTION OF STATISTICS FOR A GENERAL D-DIMENSIONAL PROCESS

Now we consider a process X given as a solution of SDE (7.1) in a general setting. Recall that the matrices Ξ_i are defined in (7.2), and each of its vector columns is distributed according to a normal law $\xi_i^j \sim \mathcal{N}(\mu_i^j, \Sigma_i^j)$, where $\mu_i^j \in \mathbb{R}^d, \Sigma_i^j \in \mathbb{R}^{d \times d}$. The mean and the variance can be seen as estimated values of the drift and diffusion coefficients, given by Euler-Maruyama scheme as in (7.4) and (7.5).

We deliberately set this notation differently from the previous section, as in the general case the expectation and the variance of each column vector cannot always be written explicitly, only estimated or approximated.

The main variable of interest in this setting is a determinant $\det \Xi_i^2$. However, unlike in 2-dimensional case, the density of $\det \Xi_i^2$ cannot be written explicitly for $d > 2$. The probabilistic properties of S are thus much harder to study. Our idea is to simplify the problem and to focus on the vector-columns of Ξ_i, which are in fact quadratic forms of normal variables and are slightly easier to study.

7.4.1   Evaluation of moments

Let us give few useful results about $\left\|\xi_i^j\right\|^2$, i.e. the norm of the $j-$th vector-column in a matrix Ξ_i:

Proposition 7.5. *The following holds:*

$$\mathbb{E}\left[\left\|\xi_i^j\right\|^2\right] = \mathbf{tr}\left(\Sigma_i^j\right) + \|\mu_i^j\|^2,$$

$$Var\left[\left\|\xi_i^j\right\|^2\right] = 2\mathbf{tr}\left(\Sigma_i^j\right)^2 + 4(\mu_i^j)^T \Sigma_i^j \mu_i^j$$

More generally, $m-$th moments of $\left\|\xi_i^j\right\|^2$ can be evaluated as:

$$\mathbb{E}\left[\left(\left\|\xi_i^j\right\|^2\right)^m\right] = \left\{\sum_{m_1=0}^{m-1}\binom{m-1}{m_1}g_i^{m-1-m_1}\sum_{m_2=0}^{m_1-1}\binom{m_1-1}{m_2}g_i^{m_1-1-m_2}\cdots\right\},$$

where

$$g_i^l = 2^l l! \left\{\mathbf{tr}\left(\Sigma_i^{l+1}\right) + (l+1)(\mu_i^l)^T\Sigma_i^l \mu_i^l\right\}$$

Proof. Follows from Theorem 3.2b.2 in Mathai and Provost (1992), by rewriting $\left\|\xi_i^j\right\|^2 = \xi_i^j I_d(\xi_i^j)^T$, where I_d is an identity $d \times d$ matrix. $\qquad\square$

Proposition 7.6. *All the moments of the $\det \Xi_i^2$ are bounded, in other words:*

$$\mathbb{E}\left[(\det \Xi_i^2)^m\right] \leq \mathbb{E}\left[\left(\prod_{j=1}^{d}\left\|\xi_i^j\right\|\right)^{2m}\right].$$

Proof. We just have to apply Hadamard inequality, obtaining:

$$\left(\det \Xi_i^2\right)^m = (\det \Xi_i)^{2m} \leq \left(\prod_{j=1}^{d}\left\|\xi_i^j\right\|\right)^{2m} \quad a.s..$$

$\qquad\square$

Now we are ready to evaluate the tail distribution of S, which will be our test statistics.

7.4.2 *Tail distribution*

In general setting it is difficult to explicitly write the probabilistic law of S, as we have done in the previous sections. Thus, we will construct the test with the help of concentration inequalities, which provide us with the information about the tail distributions of the variable S.

Lemma 7.1 (Sub-gaussian lower tail)**.** *Grant assumption (A). The following inequality holds:*

$$\mathbb{P}\left(S - \mathbb{E}[S] \leq -\varepsilon\right) \leq \exp\left(\frac{-\varepsilon^2 n^2}{4\sum_{i=1}^n \mathbb{E}[\det \Xi_i^4]}\right).$$

Proof. Consider the following transformation:

$$\mathbb{P}\left(S - \mathbb{E}[S] \leq -\varepsilon\right) = \mathbb{P}\left(e^{-\lambda(S-\mathbb{E}[S])} \geq e^{\lambda\varepsilon}\right).$$

By Markov's inequality we have $\forall \lambda > 0$:

$$\mathbb{P}\left(e^{-\lambda(S-\mathbb{E}[S])} \geq e^{\lambda\varepsilon}\right) \leq \mathbb{E}\left[e^{-\lambda(S-\mathbb{E}[S])}\right]e^{-\lambda\varepsilon}.$$

By independence of Ξ_i we note that

$$\mathbb{E}\left[e^{-\lambda(S-\mathbb{E}[S])}\right]e^{-\lambda\varepsilon} = e^{-\lambda\varepsilon}\prod_{i=1}^n \mathbb{E}\left[e^{-\frac{\lambda}{n}(\det\Xi_i^2 - \mathbb{E}[\det\Xi_i^2])}\right] =$$

$$e^{-\frac{\lambda}{n}\left(\varepsilon - \sum_{i=1}^n \mathbb{E}[\det\Xi_i^2]\right)}\prod_{i=1}^n \mathbb{E}\left[e^{-\frac{\lambda}{n}\det\Xi_i^2}\right].$$

Now consider

$$\mathbb{E}\left[e^{-\lambda\det\Xi_i^2}\right] = 1 - \frac{\lambda}{n}\mathbb{E}[\det\Xi_i^2] + \frac{\lambda^2}{2n^2}\mathbb{E}\left[2\det\Xi_i^4 \frac{e^{-\frac{\lambda}{n}\det\Xi_i^2} + \frac{\lambda}{n}\det\Xi_i^2 - 1}{(\frac{\lambda}{n}\det\Xi_i^2)^2}\right].$$

Define

$$h(u) := \frac{e^{-u} + u - 1}{u^2}.$$

Since $\lambda > 0$ and $\det\Xi_i^2 \geq 0$, the following holds:

$$h(\frac{\lambda}{n}\lambda\det\Xi_i^2) \leq h(0) = 1.$$

Then,

$$\frac{1}{n^2}\mathbb{E}\left[\det\Xi_i^4 h(\lambda\det\Xi_i^2)\right] \leq \frac{1}{n}\mathbb{E}\left[\det\Xi_i^4\right]$$

$$\mathbb{E}\left[e^{-\frac{\lambda}{n}\det\Xi_i^2}\right] \leq 1 - \frac{\lambda}{n}\mathbb{E}\left[\det\Xi_i^2\right] + \frac{\lambda^2}{n^2}\mathbb{E}\left[\det\Xi_i^4\right]$$

Finally, we obtain

$$\mathbb{P}\left(e^{-\lambda(S-\mathbb{E}[S])} \geq e^{\lambda\varepsilon}\right)$$

$$\leq e^{-\lambda\varepsilon + \frac{\lambda}{n}\sum_{i=1}^n \mathbb{E}[\det\Xi_i^2]}\prod_{i=1}^n \left(1 - \frac{\lambda}{n}\mathbb{E}\left[\det\Xi_i^2\right] + \frac{\lambda^2}{n^2}\mathbb{E}\left[\det\Xi_i^4\right]\right)$$

$$\leq \exp\left(-\lambda\varepsilon + \frac{\lambda}{n}\sum_{i=1}^n \mathbb{E}\left[\det\Xi_i^2\right] - \frac{\lambda}{n}\sum_{i=1}^n \mathbb{E}\left[\det\Xi_i^2\right] + \frac{\lambda^2}{n^2}\sum_{i=1}^n \mathbb{E}\left[\det\Xi_i^4\right]\right)$$

$$= \exp\left(-\lambda\varepsilon + \frac{\lambda^2}{n^2}\sum_{i=1}^n \mathbb{E}\left[\det\Xi_i^4\right]\right)$$

Then, it remains to maximize the above expression with respect to λ, which boils down to finding the minimal value of $-\lambda\varepsilon + \frac{\lambda^2}{n^2}\sum_{i=1}^{n}\mathbb{E}\left[\det\Xi_i^4\right]$. Taking the derivative, we obtain:

$$\frac{d}{d\lambda}\left(-\lambda\varepsilon + \frac{\lambda^2}{n^2}\sum_{i=1}^{n}\mathbb{E}\left[\det\Xi_i^4\right]\right) = -\varepsilon + 2\frac{\lambda}{n^2}\sum_{i=1}^{n}\mathbb{E}\left[\det\Xi_i^4\right].$$

Solving the equation $-\varepsilon + 2\frac{\lambda}{n^2}\sum_{i=1}^{n}\mathbb{E}\left[\det\Xi_i^4\right] = 0$ we obtain the optimal value of λ, which equals $\frac{\varepsilon n^2}{2\sum_{i=1}^{n}\mathbb{E}\left[\det\Xi_i^4\right]}$. Doing the last substitution, we obtain:

$$\exp\left(-\lambda\varepsilon + \frac{\lambda^2}{n^2}\sum_{i=1}^{n}\mathbb{E}\left[\det\Xi_i^4\right]\right) =$$

$$\exp\left(-\frac{\varepsilon^2 n^2}{2\sum_{i=1}^{n}\mathbb{E}\left[\det\Xi_i^4\right]} + \frac{\varepsilon^2 n^2}{4\sum_{i=1}^{n}\mathbb{E}\left[\det\Xi_i^4\right]}\right) = \exp\left(-\frac{\varepsilon^2 n^2}{4\sum_{i=1}^{n}\mathbb{E}\left[\det\Xi_i^4\right]}\right)$$

That gives the result. $\qquad\square$

Now our aim is to evaluate the following probability:

$$\mathbb{P}\left(S - \mathbb{E}[S] \geq \varepsilon\right). \tag{7.15}$$

The difficulty in obtaining (7.15) is that the variables $\det\Xi_i^2$ are not bounded from above. Thus, we can not use the same trick as in the previous subsection. The idea will be to split the probability space Ω in two subspaces: one (denoted by Ω_c^+) will contain the events in which $\det\Xi_i^2$ does not exceed a certain constant $\forall i$, and the other is equal to $\bar{\Omega}_c^+ = \Omega \setminus \Omega_c^+$.

We define the set $\Omega_c^+ \subset \Omega$ as follows:

$$\Omega_c^+ := \left\{\left\|\xi_i^j\right\|^2 \leq \mathbb{E}\left[\left\|\xi_i^j\right\|^2\right] + c_i^j \quad \forall j \in 1,\ldots d,\, i = 1,\ldots,n\right\}, \tag{7.16}$$

where $\|\cdot\|$ is the Euclidean norm, and denote by $\bar{\Omega}_c^+$ its complement and c_i^j is defined as follows:

$$c_i^j = tr\left(\Sigma_i^j\right)\left(d + 2\sqrt{dc} + 2c - 1\right) + 2\left\|\mu_i^j\right\|^2\sqrt{\frac{c}{d}}, \tag{7.17}$$

and the constant c is independent of i and j. Then, consider a random variable $\omega_i^+ = \det\Xi_i^2\mathbb{1}_{\Omega_c^+}$. Probability (7.15) can be bounded as follows:

$$\mathbb{P}\left(S - \mathbb{E}[S] \geq \varepsilon\right) \leq \mathbb{P}\left(\frac{1}{n}\sum_{i=1}^{n}\left(\omega_i^+ - \mathbb{E}\left[\det\Xi_i^2\right]\right) \geq \varepsilon\right) + \mathbb{P}\left(\bar{\Omega}_c^+\right).$$

The idea is then to evaluate the probability $\mathbb{P}\left(\omega_i^+ - \mathbb{E}\left[\omega_i^+\right] \geq \varepsilon\right)$ and show that $\mathbb{P}\left(\bar{\Omega}_c^+\right)$ is small (or negligible) for a good choice of the constant c. The first part of this sum can be evaluated thanks to the following Lemma:

Lemma 7.2. *Grant Assumption (A). In Ω_c^+ the following inequality holds:*

$$\mathbb{P}\left(S - \mathbb{E}[S] \geq \varepsilon\middle|\Omega_c^+\right) \leq \exp\left(-\frac{2\varepsilon^2 n^2}{\sum_{i=1}^{n}\prod_{j=1}^{d}\left(\mathbf{tr}\left(\Sigma_i^j\right) + \|\mu_i^j\|^2 + c_i^j\right)}\right),$$

with c_i^j being defined in (7.17).

Proof. First note that due to the Hadamard inequality, $\det \Xi_i^2$ is bounded by the norms of its vector-columns, which are in turn bounded on space Ω_c^+. In other words,

$$\det \Xi_i^2 \le \prod_{j=1}^d \left\| \xi_i^j \right\|^2 \le \prod_{j=1}^d \left(\mathbb{E} \left[\left\| \xi_i^j \right\|^2 \right] + c_i^j \right) \quad a.s.$$

For the bounded variable $\omega_i^+ = \det \Xi_i^2 \mathbb{1}_{\Omega_c^+}$ we can thus apply Hoeffding's inequality (see Theorem 2.8 in Boucheron et al. (2013)):

$$\mathbb{P} \left(\sum_{i=1}^n \left(\omega_i^+ - \mathbb{E} \left[\omega_i^+ \right] \right) \ge \varepsilon n \right) \le \exp \left(- \frac{2\varepsilon^2 n^2}{\sum_{i=1}^n \prod_{j=1}^d \left(\mathbb{E} \left[\left\| \xi_i^j \right\|^2 \right] + c_i^j \right)} \right).$$

Since $\mathbb{P} \left(\sum_{i=1}^n \left(\omega_i^+ - \mathbb{E} \left[\det \Xi_i^2 \right] \right) \ge \varepsilon n \right) \le \mathbb{P} \left(\sum_{i=1}^n \left(\omega_i^+ - \mathbb{E} \left[\omega_i^+ \right] \right) \ge \varepsilon n \right)$ the statement of the proposition also holds. $\square$

Now we focus on evaluating the probability $\mathbb{P}(\bar{\Omega}_c^+)$.

Lemma 7.3. *The following holds:*

$$\mathbb{P}(\bar{\Omega}_c^+) \le dne^{-c}$$

Proof. First, note that

$$\mathbb{P}(\bar{\Omega}_c^+) \;=\; \mathbb{P} \left(\bigcup_{i=1}^n \bigcup_{j=1}^d \left\{ \left\| \xi_i^j \right\|^2 \ge \mathbb{E} \left[\left\| \xi_i^j \right\|^2 \right] + c_i^j \right\} \right) \;\le\; \sum_{i=1}^n \sum_{j=1}^d \mathbb{P} \left(\left\| \xi_i^j \right\|^2 \ge \mathbb{E} \left[\left\| \xi_i^j \right\|^2 \right] + c_i^j \right)$$

Let us evaluate $\mathbb{P} \left(\left\| \xi_i^j \right\|^2 \ge \mathbb{E} \left[\left\| \xi_i^j \right\|^2 \right] + c_i^j \right)$. First, recall that vector ξ_i^j is normal with mean and variance being given by μ_i^j and Σ_i^j. In particular, it implies that $\forall \lambda \in \mathbb{R}^d$

$$\mathbb{E} \left[\exp \left(\lambda^T \left(\xi_i^j - \mu_i^j \right) \right) \right] \le \exp \left(\| \lambda \|^2 \frac{Var \left[\left\| \xi_i^j \right\| \right]}{2} \right) = \exp \left(\frac{1}{2} \| \lambda \|^2 \, tr \left(\Sigma_i^j \right) \right).$$

Then, by applying Theorem 2.1. from Hsu et al. (2012), we obtain the following:

$$\mathbb{P} \left(\left\| \xi_i^j \right\|^2 > tr \left(\Sigma_i^j \right) \left(d + \sqrt{2dc} + 2c \right) + tr \left(\mu_i^j (\mu_i^j)^T \right) \left(1 + 2 \sqrt{\frac{c}{d}} \right) \right) \le e^{-c}$$

$$\mathbb{P} \left(\left\| \xi_i^j \right\|^2 > \left(tr \left(\Sigma_i^j \right) + \left\| \mu_i^j \right\| \right) + tr \left(\Sigma_i^j \right) \left(d + \sqrt{2dc} + 2c - 1 \right) + 2 \left\| \mu_i^j \right\| \sqrt{\frac{c}{d}} \right) \le e^{-c}.$$

By Proposition 7.5 and the definition (7.16) the above expression can be rewritten as

$$\mathbb{P} \left(\left\| \xi_i^j \right\|^2 \ge \mathbb{E} \left[\left\| \xi_i^j \right\|^2 \right] + c_i^j \right) \le e^{-c}.$$

It gives the result. $\square$

Combining the results of Lemma 7.2 and 7.3, we obtain the upper tail for (7.15):

Lemma 7.4. *Grant assumption (A). The following bound holds:*

$$\mathbb{P} \left(S - \mathbb{E}[S] \ge \varepsilon \right) \le \exp \left(- \frac{2\varepsilon^2 n^2}{\sum_{i=1}^n \prod_{j=1}^d \left(\mathbf{tr} \left(\Sigma_i^j \right) + \| \mu_i^j \|^2 + c_i^j \right)} \right) + dne^{-c}, \qquad (7.18)$$

where c_i^j is defined in (7.17).

The ultimate bound for any $c \geq 0$ may be obtained by minimizing (7.18). However, the function involved in the right part of the expression is not convex, so that the existence of a global minimum is not guaranteed. However, for the practical use we do not need a global minimum. It is suffices that the probability can be bounded by an arbitrarily small value, such that the total probability of a deviation from its mean value for a variable $\det \Xi_i^2$ is bounded by a given risk. Combining Lemmas 7.1 and 7.4, we obtain the following result:

Theorem 7.1. *Grant assumption **(A)** and let*

$$z_\alpha = \frac{1}{n} C_n^d(d, \alpha) \sqrt{-\frac{1}{2} \ln \frac{\alpha}{5dn}} \sqrt{\sum_{i=1}^{n} \prod_{j=1}^{d} \left(tr\left(\Sigma_i^j\right) + \frac{2}{\sqrt{d}C_n(d, \alpha)} \left\|\mu_i^j\right\|^2 \right)},$$

where $C_n(d, \alpha) = \sqrt{d} + \sqrt{-2 \ln \frac{\alpha}{5dn}}$. Then, the following holds:

$$\mathbb{P}\left(|S - \mathbb{E}[S]| \geq z_\alpha\right) \leq \alpha,$$

Proof. Using Lemmas 7.1 and 7.4 we may apply the following restrictions on ε and c:

(i) $dne^{-c} \leq \dfrac{\alpha}{5}$,

(ii) $\exp\left(-\dfrac{2\varepsilon^2 n^2}{\sum_{i=1}^{n} \prod_{j=1}^{d} \left(\mathbf{tr}\left(\Sigma_i^j\right) + \|\mu_i^j\|^2 + c_i^j\right)}\right) \leq \dfrac{2\alpha}{5}$,

(iii) $\exp\left(\dfrac{-\varepsilon^2 n^2}{4 \sum_{i=1}^{n} \mathbb{E}[\det \Xi_i^4]}\right) \leq \dfrac{2\alpha}{5}$.

First note that condition **(i)** is equivalent to $c < -\ln \frac{\alpha}{5dn}$. Second, note that the exponent on the left side of **(ii)** grows as its denominator grows. Thus, we can embed the condition obtained on the first step into the limitations on ε. First, note that by definition (7.17), the denominator in its full form is written as follows:

$$\sum_{i=1}^{n} \prod_{j=1}^{d} \left(tr\left(\Sigma_i^j\right) \left(d + 2\sqrt{dc} + 2c\right) + 2\left\|\mu_i^j\right\|^2 \left(\sqrt{\frac{c}{d}} + 1\right) \right).$$

Using the bound on c obtained from condition **(i)**, we obtain:

$$\sum_{i=1}^{n} \prod_{j=1}^{d} \left(tr\left(\Sigma_i^j\right) \left(d + 2\sqrt{-d\ln\frac{\alpha}{5dn}} - 2\ln\frac{\alpha}{5dn}\right) + 2\left\|\mu_i^j\right\|^2 \left(\sqrt{-\frac{\ln\frac{\alpha}{5dn}}{d}} + 1\right) \right) \leq$$

$$\sum_{i=1}^{n} \prod_{j=1}^{d} \left(tr\left(\Sigma_i^j\right) \left(\sqrt{d} + \sqrt{-2\ln\frac{\alpha}{5dn}}\right)^2 + 2\left\|\mu_i^j\right\|^2 \left(\sqrt{-\frac{1}{d}\ln\frac{\alpha}{5dn}} + 1\right) \right).$$

It can be further simplified as follows:

$$\sum_{i=1}^{n} \prod_{j=1}^{d} \left(tr\left(\Sigma_i^j\right) \left(\sqrt{d} + \sqrt{-2\ln\frac{\alpha}{5dn}}\right)^2 + \frac{2}{\sqrt{d}}\left\|\mu_i^j\right\|^2 \left(\sqrt{-\ln\frac{\alpha}{5dn}} + \sqrt{d}\right) \right) \leq$$

$$\left(\sqrt{d} + \sqrt{-2\ln\frac{\alpha}{5dn}}\right)^{2d} \sum_{i=1}^{n} \prod_{j=1}^{d} \left(tr\left(\Sigma_i^j\right) + \frac{2}{\sqrt{d}\left(\sqrt{-2\ln\frac{\alpha}{5dn}} + \sqrt{d}\right)}\left\|\mu_i^j\right\|^2 \right).$$

Denote $C_n(d, \alpha) := \sqrt{d} + \sqrt{-2 \ln \frac{\alpha}{5dn}}$. Then, the bounds on ε can be obtained from the following inequality:

$$\exp\left(-\frac{2\varepsilon^2 n^2}{C_n^{2d}(d, \alpha) \sum_{i=1}^{n} \prod_{j=1}^{d} \left(tr\left(\Sigma_i^j\right) + \frac{2}{\sqrt{d}C_n(d,\alpha)} \left\|\mu_i^j\right\|^2\right)}\right) \leq \frac{2\alpha}{5}.$$

It results in the following bound:

$$\varepsilon \geq \frac{1}{n} C_n^d(d, \alpha) \sqrt{-\frac{1}{2} \ln \frac{\alpha}{5dn}} \sqrt{\sum_{i=1}^{n} \prod_{j=1}^{d} \left(tr\left(\Sigma_i^j\right) + \frac{2}{\sqrt{d}C_n(d, \alpha)} \left\|\mu_i^j\right\|^2\right)}.$$

Further, we need to consider **(iii)**, which results in

$$\varepsilon \geq \frac{2}{n} \sqrt{-\ln \frac{\alpha}{5dn} \cdot \sum_{i=1}^{n} \mathbb{E}[\det \Xi_i^4]}$$

Note that the bound obtained in (ii) is more restrictive than the bound obtained in (iii), especially when d is large. It gives the result. $\qquad\square$

7.5 CONCLUSIONS

In this Chapter we first demonstrate that under the assumption of Section 7.3 (constant and known drift), a statistical test can be proposed straightforwardly. Explicitly written density function allows us to construct a statistical test and evaluate its power. However, in order to apply the obtained test to real data, one would need to couple the testing procedure with an estimator of the drift, and prove the distribution of the test statistics in this case.

The advantage of the considered 1- and 2-dimensional toy models is that they give an idea of the behaviour of the test statistics in high-dimensional case. Indeed, it is proven in Proposition 7.1 that in a 2-dimensional case, the distribution of S is equivalent to the distribution of product of chi-squared and a normal variable. It is easy to extrapolate (using again the results from Girko (1990)) that in d-dimensional case, the centered statistics with constant diffusion coefficient would behave as a product of d chi-squared variables of $1, 2, \ldots, d$ degrees of freedom. However, the probabilistic law of such an object is not very well studied. Thus, it is difficult to propose results similar to Section 7.3 in a $d-$dimensional case, even if the case of constant coefficients is considered. In the case of non-constant coefficients, the problem becomes much more complicated. To the best of our knowledge, it is out of reach to explicitly write the distribution of the determinant of a random matrix with non-centered non-unit variance normal variables.

Luckily, we do not always need an explicit distribution to construct a test. In Section 7.4 we try to evaluate the tails of S and understand under which condition the statistics concentrates around its mean value. The inequality on the lower tail is easy to obtain, since we use the non-negativity of the test statistics (see Lemma 7.1). With the upper tail, the task is more difficult. The trouble is that the determinants, being nothing else than multivariate polynomials, are notoriously difficult to concentrate: among other things, they are not bounded and cannot be expressed as a Lipschitz

function of Gaussian variables. Most of the works, studying the law of random determinants, consider very special cases: for example, when the matrix is Hermitian (Mehta and Normand, 1998), when the dimension is going to infinity (Nguyen and Vu, 2014), when the entries are centered and independently distributed (Nyquist et al., 1954, Cicuta and Mehta, 2000, Costello and Vu, 2009). The structure of our matrix (7.2) excludes the possibility of working under these assumptions.

Thus, our idea is to reduce the problem down to studying the distribution of the norms of the vector-columns of the matrix using the matrix Hadamard inequality. They are simply quadratic forms of the normal variables and are better studied in the literature (see, for example, book Mathai and Provost (1992)). We use this trick to obtain the upper bound in Lemma 7.4. We need to note, however, that by simplifying the problem of evaluating the upper tail, we loose a lot of information about the distribution: the Hadamard inequality is easy to apply, but it is not sharp in general. Thus, the obtained quantile expression in Theorem 7.1 is rather restrictive.

In order to build a test on the obtained results, several steps need to be achieved. First, we need to be able to give an explicit expression, or a good approximation, of the first moment of S. Some approximations of the expectation of the determinant of a very general matrix are available in the literature (see Girko (1990)), but they are often difficult to apply in a non-asymptotic setting. Second, we need an efficient way to deal with the drift term of the diffusion, or be encoded in the test hypothesis one seeks to test. Indeed, the quantile in Theorem 7.1 depends on the determinant, thus we need to evaluate it prior to constructing the test. Finally, as it is said above, using the Hadamard inequality simplifies the evaluation of the tail, but causes a significant loss of information. Thus, we need either a sharper upper bound, which would depend on the moments of S exclusively, or to determine the dependency between the values of $\mathbf{tr}\left(\Sigma_i^j\right)$ (where Σ_i^j is the covariance matrix of the j-th vector-column) and the $\det \Xi_i$ (Ξ_i being the core of the statistics).

7.6   APPENDIX

7.6.1   *Note on the Lambert W function*

Lambert W function is a multivalued function, whose values are defined by the inverse relation of the function

$$f(w) = we^w,$$

where w is any complex number and e^w is the exponential function. Each branch is denoted by W_k, which is a complex-valued function of one complex argument. These functions satisfy the following property: for any complex numbers w and z, $we^w = z$ holds if and only if for some $k \in \mathbb{N}$, $w = W_k(z)$. Note that in the special case when $z \in \mathbb{R}$ and $z \geq -\frac{1}{e}$, the Lambert W function has a unique real value. More precisely, two real-valued branches of Lambert W function give the solution of the following equation:

$$ye^y = x, x \geq -\frac{1}{e},$$

and the solution as given as follows

$$y = \begin{cases} W_{-1}(x) & \text{if } x \in [-\frac{1}{e}, 0), \\ W_0(x) & \text{if } x \geq 0. \end{cases}$$

The point $-\frac{1}{e}$ is a branching point for the branch W_0 (also called a principal branch). The function can not be differentiated at this point. For the other branches the branching point is located at $x = 0$.

Part IV

AFTERWORD

CONCLUSIONS, DISCUSSIONS, FUTURE WORK

During the 3-years long PhD contract, more questions have arisen as they have been solved in the presented manuscript. The following articles were produced on the basis of the solved questions:

1. J. Chevallier, **A. Melnykova**, I. Tubikanec *"Diffusion approximation of Hawkes processes with Erlang memory kernels: Theoretical and numerical analysis"* (submitted, under review)

2. V. Calvez, S.F. Iglesias, H. Hivert, S. Méléard, **A. Melnykova**, S. Nordmann *"Horizontal gene transfer: numerical comparison between stochastic and deterministic approaches"*, ESAIM: Proceedings and Surveys, EDP Sciences, 2020, CEMRACS 2018, Vol. (67), pp.135-160, doi: 10.1051/proc/202067009

3. **A. Melnykova** *"Parametric inference for multidimensional hypoelliptic ergodic diffusion with full observations"*, Statistical Inference for Stochastic Processes, 2020, Vol. (20), pp.595–635, doi: 10.1007/s11203-020-09222-4

4. **A. Melnykova**, P. Reynaud-Bouret, A. Samson "Concentration inequalities for an estimator of covariance matrix rank in neuronal models"

The results presented in the manuscript were communicated on 6 international conferences and several seminars. The codes reproducing the results are publicly available on author's GitHub page https://github.com/melnyashka.

We devote the concluding Chapter of this thesis to the questions which remained unsolved either due to the lack of time, or because treating those questions would fall far out of the models, tools and methods presented in this work. The author hopes that the issues addressed below could inspire the interested reader to attempt their resolution.

PART I: NUMERICS

The most important message which can be taken from Chapter 4 (*Theoretical and numerical analysis of Hawkes processes with Erlang memory kernels and their diffusion approximation*) is that the stochastic diffusion, arising as a mean-field limit of PDMP model, can be used for studying such a complex system as a spiking network of neurons. There are several advantages of using stochastic diffusions in this framework: first, they are much easier and faster to simulate, since the complexity of the

algorithm does not grow with the size of a neuronal network. Second, from a mathematical point of view they are much more simple to study than the point processes. In particular, it is easier to derive the moment properties or study the long-time behaviour of the system with the SDEs, since one can use a large deviation theory (see, for example, Löcherbach (2019)). To sum up, the author hopes that the results presented in this Chapter (and respective article Chevallier et al. (2020)) could contribute towards better understanding of neuronal activity in interacting systems of neurons on a large scale.

Furthermore, the results obtained in Chapter 4 are inspiring from the statistical point of view: since it has been shown that the diffusion approximation shares the properties of the PDMP, it must be possible to use the statistical inference tools for SDEs for the parameter estimation in the presented model. It is the main subject of the ongoing collaboration between the author of the manuscript, Adeline Samson (Université Grenoble Alpes) and Susanne Ditlevsen (University of Copenhagen). To construct a parameter estimation procedure given the observations of the point processes, several steps are needed. Note that in the real life the integrated intensity process (described by a SDE) is not observed (as well as the firing intensity). So, we would need first to reconstruct the integrated intensity from the available observations of the point process. It can be conducted in several steps. First, the neurons neurons need to be clasterised by using, for example, the method of Humphries (2011). Then, the intensity rate can be estimated from spiking data with the help of kernel estimates as in Shimazaki and Shinomoto (2010), or adapting a method of Gugushvili et al. (2018). Once it is done, one may treat the resulting reconstructed process as a sample of the diffusion process. It only remains to apply the methods of parametric estimation for SDEs to the reconstructed process.

At this moment, several approaches are possible. One possible solution would be to apply the Approximate Bayesian Computation, using the numerical splitting scheme presented in Chapter 4 for simulating the paths, and taking the reconstructed integrated intensity as a reference solution. Another idea could be to adapt the contrast-type (or pseudo-maximum likelihood) estimators to the diffusion process. In that case, it is of crucial importance to determine the suitable "depth" of the memory kernel, i.e., the dimensionality of the considered diffusion. More generally, one could use other methods which can be applied directly to the observations of the point process, for example, Maximum Likelihood Estimators (see Ozaki (1979), Juditsky et al. (2020)), or Bayesian estimators (Rasmussen, 2013).

The numerical results comparing the birth-and-death (individual-based) and Hamilton-Jacobi PDE (density-based) models, obtained in Chapter 5 (and the corresponding paper Calvez, Vincent et al. (2020)) are also encouraging. In particular, we show that the Hamilton-Jacobi type PDE captures well the evolutionary rescue phenomena, and that the theoretical thresholds for changing the regime can be also applied to the individual-based model. The most straightforward application of these results would be to conduct a rigorous theoretical analysis of the resulting limiting equation. The first step to this is already done in the Chapter. However, due to the strict time limitations imposed by the CEMRACS project, we did not attempt, for example, the formal proof of convergence between the PDE and Hamilton-Jacobi integro-differential model. The same fate has doomed the proof of convergence of the semi-implicit scheme used to show the limiting behaviour of the system in a small

population size. The author hopes that the results obtained for this particular example may be carried over to other density-type models, which model the dynamics of the cancer cells under different conditions (like in Example 1.4) and many others.

PART II: STATISTICS

The results presented in Chapter 6 are interesting, first of all, from a theoretical point of view. In this chapter we highlight statistical problems which are typical for hypoelliptic diffusions and not common for elliptic case. In particular, the speed of convergence of parameters differs depending on whether or not the respective variable is driven by the Brownian motion. Also, while studying the convergence of estimator, we were forced to consider more restrictive assumptions on the drift term. Thus, the first possible extension would be to try to obtain similar results in a non-Lipschitz case: the case which includes, for example, most neuronal models considered in the manuscript.

As a second step, it could be interesting to adapt the procedure to high-dimensional systems, with an arbitrary number of smooth and rough variables. For that one would need to propose a reliable scheme, which would give a tractable discrete density. It can be done either with higher-order Itô-Taylor expansions, or a splitting scheme, adapted to a wide class of systems. For Itô-Taylor expansions, one can use a recently published preprint (Pigato, 2020), where a general result for an "extended" diffusion matrix is presented. It gives, in particular, the order of approximation which is needed for obtaining a non-degenerate density, and also the conditions under which this approximation is possible.

Finally, the proposed estimation procedure must be adapted to the case when only one variable is observable: it is the most crucial question for practical applications. The most straightforward expansion would be to embed the obtained estimator in a filtering algorithm, which would allow to treat the case of incomplete data. One could mimic the SAEM approach proposed by Ditlevsen and Samson (2017), use the Gibbs sampling as in Pokern et al. (2007) or probably input the discrete data into more modern estimation techniques, such as neuronal networks, using the contrast-type functions as the loss function.

Another question to solve before applying any parameter estimation method is to choose between the elliptic and hypoelliptic system. This is what the last chapter of this manuscript is devoted to. The author considers Chapter 7 to be a starting point in developing non-asymptotic covariance matrix rank tests for a general class of diffusion systems. By a non-asymptotic setting we mean the case when data is observed only with a fixed time step. Our initial aim is to complement the works Jacod et al. (2008), Jacod and Podolskij (2013), where the similar question is treated in asymptotic case. We choose to use the same statisics as in the above mentioned works.

In the chosen framework we are forced to deal with several difficulties: first, the drift term, which influences the accuracy of the test and needs to be either estimated from discrete data, or taken into account as an error. Second, the test statistics is challenging: it is not bounded, not a Lipschitz function, and, in general, cannot be expressed as a function of standard Gaussian variables. We are able to obtain encouraging results in the 1- and 2-dimensional case (at least in the case of the constant

drift and variance), however, the procedure for multidimensional processes needs to be improved. Several steps need to be accomplished before constructing a valid statistical test in a d-dimensional case: first, one needs to have an explicit expression or at least a good estimate of the moments of the test statistics, second, we need a sharp bound on the distribution of the upper tail. Nevertheless, the author hopes that the obtained results on the probabilistic properties of determinants of random matrix with non-centered and not i.i.d. distributed Guassian entries can be used in a various other fields, given the scarcity of the works on the subject.

BIBLIOGRAPHY

Markus Ableidinger and Evelyn Buckwar. Splitting integrators for the stochastic landau–lifshitz equation. *SIAM J. Sci. Comput.*, 38:A1788–A1806, 01 2016. doi: 10.1137/15M103529X.

Markus Ableidinger, Evelyn Buckwar, and Harald Hinterleitner. A stochastic version of the jansen and rit neural mass model: Analysis and numerics. *The Journal of Mathematical Neuroscience*, 7 (1):1, August 2017. ISSN 2190-8567. doi: 10.1186/s13408-017-0046-4. URL http://dx.doi.org/10.1186/s13408-017-0046-4.

Yves Achdou, Guy Barles, Hitoshi Ishii, and Grigory L. Litvinov. *Hamilton-Jacobi equations: approximations, numerical analysis and applications*, volume 2074 of *Lecture Notes in Mathematics*. Springer, Heidelberg; Fondazione C.I.M.E., Florence, 2013. ISBN 978-3-642-36432-7; 978-3-642-36433-4. doi: 10.1007/978-3-642-36433-4. URL https://doi.org/10.1007/978-3-642-36433-4. Lecture Notes from the CIME Summer School held in Cetraro, August 29–September 3, 2011, Edited by Paola Loreti and Nicoletta Anna Tchou, Fondazione CIME/CIME Foundation Subseries.

Yacine Aït-Sahalia. Maximum likelihood estimation of discretely sampled diffusions: a closed-form approximation approach. *Econometrica*, 70(1):223–262, 2002.

Miguel Arenas and David Posada. Coalescent simulation of intracodon recombination. *Genetics*, 184 (2):429–437, 2010. ISSN 0016-6731. doi: 10.1534/genetics.109.109736. URL http://www.genetics.org/content/184/2/429.

Miguel Arenas and David Posada. Simulation of genome-wide evolution under heterogeneous substitution models and complex multispecies coalescent histories. *Molecular Biology and Evolution*, 31 (5):1295–1301, 2014. doi: 10.1093/molbev/msu078. URL http://dx.doi.org/10.1093/molbev/msu078.

Ludwig Arnold and Wolfgang Kliemann. On unique ergodicity for degenerate diffusions. *Stochastics: an international journal of probability and stochastic processes*, 21(1):41–61, 1987.

Martina Baar, Loren Coquille, Hannah Mayer, Michael Hölzel, Meri Rogava, Thomas Tüting, and Anton Bovier. A stochastic model for immunotherapy of cancer. *Scientific reports*, 6:24169, 2016.

G. Barles. "Solutions de viscosité des équations de Hamilton-Jacobi". *Mathématiques & Applications*, vol 17, 1994.

Wolf-Jürgen Beyn, Elena Isaak, and Raphael Kruse. Stochastic c-stability and b-consistency of explicit and implicit euler-type schemes. *Journal of Scientific Computing*, 67(3):955–987, 2016.

Sylvain Billiard, Régis Ferrière, Sylvie Méléard, and Viet Chi Tran. Stochastic dynamics of adaptive trait and neutral marker driven by eco-evolutionary feedbacks. *J. Math. Biol.*, 71(5):1211–1242, 2015. ISSN 0303-6812. doi: 10.1007/s00285-014-0847-y. URL https://doi.org/10.1007/s00285-014-0847-y.

Sylvain Billiard, Pierre Collet, Régis Ferrière, Sylvie Méléard, and Viet Chi Tran. The effect of competition and horizontal trait inheritance on invasion, fixation, and polymorphism. *J. Theoret. Biol.*, 411:48–58, 2016a. ISSN 0022-5193. doi: 10.1016/j.jtbi.2016.10.003. URL https://doi.org/10.1016/j.jtbi.2016.10.003.

Sylvain Billiard, Pierre Collet, Régis Ferrière, Sylvie Méléard, and Viet Chi Tran. Stochastic dynamics for adaptation and evolution of microorganisms. *arXiv preprint arXiv:1610.00983*, 2016b.

R. Biscay, J. C. Jimenez, J. J. Riera, and P. A. Valdes. Local linearization method for the numerical solution of stochastic differential equations. *Annals of the Institute of Statistical Mathematics*, 48 (4):631–644, Dec 1996. ISSN 1572-9052. doi: 10.1007/BF00052324. URL https://doi.org/10.1007/BF00052324.

S. Blanes, F. Casas, and A. Murua. Splitting and composition methods in the numerical integration of differential equations. *Bol. Soc. Esp. Mat. Apl.*, 45, 01 2009.

Stéphane Boucheron, Gábor Lugosi, and Pascal Massart. *Concentration inequalities: A nonasymptotic theory of independence.* Oxford university press, 2013.

C. E. Bréhier and Ludovic Goudenège. Analysis of some splitting schemes for the stochastic allen-cahn equation. *Discrete Cont. Dyn.-B*, 24:4169–4190, 2019. doi: 10.3934/dcdsb.2019077.

Pierre Brémaud. *Point processes and queues: martingale dynamics*, volume 50. Springer, 1981.

Evelyn Buckwar, Massimiliano Tamborrino, and Irene Tubikanec. Spectral density-based and measure-preserving abc for partially observed diffusion processes. an illustration on hamiltonian sdes. 2019.

Calvez, Vincent, Figueroa Iglesias, Susely, Hivert, Hélène, Méléard, Sylvie, Melnykova, Anna, and Nordmann, Samuel. Horizontal gene transfer: numerical comparison between stochastic and deterministic approaches. *ESAIM: ProcS*, 67:135–160, 2020. doi: 10.1051/proc/202067009. URL https://doi.org/10.1051/proc/202067009.

Patrick Cattiaux, José R León, and Clémentine Prieur. Estimation for stochastic damping hamiltonian systems under partial observation. ii drift term. *ALEA*, 11(1):p–359, 2014.

Patrick Cattiaux, Jose R León, Clémentine Prieur, et al. Estimation for stochastic damping hamiltonian systems under partial observation. iii. diffusion term. *The Annals of Applied Probability*, 26(3):1581–1619, 2016.

Nicolas Champagnat, Régis Ferrière, and Sylvie Méléard. From individual stochastic processes to macroscopic models in adaptive evolution. *Stoch. Models*, 24(suppl. 1):2–44, 2008. ISSN 1532-6349. doi: 10.1080/15326340802437710. URL https://doi.org/10.1080/15326340802437710.

Chi-Tsong Chen. *Linear system theory and design*. Oxford University Press, Inc., 1998.

Zhengdao Chen, Baranidharan Raman, and Ari Stern. Structure-preserving numerical integrators for hodgkin–huxley-type systems. *SIAM Journal on Scientific Computing*, 42:B273–B298, 01 2020. doi: 10.1137/18M123390X.

Julien Chevallier, María José Cáceres, Marie Doumic, and Patricia Reynaud-Bouret. Microscopic approach of a time elapsed neural model. *Mathematical Models and Methods in Applied Sciences*, 25(14):2669–2719, 2015.

Julien Chevallier, Anna Melnykova, and Irene Tubikanec. Theoretical analysis and simulation methods for Hawkes processes and their diffusion approximation. working paper or preprint, March 2020. URL https://hal.archives-ouvertes.fr/hal-02513614.

Carmen Chicone. *Ordinary differential equations with applications*, volume 34. Springer Science & Business Media, 2006.

E.S. Chornoboy, L.P. Schramm, and A.F. Karr. Maximum likelihood identification of neural point process systems. *Biological Cybernetics*, 59(4-5):265–275, 1988. ISSN 0340-1200. doi: 10.1007/BF00332915. URL http://dx.doi.org/10.1007/BF00332915.

Giovanni M Cicuta and Madan Lal Mehta. Probability density of determinants of random matrices. *Journal of Physics A: Mathematical and General*, 33(45):8029, 2000.

Robert M Corless, Gaston H Gonnet, David EG Hare, David J Jeffrey, and Donald E Knuth. On the lambertw function. *Advances in Computational mathematics*, 5(1):329–359, 1996.

Manon Costa, Céline Hauzy, Nicolas Loeuille, and Sylvie Méléard. Stochastic eco-evolutionary model of a prey-predator community. *Journal of mathematical biology*, 72(3):573–622, 2016.

Kevin P Costello and Van Vu. Concentration of random determinants and permanent estimators. *SIAM Journal on Discrete Mathematics*, 23(3):1356–1371, 2009.

M. G. Crandall and P. L. Lions. Two approximations of solutions of Hamilton-Jacobi equations. *Mathematics of Computation*, 43(167):1–19, 1984. ISSN 00255718, 10886842. URL http://www.jstor.org/stable/2007396.

Angelos Dassios, Hongbiao Zhao, et al. Exact simulation of hawkes process with exponentially decaying intensity. *Electronic Communications in Probability*, 18, 2013.

François Delarue and Stéphane Menozzi. Density Estimates for a Random Noise Propagating through a Chain of Differential Equations. *Journal of Functional Analysis*, 259:1577–1630, September 2010. URL https://hal.archives-ouvertes.fr/hal-00436051.

O. Diekmann, P-E. Jabin, S. Mischler, , and B. Perthame. "The dynamics of adaptation: An illuminating example and a Hamilton-Jacobi approach". *Theoretical Population Biology*, 67(4):

257–271, 2005. ISSN 0040-5809. doi: https://doi.org/10.1016/j.tpb.2004.12.003. URL http://www.sciencedirect.com/science/article/pii/S0040580905000134.

S. Ditlevsen and A. Samson. Hypoelliptic diffusions: discretization, filtering and inference from complete and partial observations. *Journal of the Royal Statistical Society: Series B (Statistical Methodology)*, 07 2017. doi: 10.1111/rssb.12307.

Susanne Ditlevsen and Priscilla Greenwood. The morris–lecar neuron model embeds a leaky integrate-and-fire model. *Journal of Mathematical Biology*, 67(2):239–259, 2013.

Susanne Ditlevsen and Eva Löcherbach. Multi-class oscillating systems of interacting neurons. *SPA*, 127:1840–1869, 2017.

Susanne Ditlevsen and Adeline Samson. Estimation in the partially observed stochastic morris-lecar neuronal model with particle filter and stochastic approximation methods. 2012. doi: 10.1214/14-AOAS729.

Aline Duarte, Eva Löcherbach, and Guilherme Ost. Stability, convergence to equilibrium and simulation of non-linear hawkes processes with memory kernels given by the sum of erlang kernels. *ESAIM: PS*, 23:770–796, 2019. doi: 10.1051/ps/2019005. URL https://doi.org/10.1051/ps/2019005.

Stewart N Ethier and Thomas G Kurtz. *Markov processes: characterization and convergence*, volume 282. John Wiley & Sons, 2009.

Lawrence C Evans. *Partial differential equations*, volume 19. American Mathematical Soc., 2010.

William Feller. Die grundlagen der volterraschen theorie des kampfes ums dasein in wahrscheinlichkeitstheoretischer behandlung. In *Selected Papers I*, pages 441–470. Springer, 1939.

Régis Ferrière and Viet Chi Tran. Stochastic and deterministic models for age-structured populations with genetically variable traits. In *CANUM 2008*, volume 27 of *ESAIM Proc.*, pages 289–310. EDP Sci., Les Ulis, 2009. doi: 10.1051/proc/2009033. URL https://doi.org/10.1051/proc/2009033.

Susely Figueroa Iglesias. *Integro-differential models for evolutionary dynamics of populations in time-heterogeneous environments*. Theses, Université Paul Sabatier - Toulouse III, September 2019. URL https://tel.archives-ouvertes.fr/tel-02505794.

Markus Fischer and Giovanna Nappo. On the moments of the modulus of continuity of itô processes. *Stochastic Analysis and Applications*, 28(1):103–122, 2009.

Richard Fitzhugh. Impulses and physiological states in theoretical models of nerve membrane. *Biophysical Journal*, 1(6):445–466, 1961.

Danielle Florens-Zmirou. Approximate discrete-time schemes for statistics of diffusion processes. *Statistics: A Journal of Theoretical and Applied Statistics*, 20(4):547–557, 1989.

Nicolas Fournier and Sylvie Méléard. A microscopic probabilistic description of a locally regulated population and macroscopic approximations. *Ann. Appl. Probab.*, 14(4):1880–1919, 2004. ISSN 1050-5164. doi: 10.1214/105051604000000882. URL https://doi.org/10.1214/105051604000000882.

C. W. Gardiner and M. J. Collett. Input and output in damped quantum systems: Quantum stochastic differential equations and the master equation. *Phys. Rev. A*, 31:3761–3774, 1985. doi: 10.1103/PhysRevA.31.3761. URL https://link.aps.org/doi/10.1103/PhysRevA.31.3761.

V Genon-Catalot, T Jeantheau, and C Larédo. Stochastic volatility models as hidden markov models and statistical applications. bernoulli 6 1051–1079. *Mathematical Reviews (MathSciNet)*, 10:3318471, 2000.

Valentine Genon-Catalot and Jean Jacod. On the estimation of the diffusion coefficient for multidimensional diffusion processes. In *Annales de l'IHP Probabilités et statistiques*, volume 29, pages 119–151, 1993.

Valentine Genon-Catalot, Thierry Jeantheau, and Catherine Laredo. Parameter estimation for discretely observed stochastic volatility models. *Bernoulli*, 5(5):855–872, 10 1999. URL http://projecteuclid.org/euclid.bj/1171290402.

George L Gerstein and Benoit Mandelbrot. Random walk models for the spike activity of a single neuron. *Biophysical journal*, 4(1):41–68, 1964.

Wulfram Gerstner and Werner M Kistler. *Spiking neuron models: Single neurons, populations, plasticity.* Cambridge university press, 2002.

II Gikhman and AV Skhorokhod. *Stochastic differential equations. Kiev.* Naukova Dumka Publ, 1968.

Vyacheslav Girko. *Theory of Random Determinants.* Springer, 1990. doi: 10.1007/978-94-009-1858-0.

Arnaud Gloter. Discrete sampling of an integrated diffusion process and parameter estimation of the diffusion coefficient. *ESAIM: Probability and Statistics*, 4:205–227, 2000.

Arnaud Gloter. Parameter estimation for a discrete sampling of an intergrated ornstein-uhlenbeck process. *Statistics*, 35(3):225–243, 2001.

Arnaud Gloter. Parameter estimation for a discretely observed integrated diffusion process. *Scandinavian Journal of Statistics*, 33(1):83–104, 2006.

Arnaud Gloter and Michael Sørensen. Estimation for stochastic differential equations with a small diffusion coefficient. *Stochastic Processes and their Applications*, 119(3):679–699, 2009. URL https://EconPapers.repec.org/RePEc:eee:spapps:v:119:y:2009:i:3:p:679-699.

Arnaud Gloter and Nakahiro Yoshida. Adaptive and non-adaptive estimation for degenerate diffusion processes. *arXiv preprint arXiv:2002.10164*, 2020.

Joshua H. Goldwyn and Eric Shea-Brown. The what and where of adding channel noise to the hodgkin-huxley equations. 2011. doi: 10.1371/journal.pcbi.1002247.

Shota Gugushvili, Frank van der Meulen, Moritz Schauer, and Peter Spreij. Fast and scalable non-parametric bayesian inference for poisson point processes, 2018.

E. Hairer, C Lubich, and Wanner G. *Geometric numerical integration*. Springer, Heidelberg, 2006.

Peter Hall and Heyde. *Martingale limit theory and its application*. Probability and mathematical statistics. Academic Press, 1980. ISBN 0123193508,9780123193506. URL http://gen.lib.rus.ec/book/index.php?md5=4A150FD028C59EC118AA1E84CDC93370.

Alan G Hawkes. Spectra of some self-exciting and mutually exciting point processes. *Biometrika*, 58 (1):83–90, 1971.

Alan G Hawkes and David Oakes. A cluster process representation of a self-exciting process. *Journal of Applied Probability*, 11(3):493–503, 1974.

D. J. Higham and A. H. Strømenn Melbø. Numerical Simulation of a Linear Stochastic Oscillator with Additive Noise. 2004.

A. L. Hodgkin and A. F. Huxley. A quantitative description of membrane currents and its application to conduction and excitation in nerve. *Journal of Physiology-London*, 117(4):500–544, 1952.

R Höpfner, E Löcherbach, M Thieullen, et al. Ergodicity for a stochastic hodgkin–huxley model driven by ornstein–uhlenbeck type input. In *Annales de l'Institut Henri Poincaré, Probabilités et Statistiques*, volume 52, pages 483–501. Institut Henri Poincaré, 2016a.

Reinhard Höpfner, Eva Löcherbach, and Michèle Thieullen. Ergodicity and limit theorems for degenerate diffusions with time periodic drift. application to a stochastic hodgkin- huxley model. *ESAIM: Probability and Statistics*, 20:527–554, 2016b.

Reinhard Höpfner, Eva Löcherbach, and Michèle Thieullen. Strongly degenerate time inhomogeneous sdes: Densities and support properties. application to hodgkin–huxley type systems. *Bernoulli*, 23 (4A):2587–2616, 2017.

Daniel Hsu, Sham Kakade, Tong Zhang, et al. A tail inequality for quadratic forms of subgaussian random vectors. *Electronic Communications in Probability*, 17, 2012.

Mark D. Humphries. Spike-train communities: Finding groups of similar spike trains. *Journal of Neuroscience*, 31(6):2321–2336, 2011. ISSN 0270-6474. doi: 10.1523/JNEUROSCI.2853-10.2011. URL https://www.jneurosci.org/content/31/6/2321.

Martin Hutzenthaler and Arnulf Jentzen. *Numerical approximations of stochastic differential equations with non-globally Lipschitz continuous coefficients*, volume 236. American Mathematical Society, 2015.

Ildar Abdulovich Ibragimov and Rafail Zalmanovich Khasminskii. *Statistical estimation: asymptotic theory*, volume 16. Springer Science & Business Media, 2013.

Eugene M Izhikevich. *Dynamical systems in neuroscience*. MIT press, 2007.

Eduardo Abi Jaber, Martin Larsson, Sergio Pulido, et al. Affine volterra processes. *The Annals of Applied Probability*, 29(5):3155–3200, 2019.

Jean Jacod and Mark Podolskij. A test for the rank of the volatility process: the random perturbation approach. *The Annals of Statistics*, 41(5):2391–2427, 2013.

Jean Jacod and Philip Protter. *Discretization of processes*, volume 67. Springer Science & Business Media, 2011.

Jean Jacod, Antoine Lejay, Denis Talay, et al. Estimation of the brownian dimension of a continuous itô process. *Bernoulli*, 14(2):469–498, 2008.

Anders Christian Jensen. *Statistical Inference for Partially Observed Diffusion Processes*. Phd thesis, University of Copenhagen, 2014.

J.C. Jimenez and F. Carbonell. Convergence rate of weak local linearization schemes for stochastic differential equations with additive noise. *Journal of Computational and Applied Mathematics*, 279:106 – 122, 2015. ISSN 0377-0427. doi: https://doi.org/10.1016/j.cam.2014.10.021. URL http://www.sciencedirect.com/science/article/pii/S0377042714004671.

S. Jin. Efficient asymptotic-preserving (AP) schemes for some multiscale kinetic equations. *SIAM J. Sci. Comput.*, 21(2):441–454, 1999. doi: 10.1137/S1064827598334599.

Don H. Johnson. Point process models of single-neuron discharges. *Journal of Computational Neuroscience*, 3(4):275–299, Dec 1996. doi: 10.1007/BF00161089. URL https://doi.org/10.1007/BF00161089.

Anatoli Juditsky, Arcadi Nemirovski, Liyan Xie, and Yao Xie. Convex recovery of marked spatio-temporal point processes. 2020.

K. Kamimura, T. Suda, G. Zhang, and D. Liu. Advances in gene delivery systems. *Pharmaceut Med.*, 25(5):293–306, 2011.

Ioannis Karatzas and Steven E. Shreve. *Brownian Motion and Stochastic Calculus*. Graduate Texts in Mathematics. Springer, 1 edition, 1987. ISBN 9780387965352,0387965351,3540965351. URL http://gen.lib.rus.ec/book/index.php?md5=274CB8135034DBB04FE43119E28EEA52.

David G Kendall et al. On the generalized" birth-and-death" process. *The annals of mathematical statistics*, 19(1):1–15, 1948.

Mathieu Kessler. Estimation of an ergodic diffusion from discrete observations. *Scandinavian Journal of Statistics*, 24(2):211–229, 1997.

J. F. C. Kingman. On the genealogy of large populations. *J. Appl. Probab.*, (Special Vol. 19 A):27–43, 1982. ISSN 0170-9739. Essays in statistical science.

A. Klar. An asymptotic-induced scheme for nonstationary transport equations in the diffusive limit. *SIAM J. Numer. Anal.*, 35(3):1073–1094, 1998. doi: 10.1137/S0036142996305558.

A. Klar. An asymptotic preserving numerical scheme for kinetic equations in the low mach number limit. *SIAM J. Numer. Anal.*, 36(5):1507–1527, 1999.

Peter Eris Kloeden, Eckhard Platen, and Henri Schurz. *Numerical solution of SDE through computer experiments*. Universitext. Springer, 2003. ISBN 3540570748,9783540570745. URL http://gen.lib.rus.ec/book/index.php?md5=FED28E7C31D55C92DA839156DB965F99.

Thomas G Kurtz et al. Strong approximation theorems for density dependent markov chains. *Stochastic Processes and their Applications*, 6(3):223–240, 1978.

Yury A Kutoyants. *Statistical inference for ergodic diffusion processes*. Springer Science & Business Media, 2013.

H Lamba, Jonathan C Mattingly, and Andrew M Stuart. An adaptive euler–maruyama scheme for sdes: convergence and stability. *IMA journal of numerical analysis*, 27(3):479–506, 2007.

Leon Lapidus and George F Pinder. *Numerical solution of partial differential equations in science and engineering*. John Wiley & Sons, 2011.

A Le-Breton and M Musiela. Some parameter estimation problems for hypoelliptic homogeneous gaussian diffusions. *Banach Center Publications*, 16(1):337–356, 1985.

B. Leimkuhler and C. Matthews. *Molecular dynamics: with deterministic and stochastic numerical methods*. Springer International Publ., Cham, 2015. ISBN 9783319163741; 3319163744.

B. Leimkuhler, C. Matthews, and G. Stoltz. The computation of averages from equilibrium and nonequilibrium langevin molecular dynamics. *IMA. J. Numer. Anal.*, 36(1):16–79, 2016. doi: 10.1093/imanum/dru056.

Jose R. Leon and Adeline Samson. Hypoelliptic stochastic FitzHugh-Nagumo neuronal model: mixing, up-crossing and estimation of the spike rate. *Annals of Applied Probability*, 28:2243–2274, 2018. URL https://hal.archives-ouvertes.fr/hal-01492590.

P. A. W. Lewis and G. S. Shedler. Simulation of nonhomogeneous Poisson processes by thinning. *Naval Research Logistics Quarterly*, 26(3):403–413, 1979. ISSN 0028-1441. doi: 10.1002/nav.3800260304. URL http://dx.doi.org/10.1002/nav.3800260304.

José León, Luis Rodriguez, and Roberto Ruggiero. Consistency of a likelihood estimator for stochastic damping hamiltonian systems. totally observed data. 01 2018.

Loukia N. Lili, Nicholas F. Britton, and Edward J. Feil. The persistence of parasitic plasmids. *Genetics*, 177(1):399–405, 2007. ISSN 0016-6731. doi: 10.1534/genetics.107.077420. URL http://www.genetics.org/content/177/1/399.

Benjamin Lindner and Lutz Schimansky-Geier. Analytical approach to the stochastic fitzhugh-nagumo system and coherence resonance. *Physical review E*, 60(6):7270, 1999.

Benjamin Lindner, Jordi Garcıa-Ojalvo, Alexander Neiman, and Lutz Schimansky-Geier. Effects of noise in excitable systems. *Physics reports*, 392(6):321–424, 2004.

P.L. Lions. *"Generalized solutions of Hamilton-Jacobi equations"*, volume 69 of *Research notes in mathematics*. Pitman Advanced Publishing Program, Boston, 1982. ISBN 9780273085560. URL <https://books.google.fr/books?id=qxGoAAAAIAAJ>.

Eva Löcherbach. Large deviations for cascades of diffusions arising in oscillating systems of interacting hawkes processes. *Journal of Theoretical Probability*, 32(1):131–162, 2019.

Tommaso Lorenzi, Chandrasekhar Venkataraman, Alexander Lorz, and Mark AJ Chaplain. The role of spatial variations of abiotic factors in mediating intratumour phenotypic heterogeneity. *Journal of theoretical biology*, 451:101–110, 2018.

A. Lorz, S. Mirrahimi, and B. Perthame. "Dirac mass dynamics in multidimensional non local parabolic equations". *Commun. Partial Differ. Equ.*, vol. 36, (No. 6):1071–1098, 2011.

Alexander Lorz, Tommaso Lorenzi, Jean Clairambault, Alexandre Escargueil, and Benoît Perthame. Modeling the effects of space structure and combination therapies on phenotypic heterogeneity and drug resistance in solid tumors. *Bulletin of mathematical biology*, 77(1):1–22, 2015.

Lee M Henry, Jean Peccoud, Jean-Christophe Simon, Jarrod D Hadfield, Martin Maiden, Julia Ferrari, and H Charles J Godfray. Horizontally transmitted symbionts and host colonization of ecological niches. *Current biology : CB*, 23, 08 2013. doi: 10.1016/j.cub.2013.07.029.

Paul Malliavin and Anton Thalmaier. *Stochastic calculus of variations in mathematical finance.* Springer finance. Springer, 1 edition, 2006. ISBN 9783540434313,3-540-43431-3. URL <http://gen.lib.rus.ec/book/index.php?md5=A154244D1FB565DD37F6807340E79039>.

Xuerong Mao. *Stochastic differential equations and applications.* Elsevier, 2007.

A Mathai and S Provost. Quadratic forms in random variables (statistics: A series of textbooks and monographs). *Florida, USA: CRC Press*, 77:3543–3562, 1992.

Jonathan C Mattingly, Andrew M Stuart, and Desmond J Higham. Ergodicity for sdes and approximations: locally lipschitz vector fields and degenerate noise. *Stochastic processes and their applications*, 101(2):185–232, 2002.

R. Mclachlan and G. Quispel. Splitting methods. *Acta Numer.*, 11:341–434, 01 2002. doi: 10.1017/S0962492902000053.

Madan Lal Mehta and Jean-Marie Normand. Probability density of the determinant of a random hermitian matrix. *Journal of Physics A: Mathematical and General*, 31(23):5377, 1998.

Anna Melnykova. Parametric inference for hypoelliptic ergodic diffusion with full observations. *Statistical Inference for Stochastic Processes*, 20:595–635, July 2020. doi: 10.1007/s11203-020-09222-4.

G. N. Milstein and M. V. Tretyakov. Quasi-symplectic methods for langevin-type equations. *IMA Journal of Numerical Analysis*, 23(4):593–626, Oct 2003. ISSN 1464-3642. doi: 10.1093/imanum/23.4.593.

G. N. Milstein and M. V. Tretyakov. *Stochastic numerics for mathematical physics*. Scientific computation. Springer, Berlin, 2004. ISBN 3540211101.

Grigorii Noikhovich Milstein. *Numerical integration of stochastic differential equations*, volume 313. Springer Science & Business Media, 1994.

S. Mirrahimi and J. Roquejoffre. "A class of Hamilton-Jacobi equations with constraint: uniqueness and constructive approach". *J. Differential Equations*, 260(5):4717–4738, 2016. ISSN 0022-0396. URL https://doi.org/10.1016/j.jde.2015.11.027.

T. Misawa. A lie algebraic approach to numerical integration of stochastic differential equations. *SIAM J. Sci. Comput.*, 23(3):866–890, 2001. doi: 10.1137/S106482750037024X. URL https://doi.org/10.1137/S106482750037024X.

George O Mohler, Martin B Short, P Jeffrey Brantingham, Frederic Paik Schoenberg, and George E Tita. Self-exciting point process modeling of crime. *Journal of the American Statistical Association*, 106(493):100–108, 2011.

Jesper Moller and Rasmus Plenge Waagepetersen. *Statistical inference and simulation for spatial point processes*. CRC Press, 2003.

Patrick Alfred Pierce Moran. Random processes in genetics. In *Mathematical proceedings of the cambridge philosophical society*, volume 54, pages 60–71. Cambridge University Press, 1958.

Catherine Morris and Harold Lecar. Voltage oscillations in the barnacle giant muscle fiber. *Biophysical journal*, 35(1):193–213, 1981.

Jinichi Nagumo, Suguru Arimoto, and Shuji Yoshizawa. An active pulse transmission line simulating nerve axon. *Proceedings of the IRE*, 50(10):2061–2070, 1962.

Hoi H. Nguyen and Van Vu. Random matrices: Law of the determinant. *The Annals of Probability*, 42:146–167, 2014. ISSN 0091-1798. doi: 10.1214/12-aop791.

D Nualart. *Malliavin Calculus and Related Topics. Springer*. New York. 2006.

H. Nyquist, S. O. Rice, and J. Riordan. The distribution of random determinants. *Quarterly of Applied Mathematics*, 12:97–104, 1954. ISSN 0033-569X. doi: 10.1090/qam/63591.

Yosihiko Ogata. On Lewis simulation method for point processes. *IEEE Transactions on Information Theory*, 27(1):23–30, 1981.

Yosihiko Ogata. Statistical models for earthquake occurrences and residual analysis for point processes. *Journal of the American Statistical association*, 83(401):9–27, 1988.

Bernt Oksendal. *Stochastic differential equations, Universitext.* Springer,, 2003.

Thoru Ozaki. Statistical identification of nonlinear random vibration systems. *Journal of Applied Mechanics*, 56:186–191, 1989.

Tohru Ozaki. Maximum likelihood estimation of hawkes' self-exciting point processes. *Annals of the Institute of Statistical Mathematics*, 31(1):145–155, 1979.

Tohru Ozaki. *Time series modeling of neuroscience data.* Interdisciplinary statistics. Taylor & Francis, 2012. ISBN 9781420094602,1420094602. URL http://gen.lib.rus.ec/book/index.php?md5=7a5138e691b7b078e99499eee41474b8.

Volker Pernice, Benjamin Staude, Stefano Cardanobile, and Stefan Rotter. How structure determines correlations in neuronal networks. *PLOS Computational Biology*, 7(5):1–14, 05 2011. doi: 10.1371/journal.pcbi.1002059. URL https://doi.org/10.1371/journal.pcbi.1002059.

B. Perthame and G. Barles. "Dirac concentrations in Lotka-Volterra parabolic PDEs". *Indiana Univ. Math. J.*, vol. 7, :3275–3301, 2008.

W. P. Petersen. A General implicit splitting for stabilizing numerical simulations of Itô stochastic sifferential equations. *SIAM J. Numer. Anal.*, 35(4):1439–1451, 1998. doi: 10.1137/0036142996303973.

Paolo Pigato. Density estimates and short-time asymptotics for a hypoelliptic diffusion process. *arXiv preprint arXiv:2004.06541*, 2020.

Y. Pokern, A. M. Stuart, and P. Wiberg. Parameter estimation for partially observed hypoelliptic diffusions. *J. Roy. Stat. Soc.*, 71(1):49–73, 2007.

BLS Prakasa Rao. *Statistical inference for diffusion type processes*, volume 355. Arnold London, 1999.

BLS Prakasa Rao. *Nonparametric functional estimation.* Academic press, 2014.

Calyampudi Radhakrishna Rao. *Linear statistical inference and its applications*, volume 2. Wiley New York, 1973.

Jakob Gulddahl Rasmussen. Bayesian inference for hawkes processes. *Methodology and Computing in Applied Probability*, 15(3):623–642, 2013.

Yoav Raz and Emmanuel Tannenbaum. The influence of horizontal gene transfer on the mean fitness of unicellular populations in static environments. *Genetics*, 185(1):327–337, 2010. ISSN 0016-6731. doi: 10.1534/genetics.109.113613. URL http://www.genetics.org/content/185/1/327.

Basil Cameron Rennie and Annette Jane Dobson. On stirling numbers of the second kind. *Journal of Combinatorial Theory*, 7(2):116–121, 1969.

Daniel Revuz and Marc Yor. *Continuous martingales and Brownian motion*, volume 293. Springer Science & Business Media, 2013.

Patricia Reynaud-Bouret, Vincent Rivoirard, Franck Grammont, and Christine Tuleau-Malot. Goodness-of-fit tests and nonparametric adaptive estimation for spike train analysis. *The Journal of Mathematical Neuroscience*, 4(1):3, Apr 2014. doi: 10.1186/2190-8567-4-3. URL https://doi.org/10.1186/2190-8567-4-3.

Bernard Roynette. Sur les processus de diffusion de dimension 2. *Zeitschrift für Wahrscheinlichkeitstheorie und Verwandte Gebiete*, 32(1-2):95–110, 1975.

Ryszard Rudnicki and Marta Tyran-Kamińska. *Piecewise deterministic processes in biological models*, volume 1. Springer, 2017.

Adeline Samson and Michèle Thieullen. Contrast estimator for completely or partially observed hypoelliptic diffusion. *Stochastic Processes and their Applications*, 122:2521–2552, 2012. doi: 10.1016/j.spa.2012.04.006. URL https://hal.archives-ouvertes.fr/hal-00598553.

T. Shardlow. Splitting for dissipative particle dynamics. *SIAM J. Sci. Comput.*, 24(4):1267–1282, 2003. doi: 10.1137/S1064827501392879.

Hideaki Shimazaki and Shigeru Shinomoto. Kernel bandwidth optimization in spike rate estimation. *Journal of computational neuroscience*, 29(1-2):171–182, 2010.

Gordon D Smith, Gordon D Smith, and Gordon Dennis Smith Smith. *Numerical solution of partial differential equations: finite difference methods*. Oxford university press, 1985.

Charles F Stevens and Anthony M Zador. Novel integrate-and-re-like model of repetitive firing in cortical neurons. 1998.

G. Strang. On the construction and comparison of difference schemes. *SIAM J. Numer. Anal.*, 5(3): 506–517, 1968. doi: 10.1137/0705041. URL https://doi.org/10.1137/0705041.

Daniel W Stroock and SR Srinivasa Varadhan. *Multidimensional diffusion processes*. Springer, 2007.

Irene Tubikanec, Massimiliano Tamborrino, Petr Lansky, and Evelyn Buckwar. Qualitative properties of numerical methods for the inhomogeneous geometric brownian motion. 2020.

Henry C Tuckwell. *Introduction to theoretical neurobiology: volume 2, nonlinear and stochastic theories*, volume 8. Cambridge University Press, 2005.

Kenneth Uda. Ergodicity and spike rate for stochastic fitzhugh–nagumo neural model with periodic forcing. *Chaos, Solitons & Fractals*, 123:383–399, 2019.

Balthasar Van der Pol. A theory of the amplitude of free and forced triode vibrations. *Radio Review*, 1(1920):701–710, 1920.

WT Wells, RL Anderson, John W Cell, et al. The distribution of the product of two central or non-central chi-square variates. *The Annals of Mathematical Statistics*, 33(3):1016–1020, 1962.

Jeffrey West, Zaki Hasnain, Paul Macklin, and Paul K Newton. An evolutionary model of tumor cell kinetics and the emergence of molecular heterogeneity driving gompertzian growth. *SIAM Review*, 58(4):716–736, 2016.

David C Wood. The computation of polylogarithms. technical report. 1992.

Liming Wu. Large and moderate deviations and exponential convergence for stochastic damping hamiltonian systems. *Stochastic processes and their applications*, 91(2):205–238, 2001.

Xiaonan Zhang, Angelo De Milito, Maria Hägg Olofsson, Joachim Gullbo, Padraig D'Arcy, and Stig Linder. Targeting mitochondrial function to treat quiescent tumor cells in solid tumors. *International journal of molecular sciences*, 16(11):27313–27326, 2015.